Remote Sensing and GIS for Wetland Vegetation Study

Fathi Goma Al Sghair

This thesis is submitted in fulfilment of the requirements for the

Degree of Doctor of Philosophy

Institute of Biodiversity, Animal Health and Comparative Medicine

College of Medical, Veterinary and Life Sciences

University of Glasgow

September 2013

Abstract

Remote Sensing (RS) and Geographic Information System (GIS) approaches, combined with ground truthing, are providing new tools for advanced ecosystem management, by providing the ability to monitor change over time at local, regional, and global scales.

In this study, remote sensing (Landsat TM and aerial photographs) and GIS, combined with ground truthing work, were used to assess wetland vegetation change over time at two contrasting wetland sites in the UK: freshwater wetland at Wicken Fen between 1984 and 2009, and saltmarsh between 1988 and 2009 in Caerlaverock Reserve. Ground truthing studies were carried out in Wicken Fen (UK National Grid Reference TL 5570) during 14th - 18th June 2010: forty 1 m^2 quadrats were taken in total, placed randomly along six transects in different vegetation types. The survey in the second Study Area Caerlaverock Reserve (UK National Grid Reference NY0464) was conducted on 5th - 9th July 2011, with a total of forty-eight 1 m^2 quadrats placed randomly along seven transects in different vegetation types within the study area. Two-way indicator species (TWINSPAN) was used for classification the ground truth samples, taking separation on eigenvalues with high value (>0.500), to define end-groups of samples. The samples were classified into four sample-groups based on data from 40 quadrats in Wicken Fen, while the data were from 48 quadrats divided into five sample-groups in Caerlaverock Reserve.

The primary analysis was conducted by interpreting vegetation cover from aerial photographs, using GIS combined with ground truth data. Unsupervised and supervised classifications with the same technique for aerial photography interpretation were used to interpret the vegetation cover in the Landsat TM images. In Wicken Fen, Landsat TM images were used from 18th August 1984 and 23rd August 2009; for Caerlaverock Reserve Landsat TM imagery used was taken from 14th May 1988 and 11th July 2009. Aerial photograph imagery for Wicken Fen was from 1985 and 2009; and for Caerlaverock Reserve, from 1988 and 2009.

Both the results from analysis of aerial photographs and Landsat TM imagery showed a substantial temporal change in vegetation during the period of study at Wicken Fen, most likely primarily produced by the management programme, rather than being due to natural change. In Cearlaverock Reserve, results from aerial photography interpretation indicated a

slight change in the cover of shrubs during the period 1988 to 2009, but little other change over the study period.

The results show that the classification accuracy using aerial photography was higher than that of Landsat TM data. The difference of classification accuracy between aerial photography and Landsat TM, especially in Caerlaverock Reserve, was due to the low resolution of Landsat TM images, and the fact that some vegetation classes occupied an area less than that of the pixel size of the TM image. Based on the mapping exercise, the aerial photographs produced better vegetation classes (when compared with ground truthing data) than Landsat TM images, because aerial photos have a higher spatial resolution than the Landsat TM images.

Perhaps the most important conclusion of this study is that it provides evidence that the RS/GIS approach can provide useful baseline data about wetland vegetation change over time, and across quite expansive areas, which can therefore provide valuable information to aid the management and conservation of wetland habitats.

Table of Contents

Abstract ii
List of Tables vi
List of Figures ix
Acknowledgement xii
Author's Declaration xiii
Abbreviations xiv
Chapter 1 Introduction & Literature Review 1
1.1 Introduction 1
1.1.1 Types of Wetlands 2
1.2 Wetland Ecological Characteristics 7
1.3 Remote Sensing Approaches Used in Wetland Survey 11
1.3.1 Low/Medium Spatial Resolution Optical Systems 13
1.3.2 High Spatial Resolution Optical Systems 14
1.3.3 Hyperspectral Systems 17
1.3.4 Active Systems (RADAR and LiDAR) 19
1.3.5 Aerial Photography 21
1.3.6 GIS Procedures Using Imagery 22
1.4 Application of Remote Sensing Techniques on Wetland studies in the UK 24
1.5 Ecological Factors 26
1.5.1 Water Level 26
1.5.2 Soil Condition 27
1.5.3 Light Availability 28
1.6 Aims of the Study 29
Chapter 2- Methodology 30
2.1 Aerial Photographs 30
2.1.1 Orthophotography 31
2.2 LiDAR Data 33
2.3 ArcGIS Desktop 33
2.4 Landsat TM Images 37
2.5 Image Classification Approach 39
2.5.1 Unsupervised Classification 43
2.5.2 Supervised Classification 43
2.5.3 Change Detection in Wetlands with ArcMap GIS 45
2.6 Ground Truthing Analysis 47
2.6.1 Line Transect 47
2.6.2 Quadrats 47
2.6.3 TWINSPAN Classification of Ground reference Vegetation Survey Data 48
2.6.4 TABLEFIT Classification 49
2.6.5 Statistical Analysis 49
2.7 Achieving the Aims of the Investigation 49
Chapter 3- Wicken Fen study area 1 51
3.1 Introduction 51
3.2 Description of the study area 52
3.3 Airborne and Space-borne Surveys 55
3.3.1 Aerial Photography Interpretation 55
3.3.2 LiDAR image interpretation 66
3.3.3 Landsat imagery interpretation 67
3.4 TWINSPAN classification 93
3.5 TABLEFIT Classification 97

3.6 Statistical analysis 98
3.7 Discussion 102
Chapter 4- Caerlaverock Reserve study area 2 107
4.1 Introduction 107
4.2 Description of the study area (Caerlaverock NNR) 108
4.3 Airborne and Space-borne Surveys 110
4.3.1 Orthophotography interpretation 110
4.3.2 Landsat imagery interpretation 119
4.4 TWINSPAN classification 142
4.5 TABLEFIT Classification 146
4.6 Statistical analysis 147
4.7 Discussion 153
Chapter 5- General Discussion & General Comparison of Survey Approaches 158
5.1 General discussion 158
5.1.1 Aerial Photography Interpretation 158
5.1.2 Landsat TM Image Interpretation 160
5.1.3 Ground Reference Data Analysis 163
5.2 General Comparison of Survey Approaches 164
Chapter 6 Conclusions and Recommendations 166
6.1 Conclusions 166
6.2 Limitations and recommendations 170
List of References 171
Appendices 197
Appendix 1: Instructions for production of Orthophoto using BAE SYSTEMS SOCET SET (v5.6) 197
Appendix 2: Creating a seven-band image from seven TM bands, originating as seven separate TIFF files 210
Appendix 3: Showing how to produce a scene of an appropriate size for work. 220
Appendix 4a: Plant taxa recorded from 40 quadrats in Wicken Fen with common names, density and frequency. 222
Appendix 4b: Field data collected from 40 quadrats at Wicken Fen during June 2010. (T = Line transect; Q = Quadrat). 225
Appendix 4c: Environmental variables recorded from sample quadrats in June 2010 at Wicken Fen. (T = Line transect; Q = Quadrat). 235
Appendix 5: TWINSPAN Analysis depicting final Table from 40 quadrats in Wicken Fen. 237
Appendix 6: TWINSPAN groups in Wicken Fen with Ellenberg's indicator values for light -L; Moisture- F; and Reaction (soil pH or water pH) – R. 239
Appendix 7a: Plant taxa recorded from 48 quadrats in July 2011 at Caerlaverock Reserve with common names, density and frequency. 242
Appendix 7b: Field data collected from 48 quadrats at Caerlaverock Reserve during July 2011. (T = Line transect; Q = Quadrat) 245
Appendix 7c: Environmental variables recorded from sample quadrats in Caerlaverock. 257
Appendix 8: TWINSPAN Analysis depicting final Table from 48 quadrats in Caerlaverock Reserve 259
Appendix 9: TWINSPAN groups in Caerlaverock Reseve with Ellenberg's indicator values for light --L; Moisture -- F; and Salt – S. 261
Appendix 10: Shows results from digitized polygons A, B and C of Figure 3-5 five times and Figure 3-8 four times. 264

List of Tables

Table 1-1: Shows vegetation types in the UK depending on (JCCN, 2007).....4
Table 1-2: A brief summary of wetland ecology characteristics 10
Table 3-1: Explanatory example of an Error Matrix.....62
Table 3-2: Explanatory example of an Change Matrix.....62
Table 3-3: Five classes change matrix resulting from aerial photography1985 versus fieldwork 2010 for Wicken Fen. 64
Table 3-4: Two-classes change matrix resulting from aerial photography1985 versus fieldwork 2010 for Wicken Fen. 64
Table 3-5: Error matrix resulting from aerial photography 2009 vs. fieldwork 2010 for Wicken Fen, using 5 classes.....65
Table 3-6: Error matrix resulting from aerial photography 2009 vs. fieldwork 2010 for Wicken Fen, using two classes.....65
Table 3-7: Shows the possible 25 changes (including no change). 78
Table 3-8: 1984 land cover classes, showing original class name and new label.....78
Table 3-9: 2009 land cover classes, showing original class name and new label.....79
Table 3-10: Outcome pixel values and their meaning. 79
Table 3-11: Change matrix for Wicken Fen in the 1984-2009 period, values in pixels. 81
Table 3-12: Class distribution for changed land cover in Wicken Fen in the 1984-2009 period, in hectares. 81
Table 3-13: Two classes change matrix resulting from satellite imagery 1984 vs. satellite imagery 2009 of Wicken Fen. 82
Table 3-14: Six classes change matrix resulting from unsupervised classification of satellite imagery 1984 vs. fieldwork 2010 for Wicken Fen. 84
Table 3-15: Two classes change matrix resulting from unsupervised classification of satellite imagery 1984 vs. fieldwork 2010 for Wicken Fen. 85
Table 3-16: Six classes error matrix resulting from unsupervised classification of satellite imagery 2009 vs. fieldwork 2010 for Wicken Fen. 86
Table 3-17: Two classes error matrix resulting from unsupervised classification of satellite imagery 1984 vs. fieldwork 2010 for Wicken Fen. 86
Table 3-18: Five classes change matrix resulting from supervised classification of satellite imagery 1984 vs. fieldwork 2010 for Wicken Fen. 87
Table 3-19: Two classes change matrix resulting from supervised classification of satellite imagery 1984 vs. fieldwork 2010 for Wicken Fen. 88
Table 3-20: Five classes error matrix resulting from supervised classification of satellite imagery 2009 vs. fieldwork 2010 for Wicken Fen. 88
Table 3-21: Two classes error matrix resulting from supervised classification of satellite imagery 2009 vs. fieldwork 2010 for Wicken Fen. 89
Table 3-22: Five classes error matrix resulting from aerial photography 1985 vs. satellite imagery 1984 for Wicken Fen.....90
Table 3-23: Two classes error matrix resulting from aerial photography 1984 vs. satellite imagery 1985 of Wicken Fen.....90
Table 3-24: Five classes error matrix resulting from aerial photography 2009 vs. satellite imagery 2009 for Wicken Fen.....91
Table 3-25: Two classes error matrix resulting from aerial photography 2009 vs. satellite imagery 2009 of Wicken Fen. 92
Table 3-26: Shows accuracy of aerial photography 2009 versus fieldwork 2010, see Tables 3.5 and 3.6. 92

Table 3-27: Shows accuracy of satellite imagery using 1985 aerial photography for validating 1984 satellite imagery and using 2010 fieldwork for validating 2009 satellite imagery.....93
Table 3-28: TWINSPAN groups, species and indicator species after species classification 97
Table 3-29: Shows mean values and standard deviation of the mean (± SD) for a) soil pH; b) soil conductivity; c) water conductivity; d) shade; e) water depth; and f) mean vegetation height for TWINSPAN Groups, as shown by one-way ANOVA and application of Tukey's mean separation test. Mean values sharing a superscript letter in common, per variable, are not significantly different. 98
Table 3-30: Shows ean values and standard deviation of the mean (± SD) for a) Light; b) Moisture; c) soil/water pH) for TWINSPAN groups depending on Ellenberg's indicator values for plants, as shown by one-way ANOVA and application of Tukey's mean test. Mean values sharing a superscript letter in common are not significantly different. 101
Table 4-1: Explanatory example of an Error Matrix.....115
Table 4-2: Explanatory example of Change Matrix.....115
Table 4-3: Five classes change matrix resulting from aerial photography1988 (Aerial) versus 2011 fieldwork (FW) for Caerlaverock Reserve. 117
Table 4-4: Two-classes change matrix resulting from aerial photography1988 versus 2011 fieldwork for Caerlaverock Reserve. 117
Table 4-5: Error matrix resulting from aerial photography 2009 versus 2011 fieldwork for Caerlaverock Reserve, five classes. 118
Table 4-6: Error matrix resulting from aerial photography 2009 versus 2011 fieldwork for Caerlaverock Reserve, two classes. 118
Table 4-7: Shows the possible 25 changes (including no change). 127
Table 4-8: 1988 land cover classes, showing original class name and new label.....127
Table 4-9: 2009 land cover classes, showing original class name and new label.....128
Table 4-10: Outcome pixel values and their meaning. 128
Table 4-11: Change matrix for Caerlaverock Reserve in the 1988-2009 period values in pixels. 130
Table 4-12: Class distribution for changed land cover in Caerlaverock Reserve in the 1988-2009 period, in hectares. 130
Table 4-13: Two-classes change matrix for Caerlaverock Reserve in the 1988-2009 period, values in pixels.....131
Table 4-14: Six classes change matrix resulting from unsupervised classification of satellite imagery 1988 vs. fieldwork 2011 for Caerlaverock Reserve. 133
Table 4-15: Two classes change matrix resulting from unsupervised classification of satellite imagery 1988 vs. fieldwork 2011 for Caerlaverock Reserve. 134
Table 4-16: Six classes error matrix resulting from unsupervised classification of satellite imagery 2009 vs. fieldwork 2011 for Caerlaverock Reserve.....134
Table 4-17: Two classes error matrix resulting from unsupervised classification of satellite imagery 2009 vs. fieldwork 2011 for Caerlaverock Reserve.....135
Table 4-18: Five classes change matrix resulting from supervised classification of satellite imagery 1988 vs. fieldwork 2011 for Caerlaverock Reserve.....136
Table 4-19: Two classes change matrix resulting from supervised classification of satellite imagery 1988 vs. fieldwork 2011 for Caerlaverock Reserve.....136
Table 4-20: Five classes error matrix resulting from supervised classification of satellite imagery 2009 vs. fieldwork 2011 for Caerlaverock Reserve.....137
Table 4-21: Two classes error matrix resulting from supervised classification of satellite imagery 2009 vs. fieldwork 2011 for Caerlaverock Reserve.....137
Table 4-22: Five classes error matrix resulting from aerial photography 1988 vs. satellite imagery 1988 for Caerlaverock Reserve.....138

Table 4-23: Two classes error matrix resulting from aerial photography 1988 vs. satellite imagery 1988 of Caerlaverock Reserve. 139
Table 4-24: Five classes error matrix resulting from aerial photography (air) 2009 vs. satellite imagery (TM) 2009 for Caerlaverock Reserve.....140
Table 4-25: Two classes error matrix resulting from aerial photography (Air_2009) 2009 vs. satellite imagery (TM2009) 2009 of Caerlaverock Reserve. 140
Table 4-26: Shows accuracy of aerial photography 2009 versus fieldwork 2011, see Tables 4.5 and 4.6. 141
Table 4-27: Shows accuracy of satellite imagery using 1988 aerial photography for validating 1988 satellite imagery and using 2011 fieldwork for validating 2009 satellite imagery.....141
Table 4-28: TWINSPAN groups, species and indicator species after species classification 146
Table 4-29: Mean values and standard deviation of the mean (± SD) for a) soil pH; b) soil conductivity; c) shade; and d) mean vegetation height for TWINSPAN Groups, as shown by one-way ANOVA and application of Tukey's mean test Mean values per variable sharing a superscript letter in common are not significantly different.....147
Table 4-30: Mean values and standard deviation of the mean (± SD) for a) Light; b) Moisture; c) salt-tolerant) for TWINSPAN groups using Ellenberg's indicator values for plants, as shown by one-way ANOVA and application of Tukey's mean test. Mean values sharing a superscript letter in common are not significantly different.....150

List of Figures

Figure 2-1: Flowchart to create an orthophotograph from aerial photography in BAE Systems SOCET SET (v6) (Refer to Appendix 1 for further details of this process). 32
Figure 2-2: Preliminary details Wicken Fen map. 34
Figure 2-3: Preliminary details Caerlaverock Reserve map. 35
Figure 2-4: Flowcharts showing creation of mosaic map from aerial photos and LiDAR data in ArcMap GIS. 36
Figure 2-5: Flow chart showing procedure to separate TIFF bands from a Landsat TM scene and reformed as an ER Mapper as a 7 Band image. (Refer to Appendix 2 for further details of this process including displaying a natural colour image on screen using 3 bands). 38
Figure 2-6: Shows (a) gaps in Landsat 2009TM image, (b) Landsat 2009TM image, after gap filling procedure, using NASA's GapFill program a 'cosmetic'solution. The gaps reappeared after classification as differently classified stripes. 39
Figure 2-7: Procedure for choosing the Study Area from whole satellite image using the ER Mapper. (Refer to Appendix 3 for further details of this process). 40
Figure 2-8: Subset images showing the study area. 41
Figure 2-9: Landsat TM image analysis approach using ER Mapper, supporting both Unsupervised and Supervised classification. 42
Figure 3-1: Location of Wicken Fen. 53
Figure 3-2: Distribution of *Frangula alnus* in the British Isles. 54
Figure 3-3: Verrall's Fen (A), and Sedge Fen (B) in Wicken Fen 1985 aerial photograph (Black & White) 56
Figure 3-4: Verrall's Fen (A), and Sedge Fen (B) in Wicken Fen 2009 aerial photograph. 56
Figure 3-5: Cover of trees & shrubs (green) in Wicken Fen 1985, using air photo interpretation. 59
Figure 3-6: Cover of trees & shrubs (green) in Wicken Fen 1999, using Google Earth. 59
Figure 3-7: Cover of trees & shrubs (green) in Wicken Fen 2003, using Google Earth. 60
Figure 3-8: Cover of trees & shrubs (green) in Wicken Fen 2009, using air photo interpretation. 60
Figure 3-9: Height of vegetation at Wicken Fen in a mosaic map of 2004 LIDAR data (white areas are unclassified, and represent open water) 67
Figure 3-10: Ten land cover classes of 1984 Wicken Fen LandsatTM image after unsupervised classification. (See Fig. 2-8 c for the original image, prior to classification) 68
Figure 3-11: Six land cover classes of 1984 Wicken Fen LandsatTM image after unsupervised classification. 69
Figure 3-12: Six land cover classes of the 2009 Wicken Fen LandsatTM image after unsupervised classification. 70
Figure 3-13: Ten land cover classes of the 2009 Wicken Fen LandsatTM image after unsupervised classification. 71
Figure 3-14: Six classes unsupervised classification of 1984 Wicken Fen imagery 72
Figure 3-15: Six classes unsupervised classification of 2009 Wicken Fen imagery, the circled area (A) shows an obvious change in vegetation. 72
Figure 3-16: Land cover classes identified for 1984 Wicken Fen through supervised classification. 73
Figure 3-17: Land cover classes identified for 2009 Wicken Fen through supervised classification. 74
Figure 3-18: Shows scattergram created from the five class supervised classification using LandsatTM bands 2 and 4 of Wicken Fen, 1984. 75
Figure 3-19: Shows scattergram created from the five class supervised classification using Landsat TM bands 2 and 4 of Wicken Fen, 2009. 75

Figure 3-20: Wicken Fen 1984 supervised classification 76
Figure 3-21: Wicken Fen 2009 supervised classification 77
Figure 3-22: Land cover change map for Wicken Fen 1984-2009. 83
Figure 3-23: Distribution of quadrat positions (for 4 TWINSPAN sample groups) in Wicken Fen. 94
Figure 3-24: Dendrogram of the TWINSPAN classification of 40 quadrats in Wicken fen. 96
Figure 3-25: Mean (± S.D) values for soil pH for 4 sample groups. Different letters above value bars represent a significant difference between group means. 99
Figure 3-26: Mean (± S.D) values for shade height for 4 sample groups. Different letters above value bars represent a significant difference between group means. 100
Figure 3-27: Mean (± S.D) values for shade percentage for 4 sample groups. Different letters above value bars represent a significant difference between group means. 101
Figure 4-1: Map section of Caerlaverock Reserve showing Eastpark Merses study area. 109
Figure 4-2: Orthophotograph of Caerlaverock Reserve 1988.....111
Figure 4-3: Orthophotograph of Caerlaverock Reserve 2009. 111
Figure 4-4: Cover of trees (dark green) and shrubs (light green) in Caerlaverock Reserve 1988. 113
Figure 4-5: Cover of trees (dark green) and shrubs (light green) in Caerlaverock Reserve 2009. 113
Figure 4-6: Six land cover classes of the 1988 Caerlaverock LandsatTM image after unsupervised classification.....120
Figure 4-7: Ten land cover classes of the 1988 Caerlaverock LandsatTM image after unsupervised classification.....121
Figure 4-8: Six land cover classes of the 2009 Caerlaverock LandsatTM image after unsupervised classification 122
Figure 4-9: Ten land cover classes of the 2009 Caerlaverock Reserve LandsatTM image after unsupervised classification. 123
Figure 4-10: Land cover classes identified for 1988 Caerlaverock Reserve LandsatTM image through supervised classification. 124
Figure 4-11: Land cover classes identified for 2009 Caerlaverock Reserve LandsatTM through supervised classification. 124
Figure 4-12: Shows scattergram created from the five class supervised classification using LandsatTM bands 2 and 4 of Caerlaverock Reserve, 1988. 125
Figure 4-13: Shows scattergram created from the five class supervised classification using LandsatTM bands 2 and 4 of Caerlaverock Reserve, 2009. 126
Figure 4-14: Land cover change map for Caerlaverock Reserve 1988-2009. 132
Figure 4-15: Distribution of quadrat positions (in five TWINSPAN groups) in the Caerlaverock Reserve.....143
Figure 4-16: Dendrogram of the TWINSPA sample classification of 48 quadrates in Caerlaverock. 145
Figure 4-17: Mean (± S.D) values for soil pH of TWINSPAN groups. Different letters above value bars represent a significant difference between group means. 148
Figure 4-18: Mean (± S.D) values for max vegetation height for TWINSPAN groups. Different letters above value bars represent a significant difference between group means. 148
Figure 4-19: Mean (± S.D) values for soil conductivity of TWINSPAN groups. Different letters above value bars represent a significant difference between group means. 149
Figure 4-20: Mean (± S.D) values for shade percentage between TWINSPAN groups. Different letters above value bars represent a significant difference between group means. 151

Figure 4-21: Mean (± S.D) values for shade percentage between TWINSPAN groups. Different letters above value bars represent a significant difference between group means. 151
Figure 4-22: Mean (± S.D) values for shade percentage between TWINSPAN groups. Different letters above value bars represent a significant difference between group means. 152
Figure 4-23: Shows the rough grazing zone inside the yellow line that has shrubs and grasses following supervised classification for 2009 Caerlaverock Reserve Landsat TM. 157
Figure 4-24: Shows the rough grazing zone inside the yellow line that has shrubs and grasses following supervised classification for 1988 Caerlaverock Reserve LandsatTM. 157

Acknowledgement

First and foremost, I thank ALMIGHTY ALLAH for the blessing, inspiration and patience to complete my research.

I wish to express my thanks and appreciation to my two supervisors Dr. Kevin Murphy and Dr. Jane Drummond for their direction and support over the last few years to complete this research successfully; and I particularly appreciate Dr. Drummond's dedication, and time spent solving the many dilemmas in using remote-sensing methods I encountered along the way, no matter how large or small. I have learned more than I could ever have imagined from them both.

I wish to thank Elaine Benzies and Flavia Bottino, both research students at the University of Glasgow, for help in fieldwork, also to Dr. Larry Griffin at the Wildfowl & Wetlands Trust (WWT), Caerlaverock, Dumfriesshire, who provided me with information about the Caerlaverock Reserve, and as well to John Laurie, Lorna Kennedy and Florence McGarrity for their kindness and help with technical issues.

I acknowledge support, with the supply of data, from Dr. Mike Plant of the Environment Agency, the Ordnance Survey of Great Britain through Edina's Digimap service and the United States Geological Survey through its GLOVIS service.

Special thanks to my dear Libyan friends and my office mates especially Dr. Hussein Jenjan and Aiad Aboeltiyah. Also this work would not have been possible without the financial support from the Ministry of Higher Education in Libya, I am grateful to them for this opportunity.

I am most appreciative of my father, mother, brothers and sisters for their continuing support, as without reconcile from Allah then their supports and wishes, I couldn't achieve what I have achieved today.

Finally, special thanks to my wife for her patience and providing me comfort during my study, and my sons and my daughter for giving me their love, support and all joy.

Author's Declaration

I declare that the work recorded in this thesis in my own, and no part of the work here has been submitted for any other degree or qualification in any university.

Fathi G. Al Sghair

Abbreviations

AHS	Airborne Hyperspectral Scanner
ALTM	Airborne Laser Terrain Mapper
ASAR	Advanced Synthetic Aperture Radar
ATM	Airborne Thematic Mapper
AVHRR	Advanced Very High Resolution Radiometer
AVIRIS	Airborne Visible/Infrared Imaging Spectrometer
BAE Systems SOCET SET	BAE – formerly British AeroSpace SOCET – SOft Copy Exploitation toolseT
CASI	Compact Airborne Spectographic Imager
CASI	Compact Airborne Spectral Imager
DTM	Digital Terrain Models
ENVISAT	Environmental Satellite
EO	Earth Observation
ETM+	Enhanced Thematic Mapper Plus
GIS	Geographic Information System
GLOVIS	Global Visualization Viewer
GOES	Geostationary Operational Environmental Satellite
GPP	Gross Primary Production
GPS	Global Positioning Systems
IKONOS	comes from the Greek term *eikōn* for image
InSAR	Interferometric Synthetic Aperture Radar
IRS 1C LISS	Indian Remote Sensing satellites 1C Linear Imaging Self Scanning Sensor
ISODATA	Iterative Self-Organizing Data Analysis Technique algorithm
JERS-1	Japan Earth Resources Satellite -1
LIDAR	Airborne Light Detection and Ranging
MERIS	Medium Resolution Imaging Spectrometer
MIVIS	Multispectral Infrared Visible Imagine Spectrometer
MLC	Maximum Likelihood Classifier
MMU	Minimum Mapping Unit
MODIS	Moderate Resolution Imaging Spectroradiometer
MSS	Multispectral Scanner
NASA	National Aeronautics and Space Administration

NDVI	Normalized Differential Vegetation Index
NERR	National Estuarine Research Reserve
NNR	National Nature Reserves
NOAA	National Oceanic and Atmospheric Administration
NPP	Net Primary Production
NVC	National Vegetation Classification
PNG	Portable Network Graphics
PROBE-1	An airborne hyperspectral sensing system
RADARSAT-1	Canada's first-generation commercial Synthetic Aperture Radar (SAR) satellite
RADARSAT-2	Canada's second-generation commercial Synthetic Aperture Radar (SAR) satellite
RGB	Red, Green, Blue
RS	Remote Sensing
SAR	Synthetic Aperture Rader
SAV	Submerged Aquatic Vegetation
SLC	Scan Line Corrector
SPOT	Satellite Pour I'Observation de la Terre
SPOT HRV	Satellite Pour I'Observation de la Terre High Resolution Visible
SSSI	Special Scientific Interest
TIFF	Tagged Image File Format
TM	Landsat Thematic Mapper
TWINSPAN	Two-way Indicator Species Analysis
UAV's	Unmanned Aerial Vehicles
USGS	the United States Geological Survey
VHR	Very High spatial Resolution
YNNR	Yancheng National Nature Reserve

Chapter 1- Introduction & Literature Review

1

1.1 Introduction

Wetlands are sited in the landscape as ecotones that appear along elevation and hydrological gradients between terrestrial and aquatic ecosystems (Bardley and Hauer, 2007). They can be defined as regions that are transitional between terrestrial and aquatic systems, where the water table is near the surface or the land is inundated by shallow water, whether during the whole or part of the year (Frohn et al., 2009). Wetland vegetation is an important component of wetland ecosystems that plays a vital role in environmental function (Kokaly et al. 2003). Wetlands are important habitats because the heterogeneity in hydrology and soil conditions which they support results in a broad variety of ecological niches, and they usually support enormous biodiversity (McCartney and Hera, 2004).

Wetland and riparian zones supply a variety of ecological services that contribute to ecosystem functions (Ehrenfeld 2000, Mitsch and Gosselink 2000). In addition, they provide numerous valuable functions (e.g. ground water recharge, flood mitigation, regulation of pollutants and water) as well as other attributes (biodiversity support, amenity and creation, cultural heritage), and there has been increasing awareness of their functional value in recent years (Owor et al., 2007). Wetland vegetation is a significant component of wetland ecosystems, one that plays a vital role in environmental function (Kokaly et al. 2003; Lin and Liquan 2006). It is also an excellent indicator for early signs of any physical or chemical degradation in wetland environments (Adam et al. 2010). Wetlands cover 6% (seven to eight million km^2) of the world's land surface (Erwin, 2009), and occur in every climate, from the tropics to the frozen tundra, on every continent except Antarctica (Mitsch, 1994).

1.1.1 Types of Wetlands

There are many different types of wetlands. Matthews and Fung (1987) divided wetlands into 5 classes: forested bogs, non-forested bogs (where bogs are formed by infilling of shallow lakes; usually with no inflow or outflow), forested swamps, and non-forested swamps (swamps found in poorly drained areas near streams or lakes) and alluvial formations. Bogs and fens are the most common wetlands across large areas of the northern hemisphere, above 45^{o} north (Aselmann and Crutzen, 1989). It is estimated that about half of the world's wetlands are in the boreal region, mostly in the form of bogs (Matthews, 1990). According to Aselmann and Crutzen (1989), the most widespread wetland category is bogs, covering 1.9×10^{6} km^2, followed by fens and swamps, contributing about 1.5×10^{6} km^2 and 1.1×10^{6} km^2, respectively. Floodplains add another 0.8×10^{6} km^2, whereas marshes and lakes contribute only 7% to the total. Other major types of wetlands worldwide fall into the categories of coastal river deltas, inland river deltas, great riverine forests, saltmarshes, northern peatlands, inland freshwater marshes and swamps, and constructed wetlands (Mitsch, 1994).

1.1.1.1 Freshwater Wetlands in the UK

Wetlands are an important part of the British and Irish landscape, covering almost 10% of the terrestrial land area (Dawson et al., 2003), and both broad and priority habitat. The main types of wetlands are rivers, lakes, ponds, and ditches; swamps which are permanently saturated with water; and marshes which may be partially flooded for long periods (Polunin and Walters 1985). The UK has many types of freshwater wetlands, such as floodplain, swamp, fen, wet grasslands, ditches and marshes (Mitsch, 1994). Fens are dominated by graminoid (grass-like) vegetation: grasses, sedges, and rushes. Like fens, marshes are also dominated by herbaceous emergent vegetation (Mitsch and Gosselink, 2000). Common marsh species include the sedges, *Carex* and *Cyperus* spp., rushes, *Juncus* spp., and species such as cattail, *Typha* spp. (Craft, 2005). Great Britain and Ireland have almost 2,500,000 ha of bogs and fens (Taylor, 1983). The total national area of the UK is 24,159,000 ha (excluding marine areas), and the estimate of wetland coverage within the UK is 2,976,585 ha (based on Davidson and Buck 1997; UK Ramsar National Report 1999).

Lowland wetlands are classified into lowland raised bog and blanket bog, and lowland fen. The second type includes: flood-plain fen, basin fen, open-water transition fen, valley fen, springs and flushes, fen woodland, and fen meadow (JNCC, 2004). According to Barr et al. (1993), the best estimate for inland wetlands in the UK is 370,000 ha of fen, marsh and flush wetland; 1,660,000 ha of wet heath and saturated bogs; 210,000 ha of inland water bodies (i.e. lake, pond, mere, reservoir); 80,000 ha of inland watercourses (i.e. river, canal, drainage channels), and 60,000 ha of wet woodlands. England holds approximately 40% of the UK's fen and lowland raised bog, and over half of the reedbeds (Carey et al., 2008). A brief summary of vegetation types present in the UK are shown in Table 1.1.

Table 1-1: Shows vegetation types in the UK depending on (JCCN, 2007).

Vegetation types	Vegetation characteristic
Lowland Grassland Habitat Lowland meadows	Plant species occurs *Cynosurus cristatus Leucanthemum vulgare*. *Centaurea nigra, Festuca rubra, Filipendula ulmaria ,Silaum silaus*
Lowland Wetland Habitat Lowland Raised Bog	Usually various colourful *Sphagnum* mosses predominate (e.g. *Sphagnum auriculatum, S. cuspidatum, S. magellanicum, S. papillosum, S. recurvum*
Lowland Fen Poor-fens	Their vegetation is characteristically species-poor, with a moderate to high cover of *Sphagnum* bog mosses (mainly *Sphagnum cuspidatum, S. palustre, S. recurvum, S. squarrosum*) and sedges (especially Bottle sedge *Carex rostrata*),
Rich-fens	It includes mire vegetation dominated by a range of *Carex* sedges, mixed in with various vascular plants *Lychnis flos-cuculi, Pinguicula vulgaris, Ranunculus flammula, Pedicularis palustris, Caltha palustris, Cirsium palustre*
Grassland and marsh	This category includes both areas of herbaceous vegetation dominated by grasses and certain wet communities dominated by *Juncus* species, *Carex* species, *Filipendula ulmaria*.
Marsh/marshy grassland	Covering certain *Molinia* grasslands, grasslands with a high proportion of *Juncus* species, *Carex* species or *Filipendula ulmaria,* and wet meadows and pastures supporting communities of species such as *Caltha palustris* or *Valeriana* species.
Tall herb and fern	Dominated by *Pteridium aquilinum,* ,this ledge vegetation contains species such as *Angelica sylvestris, Filipendula ulmaria, Solidago virgaurea, Athyriurn fllix-femina, Trollius europaeus* and *Crepis paludosa.*
Swamp	vegetation includes both mixed and singlespecies stands of *Typha* species, *Phragmites australis; Phalaris arundinacea, Glyceria maxima, Carex paniculata, C. acutiformis, C. rostrata* or other tall sedge.
Coastal Habitat Types Saltmarsh	*Salicornia* species and *Spartina maritima*)
Bog woodland	Generally dominated by *Betula pubescens, Frangula alnus, Pinus sylvestris, Pinus rotundata* and *Picea abies*,
Scrub	*Ulex europaeus, Cytisus scoparius* and *Juniperus communis* scrub; stands of *Rubus fructicosus* and *Rosa canina* montane scrub with *Salix lapponum, S. lanata, S. myrsinites, S. arbuscula* or *S. phylicifolia;* stands of mature *Crataegus monogyna, Prunus spinosa* or *Salix cinerea*

1.1.1.2 Saltmarsh Wetlands in the UK

The plants that grow in saline habitats such as saltmarsh habitats are called halophytes. Halophytes are defined by Flowers and Colmer (2008) as species which have adaptations permitting survival and growth under saline conditions. Saltmarshes are defined as intertidal areas of fine sediment transported by water and stabilised by vegetation (Boorman, 1995). The development of saltmarshes is the result of the interplay of tides, waves, relative sea-level rise, sediment supply and vegetation (Harvey and Allan, 1998). Marshes are usually inundated with surface-water, and water levels generally vary from a few centimetres to a metre or more (Mitsch, 1994), depending on tidal and topographical location. British saltmarshes are found around much of the coast, together with a few inland marshes; the saline habitats are not solely coastal in the UK, although the number of inland saltmarshes resulting from saline groundwater and salt-bearing rocks is admittedly hugely reduced, wherever the local physiography allows their development (Adam, 1981). Saltmarshes usually arise on intertidal land (often in estuaries, but also in sea lochs in Scotland: e.g. Taubert and Murphy, 2012) within the amplitude of the usual spring tides, where halophytic plants have adapted to high salinities and are able to endure periodic immersion in seawater. They occur in a broad variety of locations, where certain conditions are present which allow a net accumulation of soft sediment, allowing the growth of halophytic plants in this zone (Burd, 1989).

British saltmarsh communities are not composed solely of halophytes, but frequently contain less-specialist species too, especially towards the upper part of the marsh (Adam, 1981). Saltmarshes in Britain are classified into three seres, the south coast sere, the east coast sere and the west coast sere; there is a fourth type in Ireland (Chapman, 1941). Within these broad geographical seres, three types of saltmarsh are usually recognised. The first type is normally ungrazed and largely restricted to southeast England; a second type is grazed and largely restricted to the Irish Sea coast of England and Wales, as well as the Scottish shore of the Solway Firth; the third type is typical of sea loch-head marshes on the west coast of Scotland (Adam, 1978). Saltmarsh zones in the UK are generally laid out as follows: lowest on the shoreline is the pioneer zone: open communities covered by all tides except the smallest range of the tide, and dominated by one or more of the following - *Spartina* spp., *Salicornia* spp., and *Aster tripolium*. Next up the shore is the low marsh zone, inundated by most tides, and characterised by a closed sward community, often

dominated by *Puccinellia maritima* and *Atriplex portulacoides*, as well as pioneer species. Often the two lowest zones are combined and referred to as the low marsh. Above this is middle marsh, covered only by spring tides, and again in general characterised by closed communities with *Limonium* spp. and/or *Plantago maritima*, as well as species found lower on the shore. Finally the uppermost part of the marsh, inundated only infrequently by the highest spring tides, is the high marsh zone: in general, this is formed of closed communities characterised by one or more of the following - *Festuca rubra*, *Armeria maritima*, *Elymus pycnanthus*, as well as plants found lower on the marsh (Boorman, 2003).

Chapman (1941) has classified the maritime saltmarshes of the world into nine main groups, with various sub-groups. The Solway area (within which lie the Caerlaverock saltmarshes that form Study Area 2 for the present work), falls into Group 1, in sub-group (a) North European Marshes: described as a "sandy and sandy mud type dominated by grasses." Generally, grasses such as *Puccinellia*, with some *Festuca* and *Agrostis*, as well as dicots such as *Armería* and *Plantago*, dominate this saltmarsh community (Marshall, 1962). National Vegetation Classification (NVC) described the communities of saltmarsh vegetation (Rodwell et al., 2000), subdividing them into thirteen communities in the lower saltmarsh, nine communities in the middle saltmarsh, and three communities in the upper saltmarsh (Boorman, 2003). Some 82.8% of the total saltmarsh area in Great Britain has officially protected conservation status, whether as Sites of Special Scientific Interest (SSSI), local Nature Reserves, or National Nature Reserves (NNR) (Burd, 1989).

Burd (1995) has described the saltmarsh sites in the United Kingdom in substantial detail. The total area of saltmarsh in the UK is 45,337 hectares, of which 71% (equivalent to 32,500 ha) is in England. A further 14.88% (equivalent to 6,748 ha) is in Scotland, 13.43% (equivalent to 6,089ha) in Wales, and 0.53% (equivalent to 239ha) in N. Ireland (Boorman, 2003). There are four dominant saltmarsh plant communities in Scotland which occur in varying proportions. Following the standard NVC classification (Rodwell et al., 2003), the first of these comprises one or both SM8 *Salicornia*/SM9 *Suaeda* communities (less abundant in the North). The second, SM10 *Puccinellia maritima*, community, is often the dominant vegetation on grazed saltmarshes. The third community is SM13, *Puccinellia Festuca*, and the fourth SM16 *Juncus gerardii* community. Large stands of the common

reed *Phragmites australis* also feature strongly in certain saltmarshes in South East Scotland, notably in the Tay Estuary saltmarshes (Burd, 1989).

As an example: in a recent study, Taubert and Murphy (2012) found that the vegetation present within a sample of Scottish saltmarshes (including both estuarine and sea loch sites) showed the three distinct vegetation zones characteristic of UK saltmarshes: (1) low marsh zone (pioneer zone) defined by soft sediments, seaweeds and a few specialist halophytes such as *Salicornia europaea* and *Puccinellia maritima*, (2) mid marsh zone (accretion zone) supporting common saltmarsh species with varying tolerance of salinity, such as *Festuca rubra, Juncus gerardii* and *Agrostis stolonifera*, and (3) upper marsh zone (mature zone) which contains species less tolerant to salt and regular submergence, such as *Elymus pycnanthus.*

1.2 Wetland Ecological Characteristics

Wetland ecosystems typically show three characteristic ecological conditions, all of which are potential stressors for plant survival and growth: periodic to continuous inundation or soil-saturation with fresh or saline water; soils that are periodically anoxic (hydric soils); and hydrosoils with rhizospheres experiencing periods of low or no oxygen availability (Craft 2005). The rooted emergent vegetation found in wetland habitats (hydrophytic vegetation) must therefore show adaptations enabling them to tolerate the stresses produced by such conditions. In addition, saltmarsh wetland plants must tolerate the osmotic stresses (which produce "physiological drought" in plant cells) produced by high salinity conditions, and which are combated by a variety of physiological adaptations involving exclusion, excretion, succulence and passive removal mechanisms (Crawford 1989).

The level of inundation, hydrosoil redox and pH are all environmental pressures, primarily affecting the edaphic (hydrosoil) habitat, which strongly influence plant survival in wetlands (Kennedy et al., 2006). Flooding is a compound stress, composed of interacting changes inside plant cells induced by the floodwater surrounding the plant (Perata et al., 2011). Plant tolerance to flooding and tissue anoxia varies widely. In response to the severity of flooding stress, terrestrial wetland species have developed a variety of strategies to resist flooding (Vartapetian and Jackson, 1997). A major constraint resulting from

excess water, at least for poorly adapted species, is an inadequate supply of oxygen to submerged tissues; diffusion of oxygen through water is 10,000 times slower than in air (Armstrong and Drew, 2002; Parent et al, 2008). The most important adaptations of plants to tolerate waterlogging in wetlands are the development of adventitious roots, which functionally replace basal roots (Parent et al., 2008). Some plants have specific adaptations, such as a capacity for anaerobic metabolism, oxygen transfer by aerenchyma, or avoidance of waterlogging using seeds or tubers (Toogood et al., 2008). In addition, one of the most important morphological adaptions to waterlogging is the development of lacunae gas spaces (aerenchyma) in the root cortex, which allows diffusion of air from leaves above the water surface down to submerged tissues (Parent et al., 2008; Jackson and Colmer, 2005).

Light is the primary source of energy for plants, and its availability may vary both within and between wetland habitats (Stuefer and Huber, 1998). Light availability explained a large part of the variation in the floristic composition of coastal wetlands (Kotowski et al., 2001). Changes in the spectral light quality had major effects on the size of modular structures (leaves, ramets), whereas changes in light quantity mainly affected their numbers (Stuefer and Huber, 1998). In herbaceous vegetation, light conditions for short species typically deteriorate over the course of the growing season, as tall dominant species build up their canopy (Edelkraut, Güsewell, 2006). Light limitation is often considered to be the mechanism excluding slow-growing, small plant species from productive or unmanaged grassland vegetation. The persistence of species in the lower canopy layers depends on their ability to tolerate low-light conditions, or to grow during periods with greater light availability (Stuefer and Huber 1998). Kotowski et al., (2001) analysed the relevance of light intensity in controlling the performance of a group of phanerogam species characteristic of sedge-moss fens. Where a tree canopy is present (as for example in fen woodland habitats, which characterise part of the area studied at Wicken Fen, Study Area 1 in the present work) shade impacts on ground-cover species may be substantial stresses for these wetland plants: most herbaceous fen species (with the exception of the tall reeds and similar species) can be classified as weak competitors for light. Some examples for shade-tolerance with Ellenberg's indicator values are *Mercurialis perennis* (3), medium shade- tolerance *Oxalis acetosella* (4), and open area *Typha latifolia* (8) (Hill et al., 1999).

The effect of grazing on wetland vegetation has been shown to be substantial in a *Phragmites australis*-dominated swamp/ wet grassland system (Vulink et al., 2000). *Phragmite*s has aerenchymatous roots well adapted to tolerate anaerobic conditions in the hydrosoil. Grazing or cutting of *Phragmites* stems at or below water-level cuts off the oxygen source for the roots, thus reducing their tolerance to the anaerobic conditions prevalent in the soft mud (Boorman and Fuller 1981). Grazing reduced the biomass of *Phragmites australis* and increased the stem densities of *Glyceria maxima*, resulting in a shift of dominance from *Phragmites* to *Glyceria* in Broadland, England (Ausden et al., 2005). In general terms, grazing increases the intensity of disturbance affecting wetland plants, which by definition are stress-tolerators (Grime 2001) and therefore have a limited genetic ability to build additional disturbance-tolerance traits (as evinced by the impacts of grazing on *Phragmites* outlined above). Grazing by herbivores such as cattle, sheep and horses is common on certain types of wetland (e.g. some saltmarsh habitats, see 1.1.2 above) and often used as a management measure, but grazing intensities are usually maintained only at a low level. Grazing has been shown to exert a considerable influence on the species composition of wetland vegetation, for example saltmarsh communities (Adam et al., 1988; Adam, 2002). Grazing (especially by larger animals, where its effect is exacerbated by trampling damage) tends to reduce the abundance of, or even eliminate species with low disturbance-tolerance characteristics, and encourage their replacement by plants with protected meristems (such as many grasses) or grazing-resistant adaptations (Andersen et al., 1990). For example, sheep grazing has been shown to have an impact on the composition and structure of saltmarsh vegetation in northern Germany: when grazing was stopped, a grass –dominated community (*Puccinellia maritima*) was rapidly replaced by a mixed forb community, with *Festuca rubra*, *Halimione portulacoides* and *Aster tripolium* (Kiehl et al., 1996).

The most important factors affecting species distribution in saltmarshes are salinity and aeration of the substrate, both of which critically influence the physiological ecology of marsh halophytes (Cooper, 1982). The availability of oxygen significantly affects plant growth, especially in the flood period saltmarsh, which affects germination, seedling growth in early stages, and root respiration (Silvestri et al., 2005). Saltmarsh plants have adopted different strategies in order to stay alive during periodic soil saturation -e.g. aerenchyma allows transport of oxygen from above-water tissues to the roots (Visser et al.,

2000) - and increased aboveground tissue pore volumes to store oxygen for respiration (Armstrong, 1982).

Saltmarsh sediments are protected from erosion by their vegetation cover; loss or weakening of the vegetation can initiate local erosion, which over time can expand to affect much larger areas (Adam, 2002). Erosion may be caused by wave action; damage may be initiated by a particular storm. In addition, in urban areas, the discharge of storm water into saltmarshes has resulted in the replacement of halophytic communities by assemblages more characteristic of brackish or freshwater marshes (Zedler et al. 1990). Table 1.2 below is shown a brief summary of wetland ecology characteristics.

Table 1-2: A brief summary of wetland ecology characteristics

Characteristic	Description
Wetland soils	Flooding, oxidation, aerobic decomposition, leaching and dehydration. The level of inundation, hydrosoil redox and pH are all environmental pressures, primarily affecting the edaphic habitat, which influence plant survival in the wetland.
Wetland hydrology	Water budgets are influenced by inflows and outflows of water, landscape, subsurface soil, and ground water; these are factors affecting the growth, development and survival of numerous plant species.
Wetland plants	Plants adaptations by morphological & anatomical changes: Physical changes in plant structure to transport oxygen to the roots. Such as, aerenchyma, adventitious roots, shallow root systems, root aeration, radial oxygen loss from roots storage of carbohydrate reserves, hypertrophied lenticels is a common change in many wood species during flooding. Metabolic adaptations: plants respond by shifting from aerobic metabolism to anaerobic metabolism, e.g. ethanol fermentation Enables wetland plants to maintain a high energy level.

1.3 Remote Sensing Approaches Used in Wetland Survey

The remote sensing options available to those concerned with wetlands' management have expanded considerably since the mid 1970s when aerial photography was almost exclusively used. Remote sensing satellite data have been applied to identify and study various wetland features such as tidal flats, lagoons, marshy vegetation, saltmarshes and saltpans. This data has also helped understand the spatial pattern, significance and extent, of wetlands to the local community (Bhuvaneswari et al. 2011), as well as identifying and monitoring them (Rani et al. 2011). Monitoring of wetlands status is increasingly seen as an important issue worldwide, because of their increasingly recognised role in ecosystem service provision, importance in maintaining human health and wellbeing, natural ecosystem biointegrity, and in carbon sequestration.

Typical of the current status of this wetland focus is the work of Dabrowska-Zielinska et al., (2009) who have applied multi-spectral remote sensing techniques to obtain data on changes in soil moisture and evapotranspiration for the management of wetlands in Poland. In wetland marshes of the Paraná River Delta in Argentina, similar procedures used radar remote sensing for water level evaluation, and to study and understand the basic interactions between the soil under different flood situations and the vegetation composition (Grings et al., 2009). Many types of remote sensing have been used to study wetlands worldwide: Prigent (2001) used satellite observation to find submerged wetlands; and Harris et al. (2005) have applied large-scale remote sensing methods to monitor near-surface peatland hydrological conditions, as well as to detect near-surface moisture stress in *Sphagnum* moss dominated habitats. In Finland, GIS and remote sensing tools have been used, combined with ground evaluations, to measure the effects of rehabilitation on the aquatic vegetation of a shallow eutrophic lake (Valta-Hulkkonen et al., 2004), whereas Mattikalli (1995) applied remote sensing and GIS to detect the landuse change of the River Glen catchments in England by acquiring data from 1931 to 1989. These techniques have also been used for detection of the landuse and landcover change in the Kainji lake Basin, Nigeria (Ikusemoran, 2009). Landsat (TM) images have been used to create a classification of the vegetation community types and plant community structure in the lower Roanoke River floodplain of north eastern North Carolina, USA (Townsend and Walsh, 2001), and for classifying coastal wetland vegetation classes in Yancheng National Nature Reserve (YNNR), China (Zhang et al., 2011); similar techniques, but with high

resolution QuickBird imagery, were used to produce a wetland typology map in the west Siberian wetlands (Peregon et al., 2009).

Meteorological satellies (GOES) and early LANDSAT imaging systems represent low spatial resolution (4000m-80m), but over the decades satellite-borne platforms have captured imagery with spatial resolutions ranging from several hundred metres to less than one metre, using passive (optical) sensors. A similar spatial resolution range is available from satellite-borne active (radar) sensors, but these products are less popular.

Turning to spectral resolution, typically space-borne passive sensors have had a spectral resolution of about 0.1microns, particularly in the visible and near-visible part of the electro-magnetic spectrum. However, the space-borne Hyperion sensor has offered a spectral resolution of about 0.01 microns, although this imagery is not universally available; such imagery is referred to as hyperspectral.
The distinctions identified above are also to be found in imagery captured from air-borne platforms, but the emphasis is on panchromatic or infrared photography and hyperspectral imagery, for the passive sensors, and radar and LiDAR for the active sensors.

The interpretation of all these different image products is enhanced when integrated with other geospatial information, this integration being particularly enabled through GIS technology. Many wetland management projects integrate processed remote sensing imagery with geospatial data in the GIS environment.

In the following sections, projects directed towards wetland management are considered under the headings:

1. Low/Medium Spatial Resolution Optical Systems;
2. High Spatial Resolution Optical Systems;
3. Hyperspectral Systems;
4. Active Systems (RADAR, SAR and LiDAR);
5. Air Photography; and,
6. GIS procedures using imagery

1.3.1 Low/Medium Spatial Resolution Optical Systems

Low spatial resolution is defined, for convenience, as images of the earth's surface at ground resolutions >50 meters; and medium resolution as > 5 meters and < 50 meters. (High spatial resolution imagery is dealt with in the next section, having resolutions of 5m or less). Low and medium spatial resolution remote sensing Earth Observation (EO) data have been used as a tool to aid the management and conservation of wetland habitats (Jones, 2009), primarily by mapping and managing wetlands, as well as for inventory assessment and monitoring (Mackay et al., 2009).

Medium resolution (30 meters) Landsat (ETM+) imagery combined with ancillary topographic and soil data have been used to map wetland and riparian systems in the Gallatin valley of South West Montana (Baker et al., 2006). To discover seasonal change, and for mapping the inundation of wetlands, Landsat (TM and ETM+) satellite imagery has been used in Uganda (Owor et al., 2007), while the same imagery combined with GIS was applied for the analysis of ecosystem decline along the River Niger Basin (Twumasi and Merem, 2007). This study also used this approach to aid riverine ecosystem management, and to compute the nature of change in the riverine environment. Landsat 5 Thematic Mapper (TM) data has been integrated with airborne hypersepctral date from the Daedalus 1268 Airborne Thematic Mapper (ATM) data, and used to map the extent of the intertidal zone in the Wash Estuary, in eastern England (Reid Thomas et al. 1995).
Low resolution satellite data have been used to map extensive wetland ecosystems: for example to obtain information on the status of aquatic vegetation and the turbidity of lake water in Punjab, India (Chopra et al., 2001). In addition, Castañeda and Ducrot (2009) used low resolution Landsat and SAR imagery for mapping land cover of wetland areas.

In peatlands, one of the most widespread wetland types (at least in the northern hemisphere), satellite sensor procedures such as Landsat (MSS, TM, ETM+ or SPOT HRV) have been used in wetland mapping for many years (Yang, 2005). The Moderate Resolution Imaging Spectroradiometer (MODIS) has been applied to map the distribution and extent of peatlands in the St. Petersburg region in Russia (Pflugmacher et al., 2007).

To analyse several ecological factors of wetlands, such as light availability, the very low (4km) resolution GOES (Geostationary Operational Environmental Satellite) weather satellite imagery and ancillary surface and atmospheric data have been used to estimate solar radiation and emergent wetland evapotranspiration in Florida, USA (Jacobs, 2004).

Medium resolution Landsat (ETM+) imagery has been used to detect and map isolated wetlands (Frohn et al., 2009); for the classification of land cover in Trabzon city (Kahya et al., 2010); and, for mapping coastal saltmarsh habitats in North Norfolk, UK (Sanchez-Hernandez et al., 2007). The same technique has been applied (combined with field survey data) to generate information on wetland resources, conservation management issues, and mapping of wetlands in the lower Mekong Basin (MacAlister and Mahaxay, 2009). Finally medium resolution Landsat, (TM and ETM+) images have been used for analysing and classifying an area covering the Sudd wetland, in the Nile swamps of southern Sudan (Soliman and Soussa, 2011).

1.3.2 High Spatial Resolution Optical Systems

Turning to high spatial resolution imagery, this is defined as images of the earth's surface at ground resolutions of less than or equal to 5 meters. Although the most recent satellite borne sensors (i.e. IKONOS, Quickbird) produce imagery of high spatial resolution, and recent sensors in the Landsat series and SPOT series have high resolutions, such resolution has traditionally been achieved from airborne platforms. The advances in the technology of remote sensing, resulting in high resolution imagery (IKONOS, with 1m to 4m resolution and Quickbird, with 0.6m to 2.8m resolution) have permitted better detection of environmental indicators, such as natural vegetation cover, wetland biomass change and water turbidity, as well as wetland loss and fragmentation.

High resolution satellite imagery may be the only image data used in a project. One study used high spatial resolution Quickbird imagery for the identification and mapping of submerged plants in Lake Mogan, which is located in central Anatolia, Turkey (Dogan, 2009). High resolution imagery (combined with the necessary ground truth measurements) was used to produce land-use/cover classification and a Normalized Differential Vegetation Index (NDVI) mapping for the Kelantan Delta, East Coast of Peninsular

Malaysia (Satyanarayana et al., 2011). QuickBird imagery was used for land cover classification and mapping plant communities in the Hudson River National Estuarine Research Reserve (NERR), New York, USA (Laba et al., 2008). Quickbird images with very high resolution (VHR) 0.61 m have been used for discrimination and mapping of saltmarsh vegetation in the Dongtan wetlands of Chongming Island, China (Ouyang et al., 2011). Another study used high resolution Quickbird data combined with medium resolution airborne laser altimetry (LiDAR) to determine plant production and the effect of land cover on gross primary production (GPP) and net primary production (NPP) in the Great Lakes region of North America (Cook et al., 2009).

High spatial resolution IKONOS satellite imagery combined with ground-based optical data was used for monitoring shallow inundated aquatic habitats in the Sound of Eriskay Scotland, UK (Malthus et al., 2003). IKONOS imagery has been used for vegetation composition mapping and estimation of green biomass in three riparian marshes in Ontario (Dillabaugh and King, 2008), and combined with airborne LiDAR altimetry data for coastal classification mapping (Lee and Shan, 2003). IKONOS high-resolution satellite imagery has been used for classification of coastal high marsh vegetation (seasonally inundated) into four classes (meadow/shrub, emergent, senescent vegetation, and rock) along the eastern shoreline of Georgian Bay, Ontario, Canada (Rokitnick-Wojcik et al. 2011). It is worth noting that the same classification was achieved using lower resolution Landsat ETM+ imagery for monitoring the changes in coastal wetlands in Chesapeake Bay, USA (Klemas, 2011).

High resolution Thematic Mapper satellite image (TM) data have been used to understand saltmarsh ecosystem function and species distribution, while canopy water content has been estimated by using Airborne Advanced Visible Infrared Imaging Spectrometer data in saltmarshes along the Petaluma River, California (Zhang et al., 1997). The same approach has also been applied, combining ETM+ images in conjunction with field observations, for the delineation and functional status monitoring of the saline wetlands, or "saladas", of the Monegros Desert, in northeast Spain (Herrero and Castañeda, 2009). In order to identify and map wetland change Zhang et al. (2009) applied high resolution Landsat MSS and TM remote sensing images in China, and this approach has also been used (combined with ETM+) for determining changes in land use in Datong basin, China (Sun et al, 2009).

High resolution Landsat Enhanced Thematic Mapper (ETM+) has been applied to classification of land cover in the Lena Delta, North Siberia (Ulrich et al., 2009), and Landsat data (TM and ETM+) imagery and multi resolution JERS-1 Synthetic Aperture Radar (SAR) data have been used to map wetlands in the Congo Basin (Bwangoy et al., 2010). High resolution Landsat Multispectral Scanner (MSS) and Thematic Mapper (TM) have been used to distinguish between saltmarsh and non – saltmarsh vegetation, and non-vegetated surfaces in the Wash, England (Hobbs and Shennan, 1986). Satellite imagery Landsat Thematic Mapper (TM) images have also been applied for mapping salt-marsh vegetation communities and sediment distribution in the Wash estuary, England (Donoghue and Shennan, 1987). More recently, it has been used with IRS 1C LISS 3 for mapping the inter-tidal habitats of the Wash (Donoghue and Mironnet, 2002).

Landsat Thematic Mapper (TM) combined with SPOT Satellite Imagery were used for mapping wetland species in the Coeur d'Alene floodplain in northern Idaho (Roberts and Gessler, 2000).

Imagery from high resolution satellite-borne sensing systems may also be integrated with similarly high resolution data from airborne platforms. A high resolution multispectral-structural approach, using IKONOS and airborne LiDAR data, has successfully mapped peatland conditions (Anderson et al., 2010), and the same tools have been used to map and distinguish types of wetland (Maxa and Bolstad, 2009). High resolution remote sensing has also been used to monitor environmental indicators, such as changes in land cover/use, riparian buffers, shoreline and wetlands (Klemas, 2001).

Another integration, that of high resolution multispectral SPOT-5 images with high spectral resolution multispectral Hyperion imagery and data from the multispectral infrared visible imagine spectrometer (MIVIS) data, has been used to map land cover and vegetation diversity in a fragmented ecosystem in Pollino National Park, Italy (Pignatti et al., 2009), and applied to monitor wetland vegetation in the Rhône delta near the Mediterranean, in southern France (Davranche et al., 2010).

High resolution QuickBird satellite images integrated with LiDAR data have been applied for classification and mapping wetland vegetation of the Ragged Rock Creek marsh, near tidal Connecticut River (Gilmore et al., 2008), and have also been applied to determine land cover types and riparian biophysical parameters in the Fitzroy catchment in

Queensland, Australia (Arroyo et al., 2010). High resolution airborne Light Detection and Ranging (LiDAR) data have been applied for detection and mapping inundation of land under the forest canopy in Choptank River USA (Lang et al., 2009), and combined with QuickBird for mapping upland swamp boundaries, and classification of vegetation communities in swamps on the Woronora Plateau, Australia (Jenkins and Frazier, 2010). The same technique has been applied to understand and map mangrove construction wetlands in southeast Queensland, Australia (Knight et al., 2009), and also been used (combined with multispectral imagery) to classify vegetation of rangeland in the Aspen Parkland of western Canada (Bork and Su, 2007).

High resolution Landsat Thematic Mapper (TM) and RADARSAT-1 image data have been integrated to study and map the wetland impact and renewal of forest from Hurricane Katrina, in the Louisiana-Mississippi coastal region of the USA (Ramsey et al., 2009).
Various types of high resolution remote sensing, including LiDAR, Radar altimetric, Landsat, TM and SPOT have been applied for analyses of riverine landscapes, such as water bodies connectivity and habitat communities (Mertes, 2002), with Landsat (TM) used to calculate the relationship between river flow and wetland inundation of the mid-Murrumbidgee River, Australia (Frazier and Page, 2009). It has also has been used for classifying coastal wetland vegetation classes in Yancheng National Nature Reserve (YNNR), China (Zhang et al., 2011).

From the foregoing, it can be seen that high spatial resolution imagery obtained from satellite and airborne sensors have become increasingly available in recent years.

1.3.3 Hyperspectral Systems

Airborne platforms are usually used to gather hyperspectral data. Hirano et al. (2003) used the hyperspectral Airborne Visible/Infrared Imaging Spectrometer (AVIRIS) with 224 spectral bands and 20m spatial resolution for mapping wetland vegetation in the Everglades National Park, Florida, USA.

The high spectral resolution Airborne Thematic Mapper (ATM) has been applied to obtain hydrological information within peatland. For example, it has been used to map the effects of water stress on *Sphagnum* spp. along the Welsh coast, using *Sphagnum* mosses as an indicator for peatland near-surface hydrology, since natural wetlands play an important role in ground water recharge and in controlling flooding (Harris et al., 2006, 2009). This approach has also been applied for mapping the distribution of aquatic macrophyte species in Cefni Reservoir on the Isle of Anglesey (Malthus and George, 1997). The same techniques combined with ground - based measurement have been used for monitoring ditch water levels of the Elmley Marshes in southeast England (Al-Khudhairy et al., 2001).

Zomer et al. (2009) used PROBE-1 airborne hyperspectral data for mapping and monitoring plant species, and the distribution of vegetation community types. A hyperspectral imaging sensor has been used to examine the evolution of wetland distribution and land coverage in monitoring of coastal wetlands (Burducci, 2008), and for identification, classification, and mapping of submerged aquatic vegetation (SAV) in the tidal Potomac River, USA (Williams et al., 2003).

The hyperspectral Compact Airborne Spectrographic Imager (CASI) and a Daedalus Airborne Thematic Mapper (ATM) have been used to provide high-resolution remote sensing data, combined with Landsat TM images, for monitoring and determination of the amount of surface water in a wetland catchment in the north Kent marshes in England (Shepherd et al., 2000). CASI has also been used to identify and map seasonal intertidal vegetation patterns in back barrier environments on the North Norfolk coast, England, UK (Smith et al., 1998), and for mapping of intertidal sediment types and saltmarshes from the Humber Estuary to North Norfolk, in eastern England, (Thomson et al., 2003). The same technique has been used in conjunction with Airborne Laser Terrain Mapper (ALTM) data for mapping the extent of coastal vegetation classes and classification of coastal habitats in the Essex Tollesbury saltmarshes (eastern England) and Ainsdale sand dunes in north west England (Brown, 2004).

Hyperspectral remote sensing data may be integrated with multispectral infrared and visible imaging spectrometer (MIVIS) data to assess the relationship between vegetation

patterns and saltmarsh morphology, and also to infer saltmarsh morphologic characteristics from vegetation mapping, in the San Lorenzo saltmarsh in the Venice lagoon, Italy (Silvestri et al., 2003). In the same location, high resolution multispectral and hyperspectral remote sensing data, accompanied by field observations, were used for mapping lagoon salt-marsh vegetation (Belluco et al., 2006), for discrimination and mapping wetland vegetation, as well as for estimating some biophysical and biochemical properties of wetland vegetation (Adam et al., 2010). The hyperspectral sensor Compact Airborne Spectral Imager (CASI) imagery has also been applied for mapping mixed vegetation communities within these saltmarshes (Wang et al., 2007).

Also, as mentioned in section 1.3.1, Landsat 5 Thematic Mapper (TM) data has been integrated with airborne hypersepctral date from the Daedalus 1268 Airborne Thematic Mapper (ATM) data and used to map the extent of the intertidal zone in the Wash Estuary, in eastern England (Reid Thomas et al. 1995).

1.3.4 Active Systems (RADAR and LiDAR)

An example of the use of radar imagery involves low resolution RADARSAT imagery, for the identification, description and mapping of wetland habitat types in Greece (Alexandridis et al., 2009). For classification of wetlands, Polarimetric RADARSAT-2 satellite imagery (with a spatial resolution of 8m) has been used in the Mer Bleue wetland, east of Ottawa, to characterise wetland vegetation species. Using this approach, it proved possible to differentiate types of wetland plant communities, such as shrub bog, sedge fen, conifer-dominated treed bog, and highland deciduous forest, under leafy status (Touzi et al., 2007).

Satellite radar imagery from ENVISAT ASAR (the Advanced Synthetic Aperture Radar instrument with 25m spatial resolution)) was used for monitoring inland boreal and sub-arctic environments, to identify inundation patterns and soil moisture change over different hydro-periods, and applied to categorise wetlands (Bartsch et al., 2007). The same approach was used for management and monitoring of wetlands, especially permafrost transition zones, where peatlands form one of the major land cover types (Bartsch et al.,

2009). ENVISAT ASAR Global Mode images have been used to monitor the dynamics of river flow and wetland areas as a response to precipitation and soil moisture variation respectively, in the upper Okavango basin and delta, Botswana (Bartsch et al., 2008).

High resolution L-band Synthetic Aperture Rader (SAR) data have been used to detect surface level changes in the Everglades wetlands in south Florida (Wdowinski et al., 2008).

Airborne Light Detection and Ranging (LiDAR) data have been used for classification of vegetation and determination of vegetation height, in Lake Hatchineha in Florida, USA (Genc et al., 2004).
High resolution LiDAR data have been applied to detect intertidal vegetation, to assess saltmarsh zonation, and to map intertidal habitats and their adjacent coastal areas in the Gulf of St. Lawrence, Canada (Collin et al., 2010), as well as for mapping coastal flooding hazard and evaluation of coastal flooding induced by surges in Cádiz Bay (SW Spain) (Raji et al., 2011). Multispectral imagery with LiDAR and GIS have been applied to carry out a geomorphological analysis of the distribution of saltmarsh features at the Great Marsh, Massachusetts, USA (Millette et al., 2010), and to model inundation and radiation characteristics within an intertidal zone located in the Minas Basin (Bay of Fundy, Nova Scotia, Canada: location of one of the biggest tidal amplitudes on Earth) (Crowell et al., 2011).

LiDAR data may be used with other DTMs. For example, high resolution LiDAR techniques combined with Global Positioning Systems (GPS) permitted accurate topographic and bathymetric mapping, including shoreline positions, in the study undertaken by Klemas (2009). Additionally, high-resolution LiDAR and Digital Terrain Models (DTM) have been used to map coastal and estuarine habitats, as well as for characterisation and monitoring of coastal environments, in the Bidasoa estuary, northern Spain (Chust et al., 2008).

LiDAR data captured from airborne platforms may be integrated with hyperspectral data from the same platforms. High resolution (LiDAR) imagery combined with high resolution

hyper-spectral imagery (CASI) has been combined with field survey to monitor hydromorphology ingredients as a component of the ecological status of river, shoreline, and estuarine habitats in the Forth Estuary, Scotland (Gilvear et al., 2004); and also applied to identify and describe stream and physical riparian habitat, in South Fork Humboldt River, Nevada, USA (Hall et al., 2009). Hyperspectral datasets and LiDAR have been used for mapping and distinguishing reedbed from surrounding vegetation types, in Cumbria, UK (Onojeghuo and Blackburn, 2011).

LiDAR has been applied for mapping elevations of tidal wetland restoration sites, and for comparing the accuracy of aerial LiDAR data with that from a singlebeam echosounder system, in the San Francisco Bay estuary, California (Athearn et al., 2010). Also, high-resolution airborne imaging spectroscopy and LiDAR have been used to map and classify the saltmarsh, mud flats and riverbank vegetation in the Scheldt basin in northern Belgium (Bertels et al., 2011).

High resolution LiDAR and GIS have been applied to inventory important wetland hydrogeomorphic features (area, volume, catchment area, hydroperiod) and structural attributes (soil, vegetation, land use) in the coastal prairie wetlands surrounding Galveston Bay, Texas, USA (Enwright et al., 2011).

1.3.5 Aerial Photography

Application of aerial photography in the coastal zone has a long history, including the study of coral reefs in the East Indies in the early part of the twentieth century. Throughout the same period in Germany, aerial photographs were being used for mapping coastlines (Baily and Nowell, 1996). Between 1973 and 1998, aerial photographs at 1:5000 scale were used, to monitor, map and quantify saltmarsh change along 440km of shoreline within the county of Essex, south-east England (Cooper et al., 2001), and have also been applied combined with Airborne Thematic Mapper (ATM) to determine vegetation change in saltmarsh communities of the Dee estuary, northwest England (Huckle et al., 2004). High resolution aerial photographs have been used for discriminating and mapping all coastal, lowland and upland habitats in Wales (Lucas et al., 2011), and to map and identify

vegetation communities on Bullo River Station, Northern Territory, Australia (Lewis and Phinn, 2011).

High spatial resolution colour-infrared aerial photography has been used to detect the change in vegetation over time in a variable tidal marsh environment, and restoring of tidal marsh in Petaluma River Marsh (Carl's Marsh) in California, USA (Tuxen, 2008), as well as to identify vegetation types present on a sub-tropical coastal saltmarsh in southeast Queensland, Australia (Dale et al. 1986).

Remote sensing using digital aerial photos has been applied to classify the Lakkasuo peatland ecosystem in Southern Finland (Huang and Sheng, 2005).

1.3.6 GIS Procedures Using Imagery

Although GIS techniques have been applied to estimate the contemporary extent of important wetlands (peatlands) in Ireland from soil and land cover maps dating from the 1970s, 1980s, and 1990s (Connolly et al., 2007), Remote Sensing (RS) integrated with the Geographic Information System (GIS) are now providing new tools for advanced ecosystem management, at local, regional and global scales over time (Zubair, 2006). Remote sensing technology and GIS are considered useful tools in analysing complex ecosystem problems.

High resolution remote sensing Landsat (TM) images and GIS have been used to determine the real extent of the cover and rate of change in wetland in Kuala Terengganu in Malaysia (Ibrahim and Jusoff, 2009). Mentioned above in section 1.3.1 is a project mapping ecosystem decline along the River Niger Basin, which integrated Landsat (TM and ETM+) satellite imagery with GIS facilities (Twumasi and Merem, 2007).

In South Carolina, United States, satellite images (medium resolution Landsat) and aerial photographs combined with GIS have been used to obtain spatial information and assess

temporal changes affecting the function and structure of wetlands over large geographic areas (Mironga, 2004).

This technique of using medium resolution remote sensing data in combination with GIS is common. It has been applied to describe the condition of wetlands along the coastline of Sri Lanka in relation to trends in land use arising from changes in agriculture and sedimentation (Rebelo et al., 2009). Identical techniques have been applied to classify and map the plant communities of wetlands in the Prairie Pothole Region of Central North Dakota (Mita et al., 2007). Medium resolution remote sensing and GIS tools have been used for habitat and species mapping, land change detection and monitoring of conservation areas (De Roeck et al., 2008), for example to acquire data on land cover/use changes, and to determine the main environmental factors affecting these changes in Lake Cheimaditida, located in Northern Greece (Papastergiadou et al., 2008).

It may seem self-evident that higher resolution imagery will provide better results. However, it can be suggested that this comes at a cost, and is not universally available. Acknowledging that higher resolution imagery is likely to provide more information, it is also useful to consider what might be adequate. Internationally there are thousands of wetlands sites to be protected, and a first step in that protection is change monitoring. Currently, Libya has almost forty coastal wetland sites (EGA-RAC/SPA, 2012) a large number of which are unprotected (Flink, 2013). To determine whether they need protection requires change monitoring. The Ramsar Convention Seretariat has published guidelines for monitoring wetlands, and the use of medium resolution imagery is supported (Lowry, 2010). Part of the research reported in this thesis will investigate whether medium resolution satellite imagery is indeed adequate for wetlands monitoring, through two British examples. Resolution is one constraint on the use of satellite imagery, but availability is another. Availability reflects price and supply. Many high resolution sensors on Earth orbiting platforms could supply data on anywhere on the Earth's surface every 2-3 weeks, or more frequently, at a price. The low cost (or no cost) suppliers exhibit some constraints; For example if they are providing free data, they may only supply imagery of a limited coverage, often only of their home nation (for example the UK's Landmap service or Canada's GeoGRATIS service); otherwise there is a charge. An exception is the GLOVIS service of the USGS. At no cost to the recipient, several decades of medium and low resolution Landsat images are available. Certainly, medium resolution data for monitoring wetlands anywhere in the world is available from this source.

As it seems that success can be achieved with medium resolution imagery (Lowry, 2010) in the context of wetlands management, and as GIS is now becoming an increasingly important management tool, the combination of low cost and universally available medium resolution imagery with GIS is attractive to those concerned with the issue. This is an important data processing environment investigated in this study.

1.4 Application of Remote Sensing Techniques on Wetland studies in the UK

A variety of remote sensing techniques have been used in the UK. Those with the longer history have involved aerial photos, but more recently successful projects have involved low, medium, and high resolution satellite imagery. Aerial photographs at 1:500 scale were used for monitoring, mapping and to quantify saltmarsh change along 440km of shoreline within the county of Essex between 1973 and 1998, southeast England (Cooper et al., 2001). High resolution aerial photographs have been applied to discriminate and map all coastal, lowland and upland habitats in Wales (Lucas et al., 2011), and also have been combined with Airborne Thematic Mapper (ATM) to determine vegetation change in salt marsh communities of the Dee estuary, northwest England, (Huckle et al., 2004). Aerial photography combined with the ground survey have been used to compare the results obtained from Landsat MSS imagery for peat detection and classification, in Cumbria, UK (Cox, 1992). Aerial photography has been formed to the very reliable, but is with increase analysis expensive.

Less expensive low / medium resolution remote-sensing data from (1984 to 1989) and GIS have been used for monitoring of land use change in the River Glen catchments in England (Mattikalli, 1995). Reid Thomas et al. (1995) have used Landsat 5 Thematic Mapper (TM) data combined with airborne hypersepctral date from the Daedalus 1268 Airborne Thematic Mapper (ATM) data to map the extent of the intertidal zone in the Wash Estuary, in eastern England. Medium resolution Landsat (ETM+) imagery has been used for mapping coastal saltmarsh habitats in North Norfolk, UK (Sanchez-Hernandez et al., 2007), also medium resolution Landsat 5 Thematic Mapper data and GIS have been used for a comprehensive survey of land cover, classification, and produce land cover map (LCM2000) for UK habitats (Fuller et al. 2005). The reliability of these approaches depends very much on the quality of ground truth available.

Better results might be expected with higher resolution, but expensive, data sets now becoming available. In the Sound of Eriskay Scotland, high spatial resolution IKONOS satellite imagery combined with ground-based optical data was used for monitoring shallow inundated aquatic habitats (Malthus and Karpouzli, 2003). High resolution Landsat (MSS) and (TM) images have been applied in the Wash, England to distinguish between salt marsh and non – salt marsh vegetation, and non-vegetated surfaces (Hobbs and Shennan, 1986). Donoghue and Shennan (1987) have used high resolution Landsat Multispectral Scanner (MSS) and Thematic Mapper (TM) to distinguish between salt marsh and non – salt marsh vegetation, and non-vegetated surfaces in the Wash, England. More recently, the same technique has been used with IRS 1C LISS 3 for mapping the inter-tidal habitats of the Wash (Donoghue and Mironnet, 2002). Multi-temporal satellite imagery (TM and ETM+) have been used for mapping and monitoring of habitats and agricultural land cover in Berwyn Mountains, North Wales, UK (Lucas et al., 2007).

Considering hyperspectral data, rather than multispectral, the high-resolution Daedalus Airborne Thematic Mapper (ATM) has been used for monitoring the distribution of aquatic macrophyte species in Cefni Reservoir, Anglesey, UK (Malthus and George, 1997). High-resolution remote sensing data (The hyperspectral Compact Airborne Spectrographic Imager (CASI) and a Daedalus Airborne Thematic Mapper (ATM)) combined with Landsat TM images have been used to monitor and determine of the amount of surface water in a wetland catchment in the north Kent marshes in England (Shepherd et al., 2000).

Thomson et al. (2003) have reported on the application of the hyperspectral Compact Airborne Spectrographic Imager (CASI) for mapping intertidal sediment types and saltmarshes from the Humber Estuary to North Norfolk in eastern England, and also CASI has been used to identify and map seasonal intertidal vegetation patterns in back barrier environments on the North Norfolk coast, England, UK (Smith et al., 1998). The same technique and (LiDAR) combined with field survey for monitoring hydromorphology ingredients as a component of the ecological status of river, shoreline, and estuarine habitats in the Forth Estuary, Scotland (Gilvear et al., 2004). Multi-spectral remotely sensed data (aerial photos and ATM) and LIDAR have been applied for mapping individual tree location, height and species broadleaved deciduous forest in the New Forest, southern England , UK (Koukoulas and Blackburn, 2005).

1.5 Ecological Factors

Remote sensing and GIS techniques offer advantages for monitoring wetland resources and provide information on wetlands. The techniques aid the detection of several ecological factors in wetlands, such as light-availability, evaporation and soil condition. The review in the following sections does not measure and assess these factors themselves, but rather explains how RS and GIS techniques can be used to do so.

1.5.1 Water Level

Radar remote sensing has been used to determine water level in wetland marshes of the Paraná River Delta in Argentina. It is based on the analysis of satellite images, taken at different places, to observe different flood situations and the composition of vegetation (Grings et al., 2009). Satellite images and GIS tools have been used, in combination with chemical and physical water analysis, to examine the impact of land use activities on vegetation cover and water quality in the Lake Victoria Basin (Twesigye et al., 2011); also, satellite images combined with ancillary ground truth data have been used for the management of water body resources in Lake Victoria (Cavalli, 2009). As already mentioned, satellite imagery, such as Landsat (TM) data, have been used for mapping lake water quality in Lake Erken, Sweden (Östlund et al., 2001), and have been also applied combined with ground truth data, to compute water turbidity and depth (Bustamante, 2009).

Multi-temporal Landsat Thematic Mapper (TM) imagery and ground – based measurement have been applied to monitor the ditch water levels of the Elmley Marshes, in southeast England (Al-Khudhairy et al., 2001); also, satellite images were used to monitor the water spread and aquatic vegetation status (and turbidity) of the Harike wetland ecosystem in the Punjab, India (Chopra et al., 2001). Along the Welsh coast, Harris et al. (2006) have applied airborne remote sensing to obtain hydrological information within peatlands, as well as to map the effects of water stress on *Sphagnum* moss. In addition, Synthetic Aperture Radar (SAR) data have been used to detect surface level changes in the Everglades wetlands, in southern Florida (Wdowinski et al., 2008), and to measure water level changes in an Amazon lake (Alsdorf et al., 2001), as well as in Amazon floodplain

habitats (Alsdorf et al., 2001). Satellite imagery (ENVISAT) has been used for monitoring and analysing water stage measurement in river and wetlands in the Amazon basin (Santos Da Silva et al., 2012).

Interferometric Synthetic Aperture Radar (InSAR) has been used for detecting water level changes in various wetlands environments around the world, including the Everglades (south Florida), the Louisiana Coast (southern USA), Chesapeake Bay (eastern USA), Pantanal wetlands of Brazil, Okavango Delta (Botswana), and the Lena Delta (Siberia) (Wdowinski et al., 2006), as well as for mapping water level changes in coastal wetlands in north China (Chou et al., 2010). The same technique has been applied for multi-temporal monitoring of wetland water levels in the Florida Everglads (Hong et al. 2010), and has also been used, combined with Radarsat-1 imagery, to map water level changes of coastal wetlands of southeastern Louisiana (Lu and Kwoun 2008).

Medium Resolution Imaging Spectrometer (MERIS) images have been used to monitor water quality in some large European lakes, Vänern and Vätter in Sweden, and Peipsi in Estonia/ Russia (Alikas and Reinart, 2008), and LiDAR data have been applied to calculate isolated wetland water storage capacity in north central Florida (Lane and D'Amico, 2010). Aerial photography and satellite imagery have been applied for study of frequent changes in water bodies and vegetation cover in Cheyenne Bottoms wetland, Kansas, USA (Owens et al., 2011).

1.5.2 Soil Condition

Advanced technologies of remote sensing provide an opportunity for studying hydrological changes in wetlands, especially peatlands, because *Sphagnum* mosses which characterise peatland vegetation, are very sensitive to changes in moisture availability. Harris et al. (2005) have applied remote sensing methods for monitoring near-surface peatland hydrological conditions, and detecting near-surface moisture stress in *Sphagnum* moss. Dabrowska-Zielinska et al. (2009) used remote sensing with various bands to obtain changes of soil moisture and evapotranspiration for management of wetlands in Poland; this technique has also been used for estimation of evaporation and soil moisture storage in the swamps of the upper Nile (Mohamed et al., 2004). Radar remote sensing (high

temporal resolution of ENVISAT ASAR WS data) has been used to observe the sensitivity of soil humidity and changes in water surface area of wetland in central Siberia (Bartsch et al., 2004). The same technique has been applied for mapping and monitoring soil moisture in wetland Biebrza National Park, Poland (Dabrowska-Zielinska et al., 2010). ENVISAT ASAR Global Mode has been used to monitor the dynamics of river discharge or inundated areas as a response to precipitation and soil moisture variation in the upper Okavango basin (Bartsch et al., 2008), and has also been used, in combination with multi-temporal C-band SAR data C-HH and C-VV from ERS-2, for investigation of inundations and soil moisture determination in Coastal Plain forested wetlands in the Mid-Atlantic Region, USA (Lang et al., 2008).

1.5.3 Light Availability

Recently developed remote sensing techniques have been used for the detection of several ecological factors in wetlands, such as light-availability, evaporation, etc. GOES satellite imagery and ancillary surface and atmospheric data have been used to estimate solar radiation and emergent wetland evapotranspiration in Florida, USA (Jacobs, 2004). For most wetlands, the rate of evapotranspiration (ET) is an important component of the wetland water cycle and often the main vector of moisture loss, especially in warmer lower latitudes. High resolution SPOT satellite image and MODIS data (MODerate-resolution Imaging Spectroradiometer) have been used to estimate evapotranspiration, humidity, and solar radiation in the Yellow River Delta wetlands of China (Jia et al., 2009). In addition, Spectral information from NOAA AVHRR data have been used to estimate water evaporation and transpiration in wetlands in Florida, USA (Chen et al., 2002). Remote sensing data (Airborne Hyperspectral Scanner AHS) has been applied to estimate evapotranspiration in the Doode Bemde Wetland in Belgium (Palmans and Batelaan, 2009), while Landsat 7/ETM+ remote sensing images have been used for estimation of evapotranspiration in Yellow River Delta Wetland, China (Li et al., 2011), and in the Nansi Lake wetland of China (Sun et al., 2011).

1.6 Aims of the Study

The aim of the study is to investigate the proposal that vegetation changes over time (e.g. scrub invasion; successional changes) have an effect on wetland plant community structure in UK wetland systems, which can be detected and quantified using remote sensing imagery. This proposed approach combines remote-sensing analysis of imagery over time with ground truth of existing wetland vegetation communities at two contrasting wetland sites in the UK.

The specific objectives of the study are:

- To assess the value of using differing forms of remote sensing imagery in the mapping and monitoring of spatial and temporal variation in wetland vegetation, with a particular view to developing procedures which can be transferred to Libya.
- To evaluate procedures by investigating temporal wetland plant community change at two contrasting UK locations by combining analysis of remote sensing data and the use of GIS techniques.

Chapter 2- Methodology

2

Selection of study areas

The study areas (Wicken Fen & Caerlaverock Reserve) were selected primarily because of their contrasting vegetation types, and also because of:

- The availability of aerial photographs and satellite images in past periods for comparison with recent images.
- The availability of previous references and studies of the plant communities in these areas, which helped in the detection of change that has happened in this area, using remote sensing techniques.
- The resemblance of the sites to wetland sites found in the author's homeland, Libya.

2.1 Aerial Photographs

Aerial photography was the first remote sensing method to be employed for mapping wetland vegetation; it is most useful for detailed wetland mapping, because of its minimum mapping unit (MMU) size (e.g. Seher and Tueller 1973; Shima et al. 1976; Howland 1980; Lehmann and Lachavanne 1997). Additionally, low-level photography, using helicopters or unmanned aerial vehicles (UAVs) can provide even smaller MMUs.

Aerial photographs at high resolution (0.25 m) of Study Area 1 (Wicken Fen) were obtained for this research from the UK Aerial Photos Database for 2009. These were received as JPEG files, of 4000 × 4000 pixels. For Wicken Fen, 1985, panchromatic images were received as JPEG files, 8267 × 8267 pixels. These Wicken Fen images were of a very flat area, and were directly taken in to ArcGIS. For Study Area 2 (Caerlaverock Reserve), aerial photographs in the form of orthophotos at high resolution (0.5m) were obtained from the UK Blue Sky for 2009, as a JPEG 11310 × 17310 pixels. Caerlaverock aerial photos for 1988, in panchromatic form were received in PNG format, 2845 × 2840 pixels. These were used to create an orthophoto in SOCET. The aerial photograph images were geometrically corrected and geocoded to the UK national grid co-ordinate systems

using the 2-D affine transformation facility available in ArcGIS. The control points were chosen from the original map (1:10,000 Ordnance Survey Map) of the study areas (at least four points per photo) for all aerial photographs.

2.1.1 Orthophotography

The orthophotography mosaic with stereo allowed easy differentiation of vegetation with differing heights, canopy shapes, and tree spacing; also, it provided a more accurate base for mapping. A Caerlaverock orthophotograph of 2009 was obtained from UK Blue Sky. As well three 1988 panchromatic photographs acquired as stereo pairs were obtained of Caerlaverock Reserve. These photographs were taken at a flying height of 12775 ft (equivalent to 3894 m) and with a focal length of 152 mm. The Caerlaverock orthophotograph 1988 was created by using BAE Systems SOCET SET (v6). There are some preliminary steps required before using BAE Systems SOCET SET. For example: converting the image from PNG to TIF format, then selecting control points from the topographic map (Ordnance Survey Map 1:10000 scale) of the Study Area; and afterwards calculating the Photographic Scale (PS) using the following formula:

$$PS = \frac{f}{H}$$

where f is the focal length, and H is the flying height. The steps adopted in this study to create the orthophoto map from aerial photos using BAE Systems SOCET SET (v6) are summarised in the flowchart shown in Figure 2.1 below.

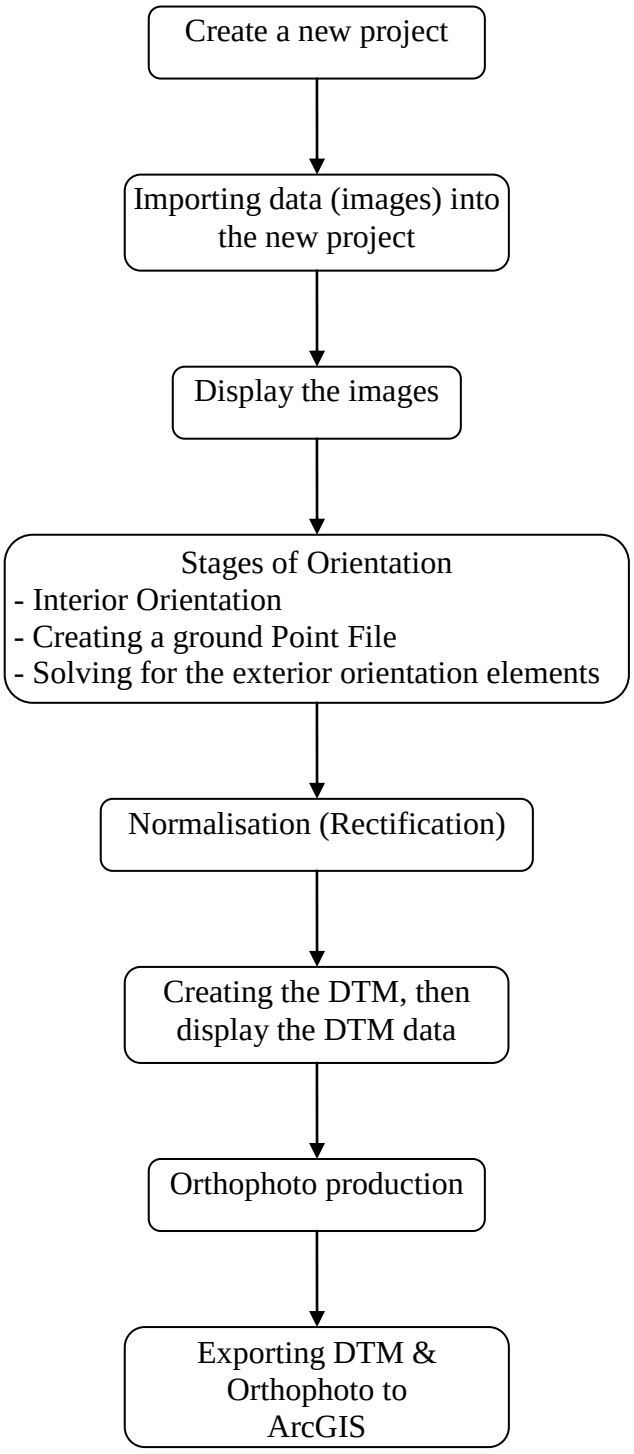

Figure 2-1: Flowchart to create an orthophotograph from aerial photography in BAE Systems SOCET SET (v6) (Refer to Appendix 1 for further details of this process).

2.2 LiDAR Data

LiDAR data were used because they greatly support the creation of a database of geographic information, adding height information to enhance surface measurement at intervals of between 1m and 2m on the ground. The quoted vertical accuracy of each height point is +/- 15 cm, and although this may be challenged in areas of variable terrain where accuracies have been found to range from 6 – 100cm (see: http://www.ctre.iastate.edu/mtc/papers/2002/Veneziano.pdf) in the flat terrain of the fens is supported. LiDAR data are easily compatible with other geographic databases available in Britain, particularly when based on the British National Grid. LiDAR is an option in remote sensing technology that optimises the precision of biophysical measurements and extends spatial analysis into the third dimension (Popeocu, 2007). It allows us to directly measure the distribution of plant canopies in three dimensions, in addition to sub-canopy topography, thus providing highly accurate approximations of vegetation height, cover, and canopy structure, and high resolution topographic maps (Lefsky et al., 2002).

LIDAR data (2 m resolution) for Wicken Fen in 2004 were acquired from the UK Environment Agency. The data were received as Digital Surface Models (DSM) and Digital Terrain Models (DTM), with all of the data referenced using the British National Grid.

2.3 ArcGIS Desktop

An important step in geographic analysis is choosing the way to represent data on the map. A Geographical Information System (GIS) is a computerised database designed for the management and use of spatial data. GIS is an essential tool for mapping existing wetlands and for identifying areas for wetland restoration or creation. GIS, such as ArcGIS, comprises spatial databases that store data as coordinates or vectors, or as grid-cells in a raster matrix (Harris, 2007). The use of GIS allows the analysis of multiple datasets, and a visual representation of mapped areas that may be suitable for wetland monitoring. ArcMap-GIS (v. 9.3) was used to produce the Wicken Fen- preliminary details map (shapefile) of the first Study Area, and the Caerlaverock Reserve- preliminary details map (shapefile) of the second Study Area (Fig.2.2 & 2.3). The ArcMap-GIS was also used to

map quadrat positions on the map that was prepared, using coordinates taken in the field by GPS in Wicken Fen during fieldwork in June 2010, and at Caerlaverock during July 2011.

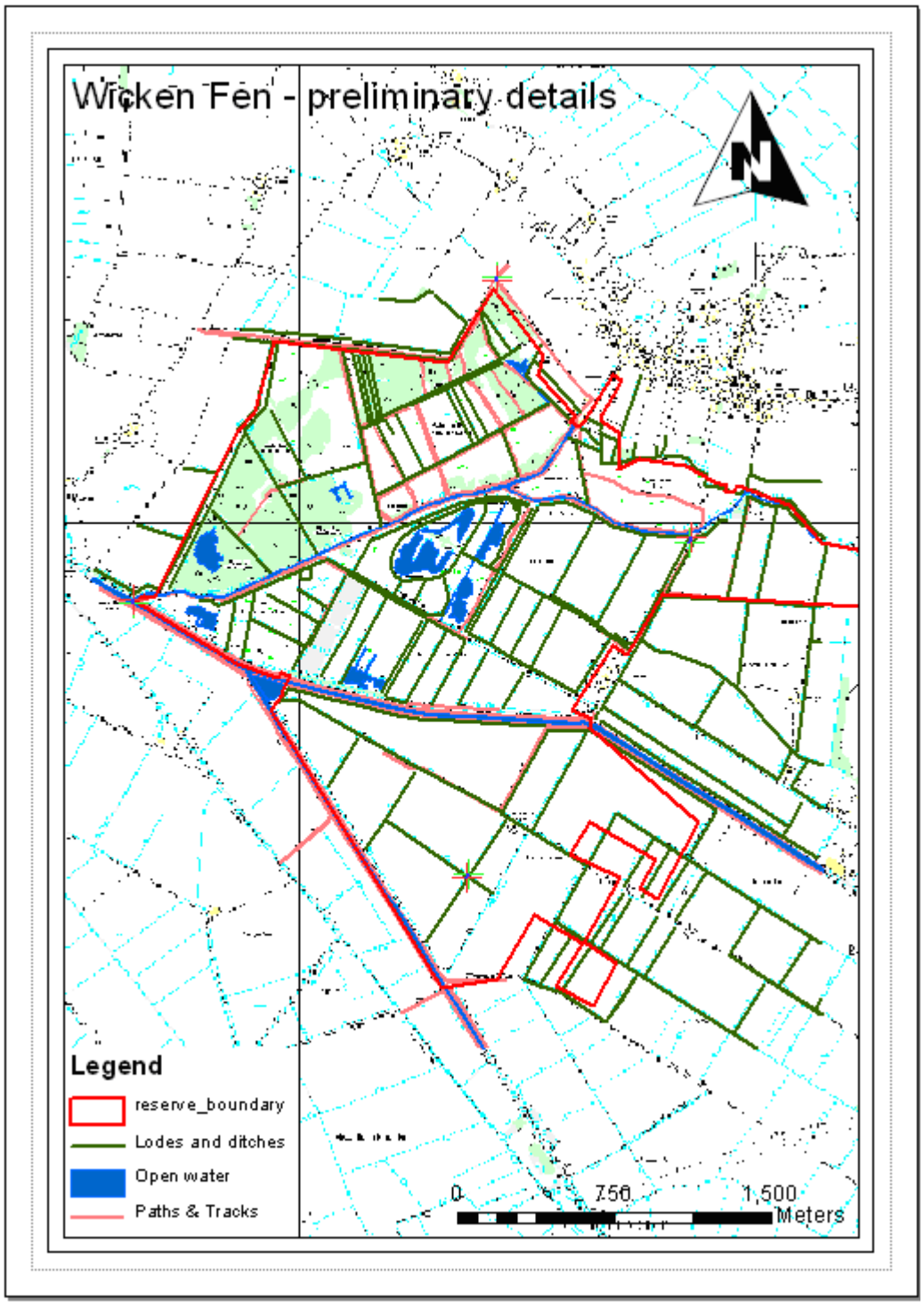

Figure 2-2: Preliminary details Wicken Fen map.

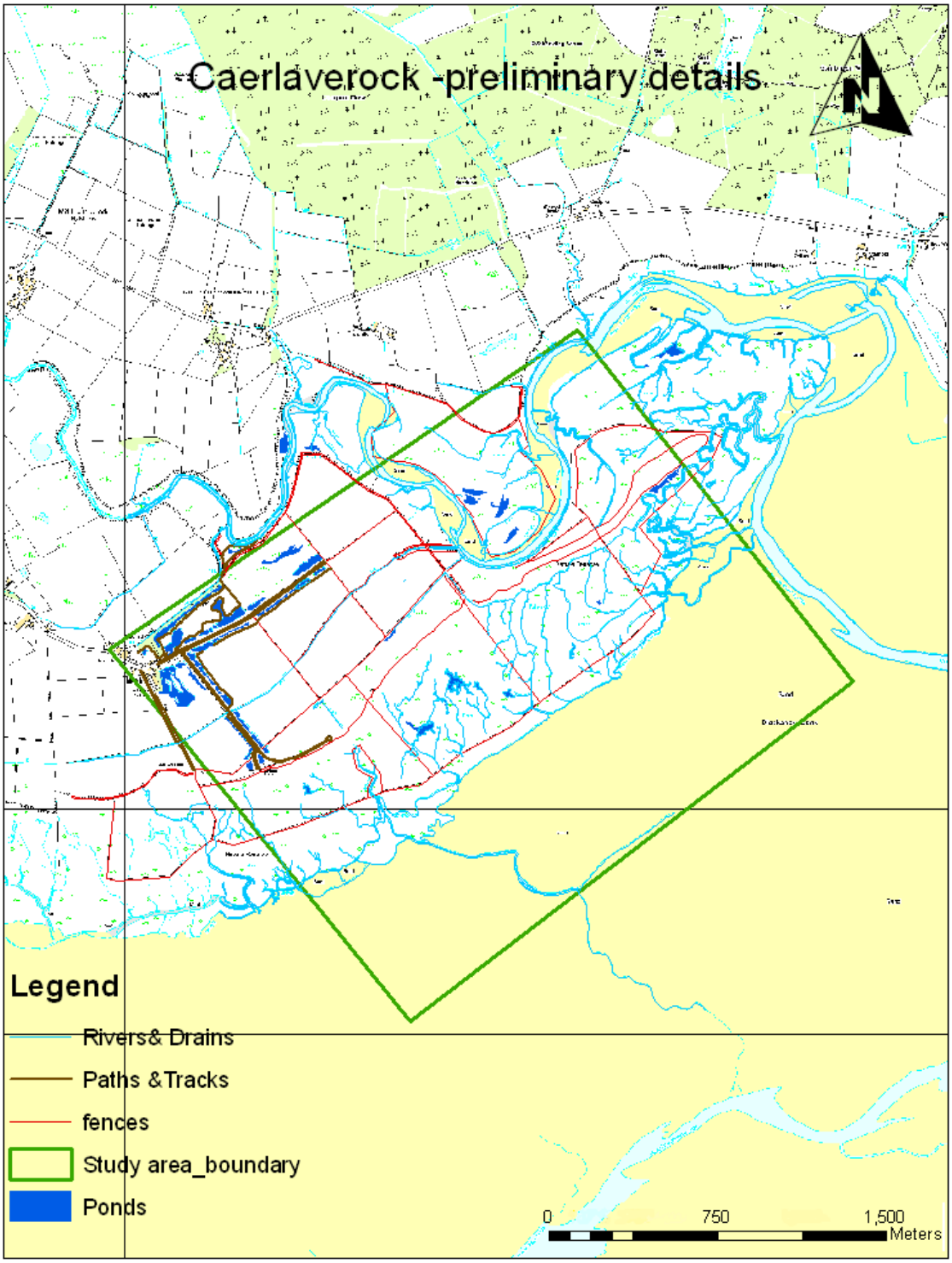

Figure 2-3: Preliminary details Caerlaverock Reserve map.

ArcMap-GIS (v.9.3) was used to calculate vegetation height by subtracting the DTM from the DSM. Then, a mosaic was created in ArcMap by using the calculations that had been performed to obtain vegetation heights to develop a single geographical representation of the Study Area. ArcMap-GIS was used to choose the control points for all aerial photographs, and for transformation to TIFF format by Georeferencing in the Geographic Information System (GIS), ArcMap. Each pixel has 8 bits with three colours (RGB) and 0.25 centimetre cell size. Pixel sets can easily be assembled to form the entire area. The steps adopted in this study to create the mosaic map from aerial photos and LiDAR data in ArcMap GIS (v9.3) are summarised in the flow chart shown in Figure 2.4 below.

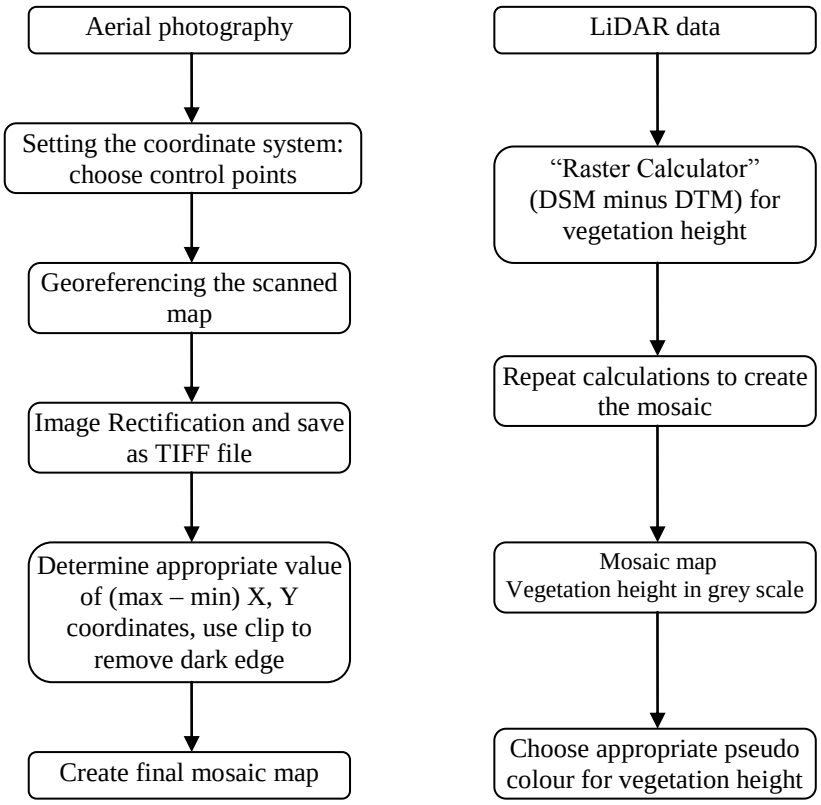

Figure 2-4: Flowcharts showing creation of mosaic map from aerial photos and LiDAR data in ArcMap GIS.

2.4 Landsat TM Images

Landsat TM and SPOT images are commonly used for mapping vegetation types in wetlands (e.g. Adam et al., 2010). Landsat 4 (TM) satellite images with 30-meter resolution, taken on 14 May 1988 for Caerlaverock Reserve, and on 18 August 1984 for Wicken Fen, were used. The Landsat (TM) scenes were obtained from the internet using the GLOVIS tool of the U.S. Geological Survey (USGS). The satellite imagery was received, with each band separated as a TIF file. All processing to convert TIF files from the single band to seven bands in a single image was done with ERDAS ER Mapper. A second set of images was used, utilising Landsat7 (TM) satellite imagery with 30 meter resolution for Caerlaverock Reserve, taken on 1 June 2009, and on 23 August 2009 for Wicken Fen. It can be noted that both sets of images were only a few days apart in their respective years, with similar cloud cover, thus radiometric balancing was not considered. These were obtained from the same agency (USGS), with each band separated as a TIF file. The same procedures were followed as above to obtain a one-layer satellite image with seven bands (Fig. 2.5). An visual interpretation of the study areas at these places where no changes seems to have occurred revealed little difference in the radiometric balance, so the ER Mapper tool was not used. In addition, a frame_and_fill program developed by the National Aeronautics and Space Administration (NASA) was used to rectify the gaps problem (SLC gap-fill) seen in 2009 Landsat imagery (Fig. 2.6). This ‘cosmetic solution’ was inappropriate; the unsupervised classification does not work effectively with the “filled” with Landsat 1 June 2009, and the gaps appeared again as differently classified bands. For this reason, the image taken on 1 June 2009 was not used, and another image for Caerlaverock Reserve, taken on 11 July 2009, was used instead.

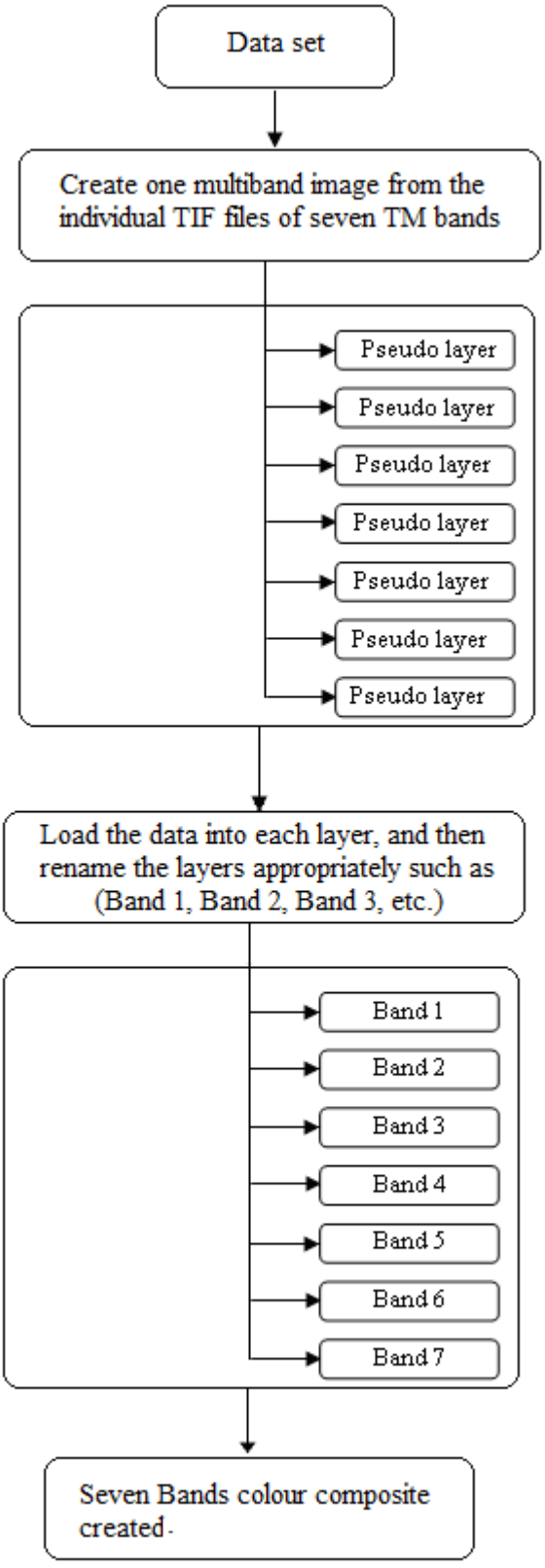

Figure 2-5: Flow chart showing procedure to separate TIFF bands from a Landsat TM scene and reformed as an ER Mapper as a 7 Band image. (Refer to Appendix 2 for further details of this process including displaying a natural colour image on screen using 3 bands).

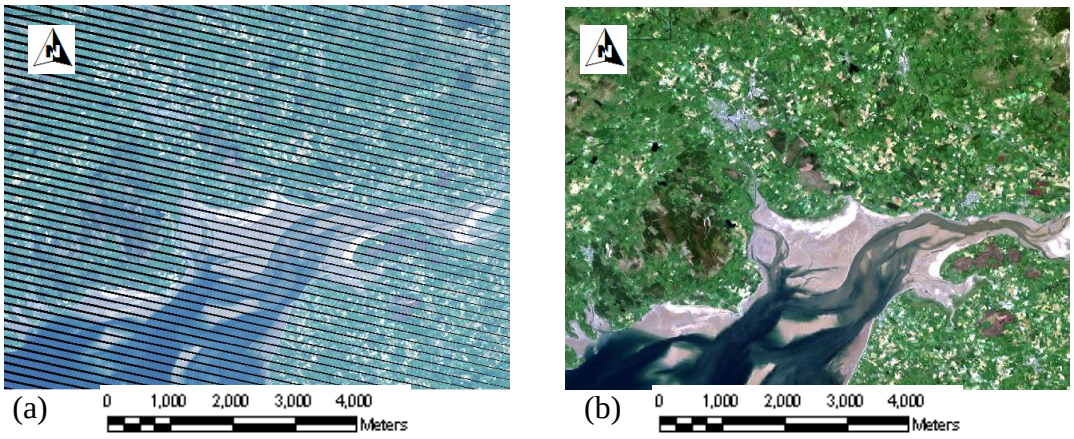

Figure 2-6: Shows (a) gaps in Landsat 2009TM image, (b) Landsat 2009TM image, after gap filling procedure, using NASA's GapFill program a 'cosmetic'solution. The gaps reappeared after classification as differently classified stripes.

2.5 Image Classification Approach

Common image analysis techniques used in mapping wetland vegetation include digital image classification (i.e. unsupervised and supervised classification: e.g. May et al. 1997; Harvey and Hill 2001) and vegetation index clustering (Yang 2007). Two remote sensing techniques were used to identify and classify vegetation in the two Study Areas.

Unsupervised and supervised satellite classifications were performed on Landsat 4 and 7 (TM) satellite images. Classifications are a computer-generated analysis of an image based on reflectance values. The classification results in a map of land cover. In order to consider only the Study Area portion of the whole image, the individual images (Wicken Fen1985TM, 2009TM, and Caerlaverock Reserve 1988TM, 2009TM) were subset to extract the Study Area, using the subset tool in ERDAS ER Mapper. The process of creating a subset involves two steps: the first identifies appropriate rows and columns for the study area (using the PAINT tool in this case), and the second uses the subset tool in ER Mapper to produce the resulting subset images (see Fig. 2.7, and Figure 2.8). The methodology adopted in this study for image preparation and vegetation classification by using ER Mapper is summarised in the flow chart shown in Figure 2.9.

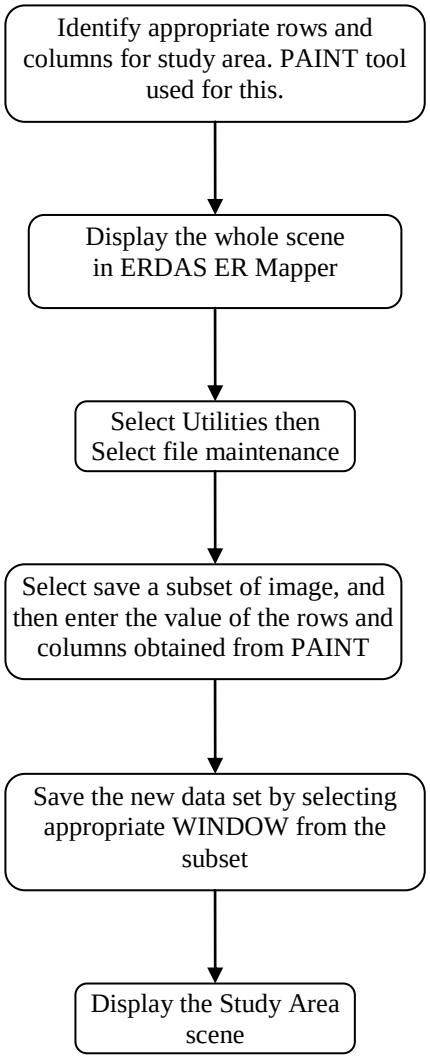

Figure 2-7: Procedure for choosing the Study Area from whole satellite image using the ER Mapper. (Refer to Appendix 3 for further details of this process).

a: Subset 1988 TM (Caerlaverock Reserve)

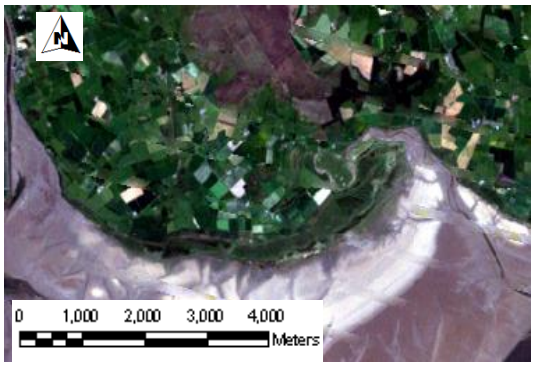

b: Subset 2009 TM (Caerlaverock Reserve)

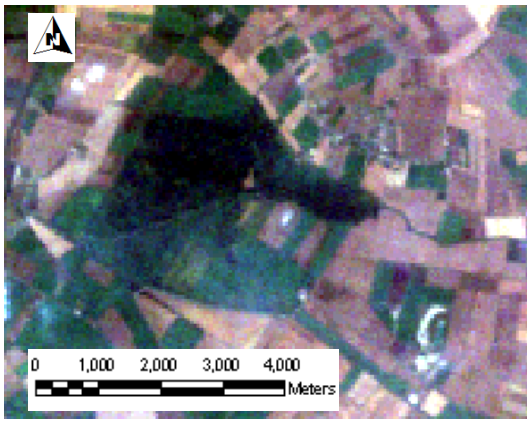

c: Subset 1984 TM (Wicken Fen)

d: Subset 2009 TM (Wicken Fen)

Figure 2-8: Subset images showing the study area.

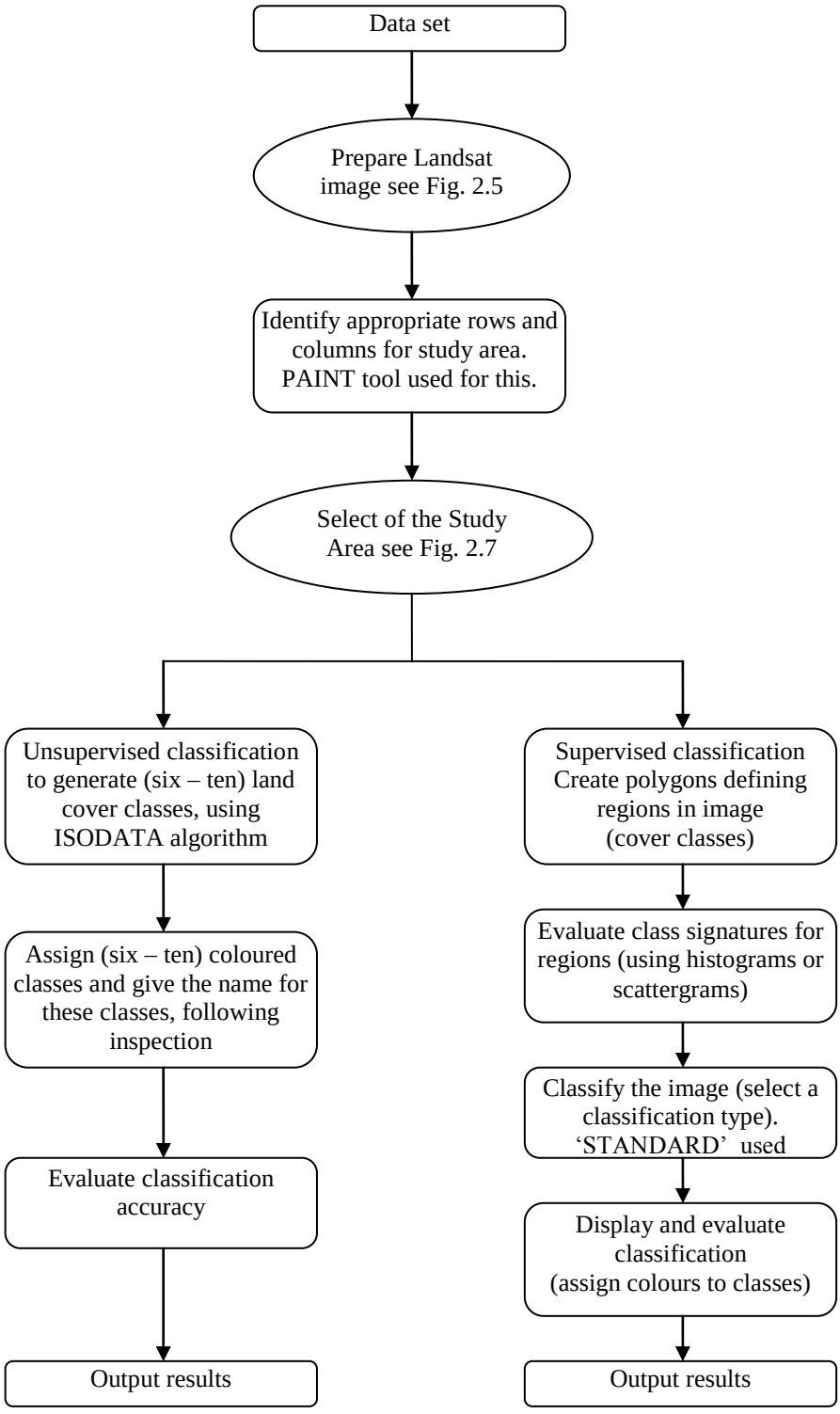

Figure 2-9: Landsat TM image analysis approach using ER Mapper, supporting both Unsupervised and Supervised classification.

2.5.1 Unsupervised Classification

Unsupervised procedures (using the ISODATA algorithm) can classify images into spectral classes, focused solely on the natural groupings derived from the image values (Govender et al., 2007). The unsupervised approach is often used in vegetation cover mapping. The benefits of unsupervised classification methods are that they involves the transfer of original image data, which provides information of higher classification accuracy (Xie et al, 2008). This classification (ISODATA algorithm) is based on the natural groupings of the spectral properties of the pixels, which are usually selected by the Remote Sensing software without any influence from the user. ISODATA is an unsupervised classification method that uses an iterative approach incorporating a number of heuristic procedures to compute classes. The ISODATA utility repeats the clustering of the image into classes until a specified maximum number of iterations has been performed, or a maximum percentage of unchanged pixels has been reached between two successive iterations (Melesse and. Jordan, 2002), for a specified number of classes.

In this study, unsupervised classification was used to produce land cover classes for each Study Area. In the unsupervised classification, the ISODATA algorithm in ERDAS ER Mapper was used, which classifies the image into a pre-selected number of classes using an iterative calculation procedure to ensure maximum statistical separability based on the spectral data. An unsupervised classification was performed on the image specifying 6 and 10 classes with 25 iterations, and a 0.98 confidence interval.

2.5.2 Supervised Classification

The maximum likelihood classifier (MLC) is a parametric classifier that assumes normal or near normal spectral distribution for each feature of interest in the target image. A supervised maximum likelihood classification algorithm was used to detect change in vegetation cover, because supervised classification depends to a greater extent than other methods on a combination of background knowledge and personal experience of the areas under investigation (Jensen, 2005). It consists of the identification of areas of specific features for each land use type or land-cover of interest to the analysis, (Govender et al., 2007).

Supervised maximum likelihood classification was chosen to compare the outputs with unsupervised classification results, which is particularly important for this study, because it identifies and locates land cover types that are known a priori through a combination of interpretation of aerial photography, Ordnance Survey map analysis, and fieldwork.

Traditional techniques of classification in remote sensing used pixel-based image classification, either using supervised or unsupervised classification. Vegetation indices are very often used in pixel based classification as an input channel to improve the classification result (Walter, 2004), pixel based approaches certainly can be useful for characterizing the land cover, and are particularly useful when landscape components of interest have very different spectral signatures (Gibbes et al., 2010). In this study pixel-based classification was used to classify the images. The analysis process in this method depends only on the spectral information in the images and it deals only with the optical value of each pixel.

Functional object based classification techniques, distinct from pixel based techniques, began to emerge in the 1990s (Janssen, 1993). The particular strength of object based techniques over pixel-based techniques has been found to be with high resolution imagery, particularly in urban environments or other patterned environments (Myint, et al. 2011; Zhou et al., 2009). However with regard to trees and shrubs (of particular interest in this research), Myint and colleagues found user and producer accuracies of 90% and 77% respectively for pixel based approaches and 84% and 86% for object oriented approaches, even with high resolution Quickbird imagery. There is thus little difference between the two approaches, for trees and shrubs, with user's accuracy in fact slightly higher for the pixel based approach, and it was concluded that the pixel based approach, for the medium resolution images used in this investigation, was adequate. The examination and development of object based approaches continue to be active research areas in the earth observation sector.

2.5.3 Change Detection in Wetlands with ArcMap GIS

Wetlands ecosystems are prone to possibly substantial change over time, in both habitat conditions and vegetation cover. ArcMap GIS 10.1 Raster calculator (an extremely flexible tool with which the author was familiar) was used to perform change detection analysis using Landsat TM. It has been assumed that all detected changes have arisen from changes in vegetation; however it must acknowledged that in British context there changes might, sometimes, arise from changes in illumination, wetness, shadow and colour; to calculate the change in the cover between the times selected in the areas of study by following the steps:

- Convert the outcome map from the ER Mapper supervised classification to TIF format (created in ER Mapper) as three separate bands for subsequent to use in ArcGIS.
- Loading the TIFF file as three separate bands in ArcGIS, because if loading it as a single image loses the details of the supervised classification.
- Use "Raster Calculator" for combining the three bands as follows:
  (1×band1+ 2×band2+3×band3) to retain the original supervised classification.
- Using "Raster Calculator Re-class" to reclassify the single image that was obtained in the previous step and re-label with the given in Tables 3.8 and 3.9.
- Obtain identical area for both images through clipping two areas by using extract by the rectangle.
- Multiply the area from image date 1 and the area from image date 2 to obtain the change detection image of vegetation zone, then interpretation the outcome pixel values, as shown in Table 3.10.

The steps adopted in this study for change detection map from Landsat TM using ArcMapGIS 10.1 are summarised in the flowchart shown in Figure 2.10 below.

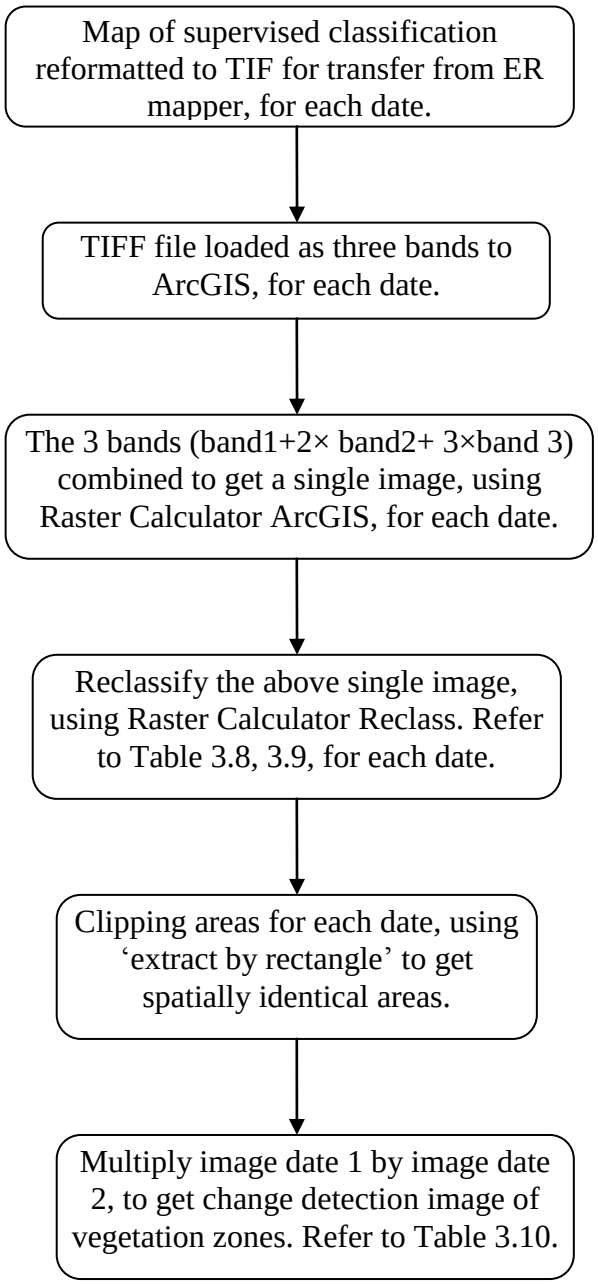

Figure 2-10: Flowchart to get change map of vegetation from Landsat TM in ArcGIS 10.1.

2.6 Ground Truthing Analysis

2.6.1 Line Transect

The line transect approach is particularly useful in studying flooded riverine and fen wetlands, which characteristically support ecotones (ecological spatial gradients). Transects had random starting points and were run in lines through the plant community, with total length depending on local conditions. Along the transect, quadrat samples were taken at intervals to record plant community composition and abundance, and relevant environmental characteristics (e.g. water depth, shade from scrub or tree vegetation, physico-chemical attributes etc). Vegetation state variables, e.g. total cover, average height and species diversity (S) were also recorded. These methods are standard for wetland vegetation survey (e.g. Kennedy et al., 2006; Timoney, 2008; De Steven et al., 2004; Bukland et al., 2007).

In this study, sampling was undertaken along six transects in Wicken Fen, in June 2010 and seven transects in Caerlaverock Reserve, in July 2011.

2.6.2 Quadrats

In Study Area 1 (Wicken Fen) the survey was conducted on 14^{th}-18^{th} June 2010: forty 1 m^2 quadrats were taken in total, placed randomly along six transects in different vegetation types (usually running from open area into shaded land) within Wicken Fen. The survey in the second Study Area was conducted on 5^{th}-9^{th} July 2011, with a total of forty-eight 1 m^2 quadrats placed completely randomly along seven transects in different vegetation types within Caerlaverock Reserve (Eastpark Farm).

In each sample quadrat, species assemblage, frequency and richness (S, number of species per m^2) was recorded within a 1m × 1m quadrat with one hundred 10cm x 10cm sub-divisions. The abundance of each plant species (as number of “hits” in sub-squares to obtain % frequency: %F) was recorded within each quadrat; see Appendix 4a, 7a.

Measurements of soil pH and soil conductivity (µS/cm) were made in each quadrat using a Hanna meter. The number of vegetation layers was recorded. Water depth was measured in some quadrats, when standing water was present; and light measurements were taken, at head height, using a SKYE PAR single-sensor meter, under, and immediately outside overhanging vegetation, when the quadrat was under or adjacent to scrub or trees, in order to assess % shade: see Appendix 4c, 7c . Paired light measurements for this purpose were taken as quickly as possible to minimise error, due to changing incoming light conditions (fortunately both surveys were undertaken during periods of hot, sunny weather which minimised this problem). The latitude and longitude of each quadrat were recorded (to 10 m accuracy) using a handheld Garmin GPS. Latitude and longitude co-ordinates measured in the field were subsequently converted to X and Y (meter) values using the website nearby.org.uk, and then input to the GIS to show the position of each guadrat on the study area map.

2.6.3 TWINSPAN Classification of Ground reference Vegetation Survey Data

In this study, Two-Way Indicator Species Analysis (TWINSPAN: version 2.3-August 2005) was used to carry out species classification of the vegetation samples (Murphy et al. 2003). Information output from the analysis is contained in the results file (results.txt). For each division, TWINSPAN identifies the strength of the division as an eigenvalue: a high eigenvalue (approaching 1.00) indicates strong separation of the two sample groups produced, with little similarity in species composition; a low eigenvalue (approaching zero) indicates strong overlap of sample groups in terms of species composition), the values were adopted more than 0.5; the indicator pseudo species (species at a predefined range of abundance, which characterises the sample group) and lists the samples assigned to each sample group. For the purposes of this study, the most useful feature of TWINSPAN is the final output two-way table (Kooh et al. 2008).

2.6.4 TABLEFIT Classification

TABLEFIT 1.0 (Hill, 1996) was used to determine UK National Vegetation Classification (NVC) categories (delineated by eigenvalues with high values (>0.500) and equivalent community types in the European CORINE biotopes classification) for the ground reference data sample-groups that were identified by TWINSPAN. Currently, national vegetation classification (NVC) is the standard phytosociological approach to the classification of natural, semi-natural and major artificial habitats in Great Britain, describing over 250 community types (Kennedy and Murphy, 2003).

2.6.5 Statistical Analysis

For normally distributed data, a one-way analysis of variance (ANOVA) was applied to determine significant differences between environmental and vegetation variables for sample groups identified by TWINSPAN. Tukey's mean comparison tests were used to determine which groups were significantly different in mean values for soil pH, conductivity, and vegetation height in the groups designated by TWINSPAN.

2.7 Achieving the Aims of the Investigation

Having developed the methodology in this chapter, it is hoped that the following two chapters will show how this has been implemented in the two study areas in order to achieve the study aims and objective, namely:

- To investigate the proposal that vegetation changes over time (e.g. scrub invasion; successional changes) have an effect on wetland plant community structure in UK wetland systems, which can be detected and quantified using remote sensing imagery. This proposal is investigated using an approach which combines remote-sensing analysis of imagery over time with ground truth of existing wetland vegetation communities at two contrasting wetland sites in the UK.

The specific objectives of the study are:

- To assess the value of using differing forms of remote sensing imagery in the mapping and monitoring of spatial and temporal variation in wetland vegetation, with a particular view to developing procedures which can be transferred to Libya.
- To evaluate procedures by investigating temporal wetland plant community change at two contrasting UK locations by combining analysis of remote sensing data and the use of GIS techniques.

Chapter 3- Wicken Fen study area 1

3

3.1 Introduction

Wicken Fen is an English fen wetland which was acquired and has been managed by the National Trust since the late 19th century. During the first half of the 20th century, cessation of cropping and falling water levels led to extensive invasion of the Fen by fen carr. In 1961, a management plan was drawn up to alter the Fen's successional decline and to restore its former habitat (Painter, 1998). A section of Wicken Fen named Wicken Sedge Fen has particular ecological and historical importance, because it is reputedly the sole undrained remnant of the Cambridgeshire Fenland. Drainage of this area for cultivation since the 17th century has dramatically reduced the area of fen and open water in Cambridgeshire until, by 1900, Wicken Sedge Fen (130 ha) was the only substantial area of fen remaining (Rowell, 1986). Many wetlands are now recognised as important ecosystem resources and have varying levels of protection in the UK, such as Special Areas of Conservation (SACs), Sites of Special Scientific Interest (SSSIs) and local nature reserves (Kennedy and Murphy, 2004).

Wicken Fen is one of the oldest and most intensively studied nature reserves in the British Isles. From the middle of the nineteenth century, it has been a prized collecting and recording ground for naturalists. As the fenland all around was drained for agriculture, the Fen become an isolated refuge for the characteristic species of fen habitats (Friday and Harley, 2000). Wicken Fen nature reserve is designated as a National Nature Reserve and is a sanctuary for birds, plants, insects and mammals, including otters and rare butterflies. The diverse landscape at Wicken Fen is made up of open fen habitats (including sedge beds, reed communities and fen meadows); aquatic habitats (such as dykes and pools); drier grassland and woodland. Intensive farmland surrounds the site, but the Fen represents an ancient landscape of high diversity and aesthetic appeal (Hine *et al.*, 2007).

3.2 Description of the study area

Wicken Fen (UK National Grid reference TL 5570) is located 15 km north-east of the city of Cambridge. It is a floodplain fen of about 130 ha, and a site of considerable natural history and conservation value, a remnant of the original peat fens of the East Anglian basin. It is bounded on its north and west sides by clay banks, on the south by a broad watercourse known as Wicken Lode, and on the east by the rising land of the Wicken ridge (Fig.3.1). The location is partly covered by fen carr with *Frangula alnus* (Alder Buckthorn) and *Salix cinerea* (grey sallow) as the most abundant tree species. *Frangula alnus* Mill. synonyms *Rhamnus frangula* L. is a small deciduous tree, or coarse shrub. Distribution of *Frangula alnus* in the British Isles, as shown in Figure (3.2), avoids permanently waterlogged and drought-prone sites. It is found on a wide range of soils, in scrub on fen peat, on the edges of raised mires, in scrub, and in woodland. It is characterised by regenerating strongly after cutting, burning or grazing; indeed, this species was planted for charcoal production (Online Atlas of the British & Irish Flora, 2013). Over 10.5 ha are covered by *Cladium mariscus* (Great Fen-sedge). The remainder of the herbaceous vegetation is dominated by *Molinia caerulea* (Purple Moor-grass), *Calamagrostis epigejos* (Wood Small-reed), *C. canescens* (Purple Small-reed), or *Phalaris arundinacea* (Reed Canary-grass) (Rowell et al., 1985; Rowell, 1986; Rowell and Harvey, 1988). Some communities at Wicken Fen are represented by National Vegetation Classification (NVC) categories M24 (*Molinia caerulea-Cirsium dissectum*) and S24 (*Phragmites australis - Peucedanum*). The M24 community is almost dominated by *Molinia*, typically with *Potentilla erecta* (Tormentil), *Succisa pratensis* (Devil's-bit Scabious), *Cirsium dissectum* (Meadow Thistle) and smaller *Carex* species. Community S24 is represented by *Phragmites australis* (Common Reed), *Peucedanum palustre* (Milk-parsley), *Peucedano-Phragmitetum australis* and *Caricetum paniculatae peucedanetosum* (tall-herb fen); this is the most widespread herbaceous community found at Wicken Fen (McCartney and de la Hera, 2004). Other plant communities present in Wicken Fen include M22 usually represented by *Juncus subnodulosus* (Blunt-flowered Rush) and *Cirsium palusture* (marsh Thistle) fen-meadow, and the W2 community (woodland) *Salix cinerea* (Grey Willow), *Betula pubescens* (Downy Birch) and *Phragmites australis* (Rodwell, 1991); this is the most botanically diverse vegetation community at Wicken Fen.

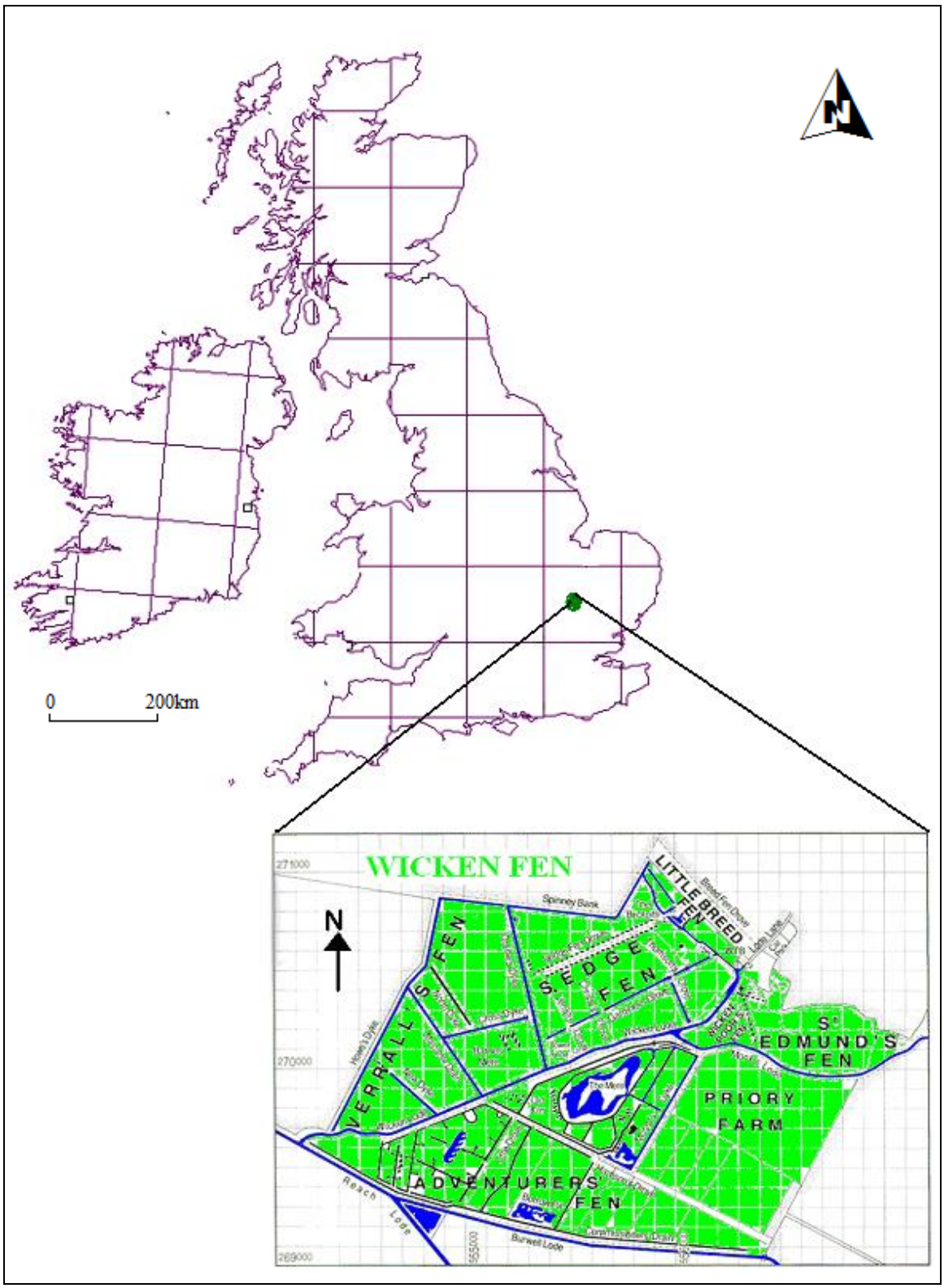

(source: www.wicken.org.uk/intro_map.htm)

Figure 3-1: Location of Wicken Fen.

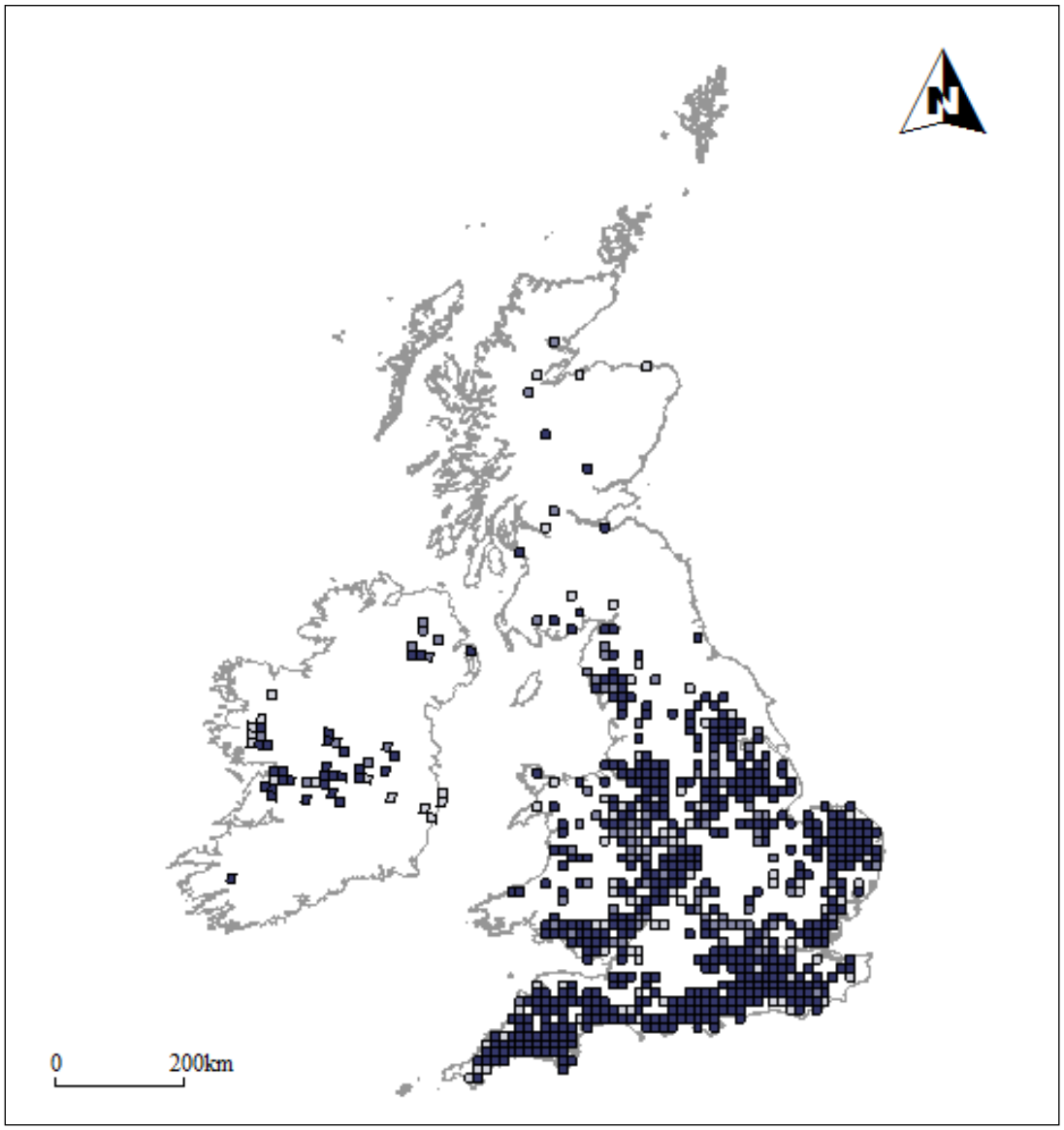

(Source:http://www.brc.ac.uk/plantatlas/index.php?q=plant/frangula-alnus)

Figure 3-2: Distribution of *Frangula alnus* in the British Isles.

3.3 Airborne and Space-borne Surveys

Aerial photographs of Wicken Fen were obtained from the UK Aerial Photos Database, and the LandsatTM scenes were obtained from the internet using the GLOVIS tool of the U.S. Geological Survey (USGS). It might be worth noting that satellite imagery is now much cheaper to acquire (using GLOVIS, for example enables acquisition with lower costs) than aerial imagery (UK Aerial Photos Database prices are about £30- £100 per photo); for this reason, satellite images were used in this study, and their results compared with those obtained from aerial photos.

3.3.1 Aerial Photography Interpretation

Geo-referenced air-photo mosaics were used as base maps from which cover types present in Wicken Fen were digitised on-screen using ArcGIS. Major structural changes in vegetation were determined by comparing vegetation maps interpreted from aerial photographs taken in 1985 (black and white) see Figure 3.3 and 2009 (true colour) see Figure 3.4. Vegetation was mapped on the basis of tree and shrub canopy cover. Areas were classified as herbaceous fen (white colour, in Figures 3.5, 3.6, 3.7, 3.8) if no trees were apparent in the photographs. The result obtained from interpretation of 2009 air-photos (Fig 3.8), when compared to air- photos of 1985 (Fig 3.5), has shown vegetation cover has changed, especially in Verrall's Fen (A), and Sedge Fen (B); see Figures 3.5 and 3.8 to compare total cover of trees and shrubs in 1985 and 2009. Details of the methodology used are given below.

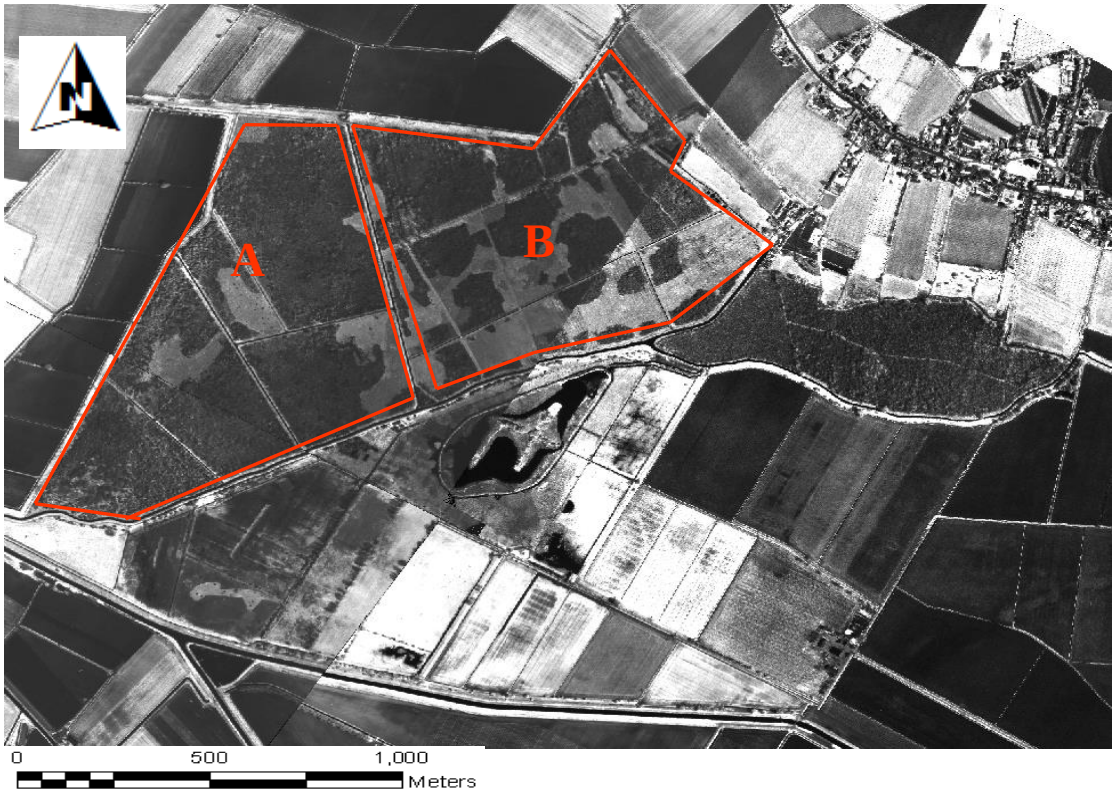

Figure 3-3: Verrall's Fen (A), and Sedge Fen (B) in Wicken Fen 1985 aerial photograph (Black & White)

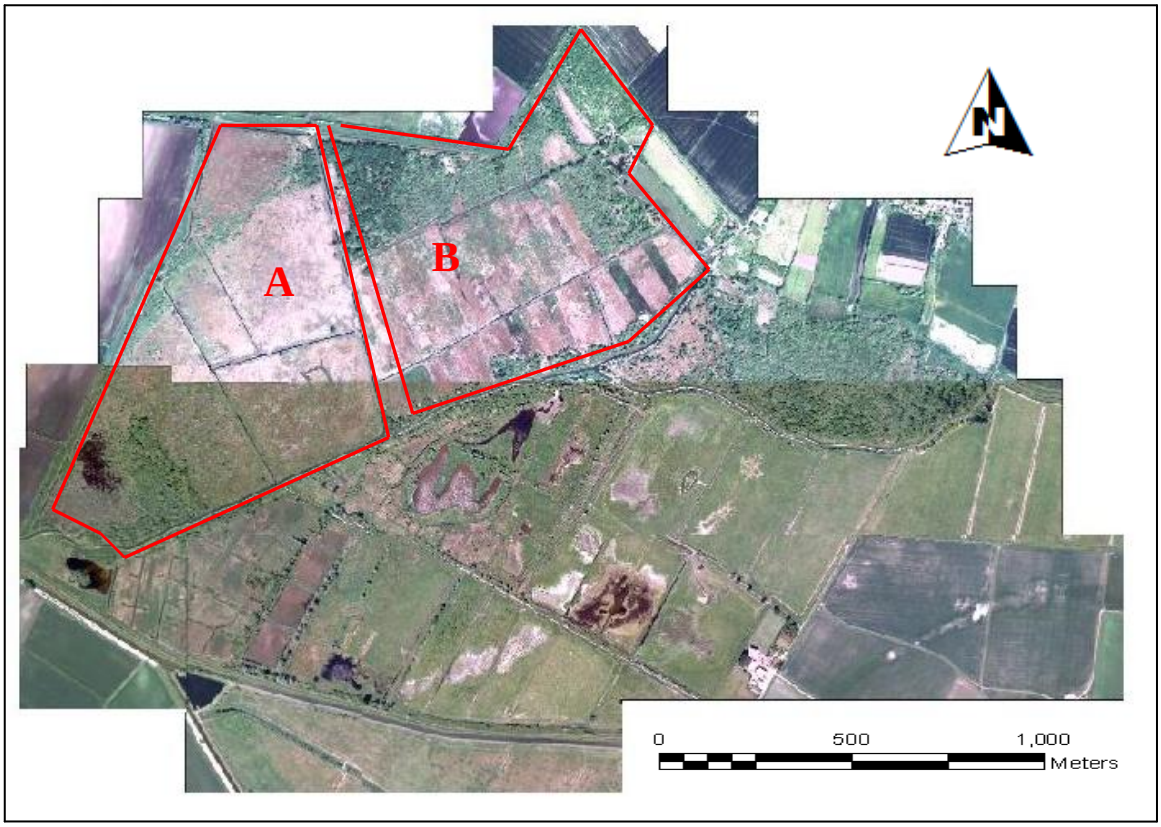

Figure 3-4: Verrall's Fen (A), and Sedge Fen (B) in Wicken Fen 2009 aerial photograph.

The total cover of trees and shrubs was delineated on-screen using the ArcMap GIS 9.3, and later ArcMap GIS 10.1, based on aerial photographs (1985, 2009), and groundtruthing fieldwork in 2010. To classify the aerial panchromatic imagery of 1985 Ordnance Survey map analysis and visual interpretation only were used. In addition, 1999 and 2003 Google Earth imagery of the study area of Wicken Fen was also delineated, and the result showed the changes in tree/shrub cover from 1999 to 2003 (Figs. 3.6 and 3.7).

Based upon the calculation of the cover of trees and shrubs in aerial photos for the target area, using ArcMap GIS, the results suggest a decrease from 1116072 m^2 (equivalent to 111.6072 ha) in 1985 (Fig. 3.5) to 671951 m^2 (equivalent to 67.1951 ha) in 2009 (Fig. 3.8) in which some 444121 m^2 (equivalent to 44. 421 ha) of tree/shrub canopy were lost.

The change rate in the cover (trees and shrubs) can be calculated using the following formula (Veldkamp et al., 1992):

$$\text{Change rate (percent, y}^{-1}) = \frac{(F_1 - F_2)/F_1}{N} \times 100$$

where:

F_1 is the cover area at the beginning of reference period;
F_2 is the cover area at the end of reference period;
N is the number of years in reference period; and,
y is a year.

The calculated annual change rate in the cover trees and shrubs from 1985 to 1999 was 2.24 %, from 1999 to 2003 was 0.28%, from 2003 to 2009 was 1.48%, and the annual change rate in the cover trees and shrubs of the whole period from 1985 to 2009 was 1.66 %.

Over the whole quarter century period (1985-2009) the percentage loss of trees and shrubs, based on the foregoing, was 39.8%. However on an annual basis the calculated change rate in the cover of trees and shrubs from 1985 to 1999 was 2.4% per annum, 0.28% from 1999 to 2003, 1.48% from 2003 to 2009, and 1.66% overall. It might be interesting to consider why the annual rate of decrease varied, but it might also be worth considering whether this

method to monitor annual change, is justified. The method relies on digitizing photo-interpreted polygons on aerial photographs; even amongst very experienced photo-interpreters this technique has associated errors could be affecting this approach, in Wicken Fen, as described in the next paragraph.

Polygons A, B and C of Figures 3-5 and 3-8 were each digitized five and four times each, respectively. The results are shown in Appendix 10. From these results it can be seen that, for Figure 3-5 (i.e. 1985), the average sizes of the polygons A,B and C were 10142.8 m^2, 88899 m^2 and 49182.8 m^2 respectively, and the standard deviation of the areas of the polygons A, B and C were respectively 95.2 m^2, 2455.05 m^2 and 2284.4 m^2. Based on these standard deviations (SDs) and assuming the digitizing error is normally distributed, it can be claimed that there is an almost 100% (strictly 99.7%, based on 3x SD) probability that the size of the polygons A,B and C are between 9857.08 m^2 and 10428.5 m^2, 81533.8m^2 and 96264.2 m^2, and 42329.6m^2 and 56036.0m^2 respectively - or the averaged area +/- 2.8%, 8.2% and 13.9% in the cases of A, B and C respectively. With digitizing precision at *this* level it becomes difficult to discuss annual changes in wood and scrub cover, but it is acceptable to discuss changes over several decades, as the percentage changes (i.e. 39.8%) are much greater than the percentage error arising from digitizing.

Repeating this discussion for Figure 3-8 (i.e. 2009), the percentage errors associated with digitizing polygons A, B and C to find their areas are 0.3%, 1.4% and 2.6% respectively. The improved quality of digitizing in the 2009 photography can be noted, but the percentage errors are still of the order of the calculated annual percentage changes, thus precluding any reliable discussion of annual rates of change.

Figure 3-5: Cover of trees & shrubs (green) in Wicken Fen 1985, using air photo interpretation.

Figure 3-6: Cover of trees & shrubs (green) in Wicken Fen 1999, using Google Earth.

Figure 3-7: Cover of trees & shrubs (green) in Wicken Fen 2003, using Google Earth.

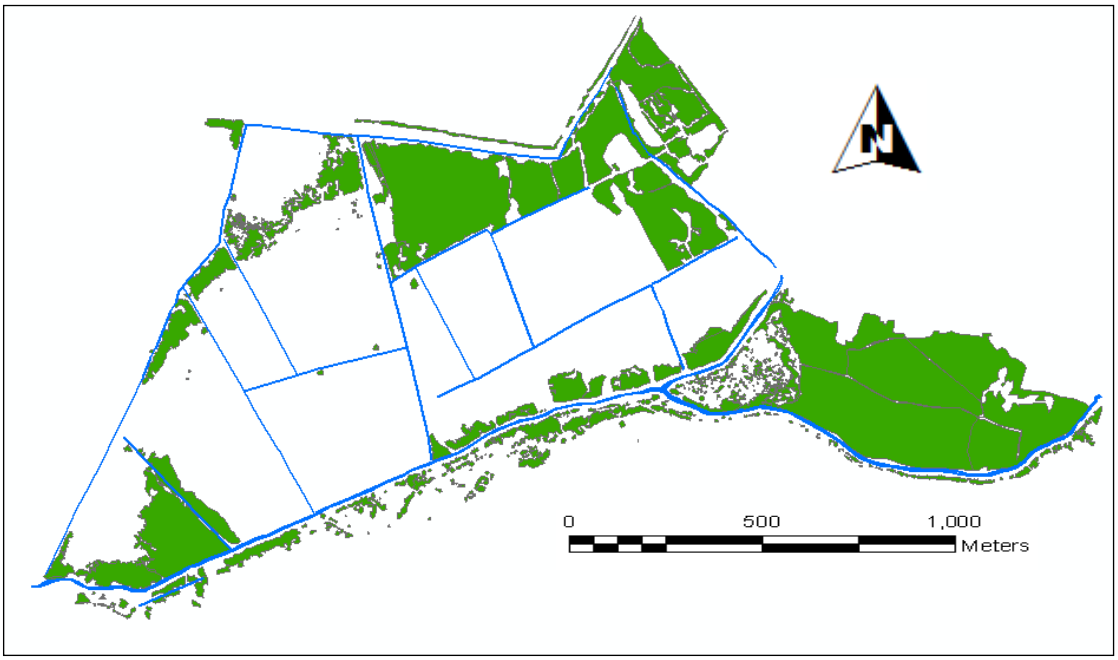

Figure 3-8: Cover of trees & shrubs (green) in Wicken Fen 2009, using air photo interpretation.

3.3.1.1 Change Matrices

A ‘change matrix’ is a development of the classical ‘misclassification matrix’ or ‘error matrix’ concept widely used in the Earth Observation sciences (see: “Remote Sensing and Image Interpretation”, edition 6, p 585, Lillesand, Kieffer and Chipman, 2008) to compare ‘ground truth’ and the outcome from a classification process.

For reasons of clarity, the creation of an error matrix is briefly described in the following three paragraphs, relating to Table 3.1.

An error matrix compares two (usually landcover) data sets. One of these is considered to be of higher accuracy than the other, and the higher accuracy set represents ‘the truth’; their comparison gives accuracy statistics for the less accurate data set. For example, the data set whose accuracy is being considered might be derived from a low resolution source, such as LandsatTM, while ‘the truth’ is provided by a higher resolution data set, such as aerial photography, orthophotography or ground observations. An error matrix provides three types of statistical information:

1. simple probability of the classification of the lower resolution data set being correct (where ‘correct’ is specified by the higher resolution data set), presented in percentage probability terms – in the simulated example below (Table 3.1) this is 70%;
2. user’s accuracy where the product provided by the producer using the lower resolution data set - such as a landcover map, in its practical use, is compared to ‘the truth’, presented in percentage probability terms, per class – in the simulated example below (Table 3.1) this is 83% in the case of Class A and 50% in the case of Class B;
3. producer’s accuracy where ‘the truth’ provided by the higher resolution product is compared to the product provided by the producer using the lower resolution data set, presented in percentage probability terms, per class – in the simulated example below (Table 3.1) this is 71% in the case of Class A, and 66% in the case of Class B.

A simulated example error matrix is provided in Table 3.1 below for two classes of land use (A,B) in a 1000 pixel site. In this example, the producers, using low resolution imagery, mapped 600 pixels of class A and 400 pixels of class B, whereas ‘the truth’ (or ‘groundtruth’) as found in high resolution aerial photography was that there were 700 pixels of class A and 300 pixels of class B (Table 3.1).

Table 3-1: Explanatory example of an Error Matrix.

PRODUCED MAP → GROUNDTRUTH ↓	CLASS A	CLASS B	∑	Producer's accuracy
CLASS A	500	200	700	500/700 (71%)
CLASS B	100	200	300	200/300 (66%)
∑	600	400		
User's accuracy	500/600 (83%)	200/400 (50%)		700/1000 (70%) (Simple probability of map being correct)

Several of these error matrices are considered subsequently in this chapter. However, a particular development of the error matrix has been to use the same statistical approach to produce a ***change matrix***. The change matrix compares two surveys considered to be of the same accuracy, but representing different dates. The statistics obtained represent change, and there has to be a modification of terminology, as shown below in Table 3.2.

Table 3-2: Explanatory example of an Change Matrix.

DATE 1 → DATE 2↓	CLASS A	CLASS B	∑	Percentage Date 2 class retained from Date 1
CLASS A	500	200	700	500/700 (71%)
CLASS B	100	200	300	200/300 (67%)
∑	600	400		
Percentage Date 1 class retained in Date 2	500/600 (83%)	200/400 (50%)		700/1000 (70%) (Overall percentage unchanged between the two dates)

It may of course be more interesting to state the above specifically in terms of percentage changed – rather than percentage unchanged, in which case there has been an overall change of 30% between the two dates, with: 17% of Date 1 Class A changing to Class B between the dates; 29% of Date 2 Class A having changed from Date 1 Class B between the dates; 50% of Date 1 Class B changing to Class A between the dates; and, 33% of Date 2 Class B having changed from Date1 Class A between the dates.

Essentially in moving from error matrices to change matrices, we are no longer considering percentages correct, but percentages unchanged.

There are several practical examples of these change matrices considered subsequently in this chapter.

3.3.1.2 Using change matrices and error matrices.

In more detail, the results of change from aerial photography 1985 versus fieldwork 2010 of the classification into five classes (trees and shrubs – T&S; pasture - P; farmland - F; herbaceous fen - HF; water - W) are shown in the change matrix Table 3.3. In Table 3.4, the results obtained from a two-class change matrix for aerial photography 1985 versus fieldwork 2010 are shown. The overall percentage unchanged between the two dates for the two and five class classifications were found to be 77.5% (Table 3.4) and 67.5% (Table 3.3), respectively.

The comparison, using error matrices between aerial photography of 2009 and fieldwork of 2010, is performed under the assumption that there will have been little change between the two dates (they are consecutive years) and the error analysis serves to confirm that aerial photography is a worthy substitute for field work – an idea which is long established amongst air photo interpreters e.g. supported by Mosbech and Hansen (1994) who mapped vegetation classes in Jameson Land, while Verheyden et al., 2002 reported that aerial photographs produced accurate vegetation maps of mangrove forests. Accuracy percentages over 90% in the two-class assessment confirm this (see Table 3.6).

Table 3-3: Five classes change matrix resulting from aerial photography1985 versus fieldwork 2010 for Wicken Fen.

Aerial 1985 → FW 2010 ↓	T&S	P	F	HF	W	∑	Percentage retained unchanged in 2010 from 1985
T&S	19	0	0	2	0	21	19/21 90%
P	0	3	0	0	0	3	3/3 100%
F	0	0	0	0	0	0	NA
HF	6	2	0	4	0	12	4/12 33.3%
W	1	2	0	0	1	4	1/4 25%
∑	26	7	0	6	1		
Percentage from 1985 retained unchanged in 2010	19/26 73.1%	3 /7 42.9%	NA	4/6 66.7%	1/1 100%		Overall % unchanged between two dates: 27/40 67.5%

Table 3-4: Two-classes change matrix resulting from aerial photography1985 versus fieldwork 2010 for Wicken Fen.

Aerial 1985 → FW 2010 ↓	T&S	Others	∑	Percentage retained unchanged in 2010 from 1985
T&S	19	2	21	19/21 90.5%
Other	7	12	19	12/19 63.2%
∑	26	14		
Percentage from 1985 retained unchanged in 2010	19/26 73.1%	12/14 85.7%		Overall % unchanged between two dates: 31/40 77.5%

The results of error matrix analysis from aerial photography 2009 versus fieldwork 2010 of the classification into five classes with user's and producer's accuracies are shown in Table 3.5. Table 3.6 shows the results obtained from two-class error matrix for aerial

photography 2009 versus fieldwork 2010. The overall accuracies for the error matrix of two and five classes were found to be 90% (Table 3.6) and 80% (Table 3.5), respectively.

Table 3-5: Error matrix resulting from aerial photography 2009 vs. fieldwork 2010 for Wicken Fen, using 5 classes.

Aerial 2009 → FW 2010 ↓	T&S	P	F	HF	W	∑	User's Accuracy
T&S	17	0	0	4	0	21	17/21 80.9%
P	0	3	0	0	0	3	3/3 100%
F	0	0	0	0	0	0	NA
HF	0	0	0	11	1	12	11/12 91.6%
W	0	1	0	2	1	4	1/4 25%
∑	17	4	0	17	2		
Producer's Accuracy	17/17 100%	3/4 75%	NA	11/17 64.7%	1/2 50%		32/40 80%

With a positive *k* ("KHAT", or "kappa") value (0.68) the classification is shown to be 68% better than classification resulting from chance.

Table 3-6: Error matrix resulting from aerial photography 2009 vs. fieldwork 2010 for Wicken Fen, using two classes.

	T&S	Other	∑	User's Accuracy
T&S	17	4	21	17/21 80.9%
Other	0	19	19	19/19 100%
∑	17	23		
Producer's Accuracy	17/17 100%	19/23 82.6%		36/40 90%

With a positive *k* ("KHAT" or "kappa") value (0.80) the classification is shown to be the classification is shown to be 80% better than classification resulting from chance.

3.3.2 LiDAR image interpretation

LIDAR data (2 m resolution) for Wicken Fen in 2004 were acquired from the Environment Agency (England and Wales). The data was received as Digital Surface Models (DSM) and Digital Terrain Models (DTM), with all of the data referenced using the British National Grid.

Initial results for vegetation height, obtained by subtracting the DTM from the DSM in ArcMap, appeared as a black and white 32 bit image. Through applying pseudo-colours in the vegetation height channel, the heights can be visualised based on the colours (Figure 3.9). In ArcMap, vegetation height values are fitted to the pseudo-colour, with the lowest value being assigned to gray, the highest to red. Trees and shrubs appeared in magenta colour and lower values of red. Figure 3.10 shows the mosaic map with the vegetation height, for visualised Wicken Fen from LIDAR data, and the OS DTM.

As indicated by Popescu (2007) LiDAR, with its multiple returns is also very useful in assessing biomass and other vegetation characteristics. Subtle differences between trees and shrubs can be detected. Determining a single "Trees &Shrubs" class does not exploit the full potential of LiDAR, and this could be investigated in future work.

The result obtained from interpretation of 2004 LIDAR data (Figure 3.9), when compared to air- photos of 1985 (see Figure 3.5), clearly shows vegetation cover change in Verrall's Fen (A), and Sedge Fen (B), over the nineteen year period.

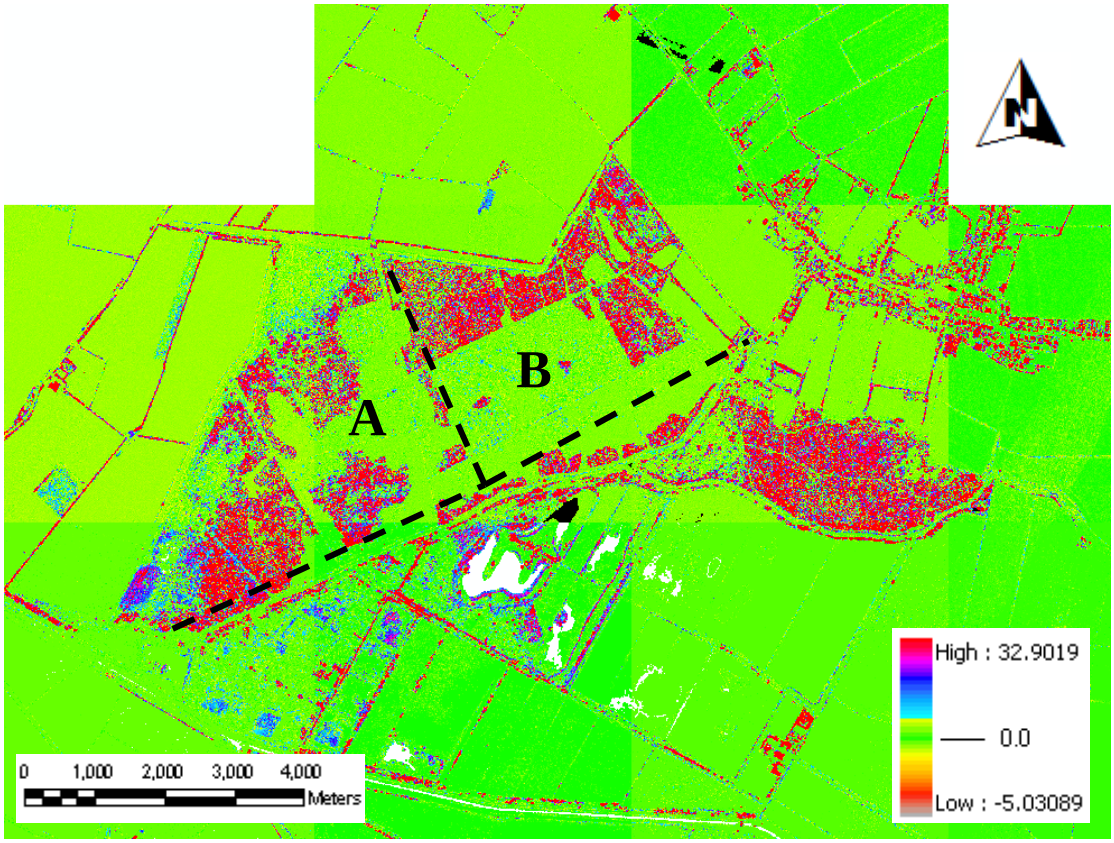

Figure 3-9: Height of vegetation at Wicken Fen in a mosaic map of 2004 LIDAR data (white areas are unclassified, and represent open water)

3.3.3 Landsat imagery interpretation

Assessment of environmental data using remote sensing is not possible without a characterisation of each land cover type following classification. Usually classification is divided into two categories, unsupervised and supervised, each of which can agglomerate remotely sensed data into meaningful groups. The unsupervised classification is often performed first, as it allows for a preliminary exploration of the data.

3.3.3.1 Unsupervised Classification

An unsupervised classification is theoretically better suited to application in a highly heterogeneous wetland environment (Harvey and Hill 2001). The results of analysis of 1984 Landsat TM imagery using unsupervised classification techniques to produce, first, ten land cover classes and then, subsequently, six land cover classes, are shown in Figures 3.10 and 3.11.

The ten class image (Fig. 3.10) is difficult to interpret; to interpret the image we need to know into which land cover type each category falls, with detailed knowledge of ground truth for the area, but it is not always easy to do that, especially in a flood plain area. In the unsupervised classification method chosen, the classes produced are based on natural breaks in the distribution of pixel values in the image. As a result, the created classes may not distinguish between the features that the user needs to resolve. For example, in this study, the reflectance of vegetation in flooded areas and open water types may be too similar for the software to separate them into distinct classes. In the six class unsupervised classification of the 1984 LandsatTM image of Wicken Fen, there appears to be an integration of open water with vegetation, see Figure 3.11 (light green) ; this has been labelled Trees and Shrubs in the figure. The six classes for the 1984 image were tall vegetation (trees, shrubs); wet grassland; pastures; waterlogged soil; and agricultural land.

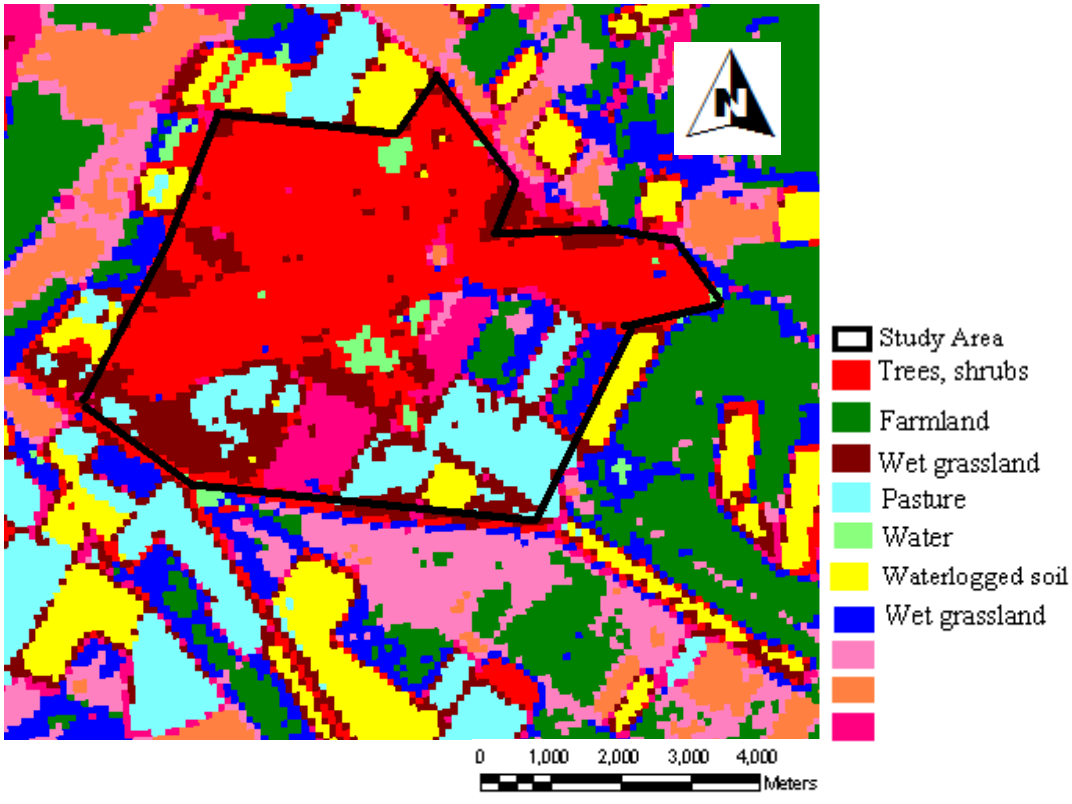

Figure 3-10: Ten land cover classes of 1984 Wicken Fen LandsatTM image after unsupervised classification. (See Fig. 2-8 c for the original image, prior to classification)

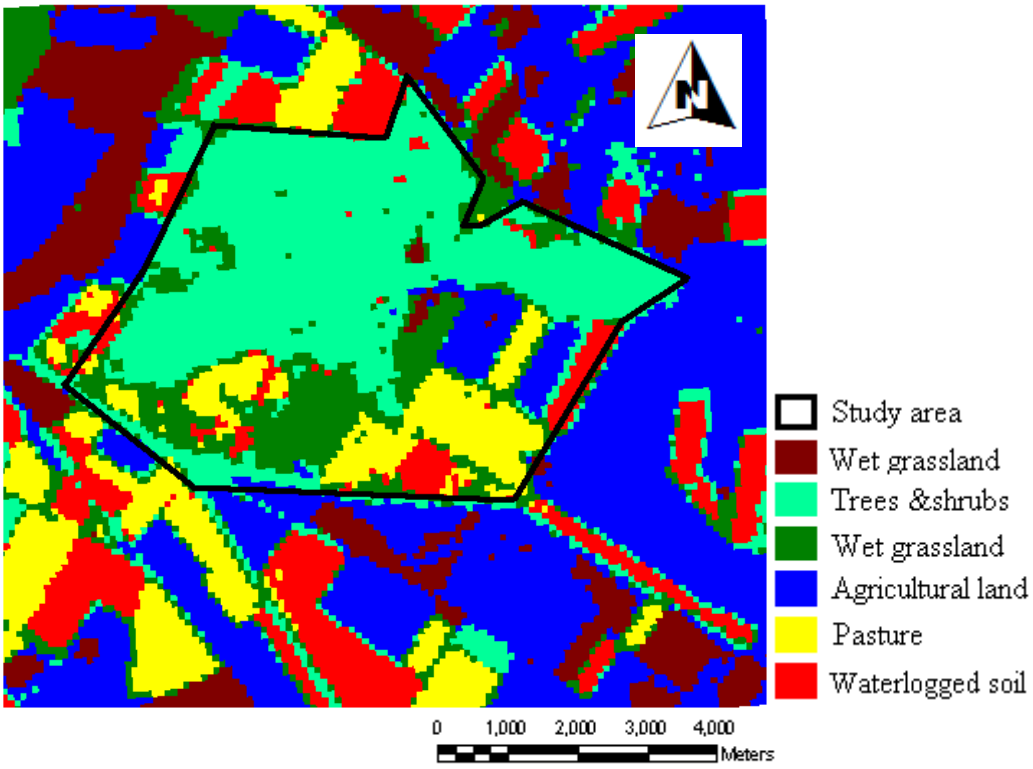

Figure 3-11: Six land cover classes of 1984 Wicken Fen LandsatTM image after unsupervised classification.

Figures 3.12 and 3.13 show the results obtained from interpretation of LandsatTM imagery for 2009, using unsupervised classifications in six and ten cover classes. The identified classes were tall vegetation (trees, shrubs), water body, wet grassland, pastures, waterlogged soil, and agricultural land.

An unsupervised classification using ten classes results in some classes in the study area which could not be identified by the author (for example Fig. 3-13). Reducing the numbers of classes to six result in a classification which matched the author's pre-existing knowledge

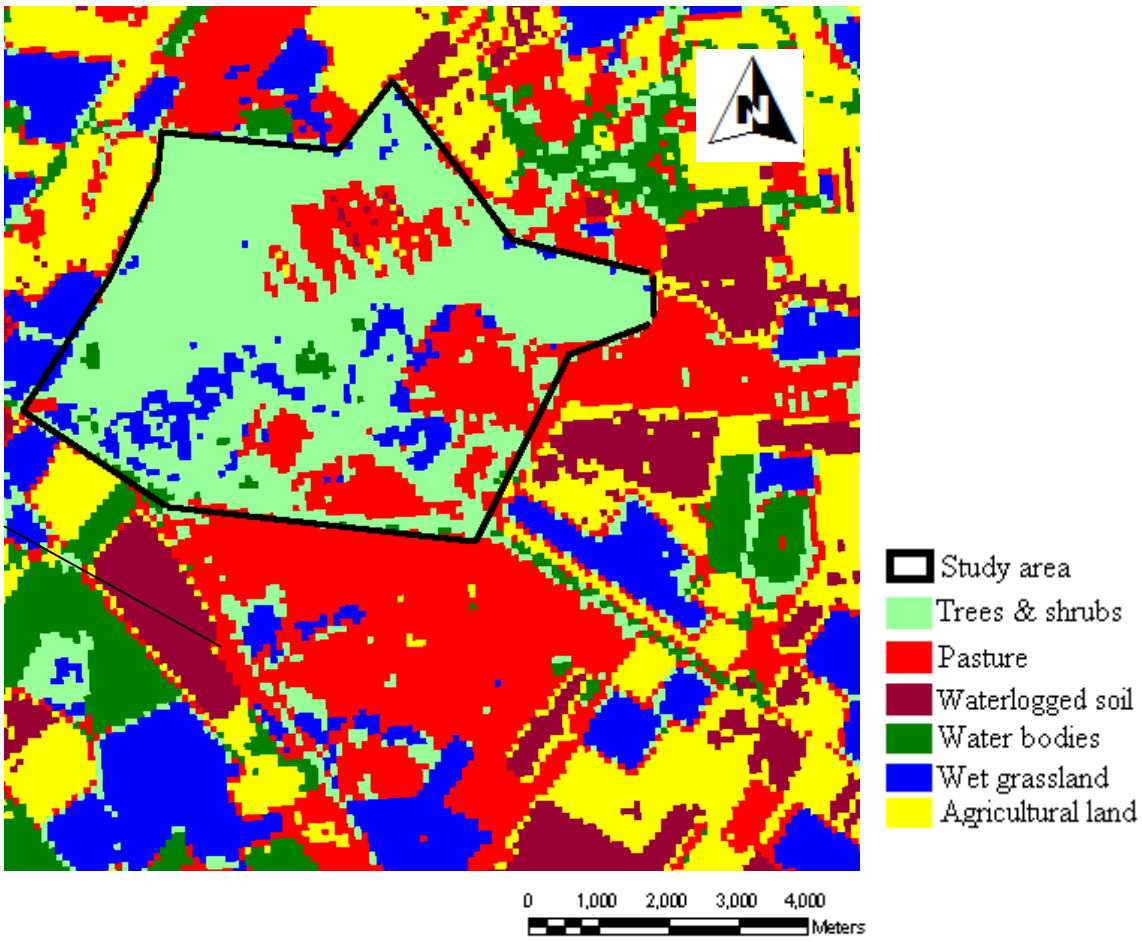

Figure 3-12: Six land cover classes of the 2009 Wicken Fen LandsatTM image after unsupervised classification.

The 10 class unsupervised classification produced classes which were difficult to identify, based on field work and knowledge of the area (see Figure 3.13).

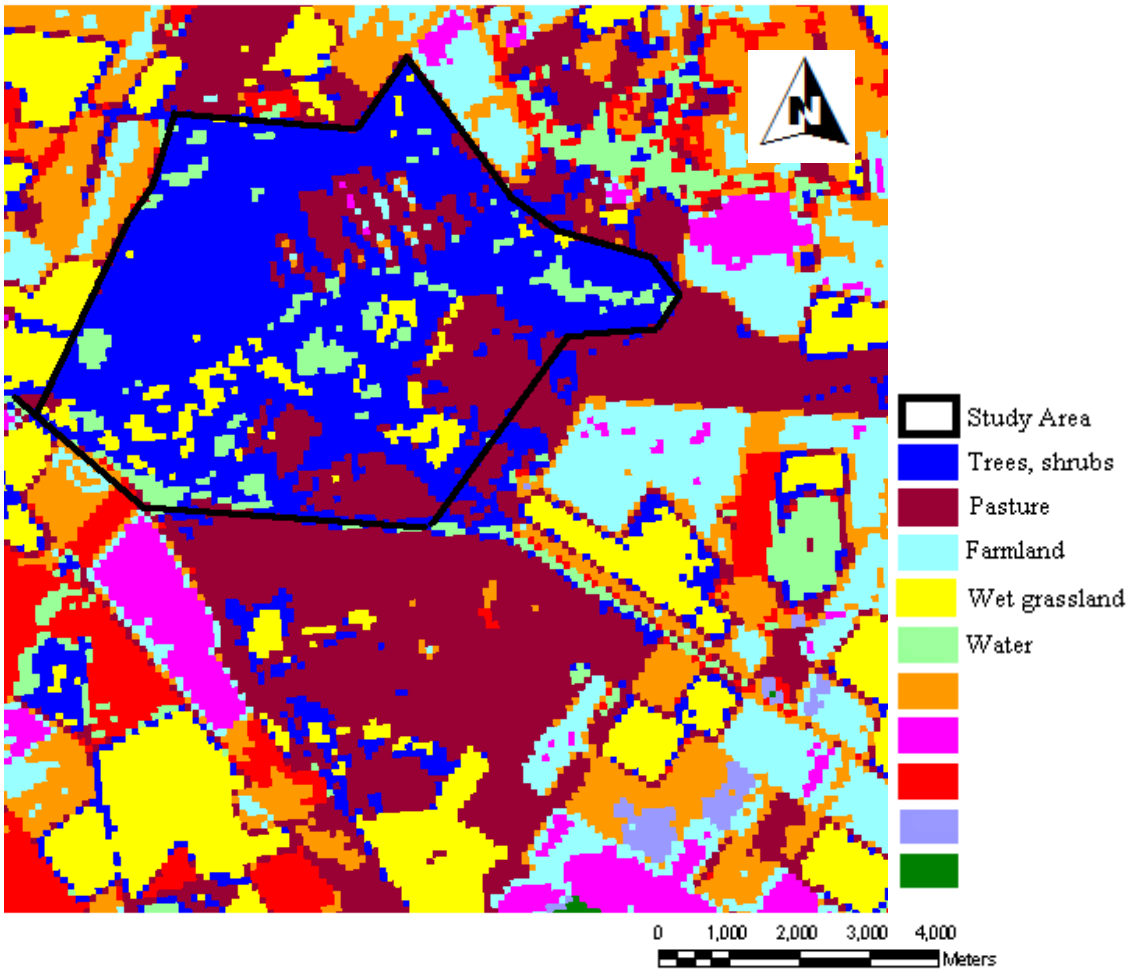

Figure 3-13: Ten land cover classes of the 2009 Wicken Fen LandsatTM image after unsupervised classification.

Results obtained from comparing the six class unsupervised classification of the LandsatTM imagery for 2009, with the similarly classified LandsatTM imagery for 1985, show that vegetation cover has changed, especially in Sedge Fen (A): see Figures 3.14 and 3.15.

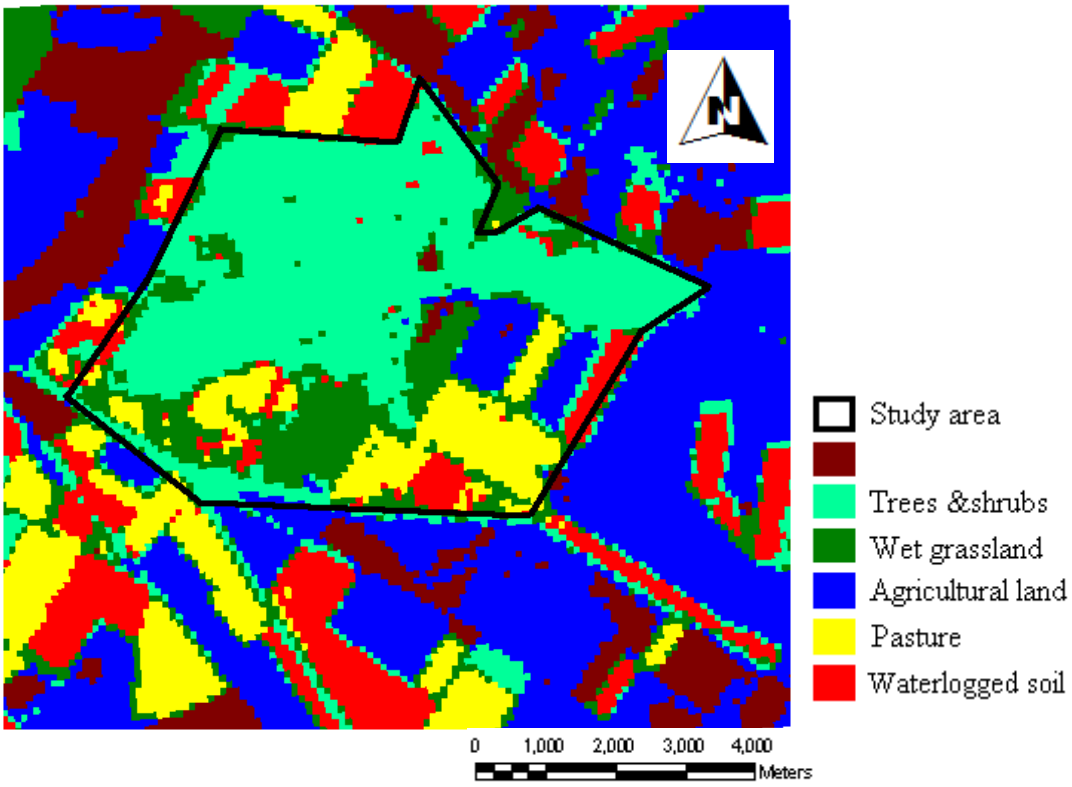

Figure 3-14: Six classes unsupervised classification of 1984 Wicken Fen imagery

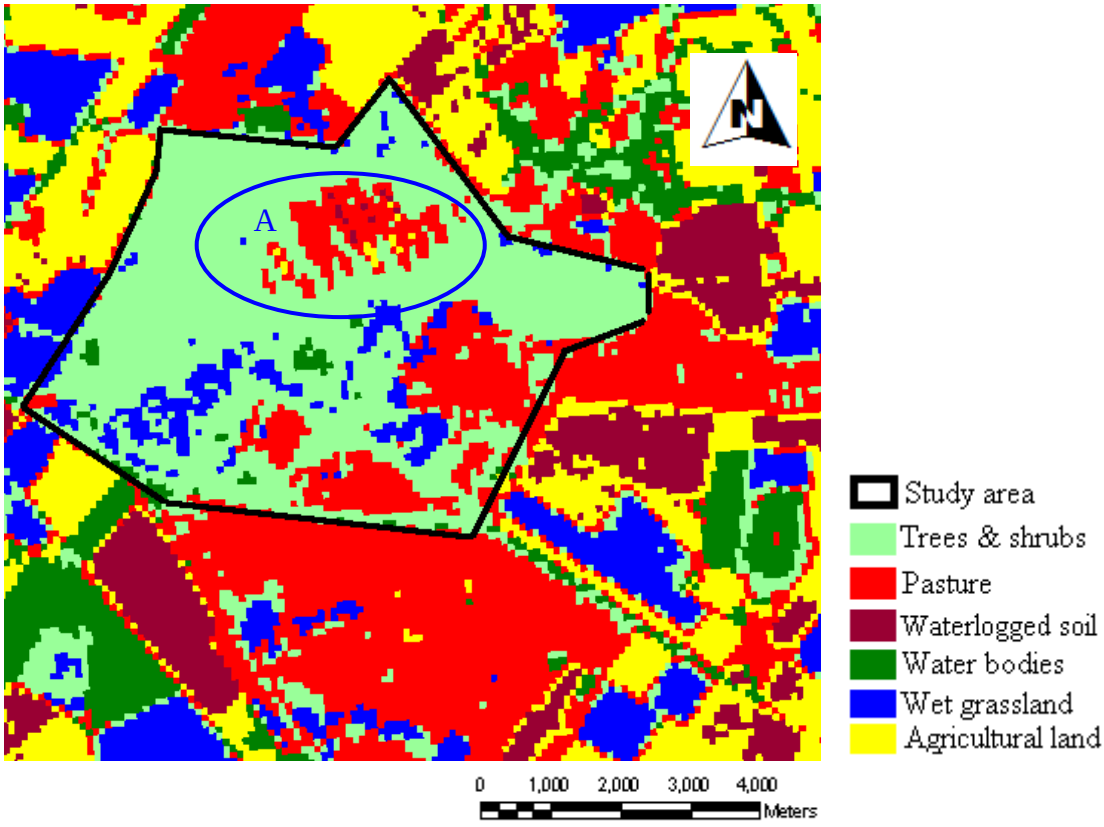

Figure 3-15: Six classes unsupervised classification of 2009 Wicken Fen imagery, the circled area (A) shows an obvious change in vegetation.

3.3.3.2 Supervised Classification

Supervised classification using maximum likelihood classification (MLC) provided better results than unsupervised classification for distinguishing Wicken Fen vegetation classes, and for subsequently monitoring change (Table 3.27). The accuracy assessment of the supervised classification classes was performed using aerial photos, Ordnance Survey maps, and fieldwork for check-values (validation sources). The Study Area was categorised into five-land cover classes; the classes were tall vegetation (trees, shrubs), pasture, farmland (crops), wet grassland, and water.

The results of the supervised classification techniques into five land cover classes for Wicken Fen LandsatTM images in 1984 and 2009 are shown in Figures 3.16 and 3.17.

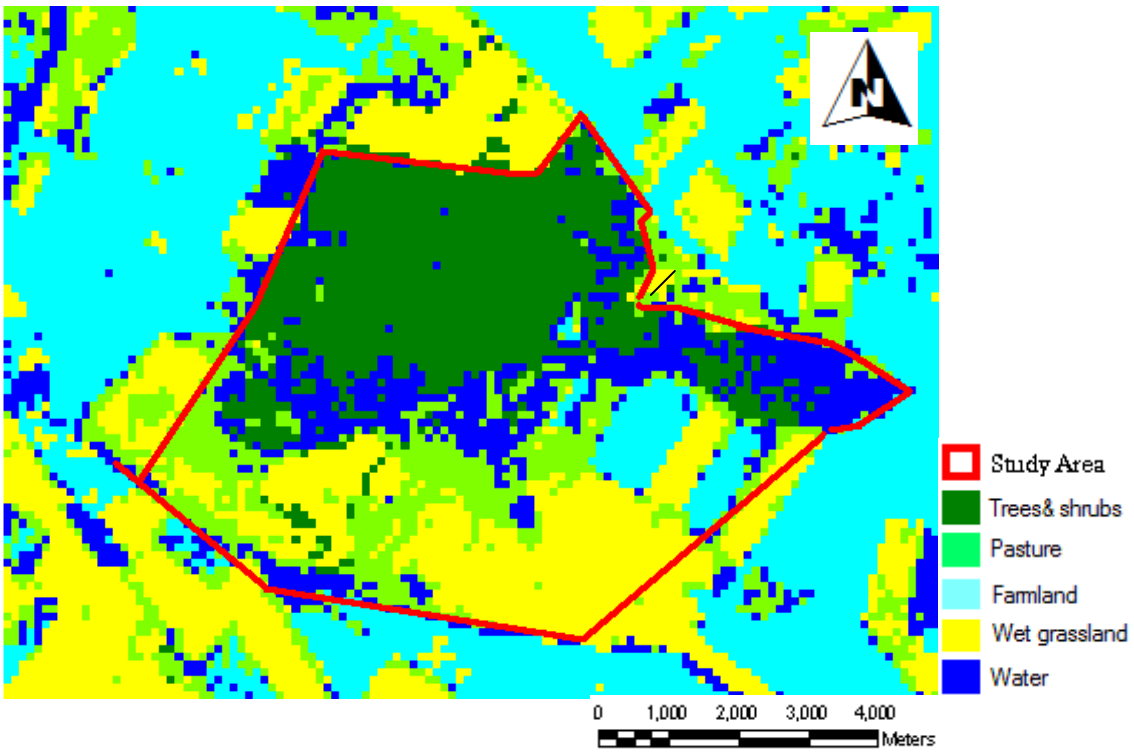

Figure 3-16: Land cover classes identified for 1984 Wicken Fen through supervised classification.

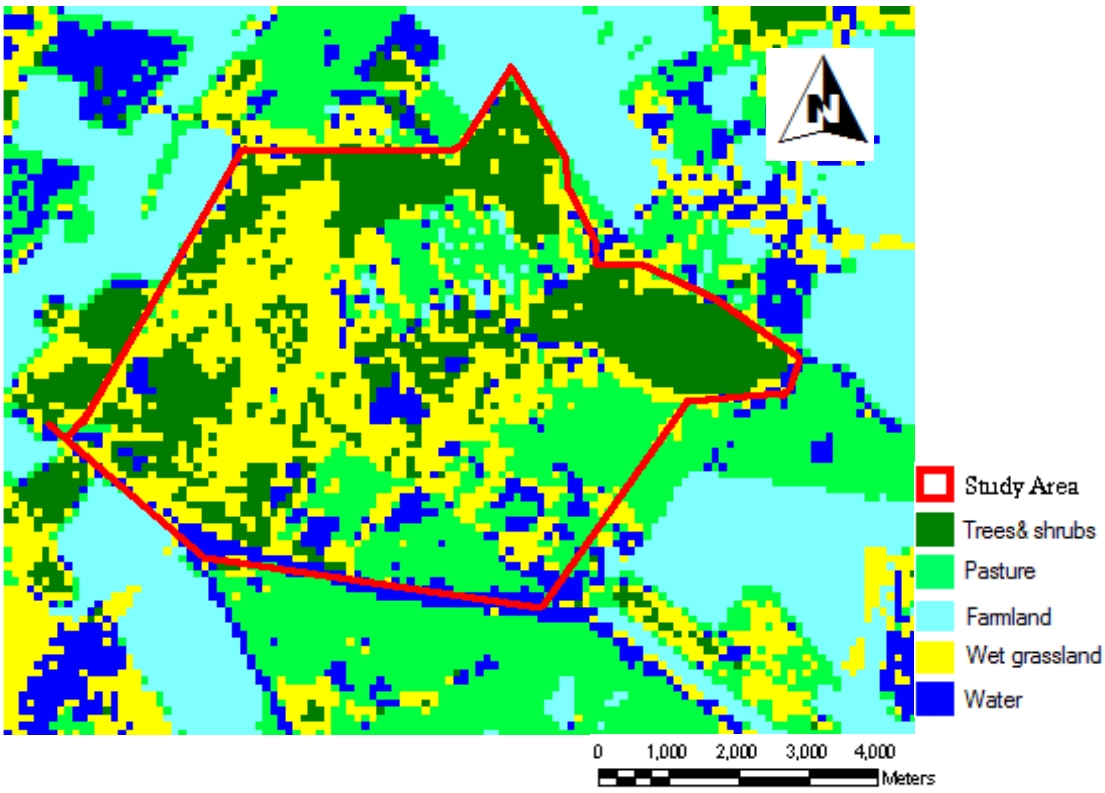

Figure 3-17: Land cover classes identified for 2009 Wicken Fen through supervised classification

Scattergrams of supervised classification for all five identified land cover classes of LandsatTM image in 1984 and LandsatTM image in 2009 for Wicken Fen are shown in Figures 3.18 and 3.19. It is noticed from interpretation of the scattergram that there is no overlap between the land cover classes; which means that the supervised classification has precisely determined land cover classes, and successfully avoided including pixels of ambiguous class (or 'mixels').

Ideally, training data should be based on in situ data collected in advance of image classification (Chen and Stow, 2002). Several spatial sampling objects are used to select training data in traditional supervised training from images: single pixel and polygons or blocks of pixels (Jensen, 1996). In this study pixel-based classification was used to classify the images. To select training areas aerial photography, Ordnance Survey maps, and fieldwork ground reference data (TWINSPAN group classification not used for training areas) have all been used as a guide for the selection of vegetation classes in supervised classification.

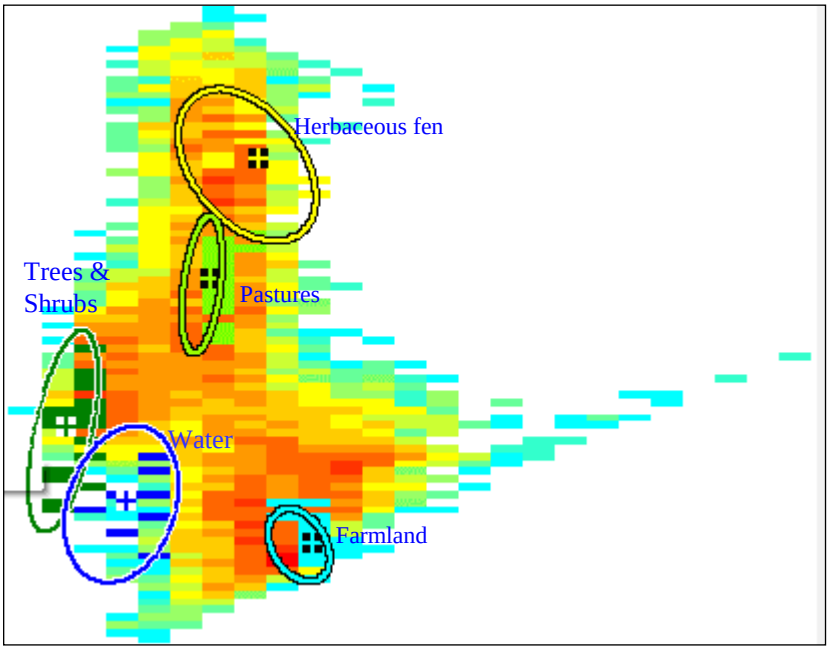

Figure 3-18: Shows scattergram created from the five class supervised classification using LandsatTM bands 2 and 4 of Wicken Fen, 1984.

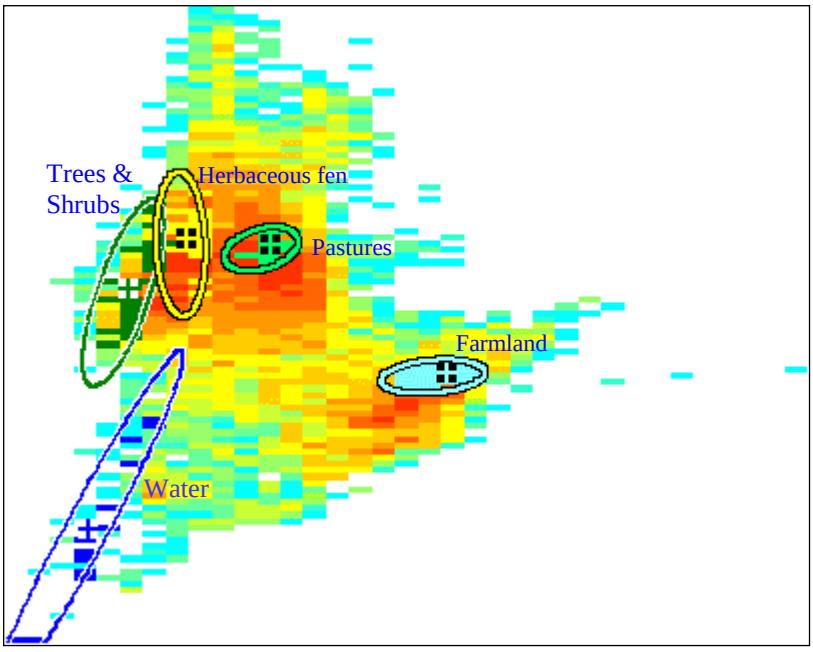

Figure 3-19: Shows scattergram created from the five class supervised classification using Landsat TM bands 2 and 4 of Wicken Fen, 2009.

The results of the supervised classification of the 2009 Landsat(TM), Fig. 3.21, data, when compared to classification of the 1985 Landsat(TM), Fig. 3.20, data, clearly show the changes in vegetation cover over this period. In 2009, Landsat(TM) imagery showed a decrease in the total cover of trees and shrubs (green) in the zones Verrall's Fen (A) and Sedge Fen (B) compared to 1984 Landsat imagery, and also showed an increase in cover of trees and shrubs in the zone Edmund's Fen (C); see Figures 3.20 and 3.21. The results obtained from the supervised classification were similar to the results obtained from aerial photo interpretation of 1985 and 2009 for Wicken Fen (Figures 3.5 and 3.8), confirming that for monitoring change to or from trees and shrubs using low resolution satellite imagery in the context of Wicken Fen, can be justified.

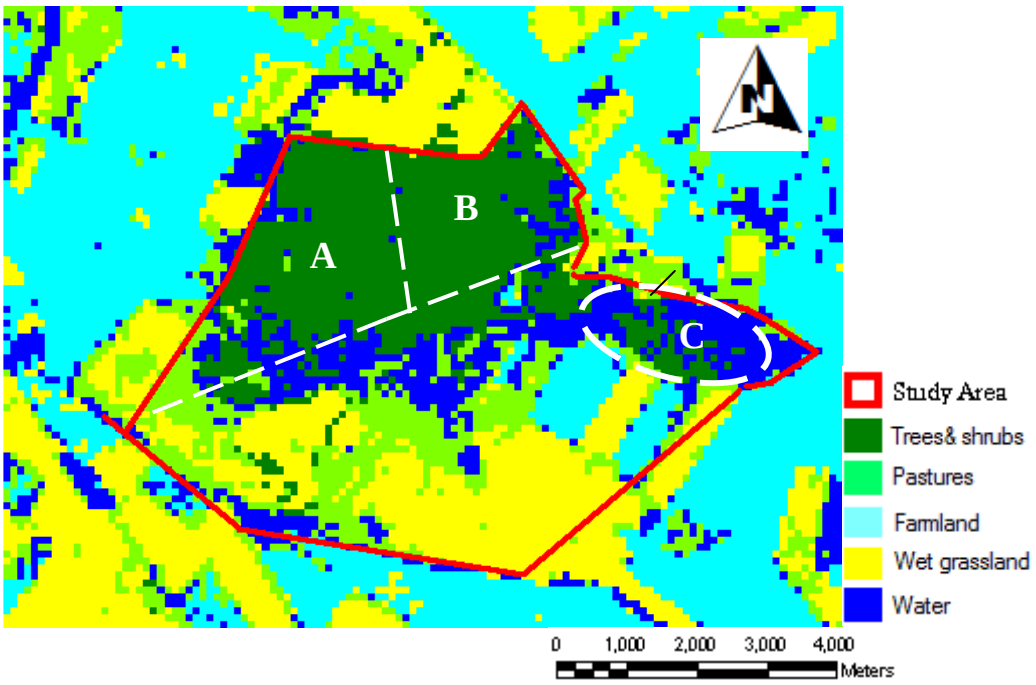

Figure 3-20: Wicken Fen 1984 supervised classification

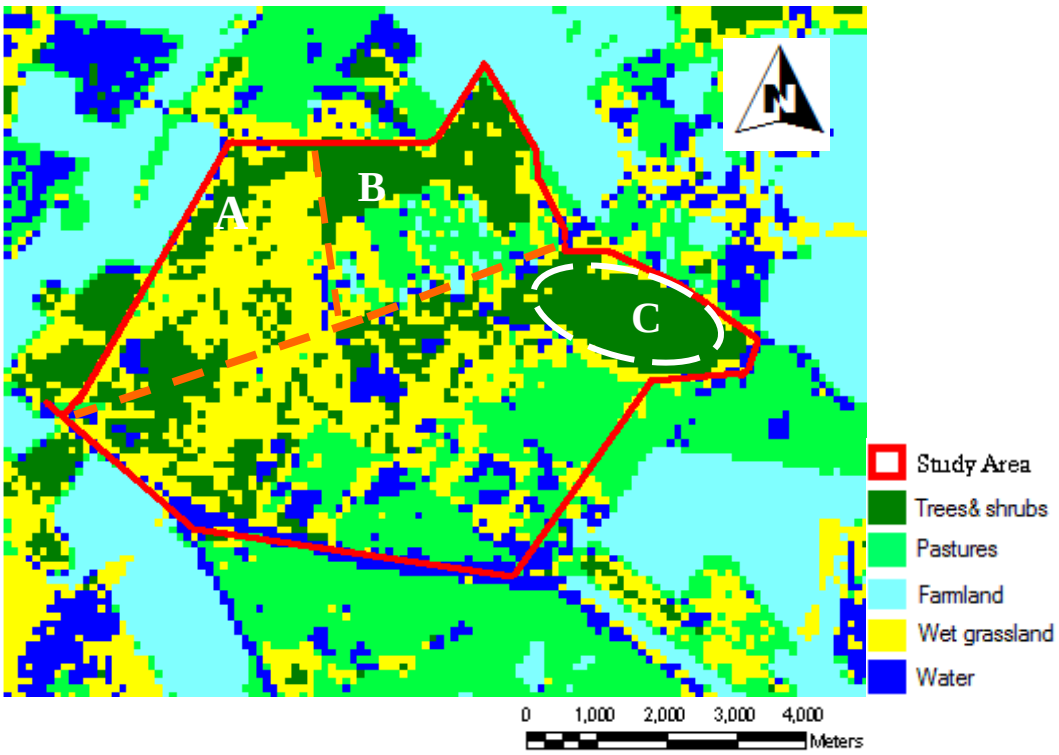

Figure 3-21: Wicken Fen 2009 supervised classification

3.3.3.3 Producing the change matrix

In this case, the two data sets being compared are from different periods (e.g. 1984 – 2009).

Following classification in ER-Mapper, the data was transferred to ArcGIS as raster data sets. The challenge is to represent and then visualise changes; that is, to produce a map showing changes between 1984-2009 (including 'no change'), and the widely used ArcGIS tool 'Map Calculus' is used to do this.

There are 5 original classes (trees and shrubs – T&S; pasture - P; farmland - F; wet grassland - WG; water - W) in each period – thus a maximum of 25 change possibilities, see Table 3.7.

Table 3-7: Shows the possible 25 changes (including no change).

#	ORIGINAL CLASS	CHANGED CLASS	COMMENT
1	T&S	T&S	No change
2	T&S	P	
3	T&S	F	
4	T&S	WG	
5	T&S	W	
6	P	T&S	
7	P	P	No change
8	P	F	
9	P	WG	
10	P	W	
11	F	T&S	
12	F	P	
13	F	F	No change
14	F	WG	
15	F	W	
16	WG	T&S	
17	WG	P	
18	WG	F	
19	WG	WG	No change
20	WG	W	
21	W	T&S	
22	W	P	
23	W	F	
24	W	WG	
25	W	W	No change

For the original class (1984) the five land cover classes were re-labelled as shown in Table 3.8.

Table 3-8: 1984 land cover classes, showing original class name and new label.

T&S	1
P	2
F	4
WG	6
W	8

For the changed class (2009) the five land cover classes were re-labelled as shown in Table 3.9.

Table 3-9: 2009 land cover classes, showing original class name and new label.

T&S	10
P	14
F	19
WG	22
W	24

Using the ArcGIS Map Calculus tool (which is called RASTER CALCULATOR), the two data sets are multiplied together, to produce a new pixel map, with the possible outcome pixel values shown in Table 3.10 below.

Table 3-10: Outcome pixel values and their meaning.

#	CLASS 1984	CLASS 2009	PRODUCT (possible outcome pixel value)	COMMENT
1	1	10	10	T&S to T&S No change
2	1	14	14	T&S to P
3	1	19	19	T&S to F
4	1	22	22	T&S to WG
5	1	24	24	T&S to W
6	2	10	20	P to T&S
7	2	14	28	P to P No change
8	2	19	38	P to F
9	2	22	44	P to WG
10	2	24	48	P to W
11	4	10	40	F to T&S
12	4	14	56	F to P
13	4	19	76	F to F No change
14	4	22	88	F to WG
15	4	24	96	F to W
16	6	10	60	WG to T&S
17	6	14	84	WG to P
18	6	19	114	WG to F
19	6	22	132	WG to WG No change
20	6	24	144	WG to W
21	8	10	80	W to T&S
22	8	14	112	W to P
23	8	19	152	W to F
24	8	22	176	W to WG
25	8	24	192	W to W No change

In the case of Wicken Fen, all possibilities were achieved, thus a palette of 25 colours was needed.

3.3.3.4 Detection of change in vegetation; results

The results obtained from change matrix analysis using the Arc Map (v10.1) are included in a chart showing class changes from 1984 to 2009 in Wicken Fen (Table 3.11 & 3.12). Based on the table change matrix, tall vegetation (trees, shrubs) covered an area of 1535 pixels (equivalent to 138.15 ha) in 1984: see Table 3.11. About 65.6% (1008 pixels equivalent to 90.7 ha) of total canopy for tall vegetation had changed by 2009 as follows: 19.0% (292 pixels equivalent to 26.28 ha) changed to pastures, 15.4% (237 pixels equivalent to 21.3 ha) changed to farmland, 34.9% (388 pixels equivalent to 34.9 ha) changed to wet grassland, and 6.1% (91 pixels equivalent to 8.19 ha) changed to water; see Table 3.12. The result obtained from the calculated change matrix confirmed that the reduction result obtained from aerial photographs indicated there has been a change in vegetation during the period 1984 to 2009 at Wicken Fen, although actual change rates differ (1.6% pa with aerial photos, 0.4% pa with supervised classification. Figure 3.22 shows the specific spatial distribution (location) of land cover change (change patterns) that have taken place between the individual cover types at Wicken Fen 1984- 2009. Table 3.13, shows the results obtained from two-class change matrix for supervised classification of satellite imagery 1984 versus satellite imagery 2009, with the overall percentage unchanged of 80%.

Table 3-11: Change matrix for Wicken Fen in the 1984-2009 period, values in pixels.

1984 → 2009 ↓	Trees & Shrubs	Pasture	Farmland	Wet grassland	Water	∑	Percentage retained unchanged in 2009 from 1984
Trees & Shrubs	527	196	550	58	42	1373	527/1373 38.4%
Pasture	292	292	446	144	235	1409	292/1409 20.7%
Farmland	237	699	536	270	490	2232	536/2232 24%
Wet grassland	388	105	288	187	201	1169	187/1169 20%
Water	91	1032	341	438	1289	3191	1289/3191 40.4%
∑	1535	2324	2116	1097	2257	9374	
Percentage from 1984 retained unchanged in 2009	527/1535 34.2%	292/2324 12.6%	536/2116 25.3%	187/1097 17%	1289/2257 57.1%		Overall % unchanged between two dates: 2831/9374 30.2%

Table 3-12: Class distribution for changed land cover in Wicken Fen in the 1984-2009 period, in hectares.

1984 → 2009 ↓	Trees & Shrubs	Pasture	Farmland	Wet grassland	Water
Trees & Shrubs		17.64	49.5	5.22	3.78
Pasture	26.28		40.14	12.96	21.15
Farmland	21.33	62.91		24.3	44.1
Wet grassland	34.92	9.45	25.92		18.1
Water	8.19	92.88	30.69	39.42	

Table 3-13: Two classes change matrix resulting from satellite imagery 1984 vs. satellite imagery 2009 of Wicken Fen.

TM 1984 → TM 2009 ↓	Trees & Shrubs	Others	∑	Percentage retained unchanged in 2009 from 1984
Trees & Shrubs	527	846	1373	527/1373 38%
Others	1008	6993	8001	6993/8001 87%
∑	1535	7839	9374	
Percentage from 1984 retained unchanged in 2009	527/1535 34.3%	6993/7839 89%		Overall % unchanged between two dates: 7520/9374 80%

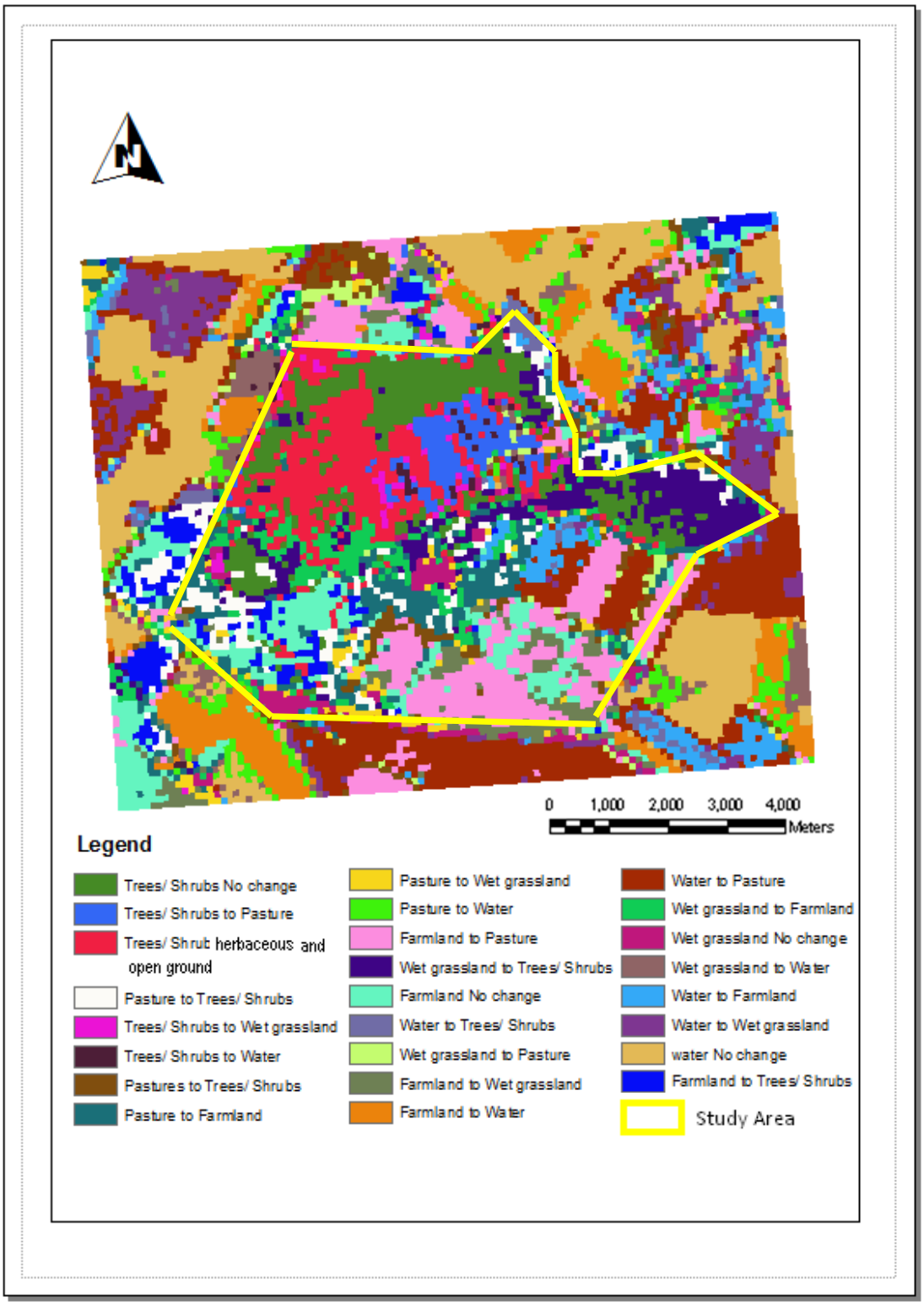

Figure 3-22: Land cover change map for Wicken Fen 1984-2009.

The results of the change matrix from the six classes of unsupervised classification of satellite imagery 1984 versus fieldwork 2010, with percentages unchanged, is shown in Table 3.14. Table 3.15, shows the results obtained from the two-class change matrix for unsupervised classification of satellite imagery 1984 versus fieldwork 2010. The overall accuracies for the change matrix of two and six classes were found to be 70% (Table 3.15) and 47.5% (Table 3.14), respectively. There are 6 original classes (trees and shrubs – T&S; pasture - P; farmland - F; wet grassland - WG; water – W; tall herbs- TH)

Table 3-14: Six classes change matrix resulting from unsupervised classification of satellite imagery 1984 vs. fieldwork 2010 for Wicken Fen.

TM1984 → FW 2010 ↓	T&S	P	F	WG	W	TH	∑	Percentage retained unchanged in 2010 from 1984
T&S	18	0	0	3	0	0	21	18/21 85%
P	0	1	2	0	0	0	3	1/3 33.3%
F	0	0	0	0	0	0	0	NA
WG	5	0	0	0	1	0	6	NA
W	2	1	1	1	0	0	5	NA
TH	2	0	2	0	1	0	5	NA
∑	27	2	5	4	2	0	19/40 47.5%	
Percentage retained unchanged in 2010 from 1984	18/27 66.7	1/2 50%	NA	NA	NA	NA		Overall % unchanged between two periods: 19/40 47.5%

Table 3-15: Two classes change matrix resulting from unsupervised classification of satellite imagery 1984 vs. fieldwork 2010 for Wicken Fen.

TM 1984 → FW 2010 ↓	T&S	Others	∑	Percentage retained unchanged in 2010 from 1984
T&S	18	3	21	18/21 85.7%
Other	9	10	19	10/19 52.6%
∑	27	13	28/40 70%	
Percentage retained unchanged in 2010 from 1984	18/27 66.6%	10/13 76.9%		Overall % unchanged between two periods :28/40 70%

The results of the error matrix from six classes unsupervised classification of satellite imagery 2009 versus fieldwork 2009, with user's and producer's accuracies, are shown in Table 3.26. Table 3.27, shows the results obtained from two-class error matrix for unsupervised classification of satellite imagery 2009 versus fieldwork 2010. The overall accuracies for the error matrix of two and six classes were found to be 65 % (Table 3.27) and 52.5% (Table 3.26), respectively, which are somewhat low results.

Table 3-16: Six classes error matrix resulting from unsupervised classification of satellite imagery 2009 vs. fieldwork 2010 for Wicken Fen.

TM 2009 → FW 2010 ↓	T&S	P	F	WG	W	TH	∑	User's Accuracy
T&S	18	2	0	1	0	0	21	18/21 85.7%
P	0	3	0	0	0	0	3	3/3 100%
F	0	0	0	0	0	0	0	NA
WG	6	0	0	0	0	0	6	NA
W	2	3	0	0	0	0	5	NA
TH	3	1	0	1	0	0	5	AN
∑	29	9	0	2	0	0	21/40 52.5%	
Producer's Accuracy	18/29 62.1%	3/9 33.3%	NA	NA	NA	NA		

With a positive *k* ("KHAT") value (0.20) the classification is shown to be better than a value on assignment of pixels, in this case 20% better than classification resulting from chance.

Table 3-17: Two classes error matrix resulting from unsupervised classification of satellite imagery 1984 vs. fieldwork 2010 for Wicken Fen.

TM 2009 → FW 2010 ↓	T&S	Others	∑	User's Accuracy
T&S	18	3	21	18/21 85.7%
Others	11	8	19	8/19 42.1%
∑	29	11	26/40 65%	
Producer's Accuracy	18/29 62.1%	8/11 72.7%		

With a positive *k* ("KHAT") value (0.28) the classification is shown to be better than a value on assignment of pixels, in this case 28% better than classification resulting from chance.

The results of the change matrix from five classes supervised classification of satellite imagery 1984 versus fieldwork 2009, with percentages unchanged, are shown in Table 3.28. Table 3.19 shows the results obtained from the two-class change matrix for supervised classification of satellite imagery 1984 versus fieldwork 2010. The overall percentages unchanged for the change matrix of two and five classes were found to be 77.5 % (Table 3.19) and 67.5% (Table3.18), respectively.

Table 3-18: Five classes change matrix resulting from supervised classification of satellite imagery 1984 vs. fieldwork 2010 for Wicken Fen.

TM 1984 → FW 2010 ↓	T&S	P	F	WG	W	∑	Percentage retained unchanged in 2010 from 1984
T&S	18	0	0	0	4	22	14/21 66.7%
P	0	3	2	0	1	6	3/6 50%
F	0	0	0	0	0	0	NA
WG	4	0	0	4	0	8	4/8 50%
W	2	0	1	0	1	4	1/4 25%
∑	24	3	3	4	6	26/40 65%	
Percentage from 1984 retained unchanged in 2010	14/24 58%	3/3 100%	NA	4/4 100 %	1/6 16.7%		Overall % unchanged between two periods: 26/40 65%

Table 3-19: Two classes change matrix resulting from supervised classification of satellite imagery 1984 vs. fieldwork 2010 for Wicken Fen.

TM 1984 → FW 2010 ↓	T&S	Others	∑	Percentage retained unchanged in 2010 from 1984
T&S	18	4	22	18/22 81.8%
Other	6	12	18	12/18 66.7%
∑	24	16	30/40 75%	
Percentage from 1984 retained unchanged in 2010	18/24 75%	12/16 75%		Overall % unchanged between two periods:30/40 75%

The results of the error matrix from the five class supervised classification of 2009 satellite imagery versus 2010 fieldwork with the user's and producer's accuracies are shown in Table 3.20. Table 3.27 shows the results obtained from the two-class error matrix for supervised classification of 2009 satellite imagery versus 2010 fieldwork. The overall accuracies for the error matrix of two and five classes were found to be 75 % (Table 3.21) and 52.5% (Table 3.20), respectively.

Table 3-20: Five classes error matrix resulting from supervised classification of satellite imagery 2009 vs. fieldwork 2010 for Wicken Fen.

TM 2009 → FW 2010 ↓	T&S	P	F	WG	W	∑	User's Accuracy
T&S	16	1	0	3	1	21	16/21 71%
P	0	1	0	2	0	3	1/3 33.3%
F	0	0	0	0	0	0	NA
WG	5	1	0	4	2	12	4/12 33.3%
W	0	1	0	3	0	4	NA
∑	21	4	0	12	3	21/40 52.5%	
Producer's Accuracy	16/21 71%	1/4 25%	NA	4/12 33.3%	0/3 NA		

With a positive *k* ("KHAT", or "kappa") value (0.23) the classification is shown to be better the classification is shown to be 23% better than classification resulting from chance.

Table 3-21: Two classes error matrix resulting from supervised classification of satellite imagery 2009 vs. fieldwork 2010 for Wicken Fen.

TM 2009 → FW 2010 ↓	T&S	Others	∑	User's Accuracy
T&S	16	5	21	16/21 71%
Other	5	14	19	14/19 73.7%
∑	21	19	30/40 75%	
Producer's Accuracy	16/21 71%	14/19 73.7%		

With a positive *k* ("KHAT" or "kappa") value (0.50) the classification is shown to be 50% better than classification resulting from chance.

The results of the error matrix from five classes of supervised classification of satellite imagery 1984 versus aerial photography 1985 with user's and producer's accuracies are shown in Table 3.22. Table 3.23, shows results obtained from the two-class error matrix for supervised classification of satellite imagery 1984 versus aerial photography 1985. The overall accuracies for the error matrix of satellite imagery vs. aerial photography of two and five classes were found to be 65 % (Table 3.23) and 52.5% (Table 3.22), respectively.

Table 3-22: Five classes error matrix resulting from aerial photography 1985 vs. satellite imagery 1984 for Wicken Fen.

AP 1985 → TM 1984 ↓	T&S	P	F	WG	W	∑	User's Accuracy
T&S	19	0	0	6	1	26	19/26 73.1%
P	0	2	0	0	0	2	2/2 100%
F	0	5	0	0	0	5	NA
WG	5	0	0	0	0	5	NA
W	2	0	0	0	0	2	NA
∑	26	7	0	6	1	21/40 52.5%	
Producer's Accuracy	19/26 73.1%	2/7 28.6%	NA	NA	NA		

With a positive *k* ("KHAT" or "kappa") value (0.13) the classification is shown to be 13% better than classification resulting from chance.

Table 3-23: Two classes error matrix resulting from aerial photography 1984 vs. satellite imagery 1985 of Wicken Fen

AP 1984 → TM 1985 ↓	T&S	Others	∑	User's Accuracy
T&S	19	7	26	19/26 73.1%
Other	7	7	14	7/14 50%
∑	26	14	26/40 65%	
Producer's Accuracy	19/26 73.1%	7/14 50%		

With a positive *k* ("KHAT" or "kappa") value (0.23) the classification is shown to be 23% better than classification resulting from chance.

The results of the error matrix from five classes supervised classification of satellite imagery 2009 versus aerial photography 2009 with user's and producer's accuracies are shown in Table 3.24. Table 3.25, shows results obtained from the two classes error matrix for supervised classification of satellite imagery 2009 versus aerial photography 2009. The overall accuracies for the error matrix of two and five classes were found to be 70 % (Table 3.25) and 52.5% (Table 3.24), respectively.

Table 3-24: Five classes error matrix resulting from aerial photography 2009 vs. satellite imagery 2009 for Wicken Fen.

AP 2009 → TM 2009 ↓	T&S	P	F	WG	W	∑	User's Accuracy
T&S	13	0	0	8	0	21	13/21 61.9%
P	1	2	0	1	0	4	2/4 50%
F	0	0	0	0	0	0	NA
WG	2	2	0	6	2	12	6/12 50%
W	1	0	0	2	0	3	NA
∑	17	4	0	17	2	21/40 52.5%	
Producer's Accuracy	13/17 76.5%	2/4 50%	NA	6/17 35.3%	NA		

With a positive *k* ("KHAT" or "kappa") value (0.25) the classification is shown to be 25% better than classification resulting from chance.

Table 3-25: Two classes error matrix resulting from aerial photography 2009 vs. satellite imagery 2009 of Wicken Fen.

AP 2009 → TM 2009 ↓	T&S	Others	∑	User's Accuracy
T&S	13	8	21	13/21 62%
Other	4	15	19	19/23 78.9%
∑	17	23	28/40 70%	
Producer's Accuracy	13/17 76.5%	15/23 65.2%		

With a positive *k* ("KHAT" or "kappa") value (0.40) the classification is shown to be 40% better than classification resulting from chance.

A summary of overall classification accuracy from two and five classes of 2009 Wicken Fen aerial photography versus fieldwork 2010 is shown in Table 3.26.

Table 3-26: Shows accuracy of aerial photography 2009 versus fieldwork 2010, see Tables 3.5 and 3.6.

Number of classes	Aerial photography	Overall classification accuracy
2	2009	90%
5	2009	80%

On the basis of Table 3.26 it was concluded that aerial photography was comparable to fieldwork and should be use to assess the quality of satellite classification. A summary of overall classification accuracy from an unsupervised classification (2 and 6 classes) and supervised classification (2 and 5 classes) for Wicken Fen satellite image using aerial photography for1984 versus fieldwork 2010 is shown in Table 3.27.

Table 3-27: Shows accuracy of satellite imagery using 1985 aerial photography for validating 1984 satellite imagery and using 2010 fieldwork for validating 2009 satellite imagery.

Classification	Class	Year of satellite imagery	Overall classification accuracy
Unsupervised classification	2	1984	70%
		2009	65%
	6	1984	47.5%
		2009	52.5%
Supervised classification	2	1984	75%
		2009	75%
	5	1984	65%
		2009	52.5%

3.4 TWINSPAN classification

TWINSPAN analysis was undertaken on the 84 species in 32 families (see Appendix 4a, 4b) recorded from 40 quadrats (coordinates captured in the field by GPS) located on 6 transects at Wicken Fen in 2010. The distribution of quadrat samples belonging to 4 TWINSPAN sample end-groups identified by the analysis (see below) along the six transects is shown in Fig. 3.23.

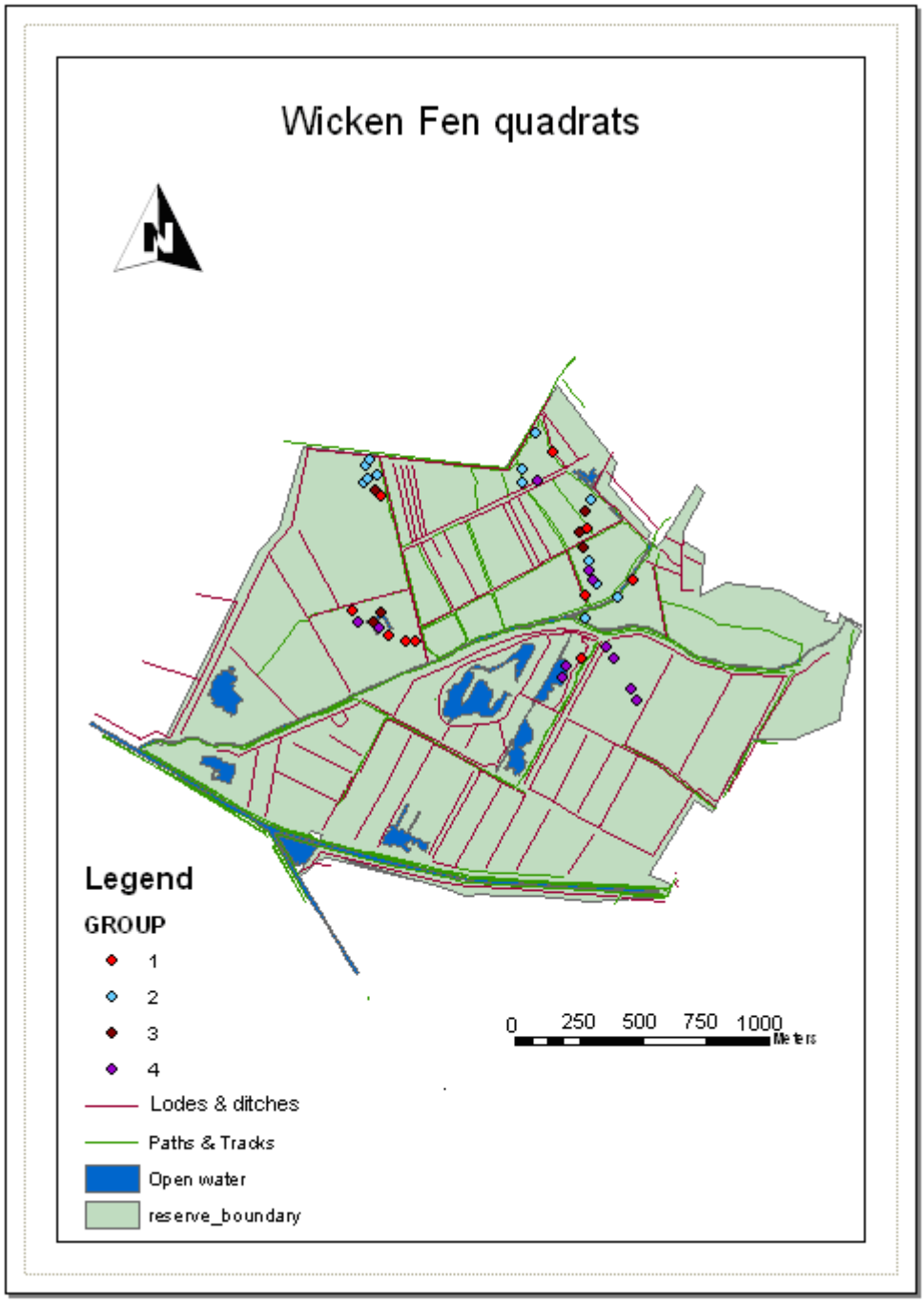

Figure 3-23: Distribution of quadrat positions (for 4 TWINSPAN sample groups) in Wicken Fen.

Sample end groups were all located at the second level of the classification, with eigenvalues for the divisions producing these groups all reasonably high, (> 0.500). For the vegetation communities that these represent, see Appendix 5. The first division [Eigenvalue = 0.541] divided the 40 quadrats into a negative (right) group including 29 quadrats, and a positive (left) group including 11 quadrats. A dendrogram showing the classification is given in Fig. 3.24 and list of species with their groups and indicator species in Table 3.28. The indicator species in the negative group were *Poa trivialis* (Rough Meadow-grass), *Galium palustre* (Common Marsh-bedstraw), *Cladium mariscus* (Great Fen-sedge) and *Symphytum officinale* (Common Comfrey). The indicators in the positive group was *Festuca rubra* (Red Fescue). The second division at the second hierarchical level [Eigenvalue = 0.502] divided the 29 quadrats into a negative group including 10 quadrats, (indicator species: *Carex distans* (Brown Sedge)), and a positive group including 19 quadrats (indicator species: *Lysimachia vulgaris*(Yellow Loosestrife), *Agrostis stolonifera* (Creeping Bent), and *Galium palustre*(Common Marsh-bedstraw)) . The fifth division [Eigenvalue = 0.520] at the same level divided the 19 quadrats into a negative group including 13 quadrats, (indicator species: *Cardamine hirsuta* (Hairy Bittercress)), and a positive group including 6 quadrats, (indicator species: *Alopecurus geniculatus* (Ground Elder)).

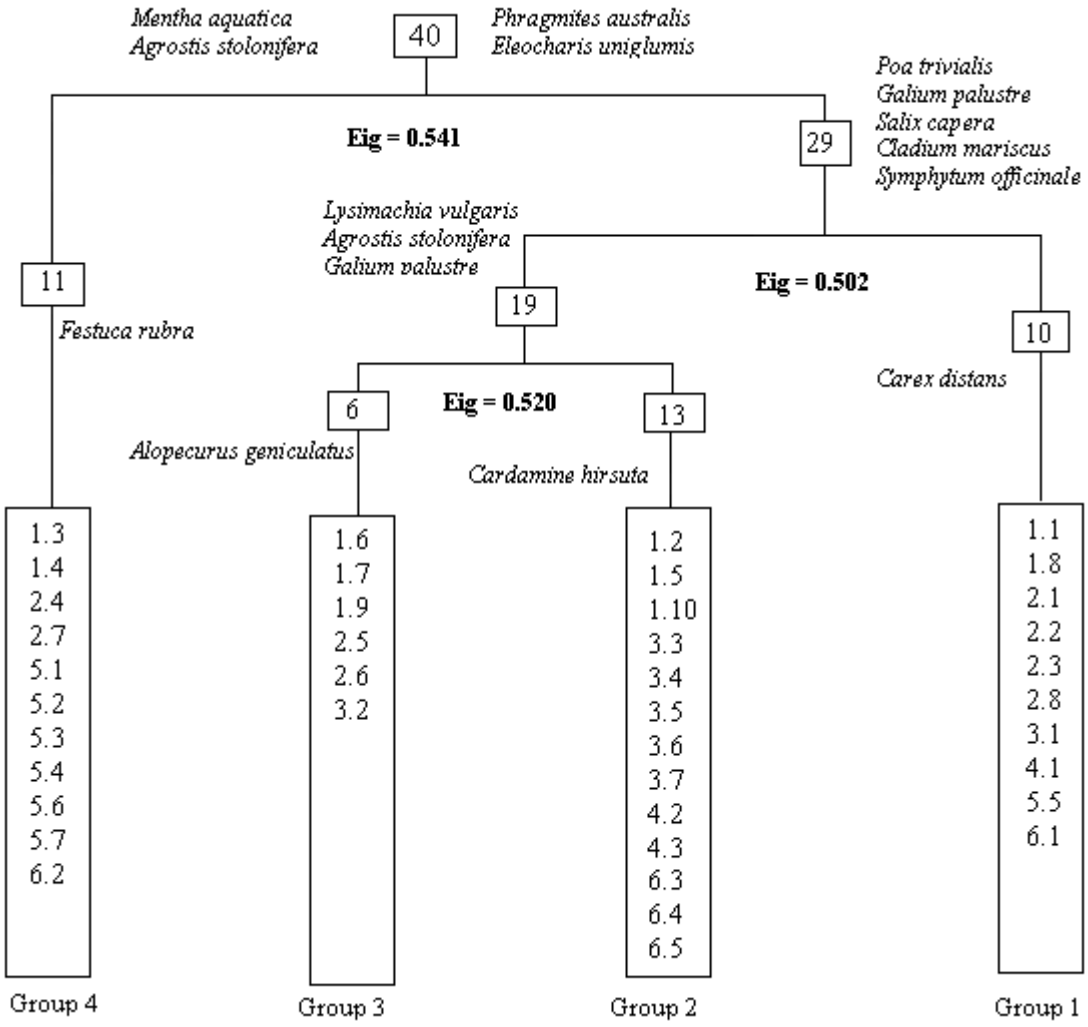

Figure 3-24: Dendrogram of the TWINSPAN classification of 40 quadrats in Wicken fen.
(3.2 = 3 means number of Line transect, 2 means number of Quadrat)

Table 3-28: TWINSPAN groups, species and indicator species after species classification (for complete species names see Appendix 4b)

Group Number	Species name abbreviations	Indicator species
1	Arel, Clma, Caac, Cadi, Capa, Ciar, Cipa, Bepe, Ephi, Feru, Gaap, Glhe, Hepu, Juin, Lope, Lyvu, Meaq, Moca, Popa, Potr, Poer, Rufr, Ruob, Sapu, Saca, Sopu, Syof, Phau, Phar	Cadi
2	Ephi, Hepu, Popa, Potr, Syof, Clma, Gaap, Rufr, Case, Cafl, Phau, Caac, Cipa, papr, Fiul, Ajre, Anod, Atfi, Cahi, Civu, Crmo, Fepr, Glhe, Jubu, Lapr, Relu, Ruhy, Sare, Sodu, Stme, Trre, Urdi, Feru, Gapa, Agat, Hola, Irps, Juef, Ciar, Juin, Phar	Cahi
3	Moca, Lyvu, Case, Phau, Caac, Cipa, Ansy, Alge, Capl, Cari, Popr, Fiul, Jubu, Urdi, Feru, Gapa, Irps, Lemi, Ratr, Tyla	Alge
4	Rafl, Ruac, Saca, Rali, Sper, Hyvu, Alpl, Mysc, Lyeu, Letr, Bepe, Chau, Caot, Ceni, Crhe, Beer, Lyfl, Thfl, Case, Cafl, Phau, Feru, Gapa, Hola, Irps, Juin, Juef, Ciar, Bepe, Capa, Dagl, LyvuMeaq, Elun, Lemi, Ratr, Tyla, Phar	Feru

3.5 TABLEFIT Classification

Depending on TABLEFIT classification to determine UK NVC categories (and equivalents in the EC CORINE biotopes classification) the first TWINSPAN group has the highest level of similarity to a recognised NVC type: OV26d *Epilobium hirsutum* tall herb wet meadow community (with goodness of fit 32; CORINE 37.7), sub community *Arrhenatherum elatius- Heracleum sphondylium* . The highest matched community type for the second group was to M28b *Iris pseudacorus - Filipendula ulmaria* tall herb wet meadow community sub community *Urtica dioica – Galium aparine* (with goodness of fit 45; CORINE 37.1). For sample-group three the highest matched community similarity to a recognised NVC type was OV26b *Epilobium hirsutum* tall herb wet meadow community (with goodness of fit 48; CORINE 37.7), subcommunity *Phragmites australis.* The last TWINSPAN group had the highest matched community type: S14c *Sparganium erectum*

swamps and tall herb fens community (with goodness of fit 42; CORINE 53.143), subcommunity *Mentha aquatic*.

3.6 Statistical analysis

The significance of differences in the mean values of environmental and botanical variables, measured at sample quadrats between the four sample groups, was tested using one-way ANOVA with mean comparison by Tukey's method, in Minitab (version 16).

Table 3.29 shows the mean values (± SD) for all measured environmental variables across the quadrats sampled in Wicken Fen, together with the results of ANOVA by Group. ANOVA tests produced no significant inter-group differences for three environmental variables (soil conductivity, water conductivity and water depth). Two environmental variables (soil pH and shade %) and one vegetation variable (plant height), did however show significant differences among the four TWINSPAN groups.

Table 3-29: Shows mean values and standard deviation of the mean (± SD) for a) soil pH; b) soil conductivity; c) water conductivity; d) shade; e) water depth; and f) mean vegetation height for TWINSPAN Groups, as shown by one-way ANOVA and application of Tukey's mean separation test. Mean values sharing a superscript letter in common, per variable, are not significantly different.

Groups	a) Soil pH	b) Cond. Soil ($\mu S\ cm^{-1}$)	c) Water Cond ($\mu S\ cm^{-1}$)	d) Shade %	e) Water depth (m).	f) Height (m)
	Mean	Mean	Mean	Mean	Mean	Mean
Group 1	7.5060^{a} ± 0.33	539.5±203.4	147.7±316.5	31.60^{ab} ±43	0.0	3.847^{ab}± 5.1
Group 2	7.4085^{a} ±0.36	640.1±130.3	0.0	68.57^{a}±41.95	0.0	7.352^{a}± 5.6
Group 3	7.2336^{a} ±0.77	551.2±177.6	392±432	$44.^{33ab}$±48.92	0.043± 0.069	4.4^{ab}±4.1
Group 4	6.9517^{a} ±0.35	870.5±587.7	462±856	0.0^{b}	0.69±0.126	1.1^{b}±0.95
$F_{3, 36}$	2.37	2.03	1.97	6.91	2.47	3.99
P	ns	n.s	n.s	***	n.s	*

* = p≤ 0.05 ** = p≤ 0.01 *** = p≤ 0.001 n.s = p >0.05

The analysis confirmed that the % shade had a significant difference between group means in group 2 and group 4 ($p = 0.001$) (Figure 3.25), with group 2 samples being largely located under tree/ shrub overstorey vegetation, while group 4 samples were much more open. There was a significant difference between height in group 2 and group 4 ($p = 0.015$) (Figure 3.26).

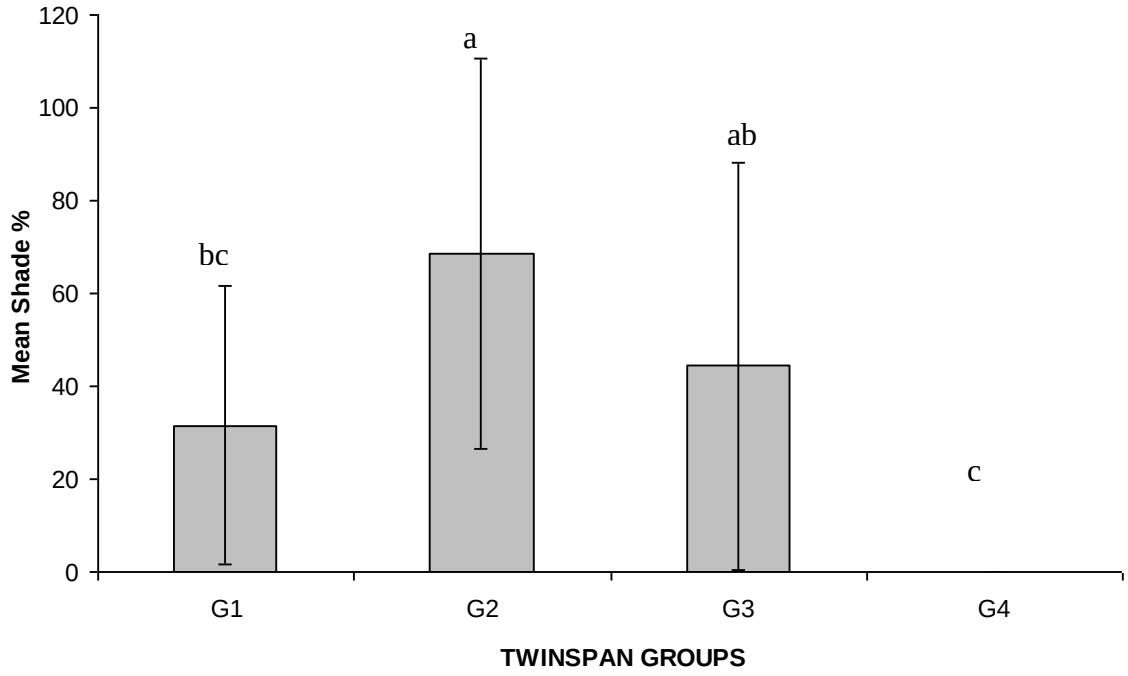

Figure 3-25: Mean (± S.D) values for soil pH for 4 sample groups. Different letters above value bars represent a significant difference between group means.

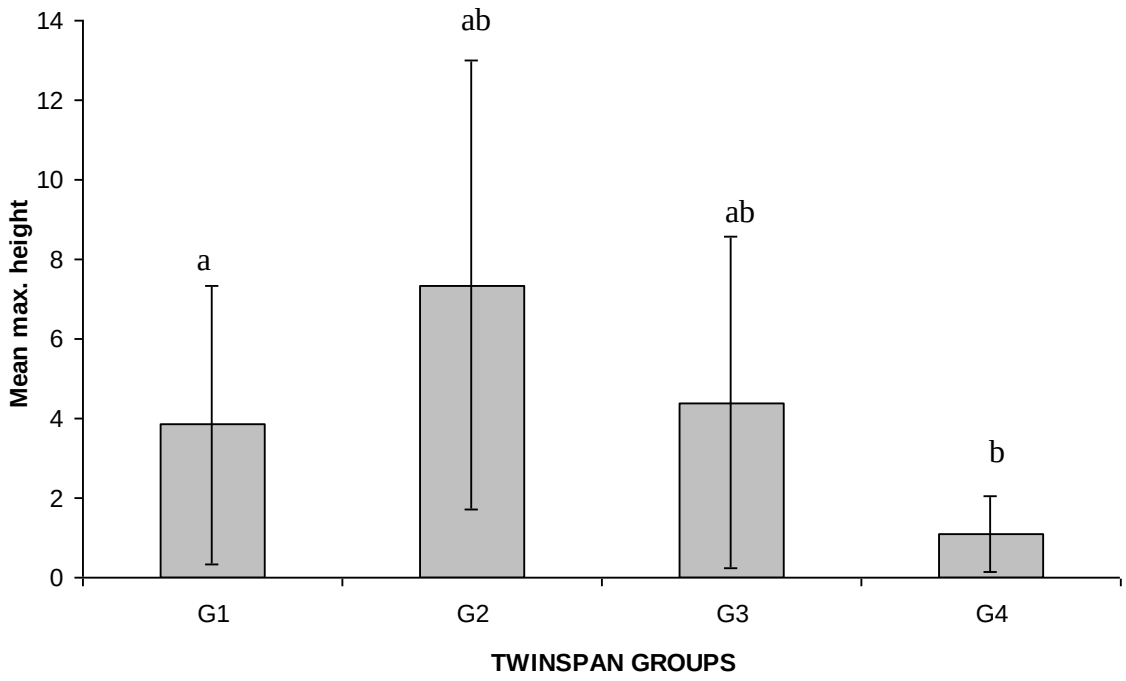

Figure 3-26: Mean (± S.D) values for shade height for 4 sample groups. Different letters above value bars represent a significant difference between group means.

In addition to testing the significance of differences in mean values of environmental and botanical variables, I measured the significance of differences in mean values of Ellenberg's indicator values, based on the data for UK plant species given by Hill et al. (2004), see Appendix 6.

Table 3.30 shows the mean values (±SD) for Ellenberg's indicator values for all plant species present in samples, comprising each sample group in Wicken Fen, together with the results of ANOVA by Group. ANOVA tests produced no significant inter-group differences for reaction (soil pH or water pH) and light. Moisture value, however, did show significant differences among the four TWINSPAN groups.

Table 3-30: Shows ean values and standard deviation of the mean (± SD) for a) Light; b) Moisture; c) soil/water pH) for TWINSPAN groups depending on Ellenberg's indicator values for plants, as shown by one-way ANOVA and application of Tukey's mean test. Mean values sharing a superscript letter in common are not significantly different.

Groups	a) Light	b) Moisture	d) Reaction (soil pH or water pH)
	Mean	Mean	Mean
Group 1	7.13 ± 0.57	6.93^{b} ± 1.57	6.3 ± 1.26
Group 2	6.93± 0.65	6.71^{b} ± 1.57	6.29 ± 0.87
Group 3	7.05 ± 0.51	8.55^{a} ± 1.7	6.2 ± 1.00
Group 4	7.09 ± 0.46	7.72^{ab} ± 2.02	6.16 ± 0.95
P	n.s	***	n.s

*** = $p \leq 0.001$ n.s = $p > 0.05$

ANOVA analysis confirmed that there was a significant difference between the four TWINSPAN groups in mean moisture ($P = 0.001$) (Figure 3.27), with samples from Group 3 supporting species with high Ellenberg soil moisture values. There were no significant differences between the four TWINSPAN groups for mean light and mean reaction (soil pH or water pH).

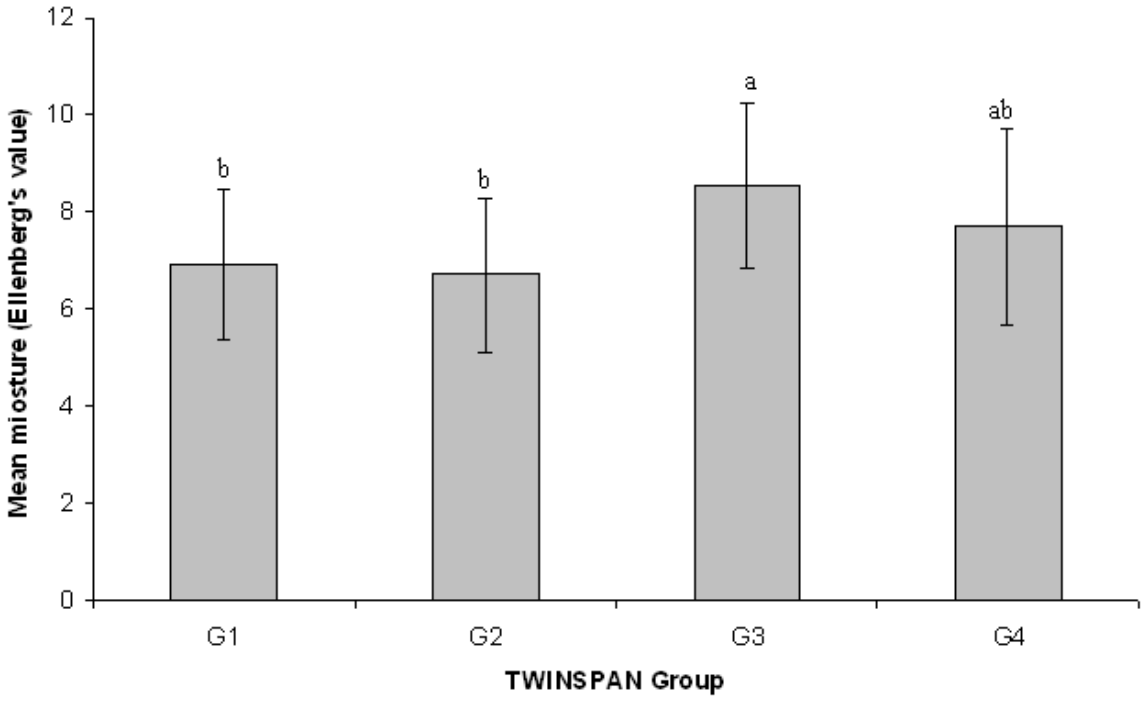

Figure 3-27: Mean (± S.D) values for shade percentage for 4 sample groups. Different letters above value bars represent a significant difference between group means.

3.7 Discussion

Successful use of aerial photography interpretation in the study of wetland vegetation ecology depends mainly on the high spatial resolution of images to provide good results for interpretation, mapping, and the comparisons between different periods. However, this investigation has shown that similar information can be acquired from satellite imagery, which is much more accessible. In the past three decades, major advances have been made in the application of remote sensing techniques to landscape characterisation, habitat monitoring, and spatial analysis of surface cover change (Ahmed et al., 2009).

Depending on the results obtained from aerial photographs and Landsat TM used in for Wicken Fen during the period between 1985 and 2009, they proved effective at detecting changes in vegetation over time. There is clearly potential to, apply this technique, elsewhere, for example to detect temporal changes in wetland vegetation in Libya. Plant communities of wetlands in semi-arid areas are particularly sensitive to any change, whether natural or change as a result of human activity (especially changing rainfall pattern, drainage etc.); so using remote sensing techniques to study these ecosystems will provide valuable information that is useful for management plans and conservation of these habitats.

Aerial photographs were used successfully for studying the vegetation cover in Wicken Fen in the period between 1985 and 2009. As is clear from interpretation of 1985 aerial photos, when comparing this period with 2009 aerial photos in Verrall's Fen and Sedge Fen (parts of Wicken Fen), the total cover of tall vegetation (trees and shrubs) has changed. Calculation of total cover of trees and shrubs and delineation using ArcMap GIS for four years 1985, 1999, 2003 and 2009, quantified the changes in tree/shrub cover. Godwin (1936) reported that some scrub, such as *Frangula* (a small tree), suffers from ″die-back″ caused by the fungi *Nectria cinnabrina* and *Fusarium* sp., and is an important cause of loss of dominance in adult carr. Also, Friday (1997) noted that in Wicken Fen a large proportion of the *Frangula* standing on all parts of the Fen became dead wood. However, undoubtedly much more important than this is active management to clear fen carr and

woodland, and restore open fen vegetation within the Nature Reserve over the study period.

The most common vegetation mapping technique in the world is aerial photography interpretation (Lewis and Phinn, 2011), which has a higher level of detailed mapping for vegetation communities, and high accuracy using manual interpretation techniques, for example in a tropical freshwater swamp (Harvey and Hill, 2001). Pollard and Briggs (1984) reported that aerial photography provided valuable information for determining the distribution of carr vegetation at Wicken Fen in 1929.

Based on morphometric measurements made from the aerial photography interpretation obtained from the delineation of total tall vegetation cover of Wicken Fen (see Figures 3.11 and 3.14), the total tall vegetation cover decreased annually by 1.7% from 1985 to 2009. This quantified change of canopy height in Wicken Fen over the study period is most likely primarily of the woodland and carr removal management programme, rather than due to natural change. Rowell and Harvey (1988) reported that the major vegetation in Wicken Sedge Fen in the 1980s was scrub, and the most abundant species were *Salix cinerea* and *Frangula* sp. A part of the carr in Sedge Fen (a part of Wicken Fen) was removed due to subsequent management operations, and evidence of recent clearance activities was personally observed during ground truth field work in 2010. Mountford et al., (2012) noted some evidence that fen herbaceous vegetation was re-establishing on Verrall's Fen (a part of Wicken Fen), where carr had been cleared.

Overall classification accuracy from aerial photography of 2009, for two and five classes (90% and 80% respectively) indicates that through my classification method, it was generally possible to correctly distinguish map classes (see Table 3.26).

The results obtained from analysis of LIDAR imagery clearly show the changes in vegetation cover in both Verrall's Fen (A) and Sedge Fen (B) (see Figure 3.8), compared with the aerial photos of 1985 and 2009. This result suggests that using LIDAR for the study of vegetation cover change has great potential for use in ecological research, because it directly measures the physical attributes of vegetation canopy structures, that are highly correlated with the basic plant communities at differeing canopy levels. Genc et al., (2004)

state that the most practical methodology for determining the size of vegetation based on height is LIDAR, providing an accurate and cost-effective alternative to mapping wetlands from the ground). Antonarakis et al. (2008) used LiDAR data to classify forest and ground types, and reported success in accurately classifying around 95%. However, it is expensive to obtain – and therefore the 'repeats' needed for monitoring may not be available.

In addition, when comparing aerial photos for 2009 with Wicken Fen-NVC map results (Colston, 1995), it can be shown that much of Verrall's Fen (a part of Wicken Fen) has changed from W2 community (*Salix cinerea, Betula pubescens, Phragmites australis*, typically a community of topogenous fen peats, encompassing most of the woodland recognised as 'fen carr' in Britain: Rodwell 1991) to OV26c (*Epilobium hirsutum*, tall herb wet meadow community: characteristic of moist but well-aerated soils, shade–sensitive, and on mesotrophic to eutrophic mineral soils and fen peats in open water: Rodwell 1991).

Colston (1995) noted that almost all of Verrall's fen (a part of Wicken Fen) carr falls into the W2 woodland community, and usually the average of soil pH based on the Ellenberg's indicator values is between 4-6. According to TABLEFIT results, it showed the W2 community changing to OV26c (tall herb wet meadow community), which prefers circumneutral soil conditions. Rodwell (1991) has described the habitat of *Epilobium hirsutum* (which is an indicator of OV26c) as tall herb wet meadow, sensitive to shade. It grows in open areas avoiding the canopy of tall trees and shrubs, indicating that areas of Verrall's Fen were cleared from their woodland canopy to become open areas suitable for growth of the tall herb community.

Unsupervised and supervised classifications are the usual methods used for satellite image interpretation. The results obtained from LandsatTM image analysis for 1984 imagery using unsupervised classification demonstrates good results using six land cover classes. A limitation of this method is that the classes are produced based on natural land cover features, which may not correspond to the features that the user needs to resolve. In the six classes, LandsatTM image analysis of the 2009 imagery succeeded in showing some change compared with 1984, with the results being fairly similar to those obtained from analysis of aerial photography. Using ten land cover classes produced classes which were

difficult to identify, based on field work and knowledge of the area (see Figure 3.12). Analysis of Landsat satellite imagery and aerial photography for the detection of land-cover changes between the two decades was done successfully elsewhere (e.g. Awotwi 2009; Adu-Poku 2010), while aerial photographs and GIS were used in an analysis of vegetation change for meadow landscape and forest watershed, and provided good results (e.g. Miller 1999; Anderson 2007). The classification of LandsatTM satellite imagery achieved a high level of accuracy, and the satellite data provides an adequate description of the major land cover for Wicken Fen wetland, but it remains apparent that aerial photography can sometimes provide information that cannot be extracted from satellite data.

Depending on the results obtained from supervised classification, maximum likelihood classification (MLC) showed better results for distinguishing Wicken Fen vegetation classes (see Table 3.27). Supervised classification often yields maps with a higher mapping accuracy (Johnston and Barson 1993), and achieves good separation of classes (Soliman and Soussa, 2011). Aerial photography, Ordnance Survey maps, and field work ground-truthing all proved useful here as a guide for the selection of vegetation classes in supervised classification.

The spectral overlap between wetland cover types is a problem frequently identified in the application of remote sensing to wetland environments (e.g. Johnston and Barson 1993, Sader et al. 1995), because, commonly, different vegetation types may possess the same spectral signature in remotely sensed images (Xie et al. 2008). The results from scattergrams of supervised classification for all land cover classes of the LandsatTM image in 1984 and LandsatTM image in 2009 showed no overlap between the land cover classes; which means that by not including class pixels other than the intended class, it was clearly possible to show decreases in the total of tall vegetation cover here between 1984 – 2009.

Results for the detection of change in vegetation using ArcMap (v 10.1) showed that cover of tall vegetation decreased by 65.6% between 1984 and 2009. More than half of the percentage change in the tall vegetation cover is change to wet grassland, with a further 19.0% change to pasture (Table 3.11). For unsupervised classification (two classes) of the LandsatTM images for 1984 and 2009 at Wicken Fen, the classification had an overall

accuracy of 70% and 65% respectively; and in six class the classification had a lower overall accuracy of 47.5% and 52.5% respectively. This is because in an unsupervised classification, the classes produced are based on natural breaks in the distribution of pixel colour in the image, and the vegetation in flooded and open water types may be too similar for the software to separate them into distinct classes. Overall classification accuracy from two classes supervised in the LandsatTM images for 1984 and 2009 were 75% (Table 3.27).

TWINSPAN classification showed that sample-group 1, the largest TWINSPAN group, representing all transects examined at the site. The indicator of the group 2 was *Cardamine hirsuta*, which has the highest level of similarity to a recognised NVC type: M28b. However, statistical analyses showed that shade % had a significant difference between group means 2 and group 4, as well as in height, suggesting that quadrats position group 2 samples being largely located under tree/ shrub overstorey vegetation, while group 4 samples were much more open.

The changes of vegetation cover that occurred in Sedge Fen and Verrall's Fen over the whole period of the study, 1985-2009, were substantial, and remote sense imagery analysis proved able to show and quantify these changes. In 1985, Verrell's Fen was almost completely covered by tall vegetation (Fig3.9), mainly fen scrub, abundant by alder *Frangula* (e.g. Rowell and Harvey 1988). Comparing aerial photos of 1985 with aerial photographs of 1999 showed some change in scrub cover change, which may be a result of successional change; and possible impact of "die-back" caused by fungal disease. A big change occurred after the deliberate removal of scrub in Verrall's Fen and Sedge Fen (B) see Figure (3.2) as part of the management plan to protect herbaceous wetland species such as *Molinia caerulea* (Purple Moor-grass), which has declined in southern England (though still common in the northern mountains and wet moors), and *Cladium mariscus* (Great Fen-sedge), which is now rare in Europe (Colston and Friday 1999).

Chapter 4- Caerlaverock Reserve study area 2

4

The reader should note that the investigation of this chapter follows the same procedures as chapter 3, and is reported in a very similar way, for reasons of ease of comparison.

4.1 Introduction

The Solway is the largest area of saltmarsh in Scotland, recognised as one of the most important estuaries in the UK (JNCC, 2004), and usually classified as one geographic unit (Harvey and Allan, 1998). Saltmarshes are commonly associated with estuaries (also called firths and sea lochs in Scotland: e.g. Taubert & Murphy, 2012). An important feature of Scottish saltmarshes is the frequent occurrence of natural transitional habitats; they are under-represented by the National Vegetation Classification (NVC: JNCC, 2004). In Scotland a transition from saltmarsh to terrestrial vegetation (e.g. grassland, freshwater swamp or woodland) commonly develops, and is often complete (Harvey and Allan, 1998).

Saltmarshes of the Solway contain a wide range of plant communities, including transitions to grassland and brackish fen, which are characteristic of Scottish marshes (Barne et al., 1996). A few surveys have examined NVC classes for Solway saltmarshes, including the merses of Caerlaverock NNR (Peberdy 1989) and estuaries entering the Solway (Zimmerman and Murphy, 2007). Other relevant studies of the Solway include geomorphological mapping (Tipping and Adams, 2007; Hansom, 2003), coastal management (Hansom and McGlashan, 2004), erosion and sediments (Allen, 1989), morphological areal changes using maps and aerial photographs (Marshall 1962).

The Scottish coasts hold about 15% (equivalent to 6748 ha) of the British 45,337 ha saltmarsh resource, of which the marshes in the Solway Firth account for 8% (equivalent to 539.8 ha: Hansom and McGlashan, 2004). The sea lochs and the coastal saltmarshes of Scotland's estuaries are the least well studied of the country's rich array of habitats, with only limited studies of Scottish saltmarshes (Harvey and Allan, 1998). In west Scotland a *Puccinellia-Festuca* community, often also with large areas of *Juncus gerardii*, commonly dominates the vegetation structure of the marshes. In northwestern marshes, a large area in

the pioneer and low marsh communities are dominated by *Salicornia, Suaeda*, sometimes with *Puccinellia*, and often also combined with *Scirpus* and *Phragmites* at some sites, though the areas are not large (Burd, 1989).

Along the northern (Scottish) shore of the Solway, the upper marsh zone is rich in sedges (*Carex* spp.) and rushes (*Juncus* spp.), and often shows transitions to freshwater and brackish marshes. Sea-purslane (*Atriplex protulacoides*) saltmarsh is less widespread than on south and east coasts due to the prevalence of grazing, mainly by cattle. The common saltmarsh-grass *(Puccinellia maritima*) is the first colonist of the mudflats in parts of the Solway, while in the main mid-to-upper marsh the vegetation type is dominated by red fescue (*Festuca rubra*) saltmarsh (Juncetum gerardii) (Barne, et al., 1996). Burd (1989) has described the saltmarshes of Scotland in considerable detail as part of the NCC survey of British saltmarshes. They are dotted all around the coast, but with only eight of the thirteen recognised NVC lower saltmarsh communities, and six of nine NVC middle saltmarsh communities being found in Scotland (Boorman, 2003).

4.2 Description of the study area (Caerlaverock NNR)

Caerlaverock National Nature Reserve (NNR) (National Grid reference NY045647) is one of 58 NNRs in Scotland. It is located 10 km south of Dumfries on the northern shore of the Solway Firth. It is the largest wetland reserve in Britain (Clyne et al., 2007), about 8 km long, and widening from less than 100 m wide at the Nith's mouth in the west, to almost 1 km wide at the Lochar Water in the east (Hansom, 2003). Caerlaverock Merse, including the 77 ha of Priestside Bank at its eastern end, extends to 563 ha (Fig.4.1 study area) (Barne, et al., 1996). Caerlaverock saltmarsh is designated a Special Area of Conservation (SAC), a Special Protection Area (SPA), a National Nature Reserve (NNR) and it is part of the Nith Estuary National Scenic Area. It contains 8.34% of the saltmarsh in Scotland (Hansom, 2003), and is dominated by a mainly *Puccinellia*, *Festuca* and *Glaux* sward with small stands of reeds (*Phragmites australis)* (Burd, 1989). Common saltmarsh-grass (*Puccinellia*) and samphire (*Salicornia*) occur in the creeks (Hansom, 2003). Within the grazed Merses of the Reserve the communities represented are SM16 *Juncus gerardii* (Saltmarsh Rush) – *Leontodon autumnalis* (Autumn Hawkbit) ; and SM16b *Festuca rubra* (Red Fescue), *Agrostis stolonifera* (Creeping Bent) and *Potentilla anserina* (Silverweed). In ungrazed merses NVC communities present include SM28 *Elymus repens* (Common

Couch) saltmarsh, with smaller amounts of *Festuca rubra*, and *Agrostis stolonifera;* and SM13d is almost dominated by *Puccinellia maritima* (Common Saltmarsh-grass) with *Plantago maritima* (Sea Plantain) and *Armeria maritima* (Thrift) (Peberdy, 1989).

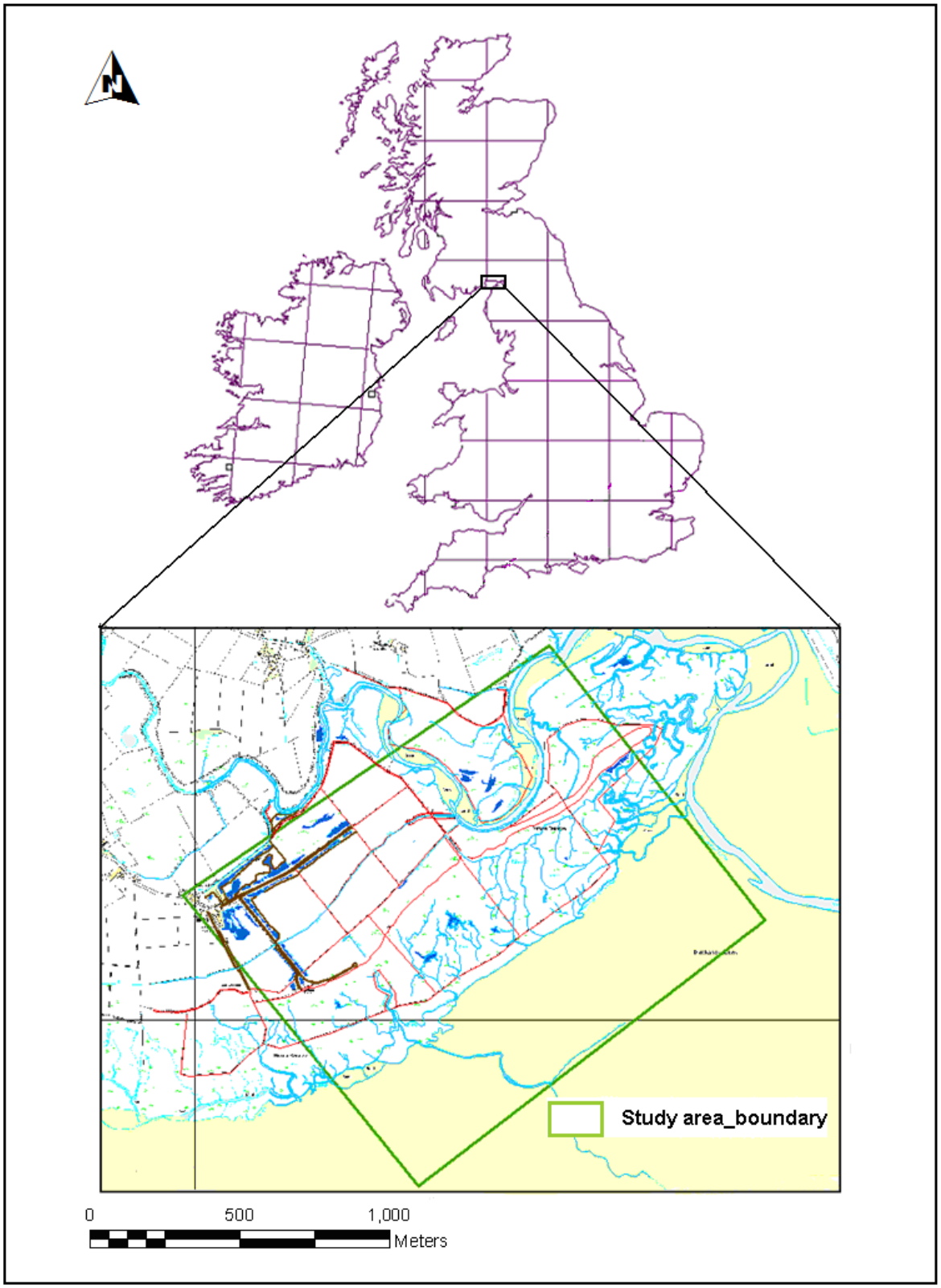

Figure 4-1: Map section of Caerlaverock Reserve showing Eastpark Merses study area.

4.3 Airborne and Space-borne Surveys

Aerial photographs of Caerlaverock Reserve were obtained from the UK company Blue Sky, and the LandsatTM scenes were obtained from the internet using the GLOVIS tool of the U.S. Geological Survey (USGS). It might be worth noting that satellite imagery is now much cheaper to acquire (using GLOVIS for example it is free to download) than aerial imagery (UK Blue Sky prices are quite high - £70 – £100 per stereo-pair); for this reason satellite images were used in this study, and their results compared with those obtained from aerial photos.

4.3.1 Orthophotography interpretation

The geo-referenced orthophotograph (produced from a stereo-pair processed in BAE System's SOCET Set) was used as a base map from which cover types present in Caerlaverock Reserve were digitised on-screen using ArcGIS. Major structural changes in vegetation were determined by comparing vegetation maps interpreted from orthophotographs produced from photography taken in 1988 (black and white) and also in 2009 (true colour): Figures (4.2 & 4.3). Canopy cover was mapped for both years on the basis of tree (symbolised using a dark green colour) and shrub (symbolised using a light green colour): Figures 4.4 and 4.5.

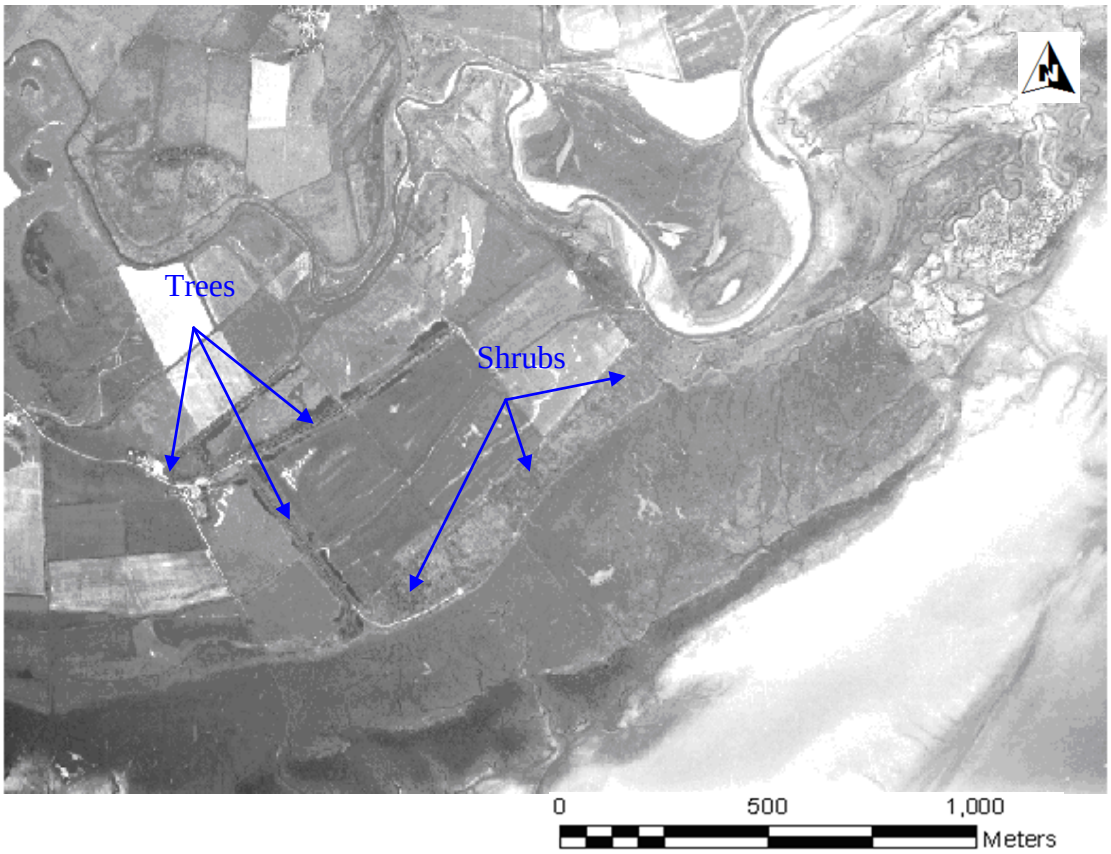

Figure 4-2: Orthophotograph of Caerlaverock Reserve 1988

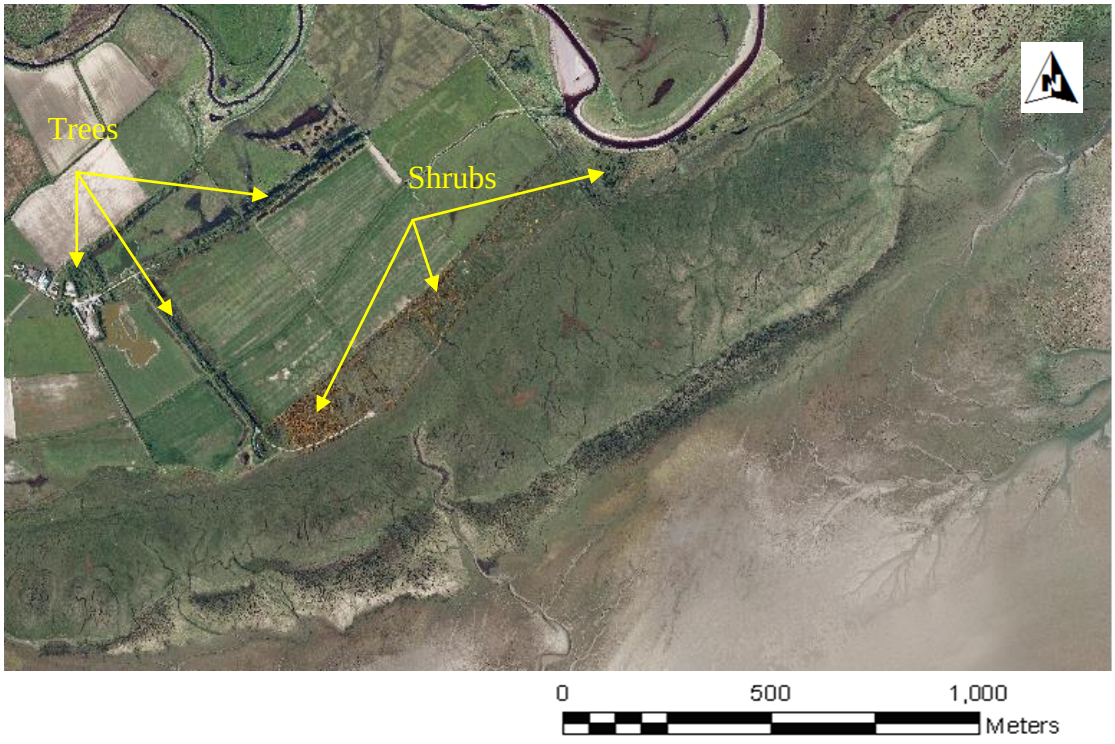

Figure 4-3: Orthophotograph of Caerlaverock Reserve 2009.

Total cover of trees and total of shrubs were delineated on-screen using the ArcMap GIS 9.3 and later ArcMap GIS 10.1 based on orthophotographs (1988, 2009), and groundtruthing fieldwork in 2011. Based upon the calculation of the cover of trees and the cover of shrubs in the orthophotographs, for the target area, using ArcMap GIS, the results showed that the cover of trees increased through the twenty-one years from 34707 m^2 (equivalent to 3.4707 ha) in 1988 (Fig. 4.4) to 47767 m^2 (equivalent to 4.7767 ha) in 2009 (Fig. 4.5), an increase of 13060 m^2 (equivalent to 1.3060 ha). Whereas, the results obtained from the cover of shrubs suggest a slight decrease in the cover from 59962 m^2 (equivalent to 5.9962 ha) in 1988 (Fig.4.4) to 59841 m^2 (equivalent to 5.9841 ha) in 2009 (Fig.4.5), a decrease of 121 m^2 of the shrub canopy through twenty-one years.

The change rate in the shrubs cover can be calculated using the following formula (Veldkamp et al., 1992):

$$\text{Change rate (percent, y}^{-1}) = \frac{(F_1 - F_2)/F_1}{N} \times 100$$

where:

F_1 is the cover area at the beginning of reference period;
F_2 is the cover area at the end of reference period;
N is the number of years in reference period; and,
y is a year.

The calculated annual change rate in the shrubs cover from 1988 to 2009 was 0.009 %, so it could be said that there is only a slight change in the shrubs cover, while a tree cover increase of 1.3% per year is a natural result for the growth of trees during the twenty-one years.

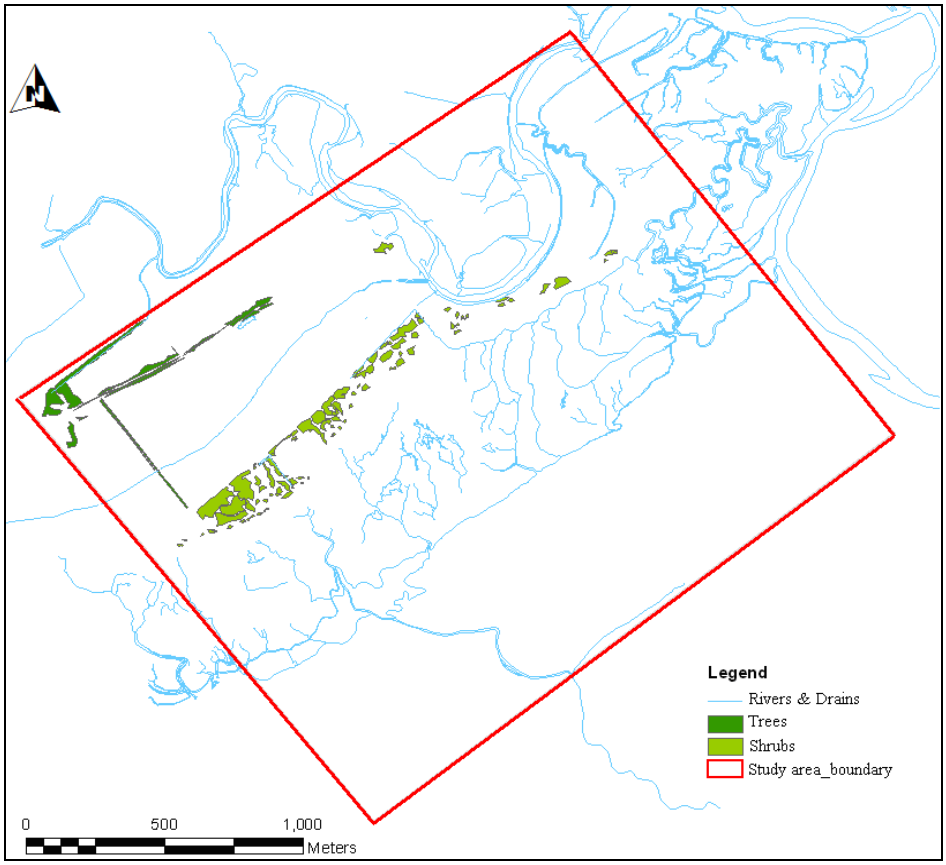

Figure 4-4: Cover of trees (dark green) and shrubs (light green) in Caerlaverock Reserve 1988.

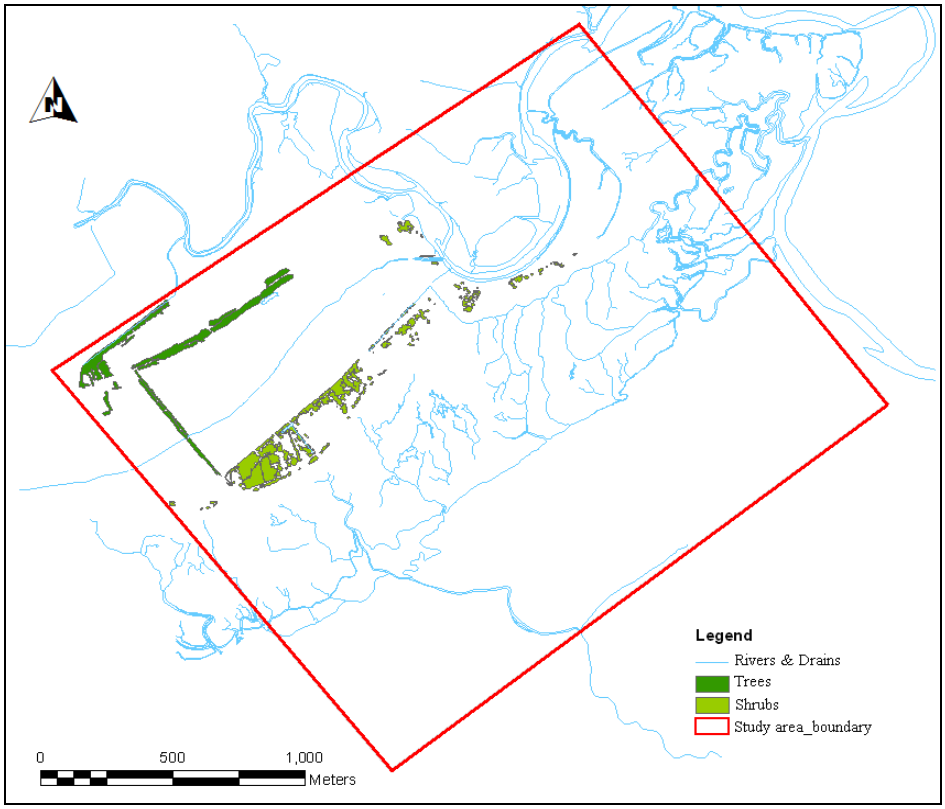

Figure 4-5: Cover of trees (dark green) and shrubs (light green) in Caerlaverock Reserve 2009.

4.3.1.1 Change Matrices

A ‘change matrix’ is a development of the classical ‘misclassification matrix’ or ‘error matrix’ concept widely used in the Earth Observation sciences (see: “Remote Sensing and Image Interpretation”, edition 6, p 585, Lillesand, Kieffer and Chipman, 2008). The error matrix compared ‘ground truth’ and the outcome from a classification process.

For reasons of clarity, the creation of an error matrix is briefly described, in the following three paragraphs, relating to Table 4.1.

An error matrix compares two (usually landcover) data sets. One of these is considered to be of higher accuracy than the other, and the higher accuracy set represents ‘the truth’; their comparison gives accuracy statistics for the less accurate data set. For example the data set whose accuracy is being considered might be derived from a lower resolution source, such as LandsatTM while ‘the truth’ is provided by a higher resolution data set, such as aerial photography, orthophotography or ground observations. An error matrix provides three pieces of statistical information:

1. simple probability of the classification of the lower resolution data set being correct (where ‘correct’ is as specified by the higher resolution data set), presented in percentage probability terms – in the simulated example below (Table 4.1) this is 70%;
2. user’s accuracy where the product provided by the producer using the lower resolution data set - such as a landcover map, in its practical use, is compared to ‘the truth’, presented in percentage probability terms, per class – in the simulated example below (Table 4.1) this is 83% in the case of Class A and 50% in the case of Class B;
3. producer’s accuracy where ‘the truth’ provided by the higher resolution product is compared to the product provided by the producer using the lower resolution data set, presented in percentage probability terms, per class – in the simulated example below (Table 4.1) this is 71% in the case of Class A and 66% in the case of Class B.

A simulated example error matrix is provided below for two classes of land use (A, B) in a 1000 pixel site. In this example, the producers, using low resolution imagery, mapped 600 pixels of class A and 400 pixels of class B, whereas ‘the truth’ (or ‘groundtruth’) as found in high resolution aerial photography was that there were 700 pixels of class A and 300 pixels of class B (Table 4.1).

Table 4-1: Explanatory example of an Error Matrix.

PRODUCED MAP → GROUNDTRUTH ↓	CLASS A	CLASS B	∑	Producer's accuracy
CLASS A	500	200	700	500/700 (71%)
CLASS B	100	200	300	200/300 (66%)
∑	600	400		
User's accuracy	500/600 (83%)	200/400 (50%)		700/1000 (70%) (Simple probability of map being correct)

There are several of these error matrices considered subsequently in this chapter. However, a particular modification of the error matrix, as also explained in Chapter 3, has been to use the same statistical approach to produce a ***change matrix***. The change matrix compares two surveys considered to be of the same accuracy, but representing different dates. The statistics obtained represent change, and there has also to be a modification of terminology, as shown below in Table 4.2.

Table 4-2: Explanatory example of Change Matrix.

DATE 1 → DATE 2↓	CLASS A	CLASS B	∑	Percentage Date 2 class retained from Date 1
CLASS A	500	200	700	500/700 (71%)
CLASS B	100	200	300	200/300 (67%)
∑	600	400		
Percentage Date 1 class retained in Date 2	500/600 (83%)	200/400 (50%)		700/1000 (70%) (Overall percentage unchanged between the two dates)

It may of course be more interesting to state the above specifically in terms of percentage changed – rather than percentage unchanged, and this would be that there has been an overall change of 30% between the two dates, with: 17% of Date 1 Class A changing to Class B between the dates; 29% of Date 2 Class A having changed from Date 1 Class B between the dates; 50% of Date 1 Class B changing to Class A between the dates; and, 33% of Date 2 Class B having changed from Date1 Class A between the dates.

Essentially in moving from error matrices to change matrices we are no longer considering percentages correct, but percentages unchanged.

There are several practical examples of these change matrices considered subsequently in this chapter.

4.3.1.2 Using change matrices and error matrices.

The results of change between 1988, based on orthophotography, and 2011, based on fieldwork, of the classification into five classes are shown in the change matrix Table 4.3. In Table 4.4, the results obtained from a two-class change matrix between the 1988 orthophotography and the 2011 fieldwork are shown. The overall percentages unchanged between the two dates for the two and five class classifications were found to be 93.4% (Table 4.4) and 83.3% (Table 4.3), respectively.

The comparison, via error matrices between aerial photography (orthophotography) of 2009 and fieldwork of 2011 (they are only two years apart) serves to confirm that aerial photography (orthophotography) is a worthy substitute for field work, which is long established amongst air photo interpreters e.g. Mosbech and Hansen (1994) state the aerial photographs had mapped vegetation classes well in Jameson Land, also Verheyden et al., 2002 reported that aerial photographs produce accurate vegetation maps of mangrove forests. Accuracy percentages over 93% in the two-class assessment of the Caerlaverock work all confirm this (see Table 4.5).

There are five original classes (trees– T; shrubs -S; wet grassland - WG; water – W; saltmarsh- SM).

Table 4-3: Five classes change matrix resulting from aerial photography1988 (Aerial) versus 2011 fieldwork (FW) for Caerlaverock Reserve.

Aerial 1988 → FW 2011 ↓	T	S	WG	W	SM	∑	Percentage retained unchanged in 2011 from 1988
T	6	0	0	0	0	6	6/6 100%
S	0	4	0	0	0	4	4/4 100%
WG	0	2	24	0	1	27	24/27 88.8%
W	0	1	2	0	0	3	NA
SM	0	0	2	0	6	8	6/8 75%
∑	6	7	28	0	7		
Percentage from 1988 retained unchanged in 2011	6/6 100%	4/7 57.1%	24/28 85.7%	NA	6/7 85.7%		Overall % unchanged between two dates: 40/48 83.3%

Table 4-4: Two-classes change matrix resulting from aerial photography1988 versus 2011 fieldwork for Caerlaverock Reserve.

Aerial 1988 → FW 2011 ↓	T&S	Others	∑	Percentage retained unchanged in 2011 from 1988
T&S	10	0	10	10/10 100%
Other	3	35	38	35/38 92.1%
∑	13	35		
Percentage from 1988 retained unchanged in 2011	10/13 76.9%	35/35 100%		Overall % unchanged between two dates: 45/48 93.4%

The results of an error matrix analysis from aerial photography 2009 versus 2011 fieldwork of the classification into five classes with user's and producer's accuracies are shown in Table 4.5 (it has been assumed that checking 2009 API against fieldwork two years newer was acceptable). Table 4.6, shows the results obtained from two-class error matrix for aerial photography 2009 versus fieldwork 2011. The overall accuracies for the error matrix of two and five classes were found to be 92% (Table 4.6) and 83.3% (Table 4.5), respectively.

Table 4-5: Error matrix resulting from aerial photography 2009 versus 2011 fieldwork for Caerlaverock Reserve, five classes.

Aerial 2009 → FW 2011 ↓	T	S	WG	W	SM	∑	User's Accuracy
T	6	0	0	0	0	6	6/6 100%
S	0	3	1	0	0	4	3/4 75%
WG	0	2	24	0	1	27	24/27 88.8%
W	0	1	2	0	0	3	NA
SM	0	0	1	0	7	8	7/8 87.5%
∑	6	6	28	0	8		
Producer's Accuracy	6/6 100%	3/6 50%	24/28 85.7%	NA	7/8 87.5%		40/48 83.3%

With a positive *k* ("KHAT" or "kappa") value (0.73) the classification is shown to be 73% better than classification resulting from chance.

Table 4-6: Error matrix resulting from aerial photography 2009 versus 2011 fieldwork for Caerlaverock Reserve, two classes.

Aerial 2009 → FW 2011↓	T&S	Other	∑	User's Accuracy
T&S	9	1	10	9/10 90%
Other	3	35	38	35/38 92%
∑	12	36		
Producer's Accuracy	9/12	35/36 97.2%		44/48 92%

With a positive *k* ("KHAT" or "kappa") value (0.76) the classification is shown to be 76% better than classification resulting from chance.

4.3.2 Landsat imagery interpretation

A characterization by land cover type is necessary for environmental assessment; classification of remotely sensed data offers this. Usually classifications are divided into two categories, unsupervised and supervised approaches that can each agglomerate remotely sensed data into meaningful groups.

4.3.2.1 Unsupervised classification

The results that were obtained from LandsatTM image in 1988 using unsupervised classification techniques to produce, first, six land cover classes and then, subsequently, ten land cover classes are shown in Figures 4.6 and 4.7. To interpret the image we need to know into which land cover types each class falls, with detailed knowledge of ground truth for the area, but it is not always easy to do that; the ten classes image is difficult to interpret, see Figure 4.7. In unsupervised classification, the classes produced are based on

natural breaks in the distribution of pixel values in the image. As a result, the created classes may not distinguish between the features that the user needs to resolve.

For example in this study, the colour (spectral response) of shrubs in wet grassland areas may be too similar for the software to separate them into distinct classes and likewise the colour (spectral response) of vegetation in flooded areas (saltmarsh) and open water. In the six classes LandsatTM image for 1988 at Caerlaverock Reserve, there appears to be an integration of open water with a part of the saltmarsh vegetation symbolised using the same colour (magenta). It might be due to the image being captured in the period of high tide; also, shrubs and wet grassland in the target area are visualised in the same colour (red), see Figure 4.6. The six classes for 1988 image were trees; shrubs; wet grassland; pastures; open water, and saltmarsh.

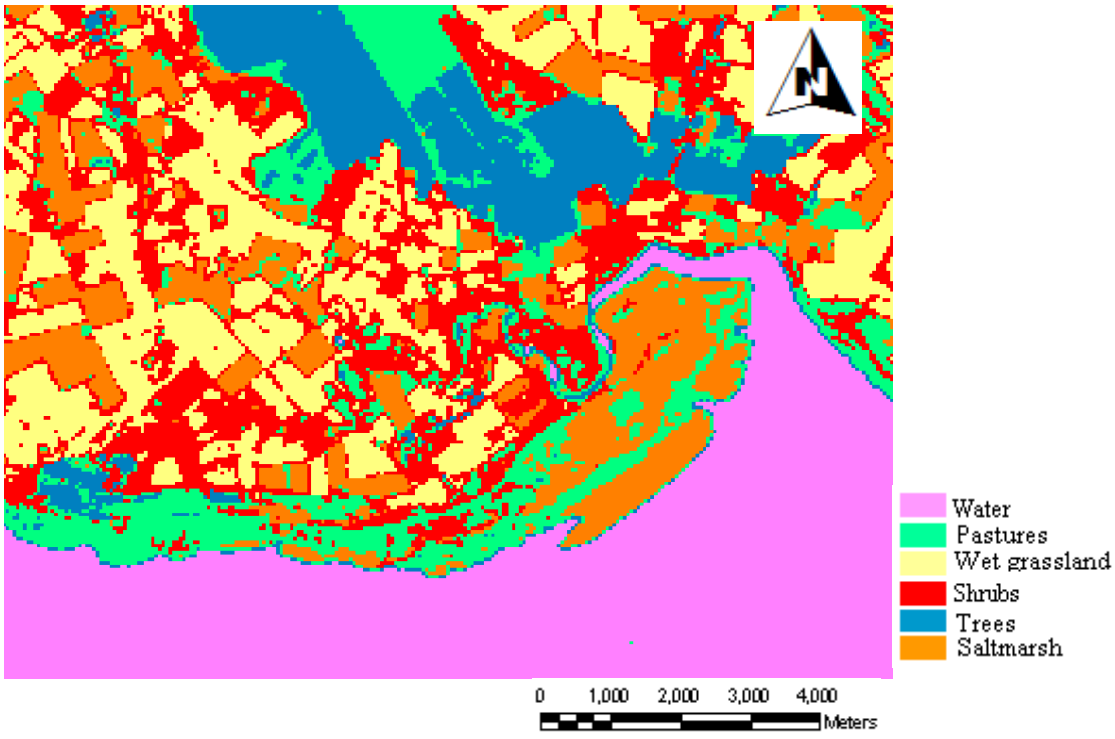

Figure 4-6: Six land cover classes of the 1988 Caerlaverock LandsatTM image after unsupervised classification.

The 10 class unsupervised classification produced classes which were difficult to identify, based on field work and a knowledge of the area (see Figure 4.7).

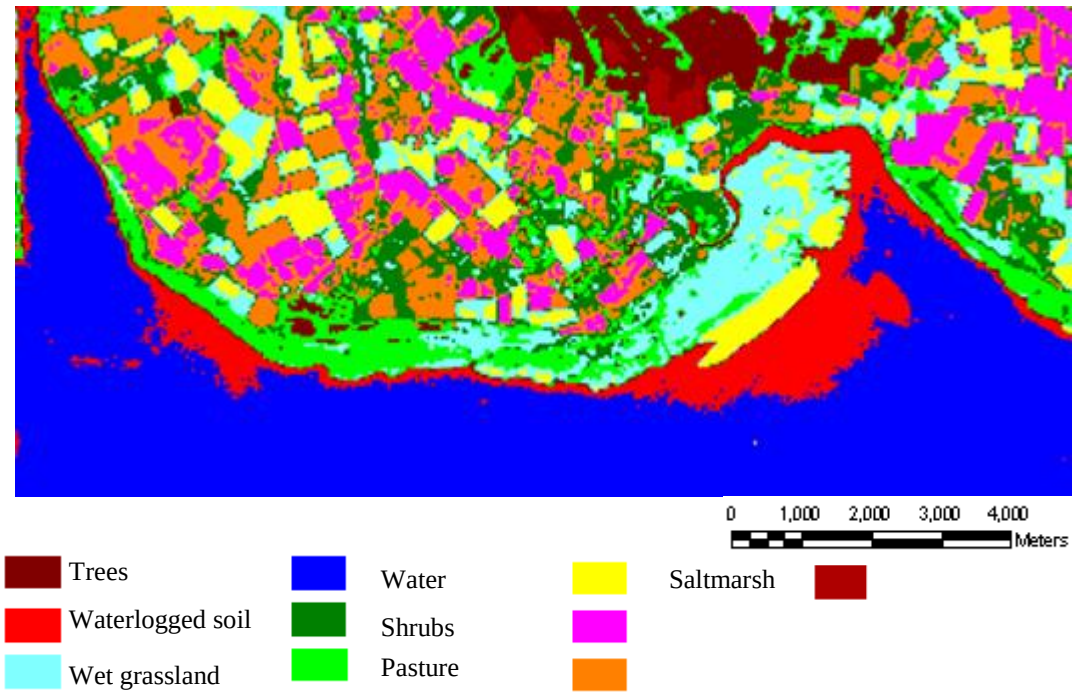

Figure 4-7: Ten land cover classes of the 1988 Caerlaverock LandsatTM image after unsupervised classification.

Figures 4.8 and 4.9 show the results that were obtained from interpretation of LandsatTM imagery for 2009 using unsupervised classifications in six and ten cover classes. The identified six classes were trees; shrubs; wet grassland; waterlogged soil; open water, and saltmarsh.

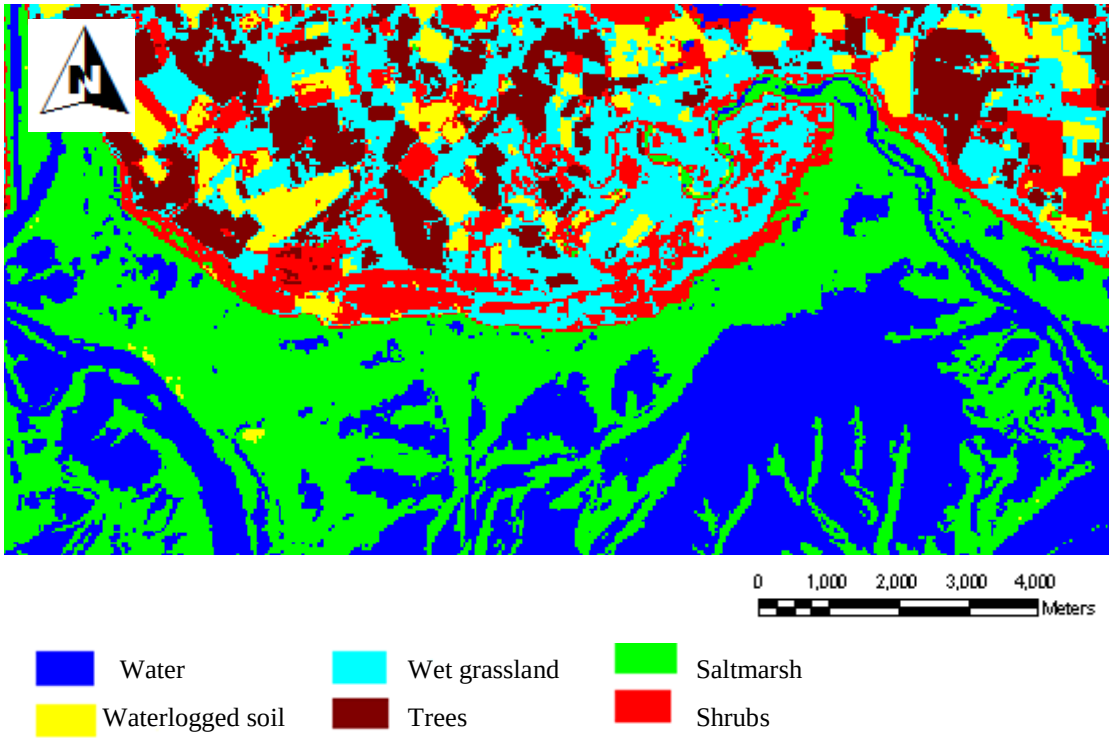

Figure 4-8: Six land cover classes of the 2009 Caerlaverock LandsatTM image after unsupervised classification .

The 10 class unsupervised classification produced classes which were difficult to identify, based on field work and a knowledge of the area (see Figure 4.9).

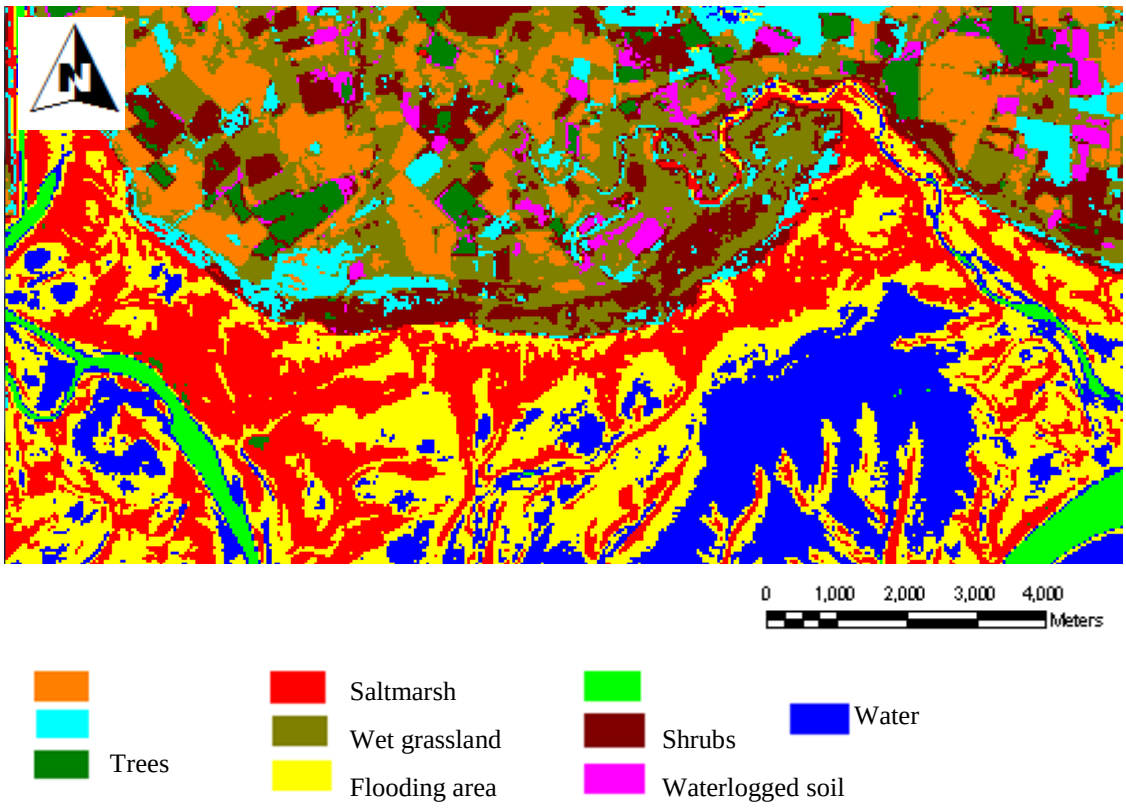

Figure 4-9: Ten land cover classes of the 2009 Caerlaverock Reserve LandsatTM image after unsupervised classification.

4.3.2.2 Supervised classification

The accuracy assessment of distinguishing the Caerlaverock Reserve vegetation classes following supervised classification was performed by using aerial photos, an Ordnance Survey map, and fieldwork as reference sources. The Study Area was categorised into five-land cover classes; the classes were trees, shrubs, wet grassland, saltmarsh and water. To select training areas aerial photography, Ordnance Survey maps, and fieldwork ground reference data (TWINSPAN group classification not used for training areas) have all been used as a guide for the selection of vegetation classes in supervised classification.

The results of the supervised classification techniques in five land cover classes for Caerlaverock Reserve LandsatTM images in 1988 and 2009 are shown in Figures 4.10, 4.11.

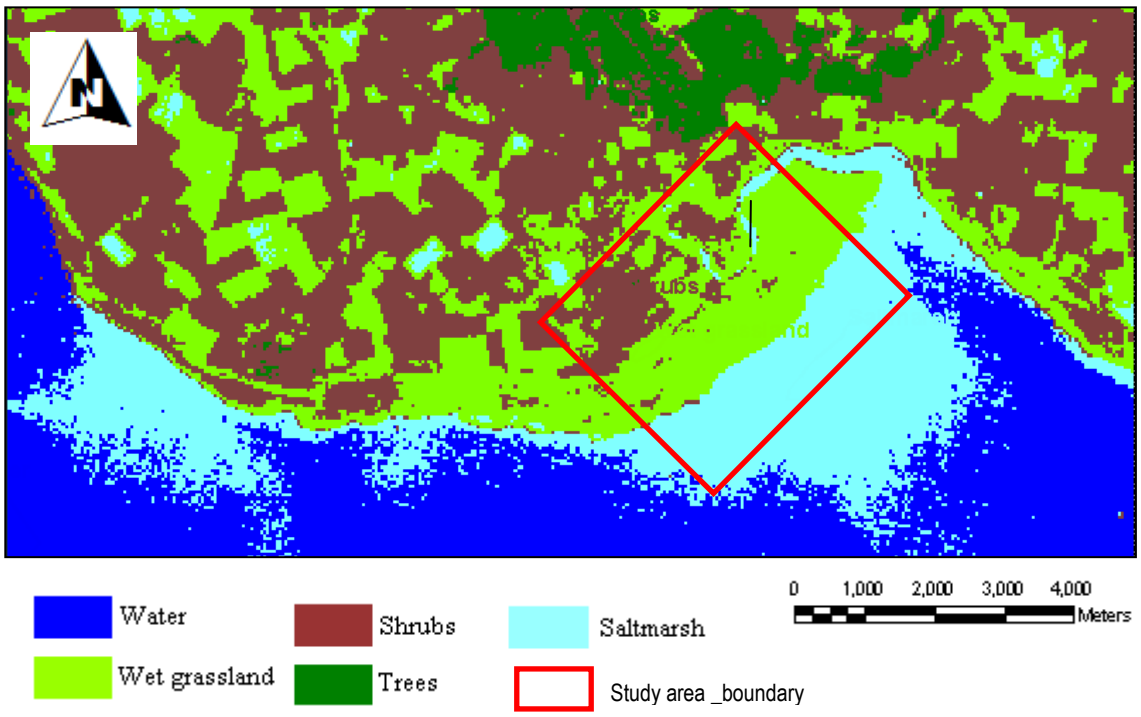

Figure 4-10: Land cover classes identified for 1988 Caerlaverock Reserve LandsatTM image through supervised classification.

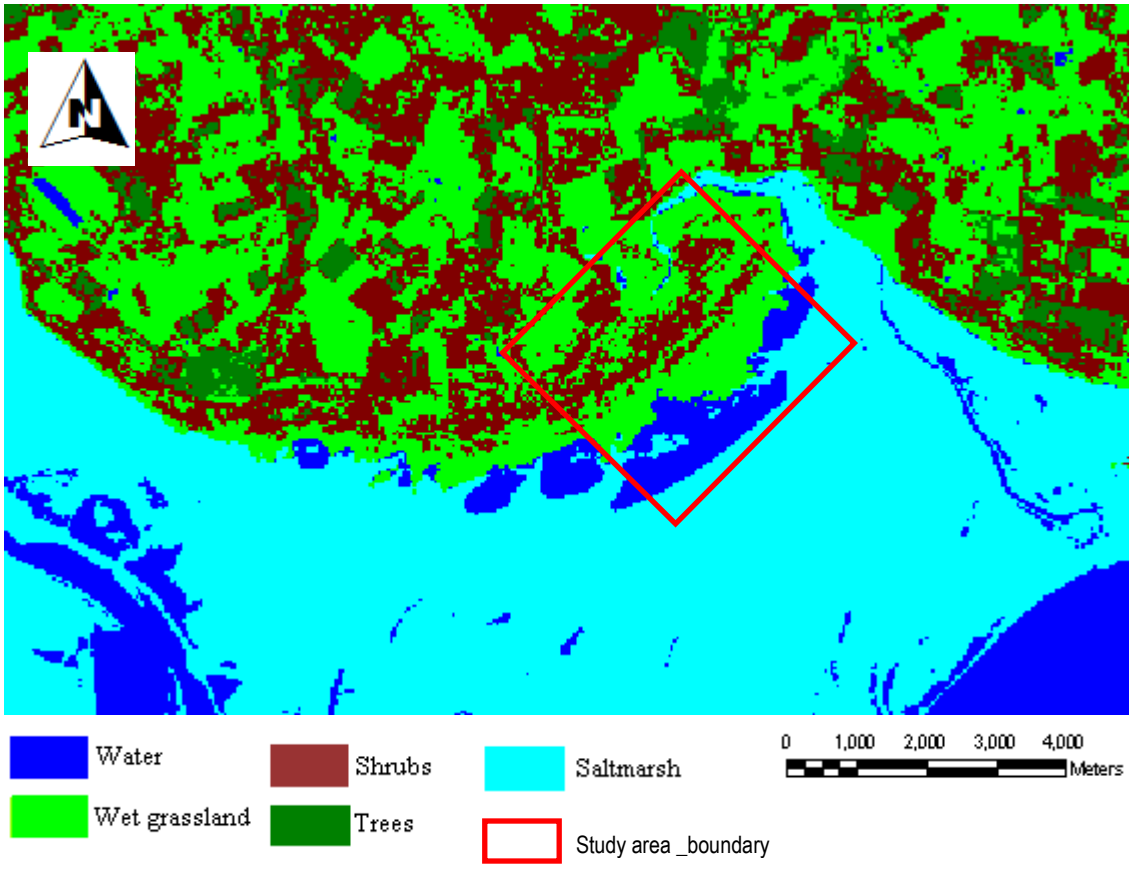

Figure 4-11: Land cover classes identified for 2009 Caerlaverock Reserve LandsatTM through supervised classification.

Scattergrams of supervised classification for all five identified land cover classes of LandsatTM image in 1988 and LandsatTM image in 2009 for Caerlaverock Reserve are shown in Figures 4.12 and 4.13. It is noticed from interpretation of the scattergram that there is no overlap between the land cover classes; which means that the supervised classification has precisely determined land cover classes and successfully avoided including pixels of ambiguous class (or 'mixels').

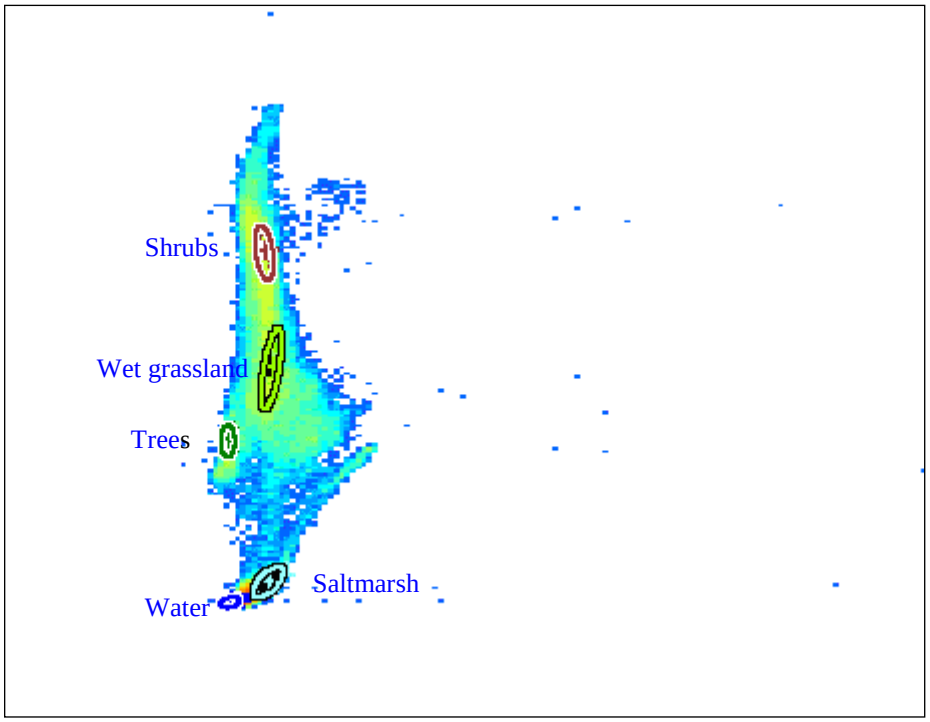

Figure 4-12: Shows scattergram created from the five class supervised classification using LandsatTM bands 2 and 4 of Caerlaverock Reserve, 1988.

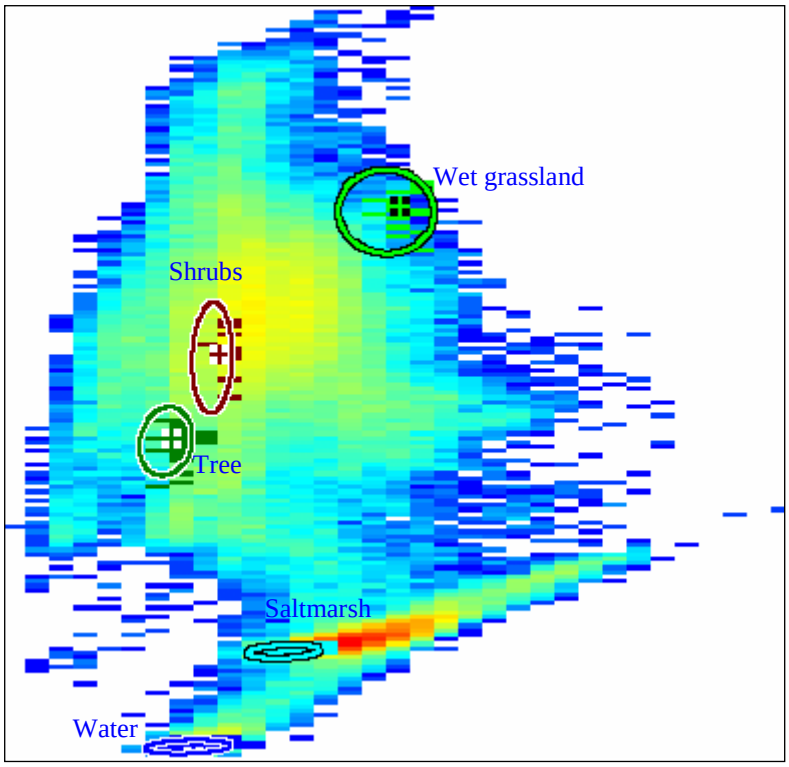

Figure 4-13: Shows scattergram created from the five class supervised classification using LandsatTM bands 2 and 4 of Caerlaverock Reserve, 2009.

4.3.2.3 Producing the change matrix

The two data sets being compared to identify change are from 1988 and 2009.

Following classification in ER-Mapper, the data were transferred to ArcGIS as raster data sets. The challenge is to represent and then visualise changes, that is to produce a map showing changes between 1988-2009 (including 'no change'), and the widely used ArcGIS tool 'Map Calculus' is harnessed to do this.

There are 5 classes (trees- T; shrubs – S; wet grassland - WG; water – W; saltmarsh- SM) in each period – thus a maximum of 25 change possibilities, see Table 4.7.

Table 4-7: Shows the possible 25 changes (including no change).

#	ORIGINAL CLASS	CHANGED CLASS	COMMENT
1	T	T	No change
2	T	S	
3	T	WG	
4	T	W	
5	T	SM	
6	S	T	
7	S	S	No change
8	S	WG	
9	S	W	
10	S	SM	
11	WG	T	
12	WG	S	
13	WG	WG	No change
14	WG	W	
15	WG	SM	
16	W	T	
17	W	S	
18	W	WG	
19	W	W	No change
20	W	SM	
21	SM	T	
22	SM	S	
23	SM	WG	
24	SM	W	
25	SM	SM	No change

The challenge is to visualise these changes, that is to produce a map showing these changes (including the no change), and GIS map calculus is used to do this.

For the original class (1988) the five land cover classes were re-labelled, using a numeric pixel value, as shown in Table 4.8.

Table 4-8: 1988 land cover classes, showing original class name and new label.

T	1
S	2
WG	4
W	6
SM	8

For the changed class (2009) the five land cover classes were re-labelled, using a numeric pixel value, as shown in Table 4.9.

Table 4-9: 2009 land cover classes, showing original class name and new label.

T	10
S	14
WG	19
W	22
SM	24

Using the ArcGIS map calculus tool (which is called RASTER CALCULATOR), the two data sets (1988 and 2009) can be multiplied together, to produce a new pixel map, with the following possible outcome pixel values shown in Table 4.10.

Table 4-10: Outcome pixel values and their meaning.

#	CLASS 1988	CLASS 2009	PRODUCT (possible outcome pixel value)	COMMENT
1	1	10	10	T to T No change
2	1	14	14	T to S Not found in study area
3	1	19	19	T to WG
4	1	22	22	T to W Not found in study area
5	1	24	24	T to SM Not found in study area
6	2	10	20	S to T
7	2	14	28	S to S No change
8	2	19	38	S to WG
9	2	22	44	S to W
10	2	24	48	S to SM
11	4	10	40	WG to T
12	4	14	56	WG to S
13	4	19	76	WG to WG No change
14	4	22	88	WG to W
15	4	24	96	WG to SM
16	6	10	60	W to T Not found in study area
17	6	14	84	W to S Not found in study area
18	6	19	114	W to WG Not found in study area
19	6	22	132	W to W Not found in study area
20	6	24	144	W to SM Not found in study area
21	8	10	80	SM to T
22	8	14	112	SM to S Not found in study area
23	8	19	152	SM to WG
24	8	22	176	SM to W
25	8	24	192	SM to SM No change

In the case of Caerlaverock Reserve, not all possibilities were achieved (i.e. 'Not found in study area'), thus a palette of only 16 colours was needed.

4.3.2.4 Detection of change in vegetation; results

The results obtained from change matrix analysis using Arc Map (v10.1) are included in a chart showing class changes from 1988 to 2009 in Caerlaverock Reserve (Table 4.11, 4.12). Based on the change matrix table, trees only covered an area of 1 pixel (equivalent to 0.09 ha), the shrubs covered an area of 18 pixels in 1988; see Table 4.11. The total canopy of shrubs had changed by 2009 as follows: 30 % (324 pixels equivalent to 29 ha) changed to trees, 67% (705 pixels equivalent to 63.45 ha) changed to wet grassland, 0.3% (3 pixels equivalent to 0.27 ha) changed to saltmarsh see Table 4.12. Figure 4.14 shows the specific spatial distribution (location) of land cover change (change patterns) that has taken place between the individual cover types at Caerlaverock Reserve from 1988 to 2009. The results obtained from the two-class change matrix for supervised classification of satellite imagery 1988 versus satellite imagery 2009, with overall percentage unchanged of 64.4% is shown in Table 4.13.

This result is unlikely to be true; the supervised classification included some grasses that were mapped as shrubs in 2009, perhaps, because of the similar reflectivity of some rough grazing areas to the shrub Gorse, the supervised classification failed to distinguish the two types. For this reason, in the outcome map of five classes using a supervised classification the cover of shrubs is greater than reality compared with aerial photographs of the same year. In addition, some wet grassland on the grounds was shrubs in the map for 1988. This could be due to the small study area and that the trees and shrubs covered an area less than one pixel size in the Landsat TM image, so probably the selected training area for TM image of 1988 included some grass with the shrubs.

Table 4-11: Change matrix for Caerlaverock Reserve in the 1988-2009 period values in pixels.

1988 → 2009 ↓	Trees	Shrubs	Wet grassland	Water	Saltmarsh	∑	Percentage retained unchanged in 2009 from 1988
Trees	1	324	1294	0	55	1674	1/1674 0.06%
Shrubs	0	18	5	0	0	23	18/23 78.26%
Wet grassland	1	705	1299	0	1129	3134	1299/3134 41.4%
Water	0	2	15	0	724	741	NA
Saltmarsh	0	3	5	0	223	231	223/231 96.5%
∑	2	1052	2618	0	2131	5803	
Percentage from 1988 retained unchanged in 2009	1/2 50%	18/1052 1.7%	1299/2618 49.6%	NA	223/2131 10.5%		Overall % unchanged between two dates: 1541/5803 26.5%

Table 4-12: Class distribution for changed land cover in Caerlaverock Reserve in the 1988-2009 period, in hectares.

1988 → 2009 ↓	Trees	Shrubs	Wet grassland	Water	Saltmarsh
Trees		29.16	116.46	0	4.95
Shrubs	0		0.45	0	0
Wet grassland	0.09	63.45		0	101.61
Water	0	0.18	1.35		65.16
Saltmarsh	0	0.27	0.45	0	

Table 4-13: Two-classes change matrix for Caerlaverock Reserve in the 1988-2009 period, values in pixels.

1988 → 2009 ↓	Trees & Shrubs	Others	∑	Percentage retained unchanged in 2009 from 1988
Trees & Shrubs	343	1354	1697	343/1697 20.2%
Others	711	3395	4106	3395/4106 82.7%
∑	1054	4749	5803	
Percentage from 1988 retained unchanged in 2009	343/1054 32.5%	3395/4749 71.5%		Overall % unchanged between two dates: 3738/5803 64.4%

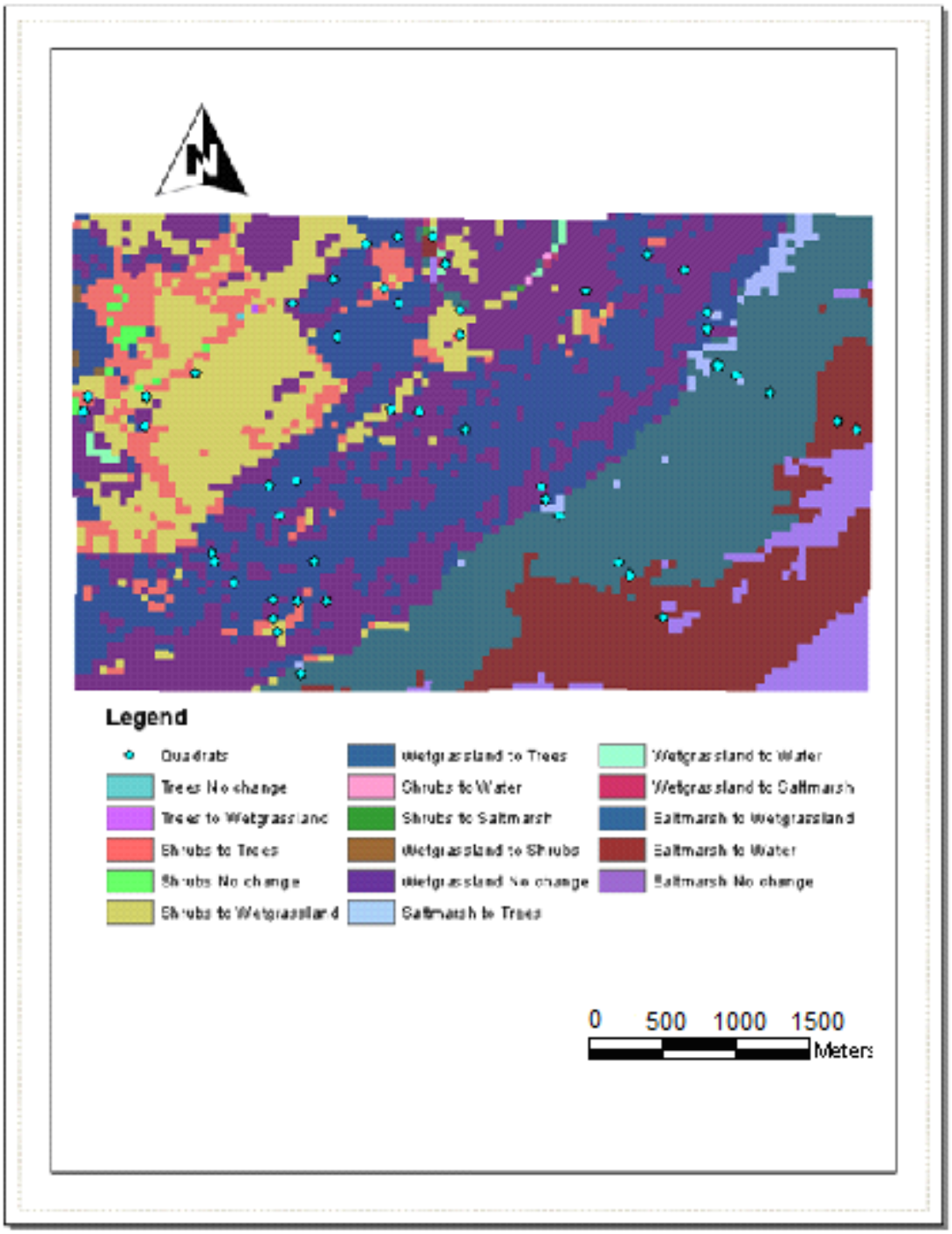

Figure 4-14: Land cover change map for Caerlaverock Reserve 1988-2009.

The change matrix from the six classes unsupervised classification of satellite imagery 1988 versus fieldwork 2011 with percentages unchanged is shown in Table 4.14. Table 4.15, shows the the two-class change matrix for the unsupervised classification of satellite imagery 1988 versus fieldwork 2011. The overall percentages unchanged for the change matrix of two and six classes were found to be 81.2% (Table 4.15) and 10.4% (Table 4.14), respectively. There are 6 original classes (trees– T; shrubs -S; wet grassland - WG; water – W; pasture - P; saltmarsh- SM)

Table 4-14: Six classes change matrix resulting from unsupervised classification of satellite imagery 1988 vs. fieldwork 2011 for Caerlaverock Reserve.

TM 1988 → FW 2011↓	T	S	WG	W	SM	P	∑	Percentage retained unchanged in 2011 from 1988
T	0	1	1	1	0	3	6	NA
S	0	0	0	0	0	4	4	NA
WG	0	4	3	1	6	11	25	3/25 12%
W	0	0	1	0	0	2	3	NA
SM	0	0	4	1	2	0	7	2/7 28.5%
P	0	1	0	1	1	0	3	NA
∑	0	6	9	4	9	20		
Percentage from 1988 retained unchanged in 2011	NA	NA	3/9 33.3%	NA	2/9 22.2%	NA		Overall % unchanged between two dates: 5/48 10.4%

Table 4-15: Two classes change matrix resulting from unsupervised classification of satellite imagery 1988 vs. fieldwork 2011 for Caerlaverock Reserve.

TM 1988 → FW 2011↓	T&S	Others	∑	Percentage retained unchanged in 2011 from 1988
T&S	6	9	15	6/15 40%
Other	0	33	33	33/33 100%
∑	6	42		
Percentage from 1988 retained unchanged in 2011	6/6 100%	33/42 78.5%		Overall % unchanged between two dates: 39/48 81.2%

The results of the error matrix from the six classes unsupervised classification of satellite imagery 2009 versus fieldwork 2011 with user's and producer's accuracies are shown in Table 4.16. Table 4.17 shows the results obtained from the two-class error matrix for unsupervised classification of satellite imagery 2009 versus fieldwork 2011. The overall accuracies for the error matrix of two and six classes were found to be 79% (Table 4.17) and 43.75% (Table 4.16), respectively.

Table 4-16: Six classes error matrix resulting from unsupervised classification of satellite imagery 2009 vs. fieldwork 2011 for Caerlaverock Reserve.

TM 2009 → FW 2011↓	T	S	WG	W	SM	P	∑	User's Accuracy
T	0	0	3	0	0	3	6	0/6 0%
S	0	0	4	0	0	0	4	0/4 0%
WG	0	0	15	0	3	7	25	15/25 60%
W	0	0	2	0	1	0	3	0/3 0%
SM	0	0	1	0	6	0	7	6/7 85.7%
P	0	0	1	0	2	0	3	0/3 0%
∑	0	0	26	0	12	10		
Producer's Accuracy	NA	NA	15/26 57.7%	NA	6/12 50%	0/10 0%		21/48 43.75%

With a positive *k* ("KHAT") value (0.20) the classification is shown to be 20% better than classification resulting from chance.

Table 4-17: Two classes error matrix resulting from unsupervised classification of satellite imagery 2009 vs. fieldwork 2011 for Caerlaverock Reserve.

TM 2009 → FW 2011↓	T&S	Others	∑	User's Accuracy
T&S	0	10	10	0/10 0%
Other	0	38	38	38/38 100%
∑	0	48		
Producer's Accuracy	NA	38/48 79%		38/48 79%

With A *k* ("KHAT") value (0) the classification is shown no better than a value on assignment of pixels, in this case 0% no better than classification resulting from chance.

The results of change matrix from five classes supervised classification of satellite imagery1988 versus fieldwork 2011 with percentages unchanged are shown in Table 4.18. Table 4.19 shows the results obtained from two-class change matrix for supervised classification of satellite imagery 1988 versus fieldwork 2011. The overall percentages unchanged for the change matrix of two and five classes were found to be 75 % (Table 4.19) and 58.3% (Table 4.18), respectively.

Table 4-18: Five classes change matrix resulting from supervised classification of satellite imagery 1988 vs. fieldwork 2011 for Caerlaverock Reserve.

TM 1988 → FW 2011↓	T	S	WG	W	SM	∑	Percentage retained unchanged in 2011 from 1988
T	0	4	2	0	0	6	NA
S	0	1	3	0	0	4	1/4 25%
WG	0	6	19	0	2	27	19/27 70.4%
W	0	1	2	0	0	3	NA
SM	0	0	0	0	8	8	8/8 100%
∑	0	12	26	0	10		
Percentage from 1988 retained unchanged in 2011	NA	1/12 8.3%	19/26 73.7%	NA	8/10 80%		Overall % unchanged between two dates: 28/48 58.3%

Table 4-19: Two classes change matrix resulting from supervised classification of satellite imagery 1988 vs. fieldwork 2011 for Caerlaverock Reserve.

TM 1988 → FW 2011↓	T&S	Others	∑	Percentage retained unchanged in 2011 from 1988
T&S	5	5	10	5/10 50%
Other	7	31	38	31/38 81.5%
∑	12	36		
Percentage from 1988 retained unchanged in 2011	5/12 41.7%	31/36 86.1%		Overall % unchanged between two dates: 36/48 75%

The results of the error matrix from the five class supervised classification of 2009 satellite imagery versus 2011 fieldwork with user's and producer's accuracies are shown in Table 4.20. Table 4.21 shows the results obtained from two-class error matrix for supervised classification of 2009 satellite imagery versus 2011 fieldwork. The overall

accuracies for the error matrix of two and five classes were found to be 52 % (Table 4.21) and 25% (Table 4.20), respectively.

Table 4-20: Five classes error matrix resulting from supervised classification of satellite imagery 2009 vs. fieldwork 2011 for Caerlaverock Reserve.

TM 2009 → FW 2011↓	T	S	WG	W	SM	∑	User's Accuracy
T	0	3	3	0	0	6	NA
S	0	2	2	0	0	4	2/4 50%
WG	0	16	10	0	2	26	12/26 38.5%
W	0	1	1	0	0	2	NA
SM	0	1	4	0	0	8	NA
∑	0	23	20	0	2		
Producer's Accuracy	NA	2/23 8.7%	10/20 50%	NA	NA		12/48 25%

With a negative *k* ("KHAT" or "kappa") value the classification is shown to be poorer than than classification resulting from chance.

Table 4-21: Two classes error matrix resulting from supervised classification of satellite imagery 2009 vs. fieldwork 2011 for Caerlaverock Reserve.

TM 2009 → FW 2011↓	T&S	Others	∑	User's Accuracy
T&S	5	5	10	5/10 50%
Other	18	20	83	20/38 52.6%
∑	23	25		
Producer's Accuracy	5/23 21.9%	20/25 80%		25/48 52%

With a negative *k* ("KHAT") value the classification is shown to be poorer than than classification resulting from chance.

The results of error matrix from five classes supervised classification of satellite imagery 1988 versus aerial photography 1988 with user's and producer's accuracies are shown in Table 4.22. In Table 4.23, shows the results obtained from two-class error matrix for supervised classification of satellite imagery 1988 versus aerial photography 1988. The overall accuracies for the error matrix of satellite imagery vs. aerial photography of two and five classes were found to be 79.2 % (Table 4.23) and 62.5% (Table 4.22), respectively.

Table 4-22: Five classes error matrix resulting from aerial photography 1988 vs. satellite imagery 1988 for Caerlaverock Reserve.

Aerial 1988 → TM 1988↓	T	S	WG	W	SM	∑	User's Accuracy
T	0	0	0	0	0	0	NA
S	4	3	5	0	0	12	3/12 25%
WG	1	4	20	0	4	29	20/29 68.9%
W	0	0	0	0	0	0	NA
SM	0	0	0	0	7	7	7/7 100%
∑	5	7	25	0	11		
Producer's Accuracy	0/5 0%	3/7 42.8%	20/25 80%	NA	7/11 63.6%		30/48 62.5%

With a positive *k* ("KHAT") value (0.40) the classification is shown to be 40% better than classification resulting from chance.

Table 4-23: Two classes error matrix resulting from aerial photography 1988 vs. satellite imagery 1988 of Caerlaverock Reserve.

Aerial 1988 → TM 1988↓	T&S	Others	∑	User's Accuracy
T&S	7	5	12	7/12 58.3%
Other	5	31	36	31/36 86.1%
∑	12	36		
Producer's Accuracy	5/12 41.7%	31/36 86.1%		38/48 79.2%

With a positive *k* ("KHAT") value (0.44) the classification is shown to be 44% better than classification resulting from chance.

The results of error matrix from five classes supervised classification of satellite imagery 2009 versus aerial photography 2009 with user's and producer's accuracies are shown in Table 4.24. In Table 4.25, shows the results obtained from two-class error matrix for supervised classification of satellite imagery 2009 versus aerial photography 2009. The overall accuracies for the error matrix of two and five classes were found to be 50 % (Table 4.25) and 27.1% (Table 4.24), respectively.

Table 4-24: Five classes error matrix resulting from aerial photography (air) 2009 vs. satellite imagery (TM) 2009 for Caerlaverock Reserve.

Air 2009 → TM 2009 ↓	T	S	WG	W	SM	∑	User's Accuracy
T	0	0	0	0	0	0	NA
S	3	2	15	0	2	22	2/22 9.1%
WG	3	4	11	0	3	21	11/21 52.4%
W	0	0	0	0	3	3	NA
SM	0	0	2	0	0	2	NA
∑	6	6	28	0	8		
Producer's Accuracy	NA	2/6 33.3%	11/28 39.3%	NA	NA		13/48 27.1%

With a negative *k* ("KHAT") value the classification is shown to be poorer than classification resulting from chance.

Table 4-25: Two classes error matrix resulting from aerial photography (Air_2009) 2009 vs. satellite imagery (TM2009) 2009 of Caerlaverock Reserve.

Air 2009 → TM 2009 ↓	T&S	Others	∑	User's Accuracy
T&S	5	17	22	5/22 22.7%
Other	7	19	26	19/26 73.1%
∑	12	36		
Producer's Accuracy	5/12 41.7%	19/36 52.8%		24/48 50%

With a negative *k* ("KHAT") value the classification is shown to be poorer than classification resulting from chance.

A summary of overall classification accuracy from two and five classes of 2009 Caerlaverock Reserve aerial photography versus fieldwork 2011 is shown in Table 4.26.

Table 4-26: Shows accuracy of aerial photography 2009 versus fieldwork 2011, see Tables 4.5 and 4.6.

Number of classes	Aerial photography	Overall classification accuracy
2	2009	92%
5	2009	83.3%

On the basis of Table 4.26 it was concluded that aerial photography was comparable to fieldwork and should be use to assess the quality of satellite classification. A summary of overall classification accuracy from an unsupervised classification (2 and 6 classes) and supervised classification (2 and 5 classes) for Caerlaverock Reserve satellite image using aerial photography for1988 versus fieldwork 2011 is shown in Table 4.27.

Table 4-27: Shows accuracy of satellite imagery using 1988 aerial photography for validating 1988 satellite imagery and using 2011 fieldwork for validating 2009 satellite imagery.

Classification	Class	Year of satellite imagery	Overall classification accuracy
Unsupervised classification	2	1988	81.2%
		2009	79%
	6	1988	10.4%
		2009	43.75%
Supervised classification	2	1988	75%
		2009	52%
	5	1988	58.3%
		2009	25%

4.4 TWINSPAN classification

TWINSPAN analysis was undertaken on the 73 species in 22 families (see Appendix 7a, 7b) recorded from 48 quadrats (coordinates captured in the field by GPS) located on seven transects at Caerlaverock Reserve in 2011. The distribution of quadrat samples belonging to five TWINSPAN sample end-groups identified by the analysis (see below) along the seven transects is shown in Fig. 4.15.

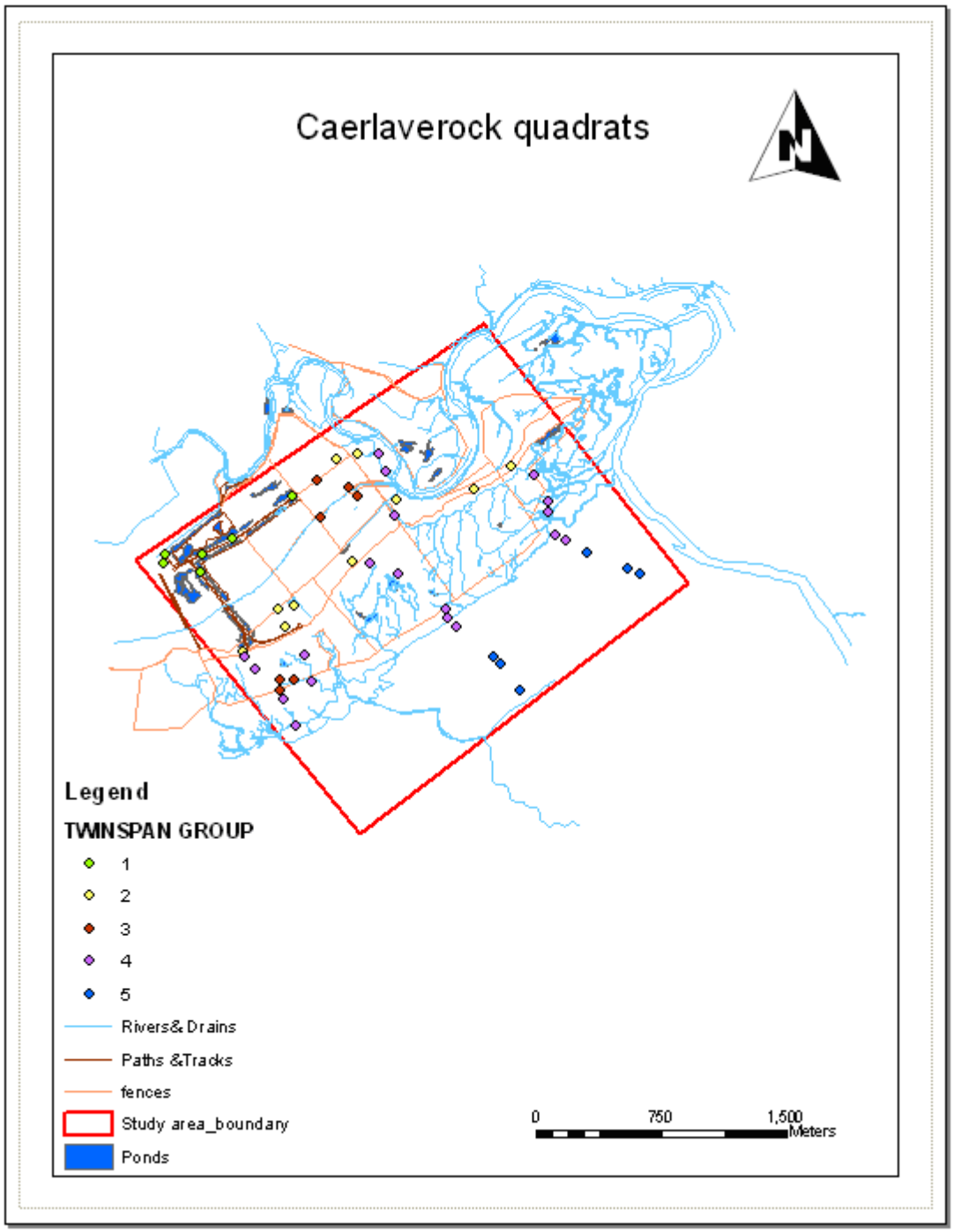

Figure 4-15: Distribution of quadrat positions (in five TWINSPAN groups) in the Caerlaverock Reserve.

Sample end groups were all located at the level of the classification that stopped at the third level of division, with eigenvalues for the divisions producing these groups all reasonably high, (> 0.500). For the vegetation communities that these represent see Appendix 8. The first division [Eigenvalue = 0.823] divided the 48 quadrats into a negative (right) group including 23 quadrats, and a positive (left) including 25 quadrats. A dendrogram showing the classification is given in Fig. 4.16 and list of species with their groups and indicator species in Table 4.28. The indicator species in the negative group were *Urtica dioica* (Common Nettle), *Galium aparine* (Cleavers), *Holcus lanatus* (Yorkshire-fog), and *Dryopteris filix-mas* (Male-fern). The indicators in positive group were *Puccinellia maritima* (Common Saltmarsh-grass) and Festuca *rubra* (Red Fescue). The second division at the second level [Eigenvalue = 0.708] divided the 23 quadrats into a negative group including 6 quadrats, (indicator species: *Bellis perennis:* Daisy), and a positive group including 17 quadrats (indicator species: *Ulex europaeus* (Gorse), *Juncus effusus* (Soft-rush) and *Trifolium repens* (White Clover). The third division [Eigenvalue = 0.701] at the same level divided the 25 quadrats into a negative group including 19 quadrats, (indicator species: *Lotus corniculatus* (Common Bird's-foot-trefoil), and a positive group including 6 quadrats, (indicator species: *Salicornia europaea* (Common Glasswort). The fifth division at the third level [Eigenvalue = 0.608] divided the 17 quadrats into a negative group including 10 quadrats, (indicator species: *Urtica dioica* (Common Nettle), and a positive group including 7 quadrats (indicator species: *Lolium perenne* (Perennial Rye-grass), *Ranunculus repens* (Creeping Buttercup), *Festuca arundinacea* (Tall Fescue), *Cynosurus cristatus* (Crested Dog's-tail), *Ranunculus acris* (Meadow Buttercup).

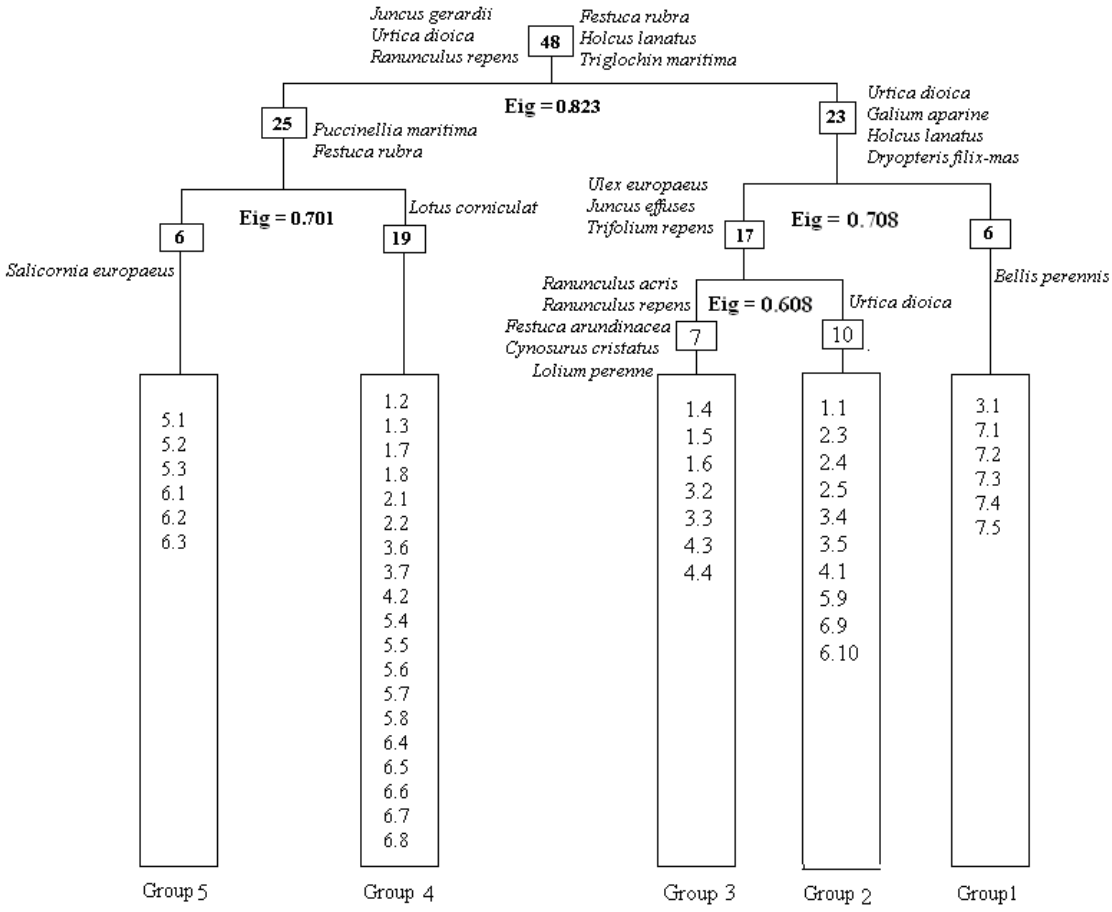

Figure 4-16: Dendrogram of the TWINSPA sample classification of 48 quadrates in Caerlaverock.

(3.1 = 3 means number of Line transect, 1 means number of Quadrat).

Table 4-28: TWINSPAN groups, species and indicator species after species classification
(For a complete species names see Appendix 7b)

Group Number	Species name abbreviations	Indicator species
1	ranu repe, ranu acri, bell pere, equi arve, dact glom, poa triv, urti dioi, gali apar, holc moll, dryo fili, hede heli, hera spho, gera robe, sile dioi elym pycn, poa subc	bell pere
2	leon autu, rubu frut, junc effu, gali palu, junc infl, symp tube, arme mari, rume acet, ulex euro, , stel nemo,junc bufo, card prat, equi arve, poly pers, epil angu, agro capi, lotu corn, eleo unig, urti dioi, gali apar, gyce decl,	urti dioi
3	fest arun, ranu acri, sene jaco, cyno cris,bell pere, lath prat, loli pere, phle prat, trip mari, caps burs, poa annu, cirs arve, elym repe, holc lana, stel holo, anth odor, agro stol, , fest rubr, ranu repe, dact glom, trif repe, care nigr, pote anse, , care flacc, oena lach,	loli pere ranu repe fest arun cyno cris ranu acri
4	agro capi, lotu corn, eleo unig, poa triv, elym pycn, trif repe, care nigr, pote anse, gyce decl, care flacc, oena lach, agro stol, leon autu, poa subc, care dist, atri hast, spar mari, fest rubr, junc gera, scir mari,ranu baud, trip mari, alop geni, care dins, coch angl, glau mari, arme mari, pucc mari, plan mari,	lotu corn
5	fest rubr, glau mari, plan mari, arme mari, sali euro,aste trip, pucc mari, coch offi	sali euro

4.5 TABLEFIT Classification

Using the TABLEFIT classification to determine NVC categories (and equivalents in the European CORINE biotopes classification) the first TWINSPAN group has the highest level of similarity to to OV24 *Urtica dioica* (Common Nettle) – *Galium aparine* (Cleavers) tall herb community (coefficient = 49.0; CORINE 87.2). The highest matched community type in the second group was to OV27b *Epilobium angustifolium* (Alpine

Willowherb) tall herb (coefficient =32; CORINE 87.2), sub community *Urtica dioica* - *Cirsium arvense* (Creeping Thistle). Group three was matched to MG12a *Festuca arundinacea* (Tall Fescue) mesotrophic grassland inundation community (coefficient = 56; CORINE 37.242), sub community *Lolium perenne* (Perennial Rye-grass) - *Holcus lanatus* (Yorkshire-fog). The fourth TWINSPAN group had a best match to MG12b *Festuca arundinacea* community (coefficient = 50; CORINE 37.242), community *Oenanthe lachenallii* (Parsley Water-dropwort). The last TWINSPAN group had a good match with SM 13d *Puccinellia* salt-marsh (coefficient = 89; CORINE 15.31), sub community *Plantago maritima* (Sea Plantain) - *Armeria maritima*.

4.6 Statistical analysis

The significance of differences in mean values of environmental and botanical variables, measured, between the five sample groups, was tested using one-way ANOVA with Tukey's method for mean comparison, in MINITAB version 16.

Table 4.29 shows the mean values (±SD) for all measured environmental variables across the quadrats in Caerlaverock Reserve, together with the results of ANOVA by Group. ANOVA tests produced significant inter-group for two environmental variables (soil conductivity, water conductivity) and one vegetation variable (plant height) among the five TWINSPAN groups.

Table 4-29: Mean values and standard deviation of the mean (± SD) for a) soil pH; b) soil conductivity; c) shade; and d) mean vegetation height for TWINSPAN Groups, as shown by one-way ANOVA and application of Tukey's mean test Mean values per variable sharing a superscript letter in common are not significantly different.

Groups	a) Soil pH	b) Cond. soil	d) Height
	Mean	Mean	Mean
Group 1	$6.0383^{b} \pm 0.37$	$215^{c} \pm 121$	$4.7800^{a} \pm 2.58$
Group 2	$5.7880^{b} \pm 0.40$	$898^{bc} \pm 1144$	$0.7060^{b} \pm 0.21$
Group 3	$6.2771^{a} \pm 0.82$	$204^{c} \pm 125$	$0.2937^{b} \pm 0.32$
Group 4	$7.0753^{a} \pm 0.51$	$1736^{b} \pm 1204$	$0.2363^{b} \pm 0.1648$
Group 5	$7.1233^{a} \pm 0.14$	$6767^{a} \pm 3404$	$0.0667^{b} \pm 0.04$
P	***	***	***

*** = $p \leq 0.001$

ANOVA analyses confirmed that there were significant differences between the five TWINSPAN groups for mean soil pH (P = 0.000) (Fig.4.17), mean soil conductivity (P = 0.000) (Fig.4.18), and mean vegetation height (P = 0.000) (Fig.4.19).

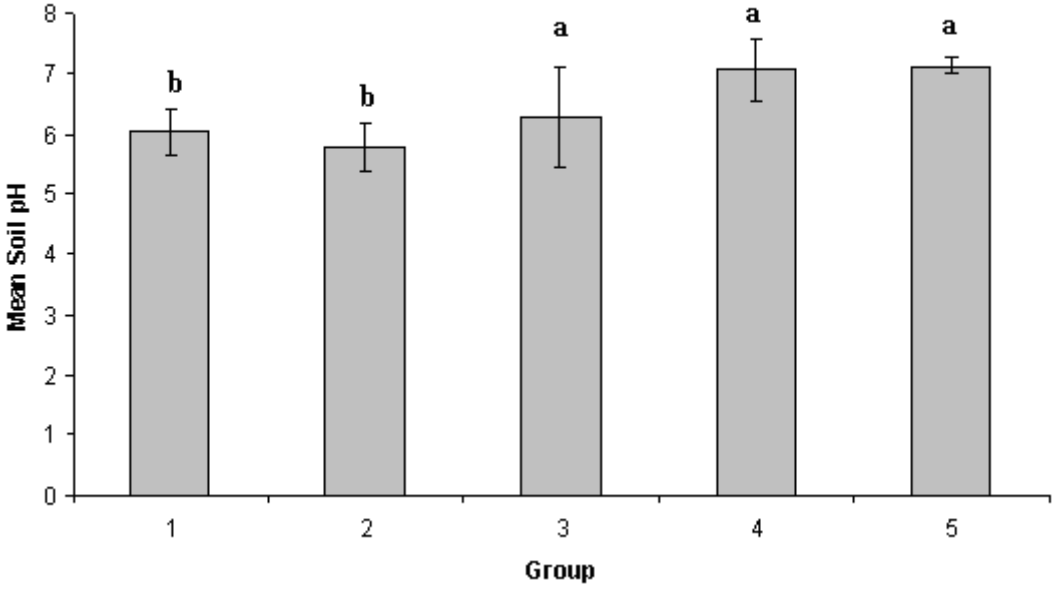

Figure 4-17: Mean (± S.D) values for soil pH of TWINSPAN groups. Different letters above value bars represent a significant difference between group means.

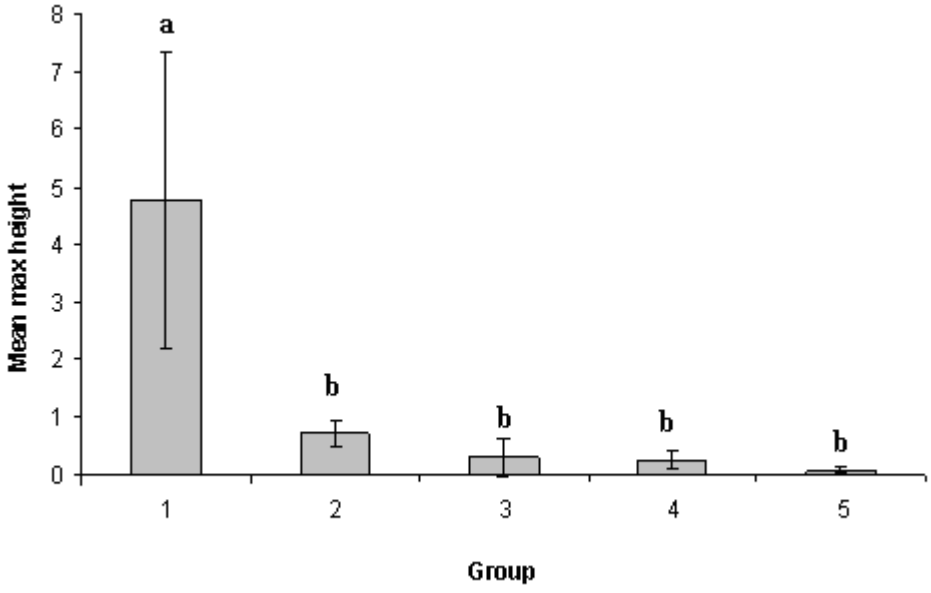

Figure 4-18: Mean (± S.D) values for max vegetation height for TWINSPAN groups. Different letters above value bars represent a significant difference between group means.

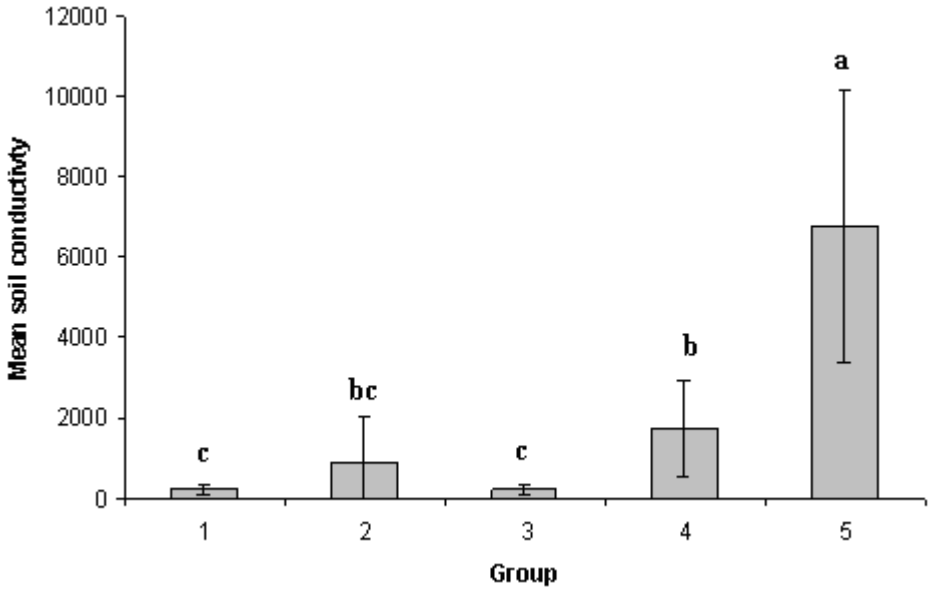

Figure 4-19: Mean (± S.D) values for soil conductivity of TWINSPAN groups. Different letters above value bars represent a significant difference between group means.

In addition to testing the significance of differences in mean values of environmental and botanical variables, I measured the significance of differences in mean values of Ellenberg's indicator values based on the data for UK plant species given by Hill et al. (1999), see Appendix 9.

Table 4.30 shows the mean values (± SD) for Ellenberg's indicator values for all plant species present at samples comprising each sample group in Caerlaverock Reserve, together with the results of ANOVA by Group. ANOVA tests produced significant difference inter-groups for light, moisture, and salt-tolerance among the five TWINSPAN groups. It is clear from the results of Ellenberg's indicator values for TWINSPAN groups that:

Group 1 somewhat shadier and drier sites, non-saline,

Group 2 somewhat moister than latter, and with a minor salt influence,

Group 3 sunnier and as dry as group 1, but with minor saline influence,

Group 4 – still better illuminated, quite moist/wet, with moderate saline influence, and

Group 5 – very well lit, wet and with marked saline influence.

Table 4-30: Mean values and standard deviation of the mean (± SD) for a) Light; b) Moisture; c) salt-tolerant) for TWINSPAN groups using Ellenberg's indicator values for plants, as shown by one-way ANOVA and application of Tukey's mean test. Mean values sharing a superscript letter in common are not significantly different.

Groups	a) Light	b) Moisture	d) Salt
	Mean	Mean	Mean
Group 1	6.20 ± 1.08	5.73 ± 0.59	0.00^{c} ± 0.00
Group 2	6.73 ± 0.88	6.41 ± 1.37	0.45^{c} ± 0.91
Group 3	7.23 ± 0.71	5.77 ± 1.18	0.50^{c} ± 0.86
Group 4	7.64 ± 0.68	6.93 ± 1.68	2.07^{b} ± 1.88
Group 5	8.37 ± 0.52	7.00 ± 1.07	4.25^{a} ± 2.19
P	***	***	***

** = p≤ 0.01 *** = p≤ 0.001

ANOVA analysis confirmed that there was a significant difference between the five TWINSPAN groups in mean light (P = 0.000) (Figure 4.20), with samples from Group 1 and Group 5 supporting species with high Ellenberg light values. There were significant differences between the five TWINSPAN groups for mean moisture (P = 0.005) (Figure 4.21), due to samples from Group 2 and Group 3 supporting species with high Ellenberg moisture values. Also ANOVA analysis confirmed that there was a significant difference between the five TWINSPAN groups in mean salt-tolerance (P = 0.000) (Figure 4.22), because of samples from Group 1, Group 3 and Group 5, supporting halophilic species with high Ellenberg salt values.

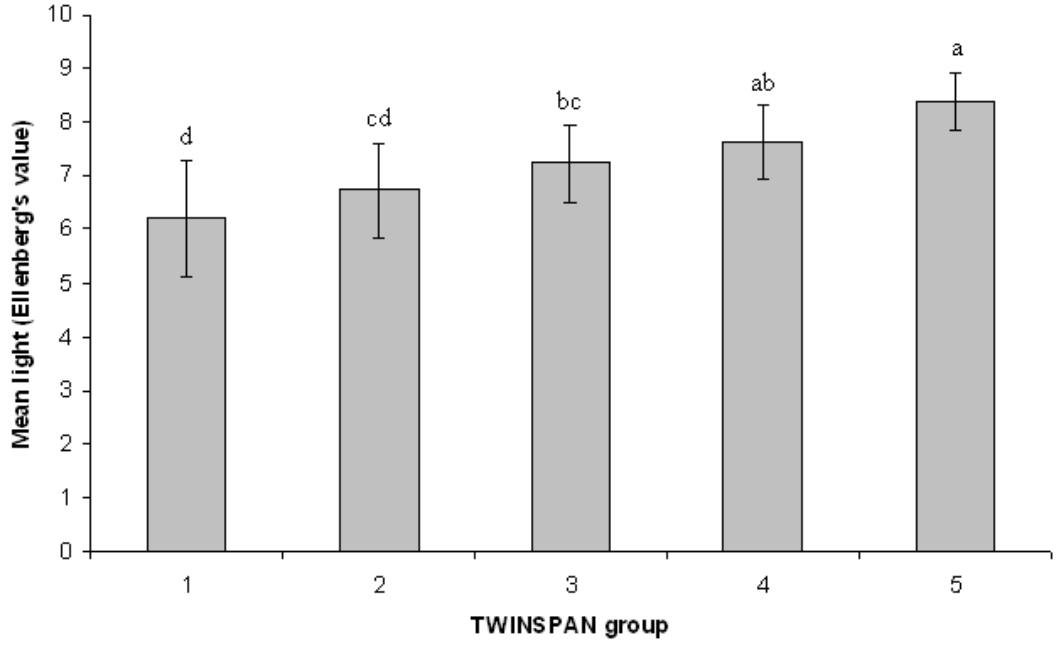

Figure 4-20: Mean (± S.D) values for shade percentage between TWINSPAN groups. Different letters above value bars represent a significant difference between group means.

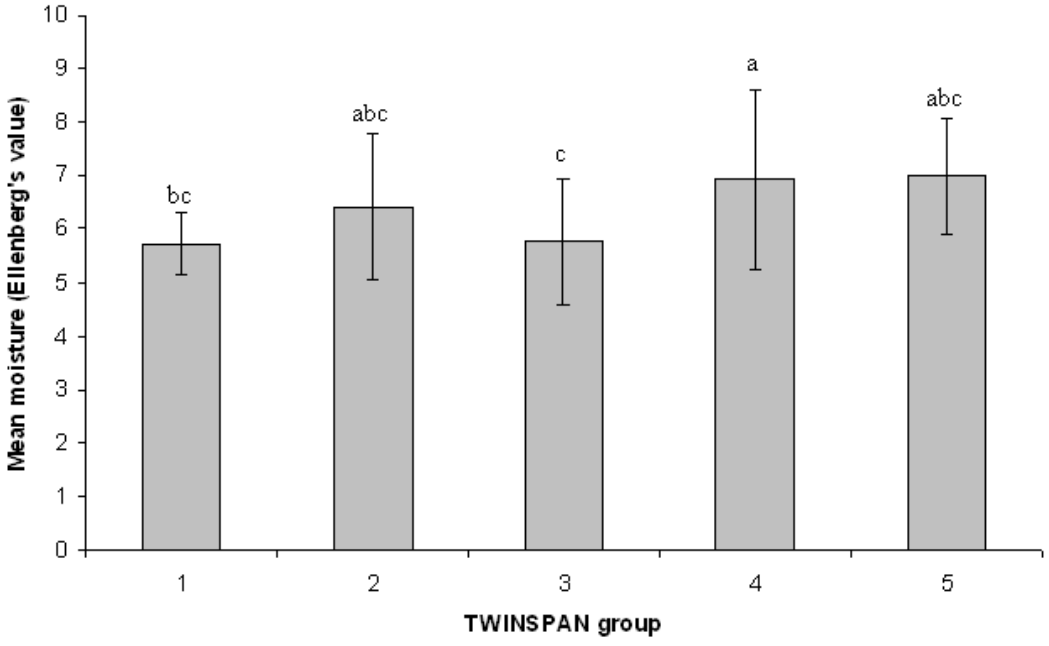

Figure 4-21: Mean (± S.D) values for shade percentage between TWINSPAN groups. Different letters above value bars represent a significant difference between group means.

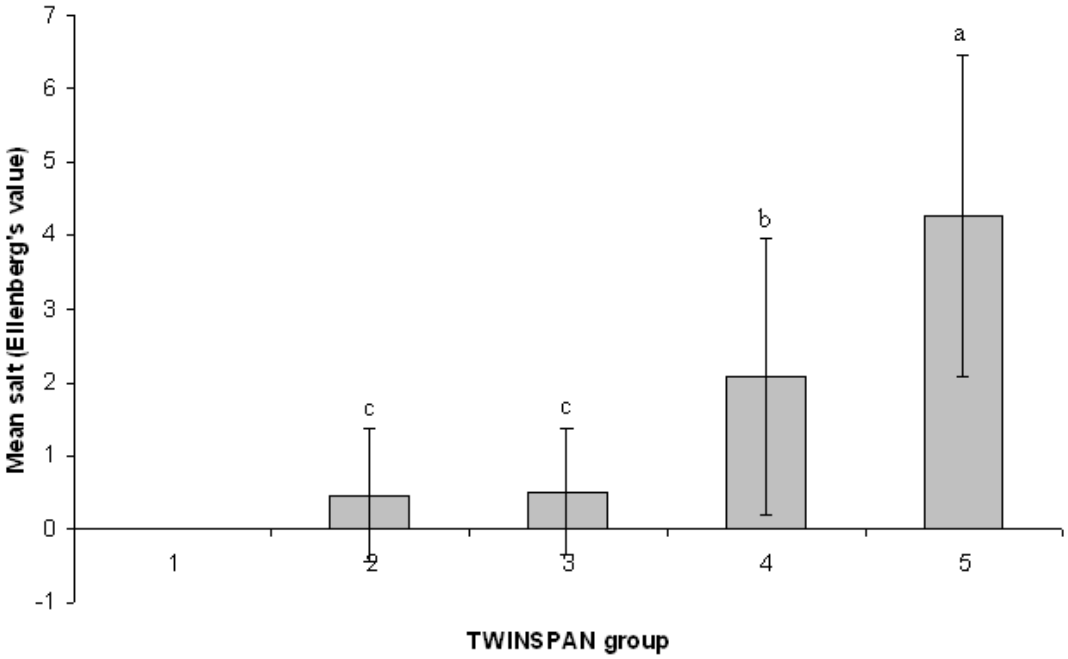

Figure 4-22: Mean (± S.D) values for shade percentage between TWINSPAN groups. Different letters above value bars represent a significant difference between group means.

4.7 Discussion

Remote sensing images are especially appropriate for reconnaissance mapping and information monitoring for different types of wetlands over large geographic areas. Successful use of remote sensing for detailed interpretation in the study of wetlands depends mainly on the spatial resolution of images to give good results for interpretation, mapping, and the comparisons between different periods. Aerial photography and orthophotography were more often used for delineation of the wetlands (Barrette et al., 2000). Duhaime et al (1997) used orthophotography as an alternative to satellite data for assessing vegetation in Block Island and Rhode Island (including freshwater and saltwater wetlands) , and provided valuable information for preparing detailed vegetation maps.

The orthophotographs were used successfully for studying the vegetation cover in Caerlaverock Reserve in the period between 1988 and 2009. As is clear from interpretation of 1988 orthophotograph when visually comparing this period with 2009 orthophotograph, the total cover of shrubs showed no change, while the total cover of trees showed a slight increase. Based on to the morphometric measurements made from the orthophotograph interpretation obtained from the delineation of total cover of trees and shrubs (see Figures 4.4 and 4.5), the total cover of shrubs slightly decreased annually by 0.009% , total cover of trees increased annually by 1.3% from 1985 to 2009. The slight decrease in the cover of shrubs, might be as a result of grazing, especially shrubs located in the grazing zone was personally observed during ground truth field work in 2011, while the percentage increased in the cover of trees as a result of the growth of trees through twenty one years.

The most common mapping technique in the world is still based on aerial photography interpretation (Lewis and Phinn, 2011) and measurement. It is used successfully for detailed mapping of vegetation communities and to a high accuracy using manual interpretation techniques, for example in a tropical freshwater swamp (Harvey and Hill, 2001). Overall classification accuracy from aerial photography of 2009, for two and five classes (92% and 83.3% respectively) indicates that through my classification method, I was generally able to correctly distinguish map classes (see Table 4.16

Unsupervised and supervised classifications are usually the methods used for Landsat TM and other remotely sensed image interpretation. The results obtained from Landsat TM image analysis for 1988 imagery using unsupervised classification show unsatisfactory results using six land cover classes, while showing a good result from two classes (Table 4.27). A limitation of this method is that the classes are produced based on natural features which may not correspond to the features that the user needs to resolve. Cawkwell et al (2007) reported that an unsupervised ISODATA classification into six classes failed to distinguish the small areas of *Juncus* and grassland in the saltmarsh habitat. Unsupervised classification (two classes) of the Landsat TM images for 1988 and 2009 at the Caerlaverock Reserve provided fairly good results, where the classification had an overall accuracy of 81.2% and 79% respectively; and in six classes the classification had a lower overall accuracy 10.4% and 43.7% respectively, because of in an unsupervised classification the classes produced are based on natural breaks in the distribution of pixel values in the image. Overall classification accuracy from two supervised classes of the Landsat TM images for 1988 and 2009 were 75% and 52% respectively (Table 4.27).

In the six classes Landsat TM image analysis of the 2009 imagery the method succeeded in showing some difference compared with 1988, with the result being fairly different to those obtained from analysis of aerial photography. Using ten land cover classes produced classes that were difficult to identify, based on field work and knowledge of the area (see Figure 4.7). A difference between the image of 1988 and the image of 2009 image may be due to the image in 1988 being captured in the high tide period and showed a large area immersed by water (Magenta colour Figure 4.6), while in 2009 the image captured in the period of low tide and it appeared that some areas were not inundated (Figure 4.8).

The classification of Landsat TM satellite imagery achieves an acceptable level of accuracy specially with the two classes unsupervised classification (Table 4.26), and the satellite data provide a description of the major land cover for Caerlaverock Reserve wetland, but it remains apparent that aerial photography at high resolution can sometimes provide better information that cannot be extracted from satellite data, especially in small areas like Caerlaverock. But it is worth remembering that Landsat TM imagery is now much cheaper to acquire (e.g. GLOVIS) than aerial imagery.

Depending on the results obtained from scattergrams of supervised classification maximum likelihood classification (MLC) showed better results for distinguishing Caerlaverock Reserve vegetation classes (Figures 4.11, 4.12). Supervised classification often yields maps with a higher mapping accuracy (Johnston and Barson 1993), and it achieves good separation of classes (Soliman and Soussa, 2011). In addition, Donoghue and Shennan (1987) noted that the maximum likelihood classification with Landsat TM showed good separation of saltmarsh vegetation communities. Aerial photography, Ordnance Survey maps, and field work ground-truthing all proved useful here as a guide for the selection of vegetation classes in supervised classification.

The spectral overlap between wetland cover types is a problem frequently identified in the application of remote sensing to wetland environments (e.g. Johnston and Barson 1993, Sader et al. 1995), because commonly different vegetation types may possess the same spectral signature in remotely sensed images (Xie et al. 2008). Sanchez-Hernandez et al (2007) state unacceptable maximum likelihood classification (MLC) for monitoring habitat in saltmarsh due and the error (or confusion) matrix illustrates that the saltmarsh class was confused with the fenland class, also Reid Thomas et al (1995) reported that the maximum likelihood classification (MLC) with Landsat TM had difficulty in mapping the vegetation of the Pioneer zone in saltmarsh vegetation due to mixed pixels of classes.

The results from scattergrams of supervised classification for all land cover classes of the Landsat TM image in 1988 and Landsat TM image in 2009 showed no overlap between the land cover classes; which means that the supervised classification has precisely determined land cover classes and successfully avoided including pixels of ambiguous class.

The results obtained from the detection of change in vegetation using ArcMap (v 10.1) showed the cover of trees between 1988 and 2009 changed by 50% to wet grassland, shrubs cover decreased by 87% in the same period. More than half of the percentage change in the shrubs cover is change to wet grassland, a further 30.0% change to trees (Table 4.11), and this result seems difficult to accept, and poor quality classification is confirmed by low k (“KHAT”) statistic. However, supervised classification included some grasses that are mapped as shrubs in an OS map (1:10000 scale) for 2009, because the reflection for some grasses from the rough grazing area is the same as the shrub Gorse

(*Ulex europaeus* L.), and supervised classification considered the same reflectivity to be one type. For this reason, in the outcome map of five classes using a supervised classification the cover of shrubs is greater than reality compared with aerial photographs of the same year, see Figure 4.23 below. In addition, some wet grassland on the grounds is shrubs in map for 1988. This could be due to the small study area, and the trees and shrubs covering an area less than one pixel size in the Landsat TM image, and probably when selected training area for TM image of 1988 includes some grass with the same colour as shrubs see Figure 4.24. Band 2 in the Landsat TM5 is (0.52-0.6 µm), this means including reflected waves for Green colour (0.500- 0.578 µm) and Yellow colour (0.578- 0.592 µm). For this reason some grass may share reflectivity with shrubs, although the scattergrams of supervised classification showed better results for all five identified land cover classes of the Landsat TM image in 1988 and Landsat TM image in 2009 for Caerlaverock Reserve (Figures 4.12 and 4.13).

According to TWINSPAN classification divided the samples into five groups depending on eigenvalues with high value (>0.500), and showed that the sample-group 4, the largest TWINSPAN group, contained quadrat representing all transects examined at the site. The indicator of the group was *Lotus corniculatus*, which has the highest level of similarity to a recognised NVC type: MG12b. The indicator species of group 5 was *Salicornia europaea*, which has the highest level of similarity to a recognised NVC type: SM13d, this community is the most widespread and extensive perennial community of the lower saltmarsh (Rodwell 2000). This group has the highest average mean conductivity and the shortest average mean vegetation height. However, statistical analyses showed the soil conductivity had a significant difference between a group means in-group 1 and group 5, as well as in mean height. Depending on the Ellenberg's indicator values, group 5 has the highest mean for salt tolerance, moisture and light, which mean these species are adapted to live in the high levels of salt and in submerged or saturated soil water and are light loving, while, the group 1 has the lowest mean for salt tolerance, moisture and light.

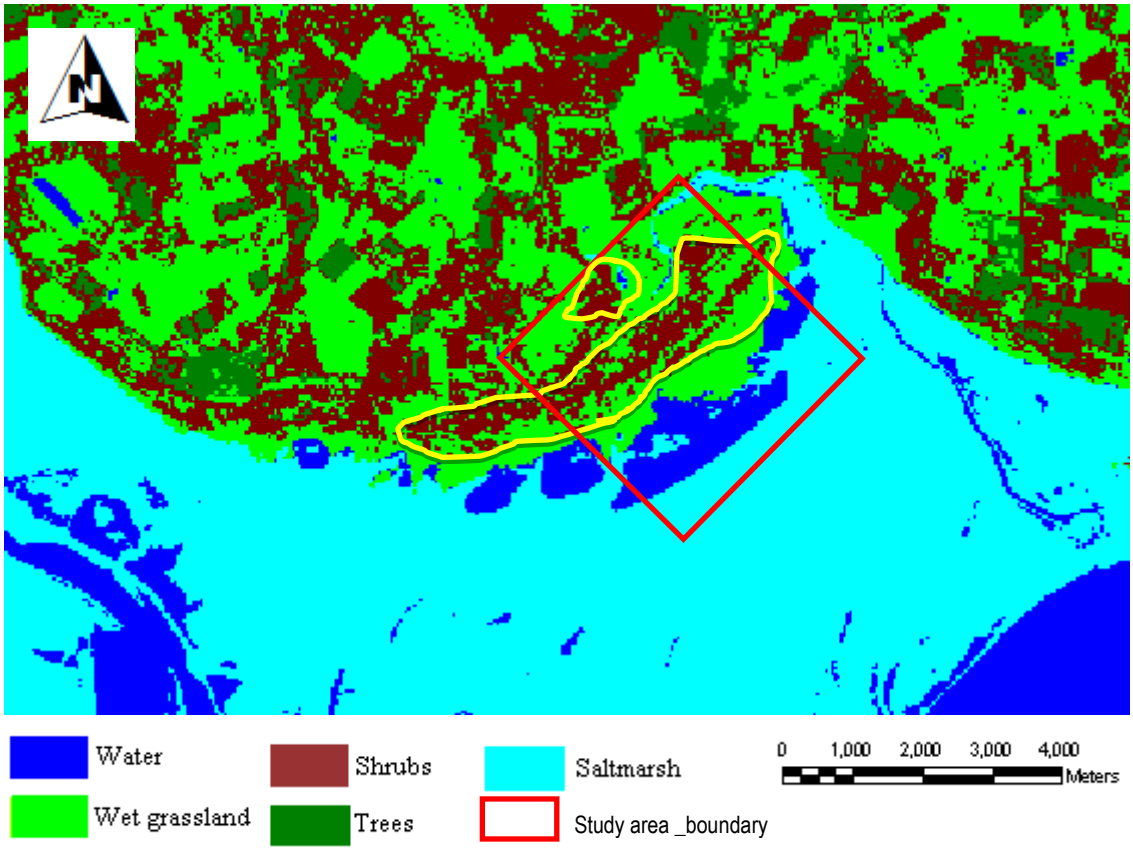

Figure 4-23: Shows the rough grazing zone inside the yellow line that has shrubs and grasses following supervised classification for 2009 Caerlaverock Reserve Landsat TM.

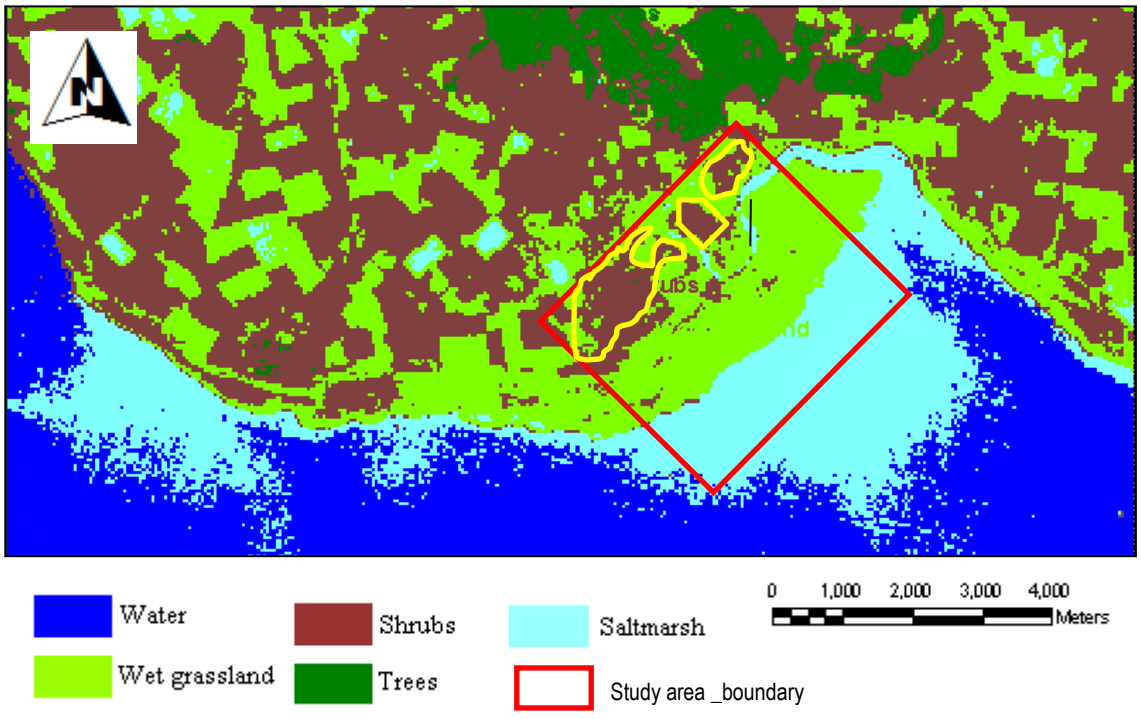

Figure 4-24: Shows the rough grazing zone inside the yellow line that has shrubs and grasses following supervised classification for 1988 Caerlaverock Reserve LandsatTM.

Chapter 5- General Discussion & General Comparison of Survey Approaches

5

5.1 General discussion

The decline of wetland resources and ecosystem services worldwide is usually closely connected with local ecological negative effects, e.g. in Libya natural conditions (drought) or abuse from human activities, or both. Using remote sensing techniques and geographic information systems will allow us to detect the change that occurs in the vegetation in the wetlands as a result of such impacts, and assist corresponding effective protection and utilization measures, as well as helping provide the scientific basis for the restoration of wetland resources and conservation.

Remote sensing imagery, analysed using GIS tools, is becoming increasingly useful for reconnaissance mapping and information monitoring of different types of wetlands over extensive geographic areas. Remote sensing tools seem to be one of the only practical ways to study environments that can be difficult to access for landscape characterisation, habitat monitoring, and spatial analysis of surface cover change (Rehnquist et al., 2001).

The aim of this project was to investigate the proposal that vegetation changes over time (e.g. scrub invasion; successional changes) have an effect on wetland plant community structure in UK wetland systems, which can be detected and quantified using remote sensing imagery. This proposal was investigated using an approach which combined remote-sensing analysis of imagery over time with ground truthing of existing wetland vegetation communities at two contrasting wetland sites in the UK

5.1.1 Aerial Photography Interpretation

In Study Area 1, Wicken Fen, interpretation performed on aerial photographs for the years 1985, 1999, 2003, and 2009, using ArcMap GIS, provided quantitative information on changing total vegetation cover (trees and shrubs, versus open herbaceous fen vegetation)

within the 24-year study period. The most significant annual change rate of Wicken Fen vegetation cover during this period, based on morphometric measurements made from aerial photography interpretation obtained from the delineation of total tall vegetation cover (trees and shrubs), is for the period between 1985 and 1999, with a 2.24% reduction per year, while the annual rate of change for the period 2003 to 2009 was a 1.48% reduction per year. Friday (1997) noted that in Wicken Fen, a wave of die-back swept through the *Frangula* carr in the 1980s, and a large proportion of the *Frangula* carr standing on all parts of the Fen became dead wood; also, in the 1990s, fire was a frequent occurrence in the dead, dry shrubs. This could be the major cause of a decrease in the tall vegetation canopy in Wicken Fen, especially Verrall's Fen in the period 1985 to 1999; and provides a likely interpretation of the high annual change rate observed in decreasing tree/shrub cover during this period.

The second significant, though lower, annual change rate, over the period 2003 to 2009 of 1.48%, is most likely due to the active woodland and carr removal management programme underway during this period, rather than to natural change. Part of the carr in Sedge Fen was removed for subsequent management operations, and evidence of recent clearance activities was personally observed during ground truth fieldwork in 2010. Mountford et al., (2012) noted that there is some evidence that fen herbaceous vegetation was re-establishing on Verrall's Fen, where carr had been cleared.

Overall classification accuracy obtained using aerial photography from 2009 for two and five classes (90% and 80% respectively) indicates that, through the classification method developed in this study, it was generally possible to correctly distinguish map classes for Wicken Fen (see Table 3.26).

In Study Area 2, an interpretation of the orthophotographs in the 21-year period between 1988 to 2009 for Caerlaverock Reserve, using ArcMap GIS, also showed changes in the total vegetation cover (trees/shrubs versus open herbaceous meadow and saltmarsh vegetation) over the study period. Based on the morphometric measurements made from the orthophotography interpretation obtained from the delineation of total tall vegetation cover of Caerlaverock Reserve using ArcGIS, the annual change rate in shrub cover was 0.009% (i.e. only a slight decrease), while tree cover increased annually by 1.3%from 1985 to 2009. This slight decrease in shrub cover might be a result of grazing of shrubs located in the grazing zone (grazing damage, by cows and Soay sheep was personally observed

during ground truth field work in 2011), while the percentage increase in the cover of trees is a result of the growth of trees over twenty one years.

Aerial photography and orthophotography are often used for delineation of wetlands (Barrette et al., 2000). Overall, approaches utilising aerial photography interpretation are still the most common technique (Lewis and Phinn, 2011).
Overall classification accuracy from aerial photography of 2009, for two and five classes (92% and 83.3% respectively) indicates that, through the classification method developed in this work, it was generally possible to correctly distinguish map classes for the Caerlaverock study area (see Table 4.26).

5.1.2 Landsat TM Image Interpretation

The Landsat TM image used in this study had a 30-meter pixel resolution, and was able to support an MMU closer to 0.1 hectares. The most important factor in distinguishing cover classes in the target area of study is the spatial resolution of the sensor. Landsat TM provided a good class separation when one class covers more than the pixel size (30×30 m) in the TM image.

In study Area 1, Wicken Fen, the Landsat TM images were classified using two methods: unsupervised and supervised. The results obtained from Landsat TM image analysis for 1984, using unsupervised classification, show good results using six land cover classes. In the six classes output map from unsupervised classification of Landsat TM image analysis for 2009, the method succeeded in showing some change when visually compared with the output map for 1984, with the result being fairly similar to those obtained from analysis of aerial photography.

Supervised classification achieves good separation of classes (Soliman and Soussa, 2011), and often yields maps with higher accuracy (Johnston and Barson 1993). Depending on the results obtained from supervised classification, maximum likelihood classification (MLC) showed better results when compared with unsupervised classification for distinguishing

Wicken Fen vegetation classes, and the best classification accuracy was achieved using a two classes supervised classification for both the 1984 and 2009 images (Table 3.27). Supervised classification is depend on the user definition for training areas; aerial photography, Ordnance Survey maps, and field work ground-truthing; all proved useful here as a guide for the selection of vegetation classes in a supervised classification.

The results from scattergrams of supervised classification for all land cover classes of LandsatTM images in 1984 and 2009 at Wicken Fen showed no overlap between the land cover classes; which indicates that the supervised classification has clearly determined land cover classes, and successfully avoided including pixels of ambiguous class (or 'mixels').

The results obtained from using ArcMap (v 10.1) for the detection of change in vegetation at Wicken Fen showed that the total cover of trees and shrubs decreased by 65.6% between 1984 and 2009, and more than half of the percentage change in the total cover is change to wet grassland. Overall classification accuracy from two classes using a supervised classification of the LandsatTM images for 1984 and 2009 was 75% (Table 3.27). A comparison of the overall accuracy was conducted to find out which method(s) provided good results. It was found that supervised classification produces more accurate results than unsupervised classification for two classes in Wicken Fen. Alrababah and Alhamad (2006) found that supervised classification worked better than unsupervised classification; also, Mohd Hasmadi et al (2009) found that supervised classification appears more accurate than unsupervised classification for land cover mapping. The same result was found in Wicken Fen.

In Study Area 2 Caerlaverock Reserve, the results obtained from Landsat TM image analysis for 1988 imagery using unsupervised classification show an unsatisfactory result using six land cover classes, but a good result from two land cover classes. The results from an unsupervised classification (two classes) of the Landsat TM images for 1988 and 2009 at Caerlaverock Reserve showed a good result, and the classification had an overall accuracy for the two years of 81.2% and 79%, respectively. In the six classes unsupervised classification the result was worse, overall accuracy in this study being only 10.4% and

43.7% respectively. A limitation of this method is that the classes are produced based on the natural groupings of the spectral properties of the pixels, selected by the remote sensing software, which may not correspond to the actual features of the vegetation.

Overall classification accuracy for the two classes supervised analysis of the Landsat TM images for 1988 and 2009 was 75% and 52% respectively (Table 4.27). Visual comparison of the outcome map of 1988 and 2009 for the Caerlaverock Reserve supervised classification showed that there was some difference between two images. This is most likely due to the timings of the captured images: in 1988, the image was captured at high tide, while in 2009 the image was captured at low tide.

A comparison of the overall accuracy was conducted to find out which method provided better results. Based on the results shown in Table 4.27, it was found that an unsupervised classification produced more accurate results than supervised classification for two classes in Caerlaverock Reserve. In this it case might be that the supervised classification has included in the training areas some grasses that were mapped as shrubs in the OS map (1:10000 scale) for 2009. Or because the reflectivity for some grasses from the rough grazing area is very similar to the shrub Gorse, and probably when selecting training areas for the TM image of 1988 using aerial photography as a guide some grass was included as shrubs. Thus for the outcome map of five classes using a supervised classification, the cover of shrubs is greater than reality for the same year, and some grass may share reflectivity with shrubs. For these reasons, when calculating the change in the cover using the results from unsupervised classification is better than supervised classification in two classes. Considering others working similarly, Rozenstein and Karnieli (2011) found that an unsupervised classification produced more accurate results than supervised classification for land use classification for the northern Negev, while Cawkwell et al (2007) working in similar areas to Caerlaverock (in N England and Wales) reported that an unsupervised classification using six classes failed to distinguish the small areas of *Juncus* and grassland in a saltmarsh habitat.

The most important problem facing the researcher in the application of remote sensing to a wetland environment, when using supervised classification, might be considered to be the

issue of overlapping classes when selecting the training area, which leads to inaccurate results in the study area. The obtained results from scattergrams of supervised classification for all land cover classes of the Landsat TM image in 1988 and Landsat TM image in 2009 showed no overlap between the land cover classes, which means that the digitised training areas were not including pixel classes other than the intended pixel classes.

The results from the detection of change in vegetation using ArcMap (v 10.1) showed that the cover, in trees, between 1988 and 2009 decreased by 50% and in shrubs by 87% (Table 4.11); this result is unlikely to be true. However, the supervised classification included some grass-covered areas as "shrubs" in the map for 2009, perhaps because the reflected wavelengths for some grasses from the rough grazing area are similar to the reflected wavelengths for the shrub Gorse (*Ulex europaeus*). For this reason, the resulting map of supervised classification showed the shrub cover of to be greater than in reality, when compared with aerial photographs of the same year. In addition, some wet grassland was recorded as "shrubs" in the map for 1988. This could be due to the small study area, the fact that trees and shrubs covered an area less than a pixel size in the Landsat TM image, and, probably, the selected training area for the TM image of 1988 included some grass with the same colour as shrubs. However, the scattergrams of supervised classification showed reasonable separation for all five identified land cover classes of the Landsat TM image in 1988 and 2009 for Caerlaverock Reserve.

5.1.3 Ground Reference Data Analysis

In Wicken Fen, TWINSPAN classification showed that the samples divided into four groups, delineated by eigenvalues with high values (>0.500). TWINSPAN classification showed that sample-group 1, the largest TWINSPAN group, and contained quadrats from all transects examined at the site. The indicator of group 2 was Cardamine hirsuta (hairy bittercress), which has the highest level of similarity to a recognised NVC type: M28b. However, statistical analyses showed that shade % had a significant difference between group means 2 and group 4, as well as in height, suggesting that quadrats position group 2 samples being largely located under tree/shrub overstorey vegetation, while group 4 samples were much more open, regardless of on which transect they occurred (transects were placed to run through several habitat conditions, e.g. wet to dry, open to woodland).

In Caerlaverock Reserve, TWINSPAN classification divided the samples into five groups, again delineated by eigenvalues with a high value (>0.500), and showed that sample-group 4, the largest TWINSPAN group, contained quadrats representing all transects examined at the site (as at Wicken, most transects were run across a range of conditions, in this case from land to seaward conditions), and had the highest level of similarity to a recognised NVC type: MG12b. Salicornia europaea (glasswort) was an indicator species of group 5, which has the highest level of similarity to a recognised NVC type: SM13d; this community is the most widespread and extensive perennial community on the lower salt marsh (Rodwell 2000). This group has the highest average mean conductivity and the shortest average mean vegetation height. However, statistical analyses showed a significant difference in soil conductivity between a group mean in group 1 and group 5, as well as in mean height. Depending on the Ellenberg's indicator values, group 5 has the highest mean for salt tolerance, moisture, and light, which means that these species are adapted to live in high levels of salt and in submerged or saturated soil water, and are light loving. In contrast, group 1 has the lowest mean for salt tolerance, moisture, and light preference.

5.2 General Comparison of Survey Approaches

Comparison of aerial photography and Landsat TM imagery classifications allowed assessment of the time taken, and which method provided a good result for mapping compared with fieldwork survey. In the aerial photos, especially in large areas, more time is required to collect the photos into a single image; this process requires several steps, and is sometimes not easy to implement (e.g. control points, clips), but these steps are necessary to get a mosaic of high quality for the entire study area. While Landsat TM images usually cover a large region (in this study, much greater than the study area), and there is a need to subset the chosen area (study area), this does not take much time and is easy to undertake.

The comparisons via error matrices - between aerial photography of 2009 and fieldwork of 2010 Wicken Fen, and aerial photography of 2009 and fieldwork of 2011 Caerlaverock Reserve, are performed under the assumption that there will have been little change during the two dates, and the error analysis serves to confirm that aerial photography is a worthy

substitute for field work, which is long established amongst aerial photo interpreters: e.g. Mosbech and Hansen (1994).

In Wicken Fen, overall classification accuracy for vegetation classes produced from aerial photography in 2009 (Table 3.26), was compared with overall accuracies obtained for vegetation classes from Landsat TM 1984 and 2009 (Table 3.27). As well, in Caerlaverock Reserve, overall accuracies for vegetation classes from Landsat TM image 1988 and 2009 (Table 4.27) were compared with the overall accuracy obtained from vegetation classes from aerial photographs 2009 (Table 4.26). The obtained result from comparisons of overall classification accuracies showed that the aerial photographs had a better overall accuracy because, it is suggested, they have a higher spatial resolution than the Landsat TM image, and in Caerlaverock Reserve, it is suggested that the areas covered, especially by shrubs, were less than the pixel size in a TM image. Hence, there were unsatisfactory results here, and low overall accuracy.

There are two restrictions when attempting to distinguish between vegetation types in satellite images. The first is that it is almost always difficult to map the vegetation class if its coverage is less than the pixel size of the TM images. The second is that distinguishing vegetation classes is not possible if there is no difference in the reflected wavelengths.

Comparisons of Landsat TM images and aerial photograph classification illustrated that at a structural level of two and five classes, Landsat TM does not facilitate a significantly higher level of mapping accuracy. However, there is no dispute that Landsat TM imagery allows for far more detailed classification than merely five classes. Generally, it has the advantage when mapping large areas, because it is fast, objective and less expensive, e.g. Mansur and Rotherham (2010) state that Landsat TM gave a good result for determination of land cover/land use changes in the Libyan Al-jabal Alakhdar region. Also, Esam et al (2012) reported that Landsat TM imagery provided good accuracy for quantifying land cover changes, and very useful information for natural resources management of the West Tahta Region, Sohage Governorate, Upper Egypt, but it still lacks the spatial resolution to map all important cover classes, especially in small areas, where the class area covered less than the pixel size in the TM image. Finally, it might be worth noting that usual costs increase roughly in proportion to increases in mapping resolution (Lunetta and Balogh 1999).

Chapter 6- Conclusion & Recommendations

6

6.1 Conclusions

Wetlands are amongst the Earth's most productive ecosystems, and are a valuable natural resource of considerable scientific value because they are associated with high biological diversity. Also they provide important ecological functions and values, such as habitat for flora and fauna species, biodiversity (Mitsch and Gosselink 1993), ground water recharge, flood mitigation, and regulation of pollutants and water. Recently, wetlands have been under increasing pressure from anthropogenic activities, including conversion to intensive agricultural use and to other industrial and residential uses. Detection and assessing changes in wetland vegetation over time is hence important for both natural resources management and ecological research (Zaman et al., 2011).

In the UK, wetlands are an important part of the landscape, covering almost 10% of the terrestrial land area (Dawson et al., 2003), e.g. Wicken Fen in England; Insh Marshes in Scotland. Traditional field investigation methods are often inadequate to achieve the detection of changes in vegetation for these ecosystems in a timely manner. Using remote sensing and GIS techniques will allow us to detect changes in these ecosystems with high accuracy and in a timely manner, and also can provide valuable information to aid the management and conservation of wetland habitat.

Wetland degradation in arid, semi-arid and sub-humid areas is strongly affected by human activities (e.g. grazing and planting crops); the application of remote sensing techniques provides accurate and timely information for mapping and monitoring vegetation cover in threatened systems. In Libya, Farwà Lagoon is an example of important coastal wetlands (Pergent et al., 2002); these are sensitive ecological systems and provide many valuable ecosystem services e.g. for tourism, recreation and fishing. Vegetation is an important component of wetland ecosystems and it also serves as an excellent indicator of early signs of any physical or chemical degradation of the land, so application of remote sensing and GIS to these ecosystems will help in the detection of change that has happened in these habitats.

Several oases in Libya, for example the Al Jufrah Oases, hold rare and important plants, and provide a natural shelter for many animals. It is difficult to monitor these systems by conventional methods such as field survey. The application of remote sensing techniques for monitoring and change detection in these ecosystems, which is essential to warn of potential collapse of these vulnerable ecosystems, can hence provide valuable information to aid the management and conservation of these habitats.

Data from Earth Observation satellites has become important in mapping the Earth's features and infrastructures, managing natural resources, and studying environmental change. The use of Remote Sensing (RS) and Geographic Information System (GIS) approaches, combined with ground truthing where appropriate, are now providing new tools for advanced ecosystem management, and assessment of change at local, regional, and global scales, over time.

Since this research started object oriented classification as supported by Definiens and open source GIS software (e.g. QGIS) have become available, there are useful uses to which these systems could be put, with regard to mapping Libya's wetlands, and this is in need of further investigation.

This study researched vegetation changes in two contrasting wetland sites in the UK: a freshwater wetland at Wicken Fen between 1984 and 2009, and saltmarsh wetland between 1988 and 2009 in Caerlaverock Reserve. The study provides the first assessment using remote sensing (Landsat TM and aerial photographs) and GIS, combined with ground truth, to assess wetland vegetation change over time at these locations. The study clearly showed the ability of the RS/GIS approach, using both satellite imagery and aerial photography, to detect spatial and temporal variation in two quite different wetland vegetation types, both provided valuable information and can aid in management and conservation.

The study found that different types of imagery, produced classification results of varying degrees of accuracy for wetland vegetation assessment. Aerial photography (airborne platforms) provided higher accuracy than Landsat TM images (satelliteborne platforms), and the results obtained here serve to confirm that aerial photography is a worthy substitute

for field work, which is long established amongst photo interpreters, because the aerial photos have a higher spatial resolution than Landsat TM images. It might be worth noting that satellite imagery is now widely applied, because medium resolution datasets are free of charge (for example using GLOVIS) and available worldwide (von Wehrden et al., 2009), whereas there are usually costs attached to obtaining aerial imagery. Direct comparison between the outcome of maps obtained from Wicken Fen (study area 1) showed that Landsat TM images provided a fairly good separation of classes, when one class occupied an area more extensive than the pixel size (30×30 m) in the TM image. In this case, the spatial resolution of the Landsat TM sensor was the most important factor in obtaining a good separation of vegetation classes in a wetland environment. (Ground reference data is important in both the interpretation of the aerial photography, and in the selection of training areas for the interpretation of the Landsat TM images, so the process can never be entirely remote.)

Satellite image (TM) information extraction was carried out using unsupervised and supervised classification to produce wetland cover classes in two study areas. Supervised classification did not provide a good result in Caerlaverock Reserve and this can be attributed to the resolution of Landsat TM image, with it not being possible to locate clearly small vegetation patches in the image. There were also problems in separating vegetation classes larger than the pixel size (30m ×30m), such as waterlogged soil, and wet grassland, (especially in selecting a training area) due to the difficulty of distinguishing between classes producing similar colours of the reflection, leading to them being coded with the same colour in the Landsat TM image.

According to TWINSPAN classification (halting the analysis at end groups produced by reasonably high separation eigenvalues:>0.500) in Wicken Fen, the samples from 40 quadrats were classified into four groups, while the data from 48 quadrats were divided into five groups in Caerlaverock Reserve. However, statistical analyses in Wicken Fen showed that shade % had a significant difference between group means 2 and group 4, as well as in height, suggesting that quadrats in group 2 samples were largely located under tree/shrub overstorey vegetation, while group 4 samples were much more open.

In Caerlaverock Reserve study area 2, statistical analyses showed that soil conductivity had a significant difference between a group means in-group 1 and group 5, as well as in mean height. In addition, depending on the Ellenberg's indicator values, group 5 has the highest mean for salt tolerance, moisture and light, while group 1 has the lowest mean for salt tolerance, moisture and light. These outcomes suggest that the ground-truthing exercise was picking up vegetation classes which reflected real environmental variation across the two sites, and which formed a real basis for the classifications detected by the RS/GIS approach.

Finally, perhaps the most important conclusion of this study is that it provides evidence that the RS/GIS approach can provide useful baseline data to monitor wetland vegetation change over time, and across quite expansive areas, which can therefore provide valuable information to aid the management and conservation of wetland habitats. Both the results obtained from aerial photographs and Landsat TM showed a change in vegetation during the period 1984 to 2009 at Wicken Fen, most likely, though not exclusively, due to active management. In contrast, in Caerlaverock Reserve, results indicated only a slight change in the vegetation cover (mainly in shrub vegetation) during the period 1988 to 2009, a result which is in line with the findings of other studies about the stability of saltmarsh communities (e.g. the recent study by Taubert and Murphy (2012), which found a high level of stability in Scottish saltmarsh plant communities over a five-decade period).

In Libya which is located in semi-arid region, many wetlands are threatened due to natural conditions (drought) e.g. Al Jufrah Oases, and/or abuse from human activities e.g. Farwà Lagoon. It is difficult to monitor these systems by conventional methods such as field survey, using remote sensing techniques and geographic information systems will allow us to detect the change that occurs in the vegetation in the wetlands as a result of such impacts, and assist corresponding effective protection and utilization measures, as well as helping provide the scientific basis for the restoration of wetland resources and conservation.

6.2 Limitations and recommendations

Some limitations noted in this study should be mentioned:

1- When creating a mosaic of aerial photographs, it is sometimes difficult to find good control points from the original map (1:10,000 Ordnance Survey Map) in some areas. Choosing control points which do not correspond with the image will provide a high error rate. Re-choosing the control points to obtain suitable points with an error of less than one pixel, to produce an acceptably good mosaic of the entire area is time consuming, and this problem will directly increase in proportion to the increasing size of the study area.

2- During selection of training areas on Landsat TM images:

- It is difficult to map a training area if a class size is less than a pixel size of the Landsat TM images.
- Distinguishing vegetation classes is not possible if there is no difference in the reflected wavelength of vegetation types involved.

To overcome this problem, several researchers have developed and used, in their studies, sub-pixel classification approaches that consider variations within pixels to overcome the mixed pixel problem and which aim to detect materials smaller than one pixel (Wang and Lang, 2009) or suppress the limitations of coarse resolution imagery (Verbeiren et al., 2008).

A recommendation for further work arising from this study is as follows: This study used RS imagery collected at fairly low spatial resolution by manned aircraft photography, and satellite imagery. It would be of considerable interest to compare the outcome of the assessments of vegetation variation at both Wicken and Caerlaverock, undertaken here, with imagery captured by photography using unmanned aerial vehicles (UAVs) which can fly much lower, and acquire remote data more rapidly and at lower cost than traditional aerial photographs, at very high spatial resolutions.

List of References

Adam E, Mutanga O & Rugege D (2010) Multispectral and hyperspectral remote sensing for identification and mapping of wetland vegetation: a review. *Wetlands Ecol Manage* , **18**, 281-296.

Adam E, Mutanga O & Rugege D (2010) Multispectral and hyperspectral remote sensing for identification and mapping of wetland vegetation: a review. *Wetlands Ecol Manage* **18**, 281-296.

Adam P, Wilson NC & Huntley B (1988) The phytosociology of coastal saltmarsh vegetation in New South Wales. *Wetlands* **7**, 35-57.

Adam P (1978) Geographical variation in British saltmarsh vegetation. *Journal of Ecology*, 339-366.

Adam P (1981) The Vegetation of British Saltmarshes. *New Phytol* **88**, 143-196.

Adam P (2002) Saltmarshes in a time of change. *Environmental Conservation* **29**, 39-61.

Adu-Poku I (2010) Land-cover Change Monitoring in Obuasi using Remote Sensing and GIS Approach. . M. Sc. Thesis, School of Geographical and Earth Sciences.

Ahmed MH, El Leithy BM, Thomposon JR, Flower RJ, Ramdani M, Ayache F & Hassan SM (2009) Application of remote sensing to site characterisation and environmental change analysis of North African coastal lagoons. *Hydrobiologia* **622**, 147-171.

AL-Khudhairy DHA, Leemhuis C, Hoffmann V, Calaon R, Shepherd IM, Thompson JR, Gavin H & asca-Tucker DL (2001) Monitoring wetland ditch water levels in the North Kent Marshes, UK, using Landsat TM imagery and ground-based measurements. *Hydrological Sciences-Journal* **46**, 585-597.

Alexandridis TK, Lazaridou E, Tsirika A & Zalidis GC (2009) Using Earth Observation to update a Natura 2000 habitat map for a wetland in Greece. *Journal of Environmental Management* **90**, 2243-2251.

Alikas K & Reinart A (2008) Validation of the MERIS products on large European lakes: Peipsi, Vنnern and Vنttern. *Hydrobiologia* **599**, 161-168.

Allen JR (1989) Evolution of salt-marsh cliffe in muddy and sandy systems: A qualitative comparison of British west-coast Estuaries. *Earth Surface Processes and Landforms* **14**, 85-92.

Alrababah MA & Alhamad MN (2006) Land use/cover classification of arid and semi arid Mediterranean landscapes using Landsat ETM. *International Journal of Remote Sensing* **27**, 2703-2718.

Alsdorf D, Birkett C, Dunne T, Melack J & Hess L (2001) Water Level Changes in a large Amazon Lake Measured with Spaceborne Radar Interferometry and Altimetry. *Geophsical Research Letters* **28**, 2671-2674.

Alsdorf DE, Smith LC & Melack JM (2001) Amazon Floodplain Water Level Changes Measured with Interferometric SIR-C Radar. *IEEE Transactions on Geoscience and Remote Sensing* **39**, 423-431.

Anderson CG (2007) Change Detection of Land Cover in a Meadow Landscape : the "Ranches" Meadow, Silver Falls State Park, Oregon. . M. Sc Thesis, The Department of Geosciences, Oregon State University.

Anderson K, Bennie JJ, Milton EJ, Hughes PDM, Lindsay R & Meade R (2010) Combining LiDAR and IKONOS data for ecohydrological classification of an ombrotrophic peatland. *Journal of Environmental Quality* **39**, 260-273.

Andresen H, Bakker JP, Brongers M, Heydemann B & Irmler U (1990) Long-term changes of saltmarsh communities by cattle grazing. *Vegetatio* **89**, 137-148.

Antonarakis AS, Richards KS & Brasington J (2008) Object-based land cover classification using airborne LiDAR. *Remote Sensing of Environment* **112**, 2988-2998.

Armstrong W (1982) Waterlogged soils. In *Environmental Plant Ecology*, pp. 290-330 [JR Etherington, editor]. Chichester: John Wiley.

Armstrong W & Drew MC (2002) Root growth and metabolism under oxygen deficiency . In *Plant roots: the hidden half*, pp. 729-761. [Y Waisel, A Eshel, and e Kafkafi U, editors]. New York: Marcel Dekker.

Arroyo LA, Johansen K, Armston J, Armston J & Phinn S (2010) Integration of LiDAR and QuikBird imagery for mapping riparian biophysical parameters and land cover types in Australian tropical savannas. *Forest Ecology and Management* **259**, 598-606.

Aselmann I & Crutzen PJ (1989) Global Distribution of Natural Freshwater Wetlands Rice Paddies, their Net Primary Productivity, Seasonality and Possible Methane Emissions. *Journal of Atmospheric Chemistry* **8**, 307-358.

Athearn ND, Takekawa JY, Jaffe B, Hattenbach BJ & Foxgrover AC (2010) Mapping Elevations of Tidal Wetland Restoration Sites in San Francisco Bay: Comparing Accuracy of Aerial LiDAR with a Singlebeam Echosounder. *Journal of Coastal Research* **26**, 312-319.

Ausden M, Hall M, Pearson P & Steudwick T (2005) The effects of cattle grazing on tall-herb fen vegetation and molluscs. *Biological Conservation* **122**, 317-326.

Awotwi A (2009) Detection of Land Use and Land Cover Change in Accra, Ghana, between 1985 and 2003 using Landsat Imagery. M Sc. Thesis, Royal Institute of Technology (KTH).

Baily B & Nowell D (1996) Techniques for monitoring coastal change: a review and case study. *Ocean &Coastal Management* **32**, 85-95.

Baker C, Lawrence R, Montagne C & Patten D (2006) Mapping wetlands and riparian areas using Landsat ETM+ imagery and decision- tree-based models. *Wetlands* **26**, 465-474.

Bardley JC & Hauer FR (2007) Effects of Hydrologic Connectivity on Water Chemistry, Soils, and Vegetation Structure and Function in an Intermontane Deprssional Wetland Landscape. *Wetlands* **27**, 719-738.

Barducci A, Guzzi D, Marcoionni P & Pippi I (2009) Aerospace wetland monitoring by hyperspectral imaging sensors: A case study in the coastal zone of San Rossore Natural park. *Journal of Environmental Management* **90**, 2278-2286.

Barne JH, Robson CF, Kaznowska SS, Doody JP & Davidson NC (1996) *Coasts and seas of the United Kingdom Region 13 Northern Irish Sea: Colwyn Bay to Stranraer, including the Isle of Man.*: Peterborough, Joint Nature Conservation Committee.

Barr CJ, Bunce RGH, Clarke RT, *et al.* (1993) *Countryside Survey 1990: main report. (Countryside 1990 vol.2).* report. London: Department of the Environment.

Barrette J, August P & Golet F (2000) Accuracy Assessment of Wetland Boundary Delineation Using Aerial Photography and Digital Orthophotography. *Photogrammetic Engineering & remote Sensing* **66**, 409-416.

Bartsch A, Kidd R, Pathe C, Shvidenko A & Wagner W (2004) Identification of wetlands in central Siberia with ENVISAT ASAR WS data.

Bartsch A, Kidd R, Pathe C, Scipal S & Wagner W (2007) Satellite radar imagery for monitoring inland wetlands in boreal and sub-arctic environments. *Aquatic Conserv. Mar Freshw Ecosyst* **17**, 305-317.

Bartsch A, Doubkova M & Wolski P (2008) River flow & Wetland Monitoring with ENVISAT ASAR Global Mode in the Okavango Basin and Delta.

Bartsch A, Wagner W, Scipal K, Pathe C, Sabel D & Wolski P (2009) Global monitoring of wetlands - the value of ENVISAT ASAR Global mode. *Journal of Environmental Management* **90**, 2226-2233.

Belluco E, Camuffo M, Ferrari S, Modenese L, Silvestri S, Marani A & Marani M (2006) Mapping salt-marsh vegetation by multispectral and hyperspectral remote sensing. *Remote Sensing of Environment* **105**, 54-67.

Bertels L, Houthuys R, Sterckx S, Knaeps E & Deronde B (2011) Large-scale mapping of the riverbanks, mud flats and saltmarshes of the Scheldt basin, using airborne imaging spectroscopy and LiDAR. *International Journal of Remote Sensing* **32**, 2905-2918.

Bhuvaneswari K, Dhamotharan R & Radhakrishnan N (2011) Remote sensing satellite data for Coastal Ecosystem and Human Interaction -A Case study in Tamilnadu, India. *International Journal of Computer Information Systems* **2**, 77-81.

Boorman LA & Fuller RM (1981) The Changing Status of Reedswamp in the Norfolk Broads. *Journal of Applied Ecology* **18**, 241-269.

Boorman LA (2003) *Saltmarsh Review. An overview of coastal saltmarshes, their dynamic and sensitivity characteristics for conservation and management.* no. 334: JNCC Report.

Boorman LA (1995) Sea level rise and the future of the British coast. Coastal Zone Topics: Process. *Ecology and Management* **1** , 10-13.

Bork EW & Su JG (2007) Integrating LIDAR data and multispectral imagery for enhanced classification of rangeland vegetation: A meta analysis. *Remote Sensing of Environment* **111** , 11-24.

Brown K (2004) Increasing classification accuracy of coastal habitats using integrated airborne remote sensing. *EARSeL eProceedings* **3**, 34-42.

Buckland ST, Borchers DL, Johnston A, Henrys PA & Marques TA (2007) Line Transect Methods for Plant Surveys. *Biometrics*, **63**, 989-998.

Burd F (1989) *The Saltmarsh Survey of Great Britain: An Inventory of British Saltmarshes, Research and Survey in Nature Conservation.* no. 17. Peterborough: Nature Conservancy Council.

Burd F (1995) *Managed retreat: a practical guide.*: English Nature, Peterborough.

Bustamante J, Pacios F, Dِaz-Delgado R & Aragonès D (2009) Predictive models of turbidity and water depth in the Doñana marshes using Landsat TM and ETM images. *Journal of Environmental Management* **90**, 2219-2225.

Bwangoy J-RB, Hansen MC, Roy DP, De Grandi G & Justice CO (2010) Wetland mapping in the Congo basin using optical and radar sensed data and derived topographical indices. *Remote Sensing of Environment* **114**, 73-86.

Carey PD, Wallis SM, Emmett BE, Maskell LC, Murphy J, Norton LR, Simpson IC & Smart SS (2008) *Countryside Survey: UK Headline Messages from 2007.*: Centre for Ecology & Hydrology.

Castañeda A & Ducrot D (2009) Land cover mapping of wetland areas in an agricultural landscape using SAR and Landsat imagery. *Journal of Environmental Management* **90**, 2270-2277.

Cavalli RM, Laneve G, Fusilli L, Pignatti S & Santini F (2009) Remote sensing water observation for supporting Lake Victoria weed management. *Journal of Environmental Management* **90**, 2199-2211.

Cawkwell FG, Dwyer N, Bartlett D, *et al.* (2007) *Saltmarsh habitat classification from satellite imagery.* Bolzano, Italy.

Chapman VJ (1941) Studies in Salt-Marsh Ecology: Section VIII. *Journal of Ecology* **29**, 69-82.

Chen J-H, Kan C-E, Tan C-H & Shih S-F (2002) Use of spectral information for wetland evapotranspiration assessment. *Agricultural Water Management* **55**, 239-248.

Chen D & Stow D (2002) The effect of training strategies on supervised classification at different spatial resolutions. *Photogrammetric Engineering & Remote Sensing* **68**, 1155-1161.

Chopra R, Verma VK & Sharma PK (2001) Mapping, monitoring and conservation of Harike wetland ecosystem, Punjab, India, through remote sensing. *Int J Remote Sensing* **22**, 89-98.

Chou X, Yun S & Zi W (2010) InSAR Analysis over Yellow River Delta for Mapping Water-Level Changes over Wetland. *Geoinformatics* **1**, 1-5.

Chust G, Galparsoro I, Borja ء, Franco J & Uriarte A (2008) Coastal and estuarine habitat mapping, using LIDAR height and intensity and multi-spectral imagery. *Estuarine, Coastal and Shelf Science* **78**, 633-643.

Clyne FJ, Garrod CJ, Tipple JR & Jeffs TM (2007) *Radiological Habits Survey: Dumfries and Galloway Coast.* Final report no. RL 08/11: Environment Report.

Collin A, Long B & Archambault P (2010) Salt-marsh characterization, zonation assessment and mapping through a dual-wavelength LiDAR. *Remote Sensing of Environment* **114**, 520-530.

Colston A (1995) National Vegetation Classification Survey of Wicken Fen NNR. Unpublished map produced for the National Trust, Wicken Fen, UK.

Colston A & Friday L (1999) Wicken Fen - 100 years either side of the Millennium. *Nature in Cambridgeshire* **41**, 46-58.

Connolly J, Holden NM & Ward SM (2007) Mapping Peatlands in Ireland using a Rule-Based Methodology and Digital Data. *Soil Science Society of America Journal* **71**, 492-499.

Cook BD, Bolstad PV, Nؤsset E, Anderson RS, Garrigues S, Morisette JT, Nikeson J & Davis KJ (2009) Using LiDAR and quickbird data to model plant production and quantify uncertainties associated with wetland detection and land cover generalizations. *Remote Sensing of Environment* **113**, 2366-2379.

Cooper A (1982) The Effects of Salinity and Waterlogging on the Growth and Cation Uptake of Saltmarsh. *New Phytologist* **90**, 263-275.

Cooper NJ, Cooper T & Burd F (2001) 25 Years of Saltmarsh Erosion in Essex: Implications for Coastal Defence and Nature Conservation. *Journal of Coastal Conservation* **7**, 31-40.

Cox C (1992) Satellite imagery, aerial photography and wetland archaeology. An interim report on an application of remote sensing to wetland archaeology: the pilot study in Cumbria, England. World Archaeology-Analytical Field Survey 24, 249-267.

Craft CB (2005) Natural and Constructed Wetlands. In *Encyclopedia of Hyrological Sciences.*, pp. 1639-1655 [A Malcom and M Jeffrey, editors]: John Wiley.

Crawford RMM (1989) *Studies in plant survival.* . Oxford: Blackwell.

Crowell N, Webster T & O'Driscoll NJ (2011) GIS Modelling of Intertidal Wetland Exposure Characteristics. *Journal of Coastal Research* **27**, 44-51.

Dabrowska-Zielinska K, Budzynska M, Kowalik W & Turlej K (2010) Soil moisture and evapotranspiration of wetlands vegetation habitats retrieved from satellite images. *Journal of Hydrology and Earth System Sciences Discussions* **7**, 5929-5955.

Dale PER, Hulsma K & Chandica AL (1986) Classification of reflectance on colour infrared aerial photographs and sub-tropical salt-marsh vegetation types. *International Journal of Remote Sensing* **7**, 1783-1788.

Darowska-Zielinska K, Gruszczynska M, Lewinski S, Hoscilo A & Bojanowski J (2009) Application of remotes and in situ information to the management of wetlands in Poland. *Journal of EnvironmentalManagement* **90**, 2261-2269.

Davidson NC & Buck AL (1997) *An inventory of UK estuaries1. Introduction and methodology* .: Joint Nature Conservation Committee, Peterborough.

Davranche A, Lefebvre G & Poulin B (2010) Wetland monitoring using classification trees and SPOT-5 seasonal time series. *Remote Sensing of Environment* **114**, 552-562.

Dawson TP, Berry PM & Kampa E (2003) Climate change impacts on freshwater wetland habitats. *J Nat Conserv* **11**, 25-30.

De Roeck ER, Verhoest NEC, Miya MH, Lievens H, Batelaan O, Thomas A & Brendonck L (2008) Remote sensing and Wetland Ecology: a South African Case Study. *Sensors* **8**, 3542-3556.

De Steven D & Toner MM (2004) Vegetation of Upper Coastal Plain Deprssion Wetlands: Environmental Templates and Wetland Dynamics within a Landscape Framework. *Wetlands* **24**, 23-42.

Dillabaugh KA & King DJ (2008) Riparian marshland composition and biomass mapping using IKONS imagery. *Can J Remote Sensing* **34**, 143-158.

Dogan OK, Akyurek Z & Beklioglu M (2009) Identification and mapping of submerged plants in a shallow lake using quickbird satellite data. *Journal of Environmental Management* **90**, 2138-2143.

Donoghue DNM & Shennan I (1987) A preliminary assessment of Landsat TM imagery for mapping vegetation and sediment distribution in the Wash estuary. *International Journal of Remote Sensing* **8**, 1101-1108.

Donoghue DNM & Mironnet N (2002) Development of an integrated geographical information system prototype for coastal habitat monitoring. *Computers and Geosciences* **28**, 129-141.

Duhaime RJ, August PV & Wright WR (1997) Automated Vegetation Mapping Using Digital Orthophotography. *Photogrammetric Engineering & Remote Sensing* **63**, 1295-1302.

Edelkraut KA & Güsewell S (2006) Progressive Effects of Shading on Experimental Wetland Communities over Three Years. *Plant Ecology* **138**, 315-327.

EGA-RAC/SPA waterbird census team (2012) *Atlas of wintering waterbirds of Libya*, 2005- 2010. Imprimerie COTIM, Tunisia.

Ehrenfeld JG (2000) Evaluating wetlands within an urban context. *Ecological Engineering* **15**, 253-265.

Enwright N, Forbes MG, Doyle RD, Hunter B & Forbes W (2011) Using Geographic Information Systems (GIS) to Inventory Coastal Prairie Wetlands along the Upper Gulf Coast, Texas. *Wetlands* **31**, 687-697.

Erwin KL (2009) Wetlands and global climate change: the role of wetland restoration in a changing world. *Wetlands Ecol Manage* **17**, 71-84.

Esam I, Abdalla F & Erich N (2012) Land Use and Land Cover Changes of West Tahta Region, Sohag Governorate, Upper Egypt. *Jounral of Geographic Information System* **4**, 483-493.

Flink S (2013) Ramsar Sites Information Service. Ramsar.wetlands.org/Portals/15/LIBYA.pdf.

Flowers TJ & Colmer TD (2008) Salinity tolerance in halophytes. *New Phytologist* **179**, 945-963.

Frazier P & Page K (2009) A reach-scale remote sensing technique to relate wetland inundation to river flow. *River Res Applic* **25**, 836-849.

Friday L (1997) *Wicken Fen the making of a wetland nature reserve.*: Harley Books (B.H. & Harley Ltd).

Friday L & Harley B (2000) *Checklist of the Flora and Fauna of Wicken Fen.*: Harley Books (B.H. & Harley Ltd).

Frohn RC, Reif M, Lane C & Autrey B (2009) Satellite remote sensing of isolated wetlands using object-oriented classification of Landsat-7 data. *Wetlands* **29**, 931-941.

Genc L, Dewitt B & Smith S (2004) Determination of Wetland Vegetation Height with LIDAR. *Turkish Journal Agriculture& Forestry* **28**, 63-71.

Gibbes C, Adhikari S, Rostant L, Southworth J & Qiu Y (2010) Application of Object Based Classification and High Resolution Satellite Imagery for Savanna Ecosystem Analysis. *Remote Sens.* **2**, 2748-2772.

Gilmore MS, Wilson EH, Barrett N, Civco DL, Prisloe S, Hurd JD & Chadwick C (2008) Integrating multi-temporal spectral and structural information to map wetland vegetation in a lower Connecticut River tidal marsh. *Remote Sensing of Environment* **112**, 4048-4060.

Gilvear D, Tyler A & Davids C (2004) Detection of estuarine and tidal river hydromorphology using hyper-spectral and LiDAR data: Forth estuary, Scotland. *Estuarine, Coastal and Shelf Science* **61**, 379-392.

Godwin H (1936) Studies in the Ecology of Wicken Fen: III. The Establishment and Development of Fen Scrub(Carr). *Journal of Ecology* **24**, 82-116.

Govender M, Chetty K & Bulcock H (2007) Areview of Hyperspectral Remote Sensing and its Application in Vegetation and Water Resource Studies. *Water South Africa*, **33**, 145-151.

Grime JP (2001) *Plant strategies, vegetation processes and ecosystem properties.*, vol. 2. Chichester: Wiley.

Grings F, Salvia M, Karszenbaum H, Ferrazzoli P, Kandus P & Perna P (2009) Exploring the capacity of radar remote sensing to estimate wetland marshes water storage. *Journal of Environmental Management* **90**, 2189-2198.

Hall RK, Watkins RL, Heggem DT, Jones KB, Kaufmann PR, Moore SB & Gregory SJ (2009) Quantifying structural physical habitat attributes using LiDAR and hyperspectral imagery. *Environmental Monitoring and Assessment* **159**, 63-83.

Hansom JD (2003) *Solway Firth (North Shore), Dumfries and Galloway. In: May, V.J.& Hansom, J.D., Coastal Geomorphology of Great Britain. Geological Conservation Review Series, 28. Joint Nature Conservation Committee, Peterborough, 541-548.*

Hansom JD & McGlashan DJ (2004) Scotland's coast: Understanding past and present processes for sustainable management. *Scottish Geographical Journal* **120**, 99-116.

Harris A, Bryant RG & Baird AJ (2005) Detecting near-surface moisture stress in *Sphagnum* spp. *Remote Sensing of Environment* **97**, 371-381.

Harris A, Bryant RG & Baird AJ (2006) Mapping the effects of water stress on *Sphagnum*: Preliminary observations using airborne remote sensing. *Remote Sensing of Environment* **100**, 363-378.

Harris A & Bryant RG (2009) A multi-scale remote sensing approach for monitoring northern peatland hydrology: Present possibilities and future challenges. *Journal of Environmental Management* **90**, 2178-2188.

Harris L (2007) *Report North East England Wetlands Feasibility Study. A partnership project by the Environment Agency and Royal Society for the Protection of Birds (RSPB).*

Harvey KR & Hill GJE (2001) Vegetation mapping of a tropical freshwater swamp in the Northern Territory, Australia: a comparison of aerial photography, Lansat TM and SPOT satellite imagery. *Int J Remote Sensing* **22**, 2911-2925.

Harvey MM & Allan RL (1998) The Solway Firth saltmarshes. *Scottish Geographical Magazine* **114**, 42-45.

Herrero J & Castañeda C (2009) Delineation and functional status monitoring in small saline wetlands of NE Spain. *Journal of Environmental Management* **90**, 2212-2218.

Hill MO (1996) TABLEFIT. [1.0] UK., Institute of Terrestrial Ecology. Ref Type: Computer Program.

Hill MO, Preston CD &. Roy DB (2004) PLANTATT, Attributes of British and Irish Plants: Status, Size, Life History, Geography and Habitats. Biological Records Centre NERC Centre for Ecology and Hydrology.

Hill MO & Šmilauer P (2005) TWINSPAN for Windows version *2.3*. Centre for Ecology and Hydrology & University of South Bohemia, Huntingdon & Ceske Budejovice.

Hine R, Peacock J & Pretty J (2007) *Green Lungs for the East of England. Report for the National Trust : University* of Essex.

Hirano A, Madden M & Welch R (2003) Hyperspectral image data for mapping wetland vegetation. *Wetlands* **23**, 436-448.

Hobbs AJ & Shennan I (1986) Remote sensing of Saltmarsh Reclamation in the Wash, England. *Jouirnal of Coastal Research* **2**, 181-198.

Hong S-H, Wdowinski S, Kim S-W & Won J-S (2010) Multi-temporal monitoring of wetland water levels in the Florida Everglades using interferometric synthetic aperture radar (InSAR). *Remote Sensing of Environment* **114**, 2436-2447.

Howland WG (1980) Multispectral aerial photography for wetland vegetation mapping. *Photogramm Eng Remote Sensing* **46**, 87-99.

Huang LX & Sheng G (2005) Classification of the Lakkasuo Peatland Ecosystem Using Remote Sensing. *Environmental Informatics Archives* **3**, 295-305.

Huckel JM, Marrs RH & Potter JA (2004) Spatial and temporal changes in saltmarsh distribution in the Dee estuary, NW England, determined from aerial photographs. *Wetlands Ecology and Management* **12**, 483-498.

Ibrahim K & Jusoff K (2009) Assessment of wetlands in Kuala Terengganu District Using landsatTM. *Journal of Geography and Geology* **1**, 33-40.

Ikusemoran M (2009) Landuse and land cover change detection in the Kainji lake Basin Nigeria using Remote Snesing and GIS approach. *BayeroJournal of Pure and Applied Sciences* **2**, 83-90.

Jackson MB & Colmer TD (2005) Response and Adaptation by Plants to Flooding Stress. *Annals of Botany* **96**, 501-505.

Jacobs JM, Anderson MC, Friess LC & Diak GR (2004) Solar radiation, longwave radiation and emergent wetland evapotranspiration estimates from satellite data in Florida, USA. *Hydrol Sci J* **49**, 461-476.

Janssen L (1993) Methodology for updating terrain object data from remote sensing data. The application of Landsat TM data with respect to agricultural fields. Doctoral Thesis, Wageningen Agricultural University, Wageningen

Jenkins RB & Frazier PS (2010) High-Resolution Remote Sensing of Upland Swamp Bounderies and Vegetation for Baseline Mapping and Monitoring. *Wetlands* **30**, 531-540.

Jensen JR (1996) Introductory Digital Image Processing: A remote sensing perspective, *2nd Edition*. NJ: Prentice-Hall, pp. 139-141.

Jensen JR (2005) *Introductory digital image processing: A remote sensing perspective* ., 3 ed. USA: Prentice Hall.

Jia L, Xi G, Liu S, Huang C, Yan Y & Liu G (2009) Regional estimation of daily to annual regional evapotranspiration with MODIS data in the Yellow River Delta wetland. *Journal of Hydrology and Earth System Sciences* **13**, 1775-1787.

JNCC (2004) *Common Standards Monitoring guidance for lowland wetland habitats. Version August 2004. ISSN 1743-8160 (online).*

JNCC (2004) *Common Standards Monitoring Guidance for Saltmarsh Habitats*.

Johnston R & Barson M (1993) Remote sensing of Australian wet- lands: An evaluation of Landsat TM data for inventory and classification. *Australian Journal of Marine and Freshwater Research* **44**, 235-252.

Jones K, Lanthier Y, Voet P, Valkengoed E, Doug Taylor D & Fernandez-Prieto D (2009) Monitoring and assessment of wetlands using Earth Observation: The Glob Wetland project. *Journal of Environmental Management* **90**, 2154-2169.

Kahya O, Bayram B & Reis S (2010) Land cover classification with an expect system approach using Landsat ETM imagery: a case study of Trabzon. *Environmental Monitoring and Assessment* **160**, 431-438.

Kennedy MP & Murphy KJ (2003) Hydrological and hydrochmical conditions characterising *Carex chordorrhiza* L. fil. (String Sedge) habitat in a Scottish riverine floodplain wetland. *Aquatic Botany* **77**, 243-255.

Kennedy MP, Murphy KJ & Gilvear DJ (2006) Predicting interactions between wetland vegetation and the soil-water and surface-water environment using diversity, abundance and attribute values. *Hydrobiologia* **570**, 189-196.

Kiehl K, Eischeid I, Gettner S & Walter J (1996) Impact of different sheep grazing intensities on saltmarsh vegetation in northern Germany. *Journal of Vegetation Science* **7**, 99-106.

Klemas V (2011) Remote Sensing of Wetlands: Case Studies Comparing Practical Techniques. *Journal of Coastal Research* **27**, 418-427.

Klemas VV (2001) Remote Sensing of Landscape-Level Coastal Environmental Indicators. *Environmental Management* **27** , 47-57.

Klemas VV (2009) Remote Sensing of Coastal Resources and Environment. *Environmental Research, Engineering and Management* **2**, 11-18.

Knight JM, Dale PER, Spencer J & Griffin L (2009) Exploring LiDAR data for mapping the micro-topography and tidal hydro-dynamics of mangrove systems: An example from southeast Queensland, Australia. *Estuarine, Coastal and Shelf Science* **85**, 593-600.

Kokaly RF, Despain DG, Clark RN & Livo KE (2003) Mapping vegetation in ellowstone National Park using spectral feature analysis of AVIRIS data. *Remote Sens Environ* **84**, 437-456.

Kooch Y, Jalilvand H, Bahmanyar AM & Pormajidian RM (2008) Application of the Two Way Indicator Species Analysis in Lowland Plant Types Classification. *Pakistan Journal of Biological Sciences,* **11**, 752-757.

Kotowski W, van Andel J, van Diggelen R & Hogendorf J (2001) Responses of fen plant species to groundwater level and light intensity. *Plant Ecology* **155**, 147-156.

Koukoulas S & Blackburn GA (2005) Mapping individual tree location, height and species in broadleaved deciduous forest using airborne LIDAR and multi-spectral remotely sensed data. International Journal of Remote Sensing 26, 431-455.

Laba M, Downs R, Smith S, Welsh S, Neider C, White S, Richmond M, Philpot W & Baveye P (2008) Mapping invasive wetland plants in the Hudson River National Estuarine Research Reserve using quickbird satellite imagery. *Remote Sensing of Environment* **112**, 286-300.

Lane CR & D'Amico E (2010) Calculating the Ecosystem Service of Water Storage in Isolated Wetlands using LiDAR in North Central Florida, USA. *Wetlands* **30**, 967-977.

Lang MW, Kasischke ES, Prince SD & Pittman KW (2008) Assessment of C-band synthetic aperture radar data for mapping and monitoring Coastal Plain forested

wetlands in the Mid-Atlantic Region, U.S.A. *Remote Sensing of Environment* **112**, 4120-4130.

Lang MW & McCarty GW (2009) LiDAR intensity for improved detection of inundation below the forest canopy. *Wetlands* **29**, 1166-1178.

Lee DS & Shan J (2003) Combining Lidar Elevation Data and IKONOS Multispectral Imagery for Coastal Classification Mapping. *Marine Geodesy* **26**, 117-127.

Lefsky MA, Cohen WB, Parker GG & Harding DJ (2002) Lidar Remote Sensing for Ecosystem Studies. *Bioscience* **52**, 19-30.

Lehmann A & Lachavanne JB (1997) Geographic information system and remote sensing in aquatic botany. *Aquat Bot* **58**, 195-207.

Lewis DL & Phinn S (2011) Accuracy assessment of vegetation community maps generated by aerial photography interpretation: perspective from the tropical savanna, Australia. *Journal of Applied Remote Sensing* **5: 053565.**

Li H, Wang H, Kong Y & Li L (2011) Estimation of Evapotranspiration in Yellow River Delta Wetland Based on Two-Source Energy Balance (TSEB) Model. *IEEE Geoinformatics*, 19th *Internatonal Conference* 24-26 June 2011.

Lillesand TM, Kiefer WR & Jonathan WC (2008) *Remote Sensing and Image Interpretation.* 6 ed. River Street, Hoboken, Wiley and Sons.

Lin Y & Liquan Z (2006) Identification of the spectral characteristics of submerged plant Vallisneria spiralis. *Acta Ecologica Sinica* **26**, 1005-1011.

Lowry J (2010) *A Framework for a Wetland Inventory Metadatabase. Ramsar Technical Report No. 4. Ramsar Convention Secretariat, Gland, Switzerland.*

Lu Z & Kwoun O (2008) Radarsat-1 and ERS InSAR Analysis over Southeastern Coastal Louisiana: Implications for Mapping Water-Level Changes Beneath Swamp Forests. *IEEE Transactions on Geoscience and Remote Sensing* **46**, 2167-2184.

Lucas R, Rowlands A, Brown A, Keyworth S & Bunting P (2007) Rule-based classification of multi-temporal satellite imagery for habitat and agricultural land cover mapping. ISPRS Journal of Photogrammetry and Remote Sensing 62, 162-185.

Lucas R, Medcalf K, Brown A, Bunting P, Breyer J, Clewley D, Keyworth S & Blackmore P (2011) Updating the Phase 1 habitat map of Wales, UK, using satellite sensor data. *ISPRS Journal of Photogrammetry and Remote Sensing* **66**, 81-102.

Lunetta RS & Balogh ME (1999) Application of Multi-Temporal Landsat 5 TM Imagery for Wetland Identification. *Photogrammetric Engineering & Remote Sensing* **65**, 1303-1310.

MacAlister C & Mahaxay M (2009) Mapping wetlands in the Lower Mekong Basin for wetland resource and conservation management using Landsat ETM images and field survey data. *Journal of Environmental Management* **90**, 2130-2137.

MacKay H, Finlayson CM, Fernˌndez-Prieto D, Davidson N, Pritchard D & Rebelo L-M (2009) The role of Earth Observation (EO) technologies in supporting implementation of the Ramsar Convention on Wetlands. *Journal of Environmental Management* **90**, 2234-2242.

Malthus TJ & George DG (1997) Airborne remote sensing of macrophytes in Cefni Reservoir, Anglesey, UK. *Aquatic Botany* **58**, 317-332.

Malthus TJ & Karpouzli E (2003) Integrating field and high spatial resolution satellite-based methods for monitoring shallow submersed aquatic habitats in the Sound of Eriskay, Scotland, UK. . *International Journal of Remote Sensing* **24**, 2585-2593.

Marshall JR (1962) The morphology of the upper Solway saltmarshes. *Scottish Geographical Magazine* **78**, 81-99.

Matthews E & Fung I (1987) Methane emissions from natural wetlands: Global distribution, area, and environmental characteristics of sources. *Global Biogeochem* **1**, 61-86.

Matthews E (1990) Global data bases for evaluating trace gas sources and sinks. In *Soils and the Greenhouse Effect.*, pp. 311-325 [AF Bouwman, editor]. Chishester: John Wiley and Sons.

Mattikalli NM (1995) Integration of remotely-sensed raster data with a vector-based geographical information system for land-use change detection. *Int J Remote Sensing* **16**, 2813-2828.

Maxa M & Bolstad P (2009) Mapping northern wetlands with high resolution satellite images and LiDAR. *Wetlands* **29**, 248-260.

May AMB, Pinder JE & Kroh GC (1997) A comparison of LANDSAT Thematic Mapper and SPOT multi-spectral imagery for the classification of shrub and meadow vegetation in Northern California, USA. *International Journal of Remote Sensing* **18**, 3719-3728.

McCartney MP & Hera A (2004) Hydrological assessment for wetland conservation at Wicken Fen. *Wetlands Ecology and Management* **12**, 189-204.

Melesse AM & Jordan JD (2002) A Comparison of Fuzzy vs. Augmented-ISODATA Classification Algorithms for Cloud-Shadow Discrimination from Landsat Images. *Photogrammetric Engineering & Remote Sensing* **68**, 905-911.

Mertes LAK (2002) Remote sensing of riverine landscapes. *Freshwater Biology* **47**, 799-816.

Miller M (1999) Use of historic aerial photography to study vegetation change in the Negrito Creek Watershed, Southwestern New Mexico. *The Southwestern Naturalist* **44**, 121-137.

Millette TL, Argow BA, Marcano E, Hayward C, Hopkinson CS & Valentine V (2010) Saltmarsh Geomorphological Analyses via Integration of Multitemporal Multispectral Remote Sensing with LIDAR and GIS. *Journal of Coastal Research* **26**, 809-816.

Mironga JM (2004) Geographic Information Systems (GIS) and remote sensing in the management of shallow tropical lakes. *Applied Ecology and Environmental Research* **2**, 83-103.

Mita D, DeKeyser E, Kirby D & Easson G (2007) Developing a wetland condition prediction model using landscape structure variability. *Wetlands* **27**, 1124-1133.

Mitsch MJ (1994) *Global Wetlands Old World and New.* Amsterdam, The Netherlands: Elsevier Science B. V.

Mitsch WJ & Gosselink JG (2000) The value of wetlands: importance of scale and landscape setting. *Ecological Economics* **35**, 25-33.

Mnsur S & Rotherham ID (2010) Using TM and ETM+ data to determine land cover/land use changes in the Libyan Al-jabal Alakhdar region. *Landscape Archaeology and Ecology End of Tradition* **8**, 132-138.

Mohamed YA, Bastiaanssen WGM & Savenije HHG (2004) Spatial variability of evaporation and moisture storage in the swamps of the upper Nile studied by remote sensing techniques. *Journal of Hydrology* **289**, 145-164.

Mohd Hasmadi I, Pakhriazad HZ & Shahrin MF (2009) Evaluating supervised and unsupervised techniques for land cover mapping using remote sensing data. *Malaysian Journal of Society and Space* **5**, 1-10.

Mosbech A & Hansen BU (1994) Comparison of satellite imagery and infrared aerial photography as vegetation mapping methods in an arctic study area; Jameson Land, East Greenland. *Polar Research* **13**, 139-152.

Mountford O, Stroh P & Selby J (2012) *National Trust, Wicken Fen, Recording and Research Newsletter. New Edition 4.*

Murphy KJ, Dickinson G, Thomaz SM, *et al.* (2003) Aquatic plant communities and predictors of diversity in a sub-tropical river floodplain: the Upper Rio Paranل, Brazil. *Aquatic Botany* **77**, 276.

Myint SW, Gober P, Brazel A, Grossman-Clarke S & Weng Q (2011) Per-pixel vs. object-based classification of urban land cover extraction using high spatial resolution imagery. *Remote Sensing of Environment* **115**, 1145–1161.

Onojeghuo AO & Blackburn GA (2011) Optmising the use of hyperspectral and LiDAR data for mapping reedbed habitats. *Remote Sensing of Environment* **115**, 2025-2034.

Ouyang Z, Zhang M, Xie X, Shen Q, Guo H, Zhao B & Zhao B (2011) A comparison of pixel-based and object-oriented approaches to VHR imagery for mapping saltmarsh plants. *Ecological Informatics* **6**, 136-146.

Owens L, Aber JS & Aber SW (2011) Remote sensing half-century record of environmental changes at Cheyenne Bottoms, Kansas. *Emporia State Research Studies* **47**, 1-10.

Owor M, Muwanga A & Pohl W (2007) Wetland change detection and inundation north of Lake George, western Uganda using landsat data. *African Journal of Science and Technology (AJST) Science and Engineering Series* **8**, 94-106.

Östlund C, Flink P, Str¨ombeck N, Pierson D & Lindell T (2001) Mapping of the water quality of Lake Erken, Sweden, from Imaging Spectrometry and Landsat Thematic Mapper. *The Science of the Total Environment* **268**, 139-154.

Painter D (1998) Effects of Ditch Management Patterns on Odonata at Wicken Fen, Cambridgeshire, UK. *Biological Conservation* **84**, 189-195.

Palmans T & Batelaan O (2009) Estimating evapotranspiration in the Doode Bemde wetland from AHS data. *Geophysical Research Abstracts* **11**, EGU2009-7602.

Papastergiadou ES, Retalis A, Apostolakis A & Georgiadis Th (2008) Environmental Monitoring of Spatio-temporal Changes Using Remote Sensing and GIS in a Mediterranean Wetland of Northern Greece. *Water Resour Manage* **22**, 579-594.

Parent C, Capelli N, Berger A, Crèvecoeur M & Dat JF (2008) An Overview of Plant Responses to Soil Waterlogging. *Plant Stress* **2**, 20-27.

Peberdy K (1989) A survey of the Caerlaverock NNR merses. London, unpublished report of Wildfowl & Wetlands Trust & Scottish Natural Heritage.

Perata P, Armstrong W & Voesenek LACJ (2011) Plants and flooding stress. *New Phytologist* **190**, 269-273.

Peregon A, Maksyutov S & Yamagata Y (2009) An image-based inventory of the spatial structure of West Siberian wetlands. *Environ Res Lett* **4 045014**.

Pflugmacher D, Krankina ON & Cohen WB (2007) Satellite-based peatland mapping: Potential of the MODIS sensor. *Global and Planetary Change* **56**, 248-257.

Pignatti S, Cavalli RM, Cuomo V, Fusilli L, Pascucci S, Poscolieri M & Santini F (2009) Evaluating Hyperion capability for land cover mapping in a fragmented ecosystem: Pollino National Park, Italy. *Remote Sensing of Environment* **113**, 622-634.

Pollard AJ & Brigges D (1984) Genecologyical Studies of *Urtica dioica* L, II. Patterns of Variation at Wicken Fen, Cambridgeshire, England. *New Phytol* **96** , 483-499.

Polunin O & Walters M (1985) *A Guide to the Vegetation of Britain and Europe.* Oxford: Oxford University Press.

Popescu SC (2007) Estimating biomass of individual pine trees using airborne lidar. *Biomass and Bioenergy* **31**, 646–655.

Prigent C, Matthews E, Aires F & Rossow WB (2001) Remote sensing of global wetland dynamics with multiple satellite data sets. *Geophysical Research Letters* **28**, 4631-4634.

Raji O, Rچo LD, Gracia FJ & Benavente J (2011) The use of LIDAR data for mapping coastal flooding hazard related to storms in Cلdiz Bay (SW Spain). *Journal of Coastal Research* **64**, 1881-1885.

Ramsey E, Rangoonwala A, Middleton B & Lu Z (2009) Satellite optical and Radar data used to track wetland and forest impact and short-term recovery from hurricane Katrina. *Wetlands* **29**, 66-79.

Rani M, Kumar P, Yadav M & Hooda RS (2011) Wetland Assessment and Monitoring Using Image Processing Techniques: A Case Study of Ranchi, India. *Journal of Geographic Information System* **3**, 345-350.

Rebelo LM, Finlayson CM & Nagabhatla N (2009) Remote sensing and GIS for wetland inventory, mapping and change analysis. *Journal of Environmental Management* **90**, 2144-2153.

Reid Thomas DC, Donoghue DNM & Shennan I (1995) Intertidal mapping of the Wash Estuary. *EARSeL Advances in Remote Sensing* **4**, 135-142.

Roberts FM & Gessler PE (2000) *Using Landsat Thematic Mapper and SPOT Satellite Imagery to inventory wetland plants of the Coeur d'Alene Floodplain. In: Hansen,Mark; Burk,Tom,eds. Integrated tools for natural resources inventories in the 21st century.*: Gen.Tec.Rep.NC-212. St. Paul, MN: U.S Dept. of Agriculture, Forest Service, North Central Forest Experiment Station.

Rodwell JS (1991) *British Plant Communities. Woodlands and scrub*. Cambridge, UK: Cambridge University Press.

Rodwell JS, Dring JC, Averis ABG, Proctor MCF, Malloch AJC, Schaminée JNJ & Dargie TCD (2000) *Review of coverage of the National Vegetation Classification.* no. 302: JNCC, Peterborough.

Rokitnick-Wojcik D, Wei A & Chow-Fraser P (2011) Transferability of object-based rule sets for mapping coastal high marsh habitat among different regions in Georgian Bay, Canada. *Wetlands Ecol Manage* **19**, 223-236.

Rowell TA, Guarino L & Harvey HJ (1985) The Experimental Management of Vegetation at Wicken Fen, Cambridgeshire. *Journal of Applied Ecology* **22**, 217-227.

Rowell TA (1986) The History of Drainage at Wicken Fen, Cambridgeshire, England, and its Relevance to Conservation. *Biological Conservation* **35**, 111-142.

Rowell TA & Harvey HJ (1988) The Recent History of Wicken Fen, Cambridgeshire, England: A guide to Ecological Development. *Journal of Ecology*, **76**, 73-90.

Rozenstein O & Karnieli A (2011) Comparison of methods for land-use classification incorpoating Remote Sensing and GIS inputs. *Applied Geography* **31**, 533-544.

Rundquist DC, Narumalani S & Narayanan RM (2001) A review of wetlands remote sensing and defining new considerations. *Remote Sensing Reviews* **20**, 207-226.

Sader SA, Ahl D & Wen-Shu L (1995) Accuracy of Landsat-TM and GIS rule-based methods for forest wetland classification in Maine. *Remote Sensing of the Environment*, **53**, 133-144.

Sanchez-Hernandez C, Boyd DS & Foody GM (2007) Mapping specific habitats from remotely sensed imagery: Support vector machine and support vector data description based classification of coastal saltmarsh habitats. *Ecological Infromatics* **2**, 83-88.

Santos Da Silva J, Seyler F, Calmant S, Filho OCR, Roux E, Araٜjo AAMA & Guyot JL (2012) Water level dynamics of Amazon wetlands at the watershed scale by satellite altimetry. *International Journal of Remote Sensing* **33**, 3323-3353.

Satyanarayana B, Mohamad KA, Idris IF, Husain M & Dahdouh-Guebas F (2011) Assessment of mangrove vegetation based on remote sensing and ground-truth measurements at Tumpat, Kelantan Delta, East Coast of Peninsular Malaysia. *International Journal of Remote Sensing* **32**, 1635-1650.

Seher J & Tueller P (1973) Colour aerial photos for marshland. *Photogramm Eng Remote Sensing* **39**, 489-499.

Shepherd I, Wikinson G & Thompson J (2000) Monitoring surface water storage in the north Kent marshes using Landsat TM images. *Int J Remote Sensing* **21**, 1843-1865.

Shima LJ, Anderson RR & Carter VP (1976) The use of aerial color infrared photography in mapping the vegetation of freshwater marsh. *Chesapeake Science* **17**, 74-85.

Silvestri S, Marani M & Marani A (2003) Hyperspectral remote sensing of saltmarsh vegetation, morphology and soil topography. *Physics and Chemistry of the Earth* **28**, 15-25.

Silvestri S, Defina A & Marani M (2005) Tidal regime, salinity and saltmarsh plant zonation. *Estuarine, Coastal and Shelf Science* **62**, 119-130.

Smith GM, Spencer T, Murray AL & French JR (1998) Assessing seasonal vegetation change in coastal wetlands with airborne remote sensing: an outline methodology. *Mangroves and Saltmarshes* **2**, 15-28.

Soliman G & Soussa H (2011) Wetland change detection in Nile swamps of southern Sudan using multitemporal satellite imagery. *Journal of Applied Remote Sensing* **5: 053517**.

Stuefer JF & Huber H (1998) Differential effects of light quantity and spectral light quality on growth, morphology and development of two stoloniferous Potentilla species. *Oecologia* **117**, 1-8.

Sun Z, Ma R & Wang Y (2009) Using Landsat data to determine land use changes in Datong basin, China. *Environ Geol* **57**, 1825-1837.

Sun Z, Wei B, Su W, Shen W, Wang C, You D & Liu Z (2011) Evapotranspiration estimation based on the SEBAL model in the Nansi Lake Wetland of China. *Mathematical and Computer Modelling* **54**, 1086-1092.

Taubert R & Murphy KJ (2012) Long-term dynamics in Scottish saltmarsh plant communities. *Glasgow Naturalist* **25**, 111-118.

Taylor JA (1983) The Peatlands of Great Britain and Ireland. In *Ecosystems of the World (4a). Mires: Swamp, Bog, Fen. and Moor,* pp. 1-46 [AJP Gore, editor]. Amsterdam: *Elsevier*.

Thomson AG, Fuller RM, Yates MG, Brown SL, Cox R & Wadsworth RA (2003) The use of airborne remote sensing for extensive mapping of intertidal sediments and saltmarshes in eastern England. *Int J Remote Sensing* **24**, 2717-2737.

Timoney K (2008) Factors influencing wetland plant communities during a flood-drawdown cycle in Peace-Athabasca Delta, Northern Alberta, Canada. *Wetlands* **28**, 450-463.

Tipping R & Adams J (2007) Structure, composition and significance of Medieval storm beach ridges at Caerlaverock, Dumfries and Galloway. *Scottish Journal of Geology* **43**, 115-123.

Toogood SE, Joyce CB & Waite S (2008) Response of Floodplain Grassland Plant Communities to Altered Water Regimes. *Plant Ecology* **197**, 285-298.

Touzi R, Deschamps A & Rother G (2007) Wetland characterization using polarimetric RADARSAT-2 capability. *Can J Remote Sensing* **33**, 56-67.

Townsend PA & Walsh SJ (2001) Remote sensing of forested wetlands: application of multitemporal and multispectral satellite imagery to determine plant community composition and structure in southeastern USA. *Plant Ecology* **157**, 129-149.

Tuxen KA, Schile LM, Kelly M & Siegel SW (2008) Vegetation Colonization in a Restoring Tidal Marsh: A Remote Sensing Approach. *Restoration Ecology* **16**, 313-323.

Twesigye CK, Onywere SM, Getenga ZM, Mwakalila SS & Nakiranda JK (2011) The Impact of Land Use Activities on Vegetation Cover and Water Quality in the Lake Victoria Watershed. *The Open Environmental Engineering Journal* **4**, 66-77.

Twumasi YA & Merem EC (2007) Using Remote Sensing and GIS in the Analysis of Ecosystem Decline along the River Niger Basin: The Case of Mali and Niger. *Int J Environ Res Public Health* **4**, 173-184.

UK Ramsar (1999) *Convention on Wetlands of International Importance Especially as Waterfowl Habitat Ramsar Convention. UK National Report to the 7th Meeting of the Conference of the Contracting Parties Site Supplement San José*. Costa Rica.

Ulrich M, Grosse G, Chabrillat S & Schirrmeister L (2009) Spectral characterization of periglacial surface and geomorphological units in the Arctic Lena Delta using field spectrometry and remote sensing. *Remote Sensing of Environment* **113**, 1220-1235.

Valdkamp E, Weitz AM, Staritsky IG & Huising EJ (1992) Deforestation trends in the Atlantic Zone of Costa Rica: a case study. *Land Degradation & Rehabilitation* **3**, 71-84.

Valta-Hulkkonen K, Kanninen A & Pellikka P (2004) Remote sensing and GIS for detecting changes in the aquatic vegetation of a rehabilitated lake. *Int J Remote Sensing* **25**, 5745-5758.

Vartapetian BB & Jackson MB (1997) Plant adaptations to anaerobic stress. *Annals of Botany* **79**, 3-20.

Verheyden A, Dahdouh-Guebas F, Thomaes K, De Genst W, Hettiarachchi S & Koedam N (2002) High- resolution Vegetation Data for Mangrove Reseach as obtained from Aerial photography. *Environment, Development and Sustainability* **4,** 113-133.

Verbeiren S, Eerens H, Piccard I, Bauwens I & Orshoven JV (2008) Sub-pixel classification of SPOT-VEGETATION time series for the assessment of regional crop areas in Belgium. *International Journal of Applied Earth Observation and Geoinformation* 10, 486-497.

Visser EJW, Colmer TD, Blom CWPM & Voesenek LACJ (2000) Changes in growth, porosity, and radial oxygen loss from adventitious roots of selected mono- and dicotyledonous wetland species with contrasting types of aerenchyma. *Plant, Cell and Environment* **23**, 1237-1245.

von Wehrden H, Zimmermann H, Hanspach J, Ronnenberg K & Wesche K (2009) Predictive Mapping of Plant Species and Communities Using GIS and Landsat Data in a Southern Mongolian Mountain Range. *Folia Geobot,* **44**, 211-225.

Vulink JT, Drost HJ & Jans L (2000) The infl uence of different grazing regimes on phragmites and shrub vegetation in the well-drained zone of a eutrophic wetland. *Applied Vegetation Science* **3**, 73-80.

Walter V (2005) Object-based classification of remote sensing data for change detection. *ISPRS Journal of Photogrammetry & Remote Sensing* **58**, 225–238.

Wang C, Menenti M, Stoll M-P, Belluco E & Marani M (2007) Mapping mixed vegetation communities in saltmarshes using airborne spectral data. *Remote Sensing of Environment* **107**, 559-570.

Wang J & Lang PA (2009) Detection of Cypress Canopies in the Florida Panhandle Using Subpixel Analysis and GIS. *Remote Sens***1**, 1028-1042.

Wdowinski S, Kim S, Amelung F & Dixon T (2006) Wetland InSAR: A new space-based hydrological monitoring tool of wetlands surface water level changes. p. -6. Frescati, Itali.

Wdowinski S, Kim S-W, Amelung F, Dixon TH, Miralles-Wilhelm F & Sonenshein R (2008) Space-based detection of wetlands' surface water level changes from L-band SAR interferometry. *Remote Sensing of Environment* **112**, 681-696.

Williams DJ, Rybicki NB, Lombana AV, O'Brien TM & Gomez RB (2003) Preliminary investigation of submerged aquatic vegetation mapping using hyperspectral remote sensing. *Environmental Monitoring and Assessment* **81**, 383-392.

Xie Y, Sha Z & Yu M (2008) Remote sensing imagery in vegetation mapping: a review. *Journal of Plant Ecology,* **1**, 9-23.

Yang X (2005) Remote sensing and GIS applications for estuarine ecosystem analysis: an overview. *International Journal of Remote Sensing* **26**, 5347-5356.

Yang X (2007) Integrated use of remote sensing and geographic information systems in riparian vegetation delineation and mapping. *International Journal of Remote Sensing* **28**, 353-370.

Zedler JB, Paling E & McComb A (1990) Differential salinity responses to help explain the replacement of native *Juncus kraussii* by *Typha orientalis* in Western Australian saltmarshes. *Australian Journal of Ecology* **15,** 57-72.

Zhang C, Lu D, Yang B, Sun C & Sun M (2011) Coastal wetland vegetation classification with a Landsat Thematic Mapper image. *International Journal of Remote sensing* **32**, 545-561.

Zhang J, Zhang Y, Liu L, Ding M & Zhang X (2011) Identifying Alpine Wetlands in the Damqu River Basin in the Source Area of the Yangtze River Using Object-based Classification Method. *Journal of Resource and Ecology* **2**, 186-192.

Zhang M, Ustin SL, Reimankova E & Sanderson W (1997) Monitoring pacific coast saltmarshes using Remote Sensing. *Ecological Applications* **7**, 1039-1053.

Zhang S, Na X, Kong B, Wang Z, Jiang H, Yu H, Zhao Z, Li X, Liu C & Date P (2009) Identifying wetland change in China's Sanjiang Plan using Remote Sensing. *Wetlands* **29**, 302-313.

Zhou W, Huang G, Troy A & Cadenasso ML (2009) Object-based land cover classification of shaded areas in high spatial resolution imagery of urban areas: A comparison study. *Remote Sensing of Environment* **113**, 1769–1777.

Zimmermann S & Murphy KJ (2007) Plant communities and vegetation diversity in Scottish saltmarshes in relation to land use. *Botanical Society of Scotland News* **89**, 26-31.

Zomer RJ, Trabucco A & Ustin SL (2009) Building spectral libraries for wetlands land cover classification and hyperspectral remote sensing. *Journal of Environmental Management* **90**, 2170-2177.

Zubair AO (2006) Change detection in land use and land cover using Remote sensing data and GIS. MSc Thesis, Department of Geography, University of Ibadan.

Web Sites

Wicken Fen map.
www.wicken.org.uk/intro_map.htm

Online Atlas of the British & Irish Flora. Online access January 2013
http://www.brc.ac.uk/plantatlas/index.php?q=plant/frangula-alnus
http://www.ctre.iastate.edu/mtc/papers/2002/Veneziano.pdf)

Appendices

Appendix 1: Instructions for production of Orthophoto using BAE SYSTEMS SOCET SET (v5.6)

Login as 'workstation only', using the following:

User name: **SHTOPO**
Password: **topoontour**

Start the Socet Set software by clicking on the green icon on the desktop.

Several windows open towards the left side of the screen (quite slow!).

1. The first step is to CREATE A NEW PROJECT

From the menus select :

Project>Create/Edit Project - a dialogue box will appear at the right side of the screen

We want to create a new project so select **File>New.** The dialogue box will refresh (ignore warning box if it appears).

Project path	F:\users\shtopo\data**JED** (use your initials not JED!)
Options/select datum	Ordnance_Survey_of_Great_Britain_1936(Scotland) ….. way down the list!
Units	metres
Co-ordinate system	LSR local
Vertical reference	MSL (mean sea level) / EGM96
Minimum ground elevation (estimated)	0
Maximum ground elevation (estimated)	500
LOCATION	DEFAULT
Options/LSR Origin (This and respect to	Lat 49:00:00 and Long –2:00:00 Rotation 0 is the origin of the National Grid in latitude longitude values, and its rotation with the meridian direction)

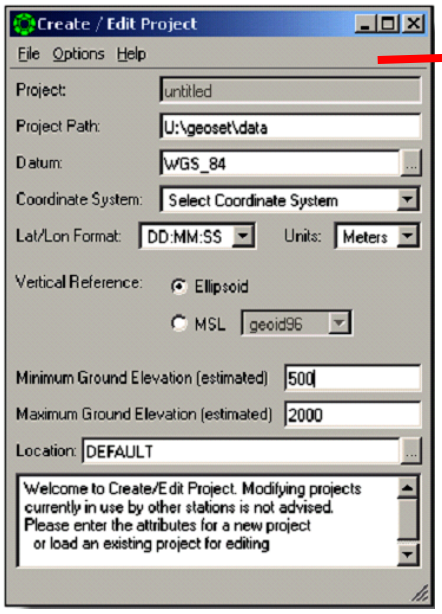

File>save as - JED - OK
Message appears - Project JED.prj created

File> Exit **(**confirm with 'Yes' to project modification in a subsidiary window – if it appears**)**

Enter Project Name (in subsidiary window) JED - OK
File>Load project -select **JED**.prj (in subsidiary window)

OK

2. IMPORTING DATA INTO THE NEW PROJECT

From the menus which appear along the top of the project box select:
Preparation>Import>Image>Frame (… the Frame Import dialogue box appears)

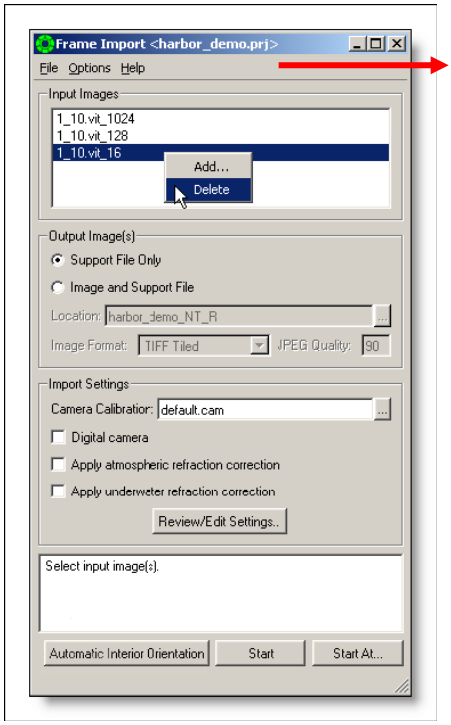

Select **File > open** and navigate to the images to be imported.

Select each to be imported and click **OPEN,** using **right click** and **ADD** in the Input Images space, for further images.

In the dialogue box below (Output Image(s)), select **Image and Support File**

Select **Image Format** as **VITEC(but TIFF is fine!)**

In the **Import Settings** section select the correct Camera calibration file **(Balmacara05.cam)** and click **OPEN**

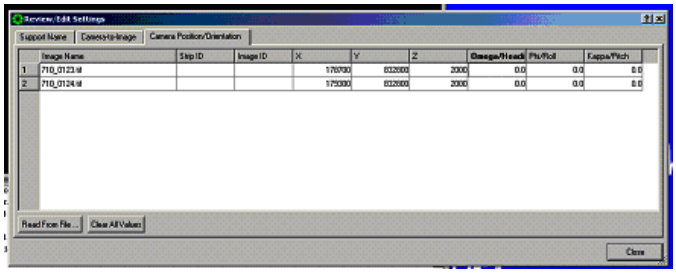

Only apply **atmospheric and water refraction** correction if necessary.

In the **Review/Edit Settings** dialogue box complete the section for:

Camera Position/Orientation by adding the approximate co-ordinates for the Centre of each photo and add the approximate flying height for each image – to give approximate values for the camera position. **CLOSE**

In the **Frame Import** window **Options** menu choose to create minifications (**Auto Minify**) and then click **START**. This takes several seconds and includes the minification process.

Once the process has completed select: **File>Exit**

3. TO DISPLAY THE IMAGES

Make sure that split screen is selected
File>Load images
Image Loader window appears
Select 710_0123.sup (as LH image)
Select 710_0124.sup (as RH image)
Load
(Select **Close** to put the Image Loader window away)

4. STAGES OF ORIENTATION

a) Interior Orientation

From the main menu - Preparation>Interior Orientation/Manual Interior Orientation

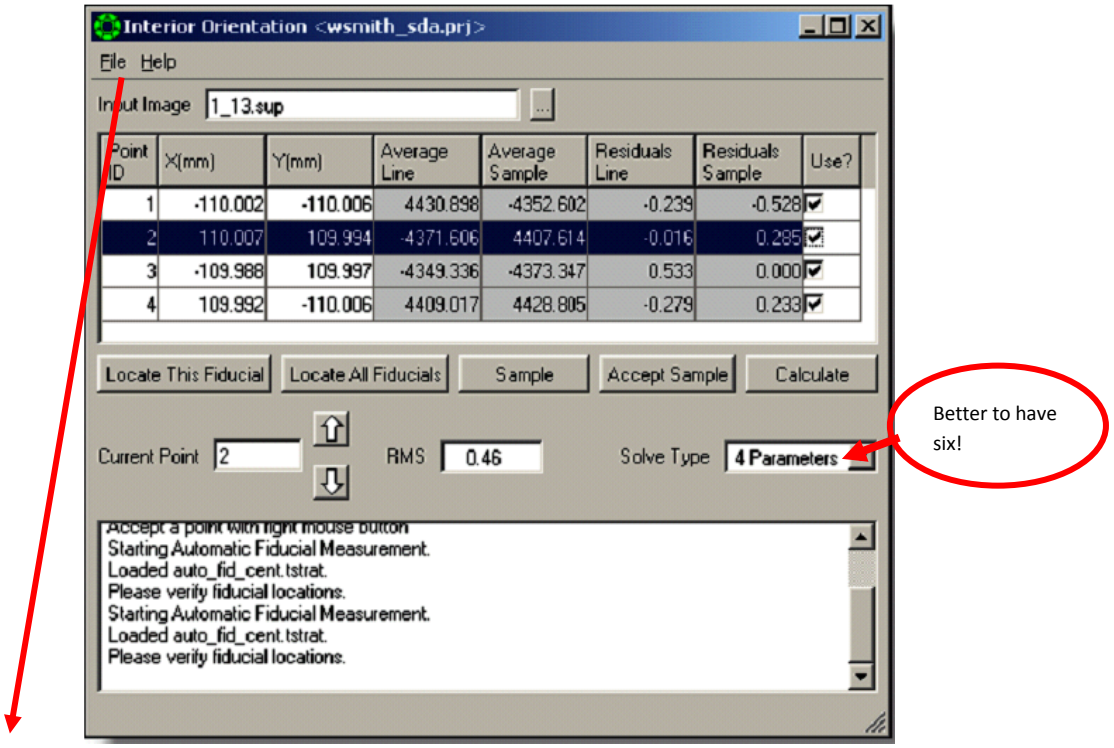

Click File>Open

***Select image **710_0123.sup** **OPEN**

The above dialogue box will appear; the view should be changed to **Mono.**

-The cursor will move to the approximate position of the first fiducial.

-**Locate this fiducial** (screen cursor should automatically centre over the centre of the fiducial cross – as long as it was 'within' the fiducial mark – and if this does not work, then do position the screen cursor within the fiducial mark manually using the Extraction cursor/3D cursor) Position the mark exactly using the Extraction cursor.
-**Sample** the point and **Accept sample**
-**Next Point -** (the cursor will move to the approx position of the second point)
-**Locate this fiducial** (repeat as before)
-**Accept sample** (once you are satisfied that you have the best position)
-Repeat the above steps for each of the fiducials available.
-Once all fiducials have been measured and the RMS value is acceptable (in the case of Balmacara less than 1)
-**File>save**
-**Repeat from ***** above for the right hand image **710_0124.sup** and exit, saving points and solution.
-**File>exit**

b) Preparation for exterior orientation: creating a Ground Point File

Select – Preparation>Control point editor
A new dialogue box (Control Point Editor) appears

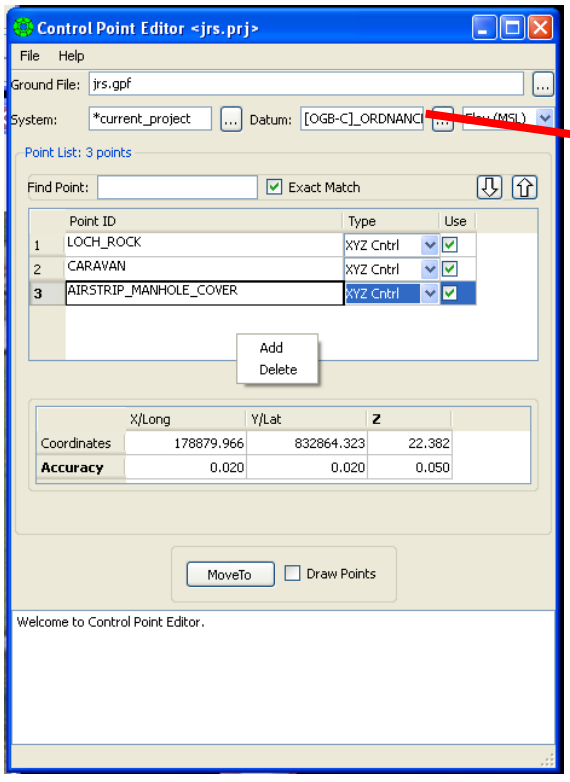

Datum select OSGB… OK
Elev (MSL)

**Right click in the box below Point ID and choose - Add

Add the following information

Point ID	type name of point
PT type	select - x,y,z
Use	select – ON (tick)
X/Long	type easting value
X/Long accuracy	type relevant accuracy from GPS result sheet eg 0.02
Y/Lat	type northing value
Y/Lat - accuracy	type relevant accuracy from GPS result sheet eg 0.02
Z/Elev	type height value
Z/Elev - accuracy	type relevant accuracy from GPS result sheet eg 0.05

Repeat from ** for the remaining control points in the model.

When all points have been added **File>Save as JED.gpf**
File exit

C) Solving for the exterior orientation elements

Select - Preparation>Multi-Sensor Triangulation

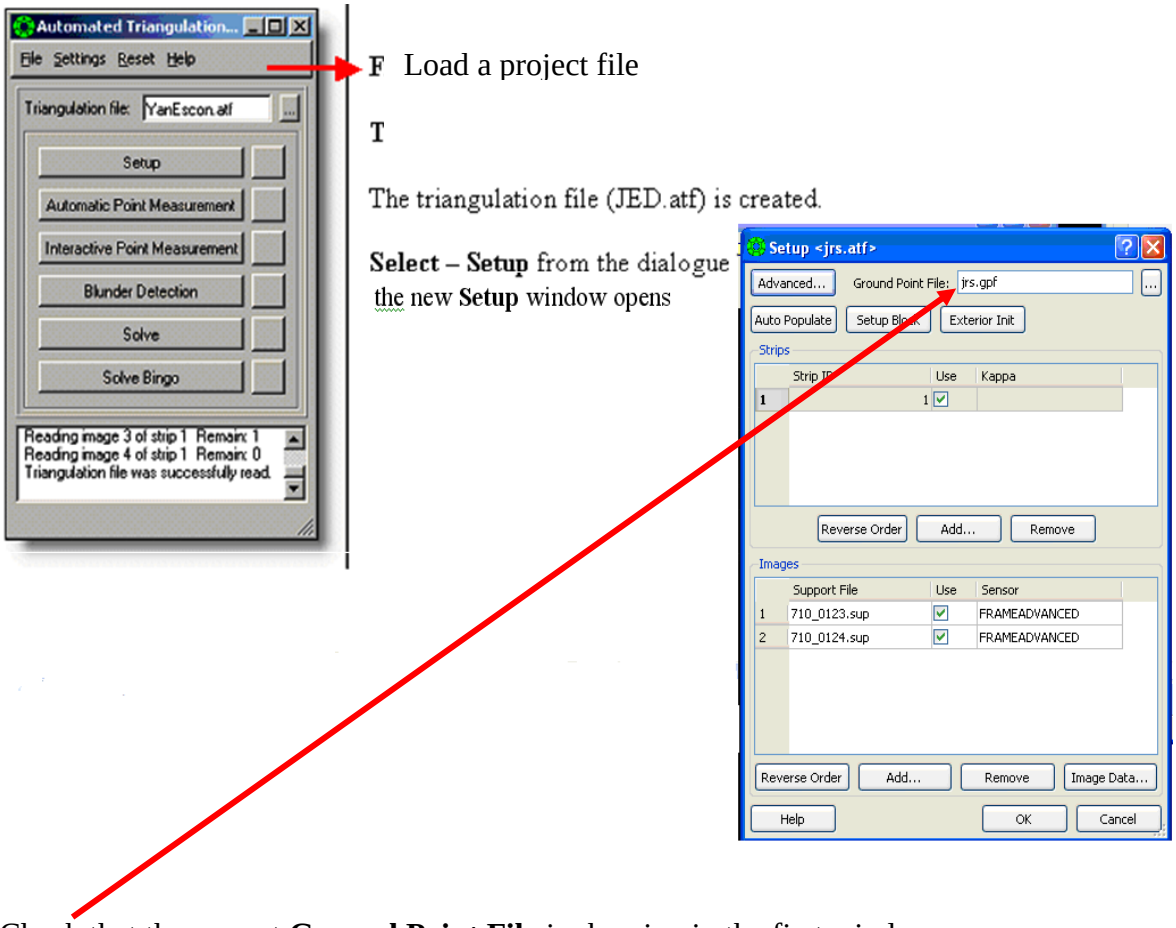

Check that the correct **Ground Point File** is showing in the first window.

In the section headed **STRIPS**, select **Add** and type **1** in the dialogue box which appears (as we only have a pair of photos)

Click OK

From the window (**Select Support Files**) which opens with the images, select the correct images (710_123.sup, 710_124.sup). **Click OK.**

Click the button for **Exterior Initialise** and accept any warnings which appear.

Click **OK**.

The window returns to the **Automated Triangulation** window.

Next **Select - Interactive Point Measurement**

Interactive Point Measurement

This stage involves measuring the photo co-ordinates for each of the ground control points.

**** Highlight** the first point to be measured in the point list.

Right click in the box under Image Points and **add the 2 images**.

Make sure the correct image is on the **Left.** On the main window select zoom of 1:32 or 1:64 to enable the whole model to be shown and display both images with the split screen.

Find the approximate position of the first control point on each photo using paper prints and control point diagrams to assist.

Next using the **Extraction cursor** as demonstrated, along with the LOCKING of images alternately, position the cursor as accurately as possible at maximum zoom over the ground control point in each photo

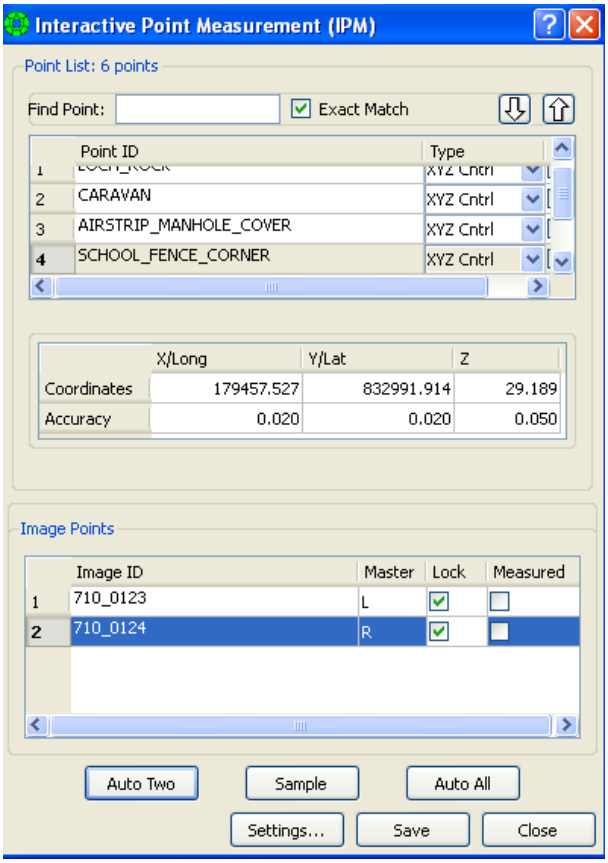

Check the position stereoscopically to achieve the best position on each image.

Once satisfied that no improvement can be made select SAMPLE from the menu and repeat from ** for the remainder of the control points.

SAVE
CLOSE

From the **SETUP** menu select **SOLVE**

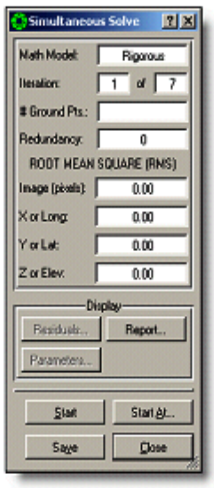

In the window which appears, click start and wait until the calculations have been completed. Examine the residuals and RMS values to ensure they are acceptable. If not, then re-measure points as appropriate.
(If you require to re-measure points, then do not save the solution until you are happy with the results – so answer NO to the question about saving!)

Click – CLOSE

File>Save Triangulation File

File>Exit
The Orientation phase has now been completed and the images should be reloaded with the Image Load function in their correct position with respect to each other.

5. NORMALISATION (Rectification)

Preparation>Resample>Rectification>Pairwise

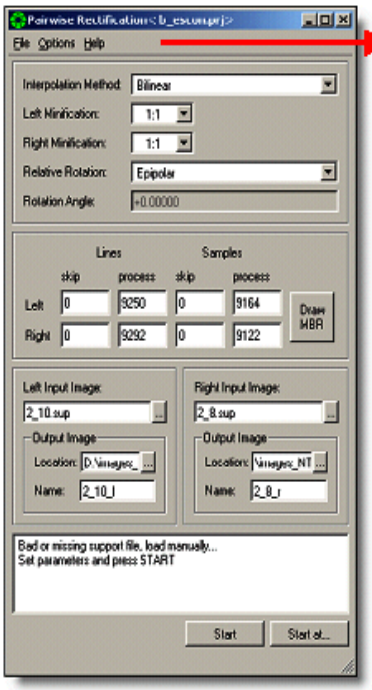

File>Select Left support File	710_0123.sup	Click
File>Select Right support file	710_0124.sup	Click
Interpolation method	Bilinear	
Left minification	1:1	
Right minification	1:1	
Relative orientation	epipolar	
Rotation angle	0.0	

(Since the whole image is going to be rectified, there is no need to specify the area.)

Check that the correct names will be created for your new files – ie 710_0123_l.sup and 710_0124_r.sup. This means there will be a new version of each image created with the effects of tilts removed when 123 is the left hand image and 124 is the right hand image.

Select **Options>Autominify** - ON

Select - START
This takes a few minutes and once complete select **File/Exit.**
There will now be 2 more images available to load - ie **710_0123_l.sup** and **710_0123_r.sup.**

6. CREATING THE DTM.

File>Load images (menu as before)

Select images 710_0123_l.sup and 710_0124_r.sup

From the main menu bar – Extraction>Terrain>Automatic Extraction

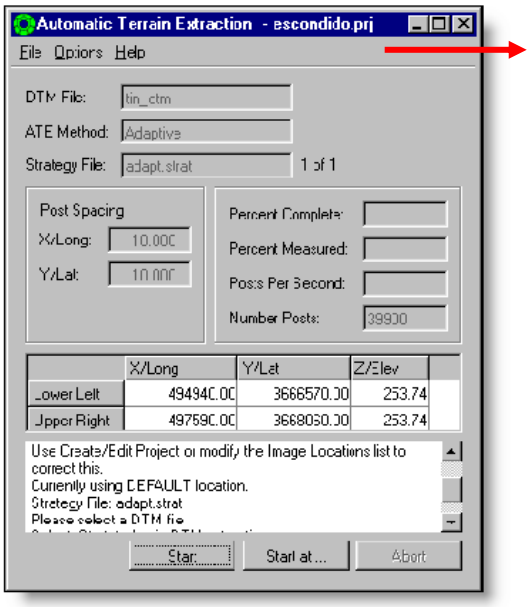

File> Create DTM

The Create DTM window appears:

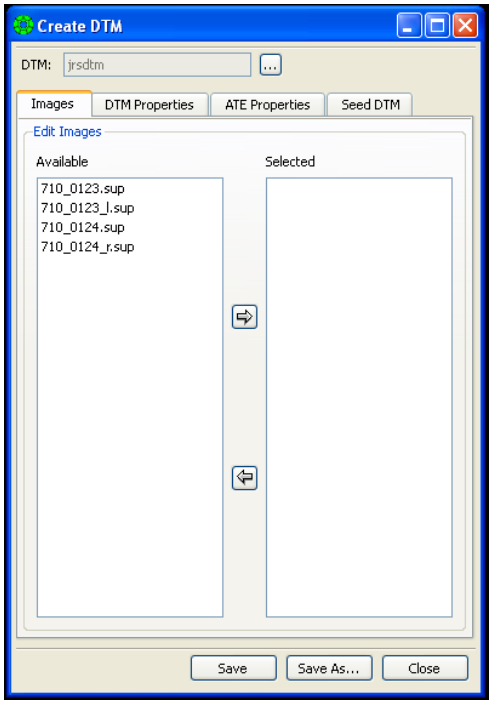

Use the browse button to name (or find) the DTM file, in the new window (Select a DTM(s)). The name for the new DTM should be added (e.g. jeddsm) or selected. Click OK:

In Create DTM select DTM properties and work through the first three tabs:

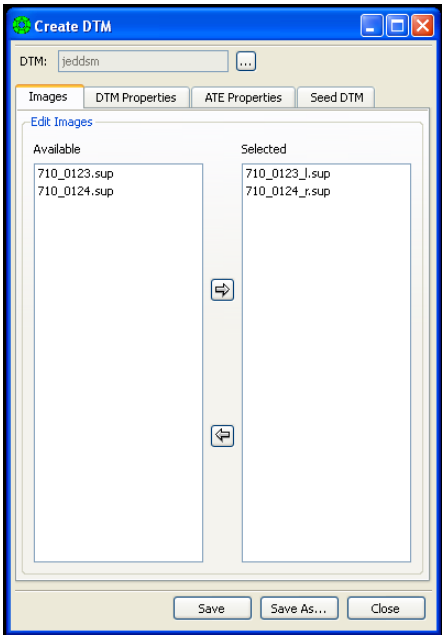

In the first tab, select the two rectified files to be used for image matching.

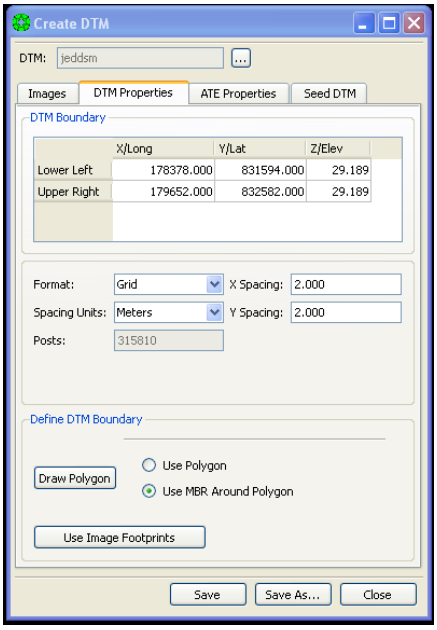

In the second tab, for the post spacing in the DTM select 2 metres for x and y.

To choose the area (Define DTM boundary) for the DTM select **Use MBR Around Polygon** and using the ‘mouse-trak’ extraction cursor draw a polygon (click Draw Polygon) for the area to be included in the DTM (red rectangle around green quadrilateral should appear).

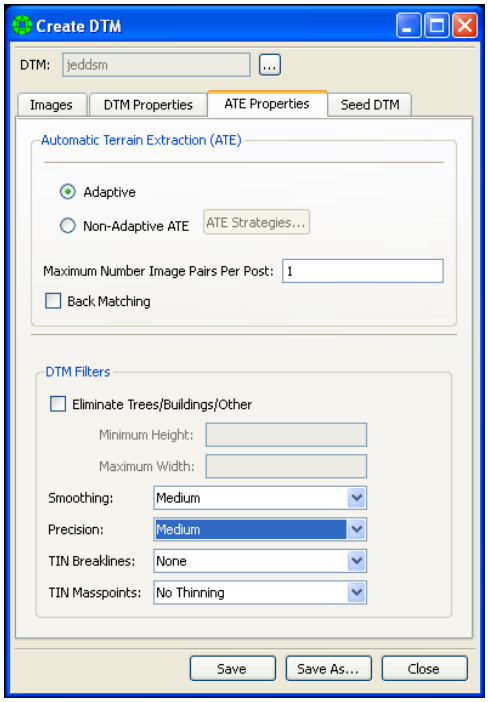

In the third tab from **CREATE DTM, i**n ATE properties:

Select **adaptive**
Select **smoothing - medium**
precision - medium
SAVE
START **(in Automatic Terrain Extraction window)**

This process takes several minutes depending on the spacing of the points chosen and the size of the area chosen. It also involves 7 passes, during which the image matching (and hence DTM quality) is refined.

Once the process is complete, there will be a message which states

Saving DTM after last pass then **DTM collection complete**

File>Exit

7. TO DISPLAY THE DTM DATA

File>Load images as before
Select the rectified image support files eg 016_l.sup and 017_r.sup

Extraction/Terrain>Interactive Edit (Interactive Terrain Edit Window appears)

File>open DTM

The 'Select a DTM(s)' window appears

Select (e.g.) jedsm OK

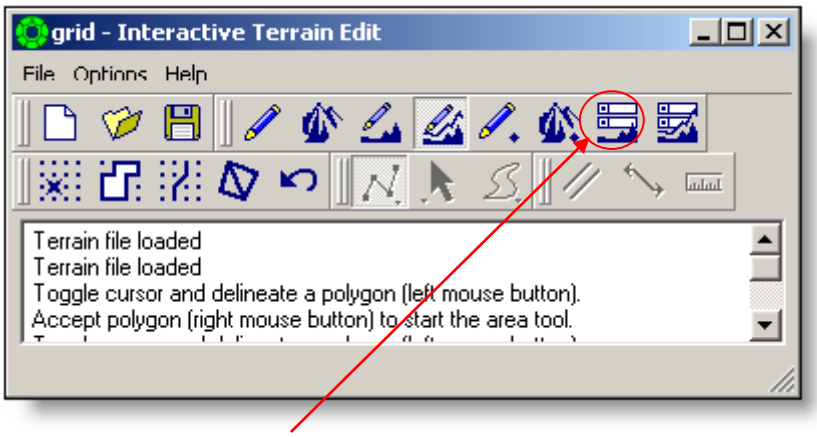

Choose Set Up DTM button and from the 'Preferences' menu select

Mode	Editable contours
Line style	solid
Graphics width	thin
Rendering	quick
Contour interval	1
Index interval	50
x-steps off set	1 0
y-steps offset	1 0
Colour source	Elevation (click Edit Ranges to ensure the correct values are available)

Apply
OK

From the Interactive Terrain Edit menu
select **DRAW terrain graphics** (a pencil symbol!)

The images will display with contours overlaid. (These contours cannot be directly exported but the DTM can be exported for use in a Terrain modelling package such as 3D Analyst in ArcView or Vertical Mapper in MapInfo.)

(You might care to inspect these contours under magnification and in stereo – but beware forest areas are quite confusing….)

File>Exit

8. ORTHOPHOTO PRODUCTION

Products>Orthophoto generation
A new window appears with various sections to be completed.

On the first screen/tab select 'Orthophoto'

On the second (input) screen the Primary image should be selected from the pair of photos. Choose the rectified image which you think will be clearer to Digitise.

At the right hand side of the screen – choose to get height from the DTM and enter the file name for your own DTM.

On the third (output) screen, the area to be converted to the Orthophoto is selected. In the calculate box Primary Image drop down menu, choose the DTM as the area for the Orthophoto and click the 'UPDATE' button.

In **Output Options**:

Name:	e.g. JED_0123_ortho	
Output file format	select	**Tif** (this means it can be used directly in other packages eg ArcGIS etc
GSD (ground separation distance)		1

On the **Options** screen complete as instructed :

Eg Gridlines?	
Select grid spacing	200 or 500 or 1000?
Select grid grey	254 (for white lines) or 1 for black lines
CreateWORLD file?	Do this if you intend taking the orthophoto into ArcGIS. This step creates a .tfw file to allow the image to be added directly to ARCGIS
Options/Auto minify	(ensure this is selected)

Start (the process begins and again takes a few minutes)

Once the orthophoto has been produced, it is possible to create a stereomate to enable the orthophoto to be viewed stereoscopically. **Repeat the process above** for creating an orthophoto but this time select

Options/Stereomate
Select base to height ratio 1
Select Left mate
OK
and give a suitable (but different) name to the image to be created eg **XXXmate**.
(NB Do not choose to make grid lines this time)

File/EXIT

9. EXPORTING DTM TO MAPINFO/ARCVIEW

To export DTM files – in ARC Grid format
From the Output menu select Output/File Export/Terrain/Arc Grid

The **ASCII ArcGrid Export** dialogue window appears.

Select the input DTM file,
Grid spacing,
Output file name
Start

To export the orthophoto to ArcMAP ensure you have produced the tfw file and the tif file as mentioned in the previous section (8).

10. ArcGIS

For the orthophoto:
In ArcGIS use ADD with the TIF file (the orthophoto) (in ArcMap) to bring it into ArcMAP. (PLEASE NOTE the .TFW file must be in exactly the same directory as the .TIF file or the coordinates revert to pixel coordinates.)

For the DTM:
Change the extension for the DTM file from .OUT to .ASC.
In ArcGIS the DTM file will need to be converted from ASCII to raster, using:
ArcToolbox/Conversion Tools/To Raster/ASCII to Raster.
(For contouring the DEM us Spatial Analyst/Surface/Contour)

The data are now ready for subsequent GIS editing and processing.

Jane Drummond, Nov. 2012

Appendix 2: Creating a seven-band image from seven TM bands, originating as seven separate TIFF files.

Unsupervised Classification

To create a seven-band image from seven separate TIFF (.tif) bands from a Landsat TM scene in ER mapper

OBJECTIVE:

The bands we have are:

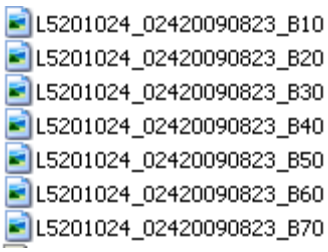

Which are the seven Landsat thematic mapper (TM) bands.

***This* description shows you how to create a seven-band image from seven TM bands, originating as seven separate TIFF files**

STEPS:

1. **Open ER-mapper**
2. **Click the Edit Algorithm button**

The following algorithm appears:

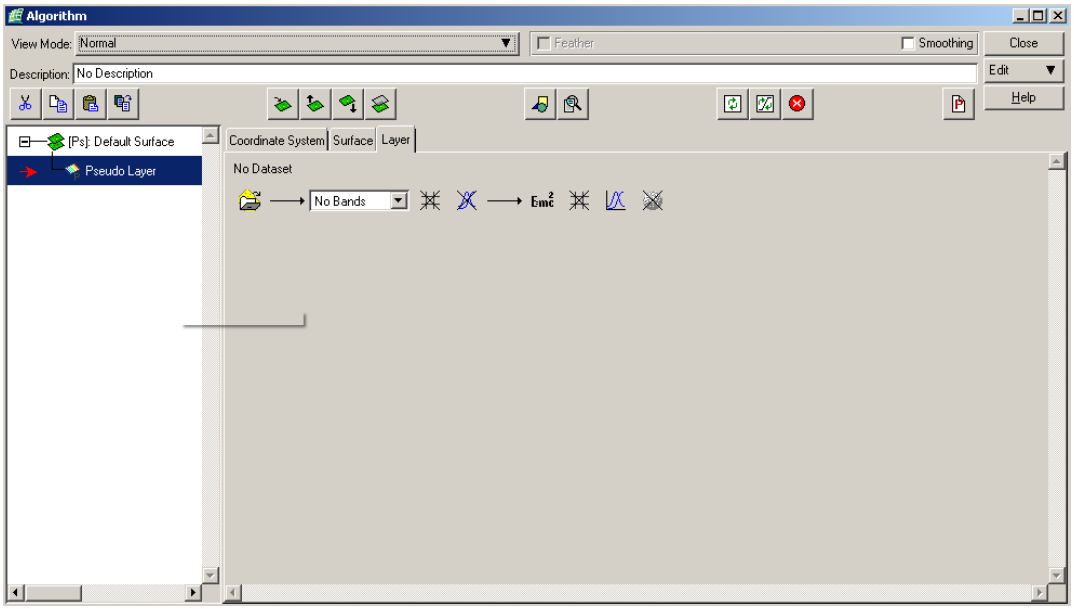

3. To create seven layers activate the Pseudo Layer which has appeared and using the duplicate button six times, create 7 pseudo layers.

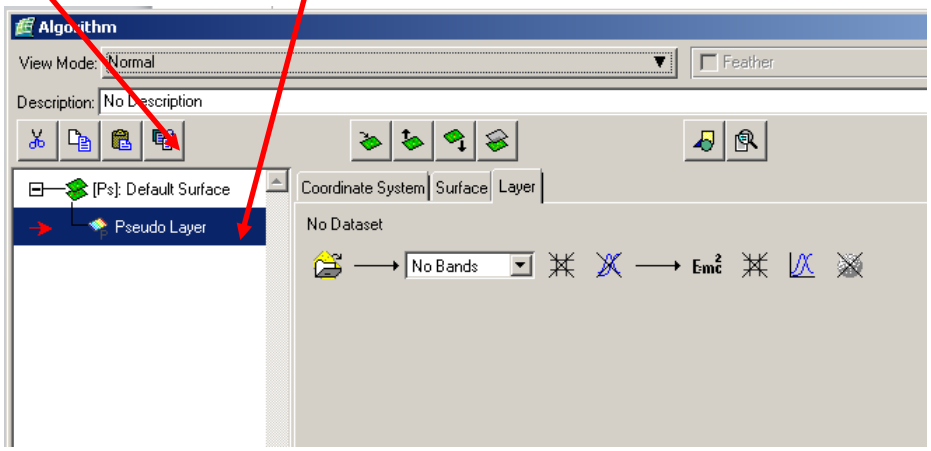

The following algorithm appears:

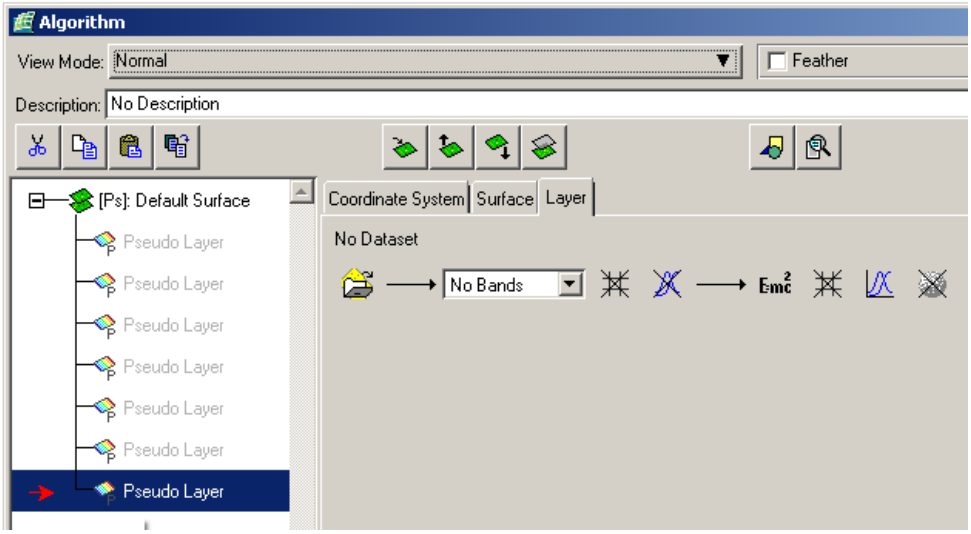

4. To load the data into each layer:

activate the layer;

click the Load dataset button;

select the data set you want in that layer;

click Apply this layer only; and,

click OK.

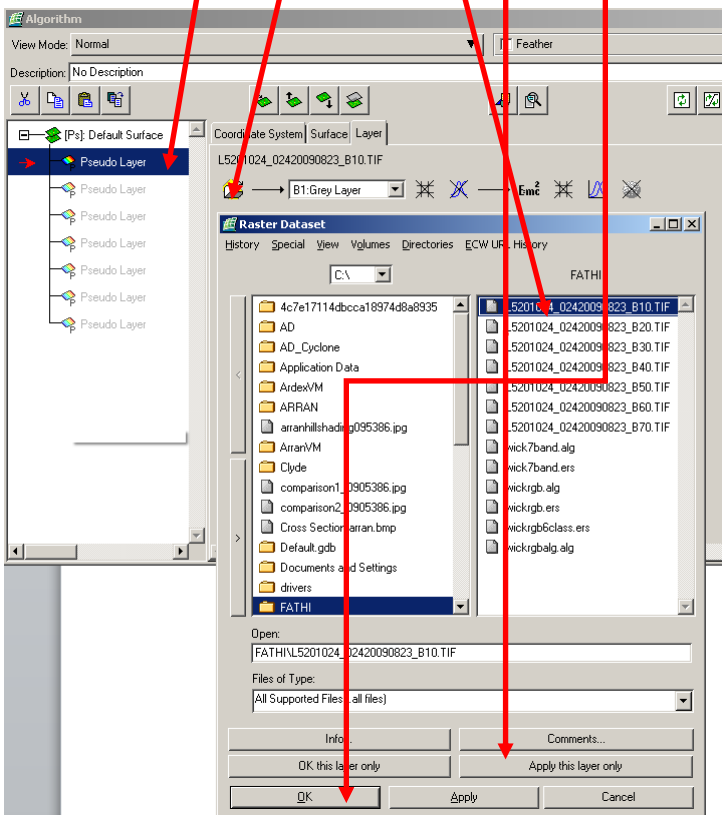

The following algorithm appears:

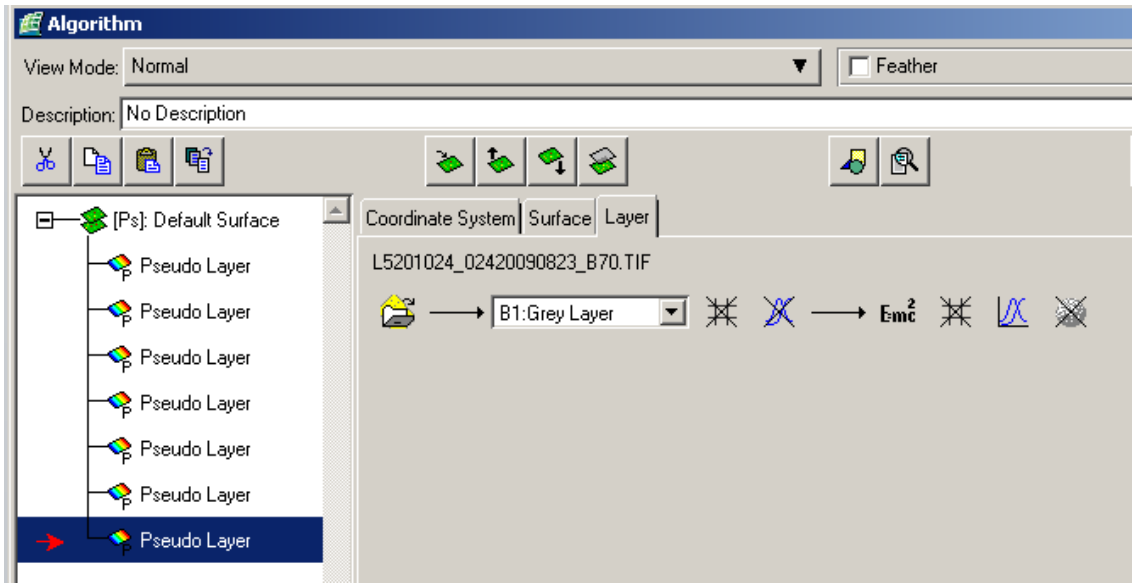

5. To rename the layers appropriately, double click on each layer's name (currently Pseudo Layer) and rename them, such as Band 1, Band 2, Band 3, etc.

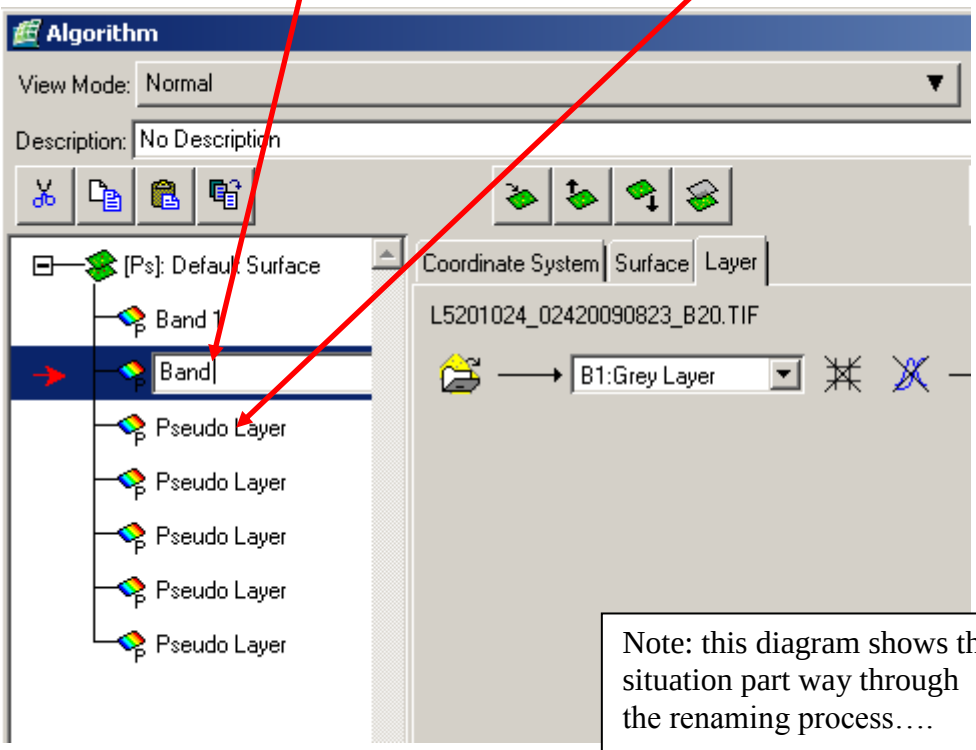

The following algorithm appears:

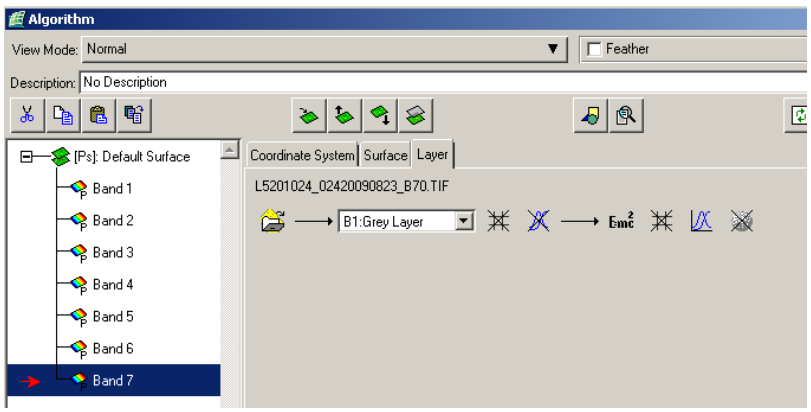

6. To save as an ER-mapper format dataset (.ers):

Click Save As;

Choose an appropriate volume for saving;

Choose an appropriate out put file type (i.e. .ers);

Choose an appropriate file name; and

Click OK.

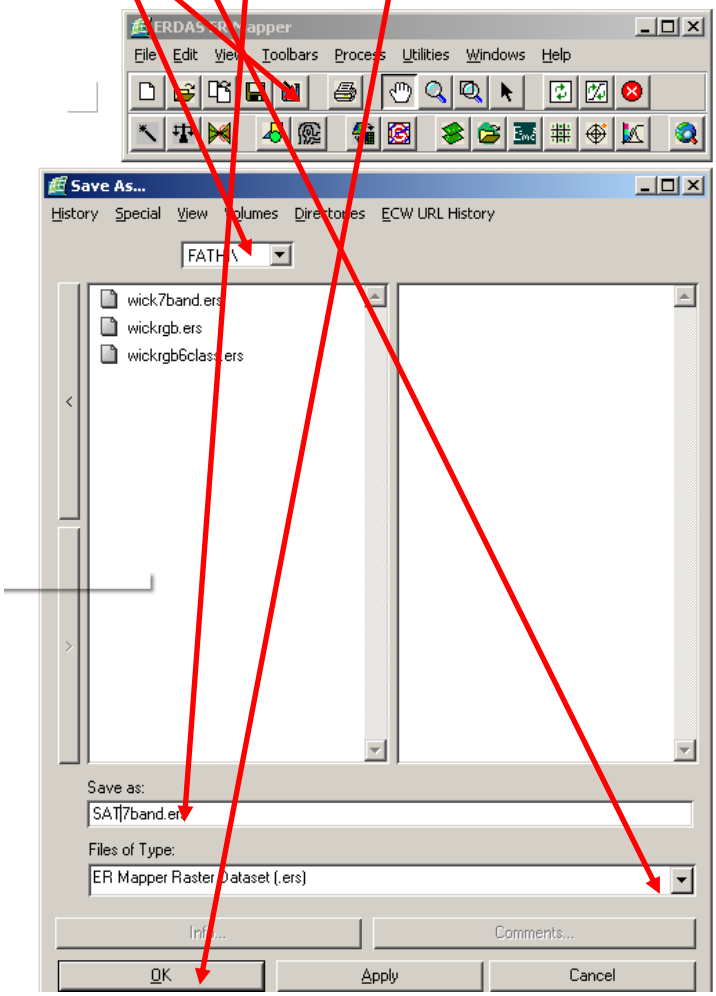

Then……

Tick Delete output transforms; select Output Type Multi layer; click OK (x2)

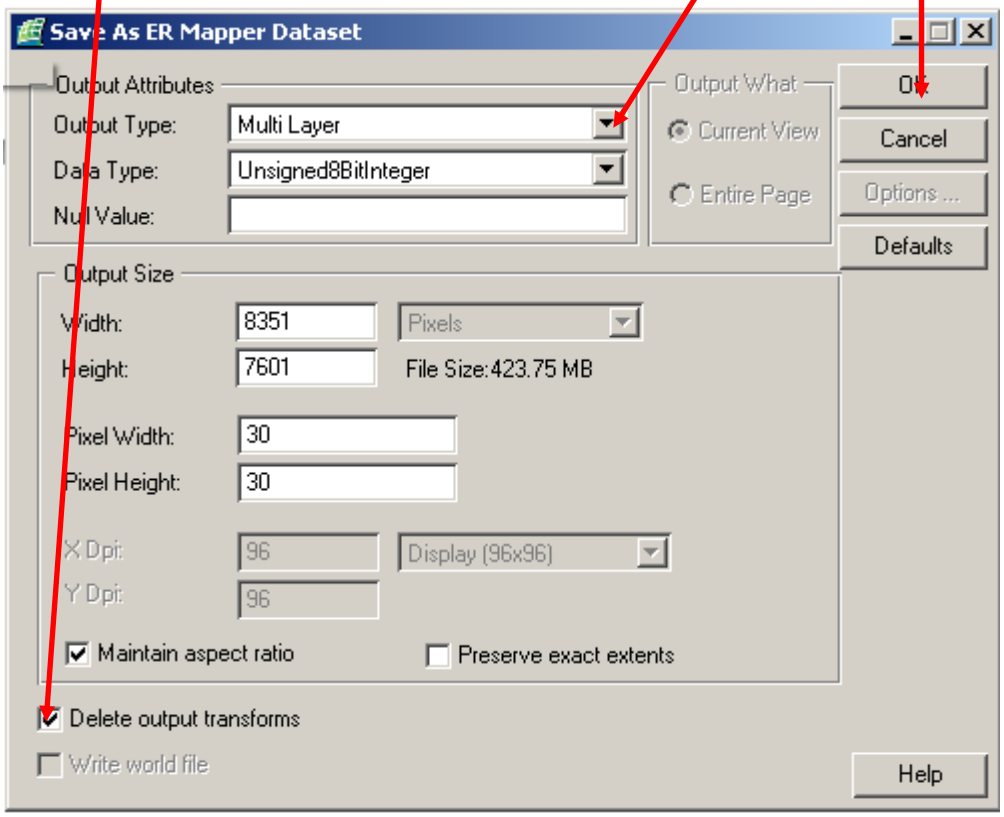

…to finish saving the .ers data file.

7. To save the algorithm

Click Save As;

Choose an appropriate volume for saving;

Choose an appropriate out put file type (i.e. .alg);

Choose an appropriate file name; and

Click OK.

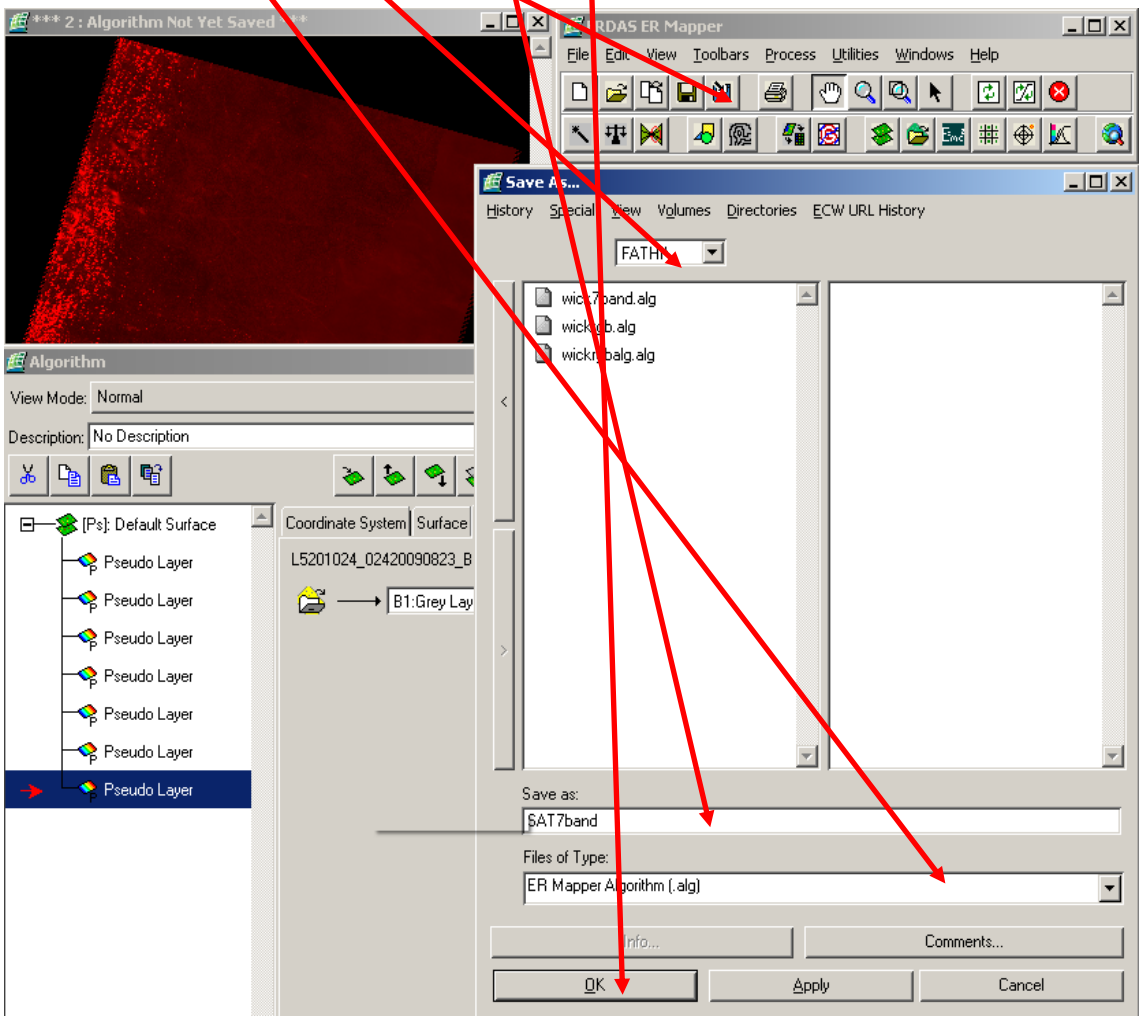

8. To check all is well – 1! (We'll make an RGB display)

Close the Algorithm and display windows.

Click the open button and select the newly created .ers file (i.e. SAT7band.ers), click OK

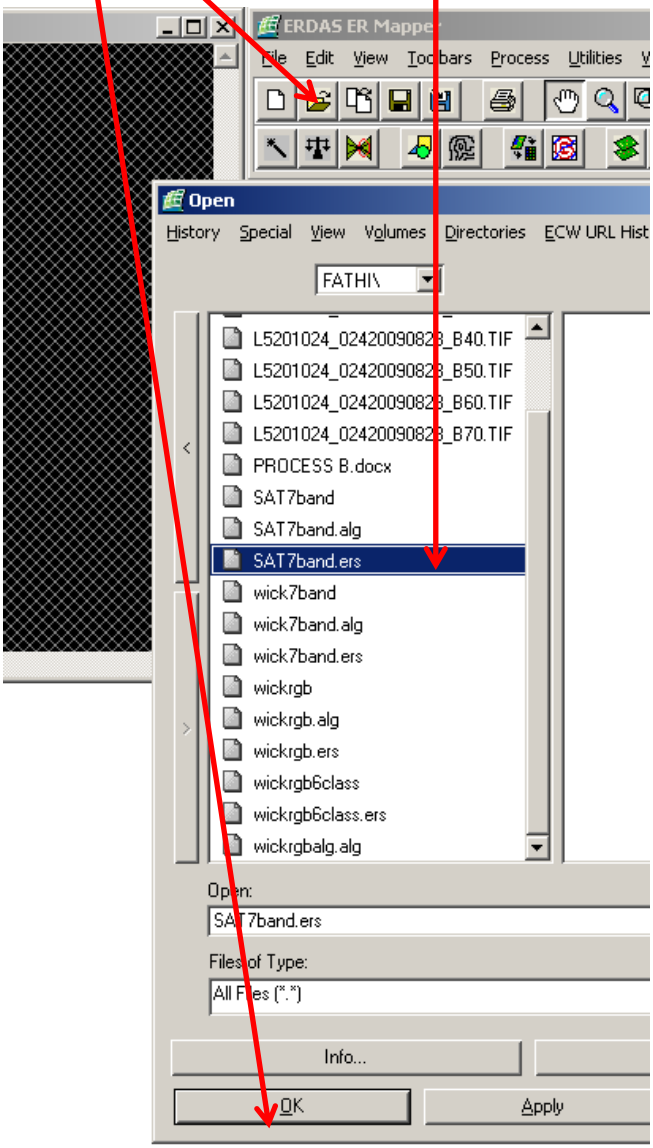

and ensure it displays.

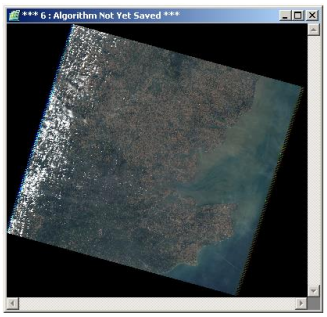

9. To check all is well – 2! (We'll highlight vegetation using NDVI)

Add the Forestry (or Remote Sensing) tool bar to ER-Mapper

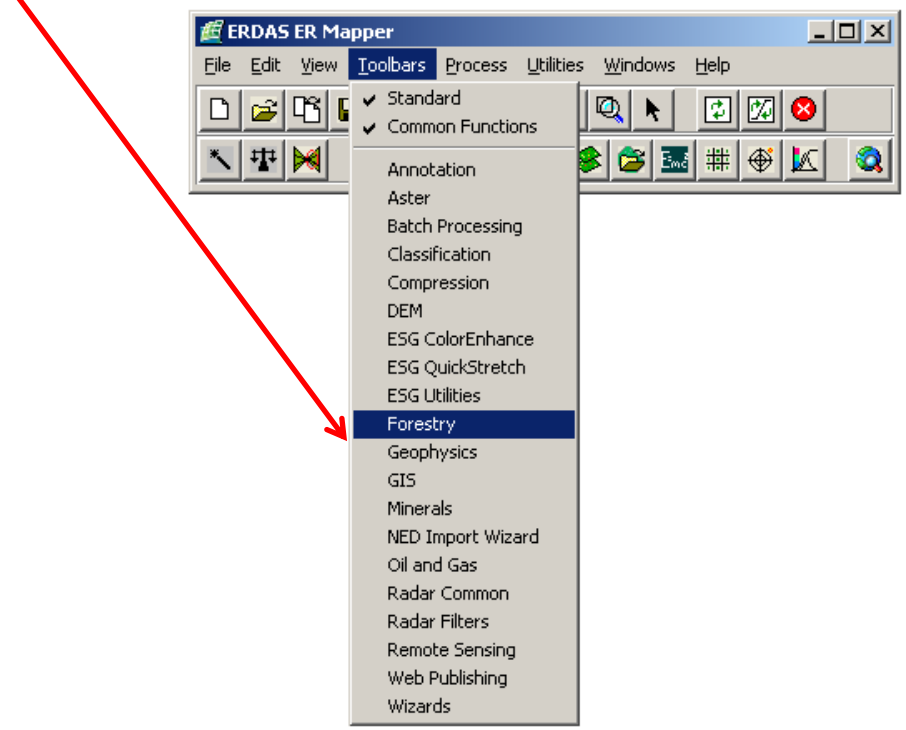

Run the NDVI process:

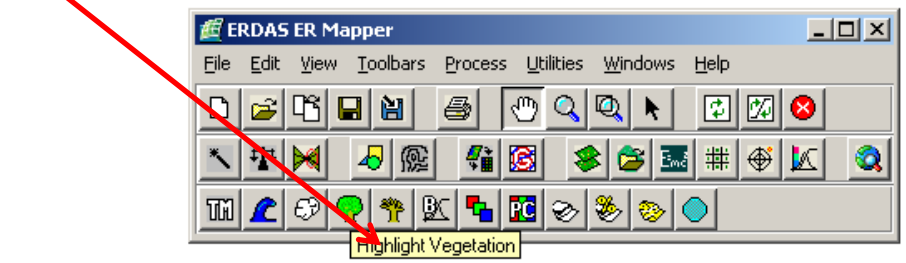

…achieving the outcome:

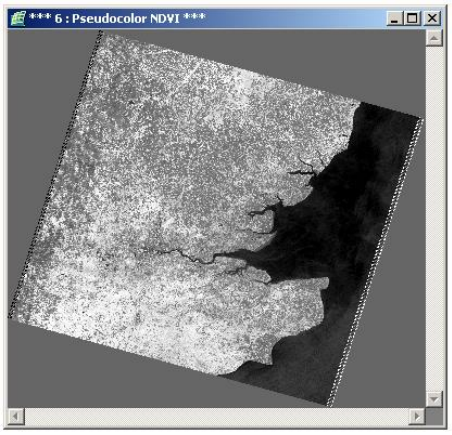

10. To check all is well – 3! (We'll use the TM tool to ensure our .ers data set (which we have made from the 7 TIFF files, behaves like a 7 band TM image):

choose the TM process and the appropriate .ers file.

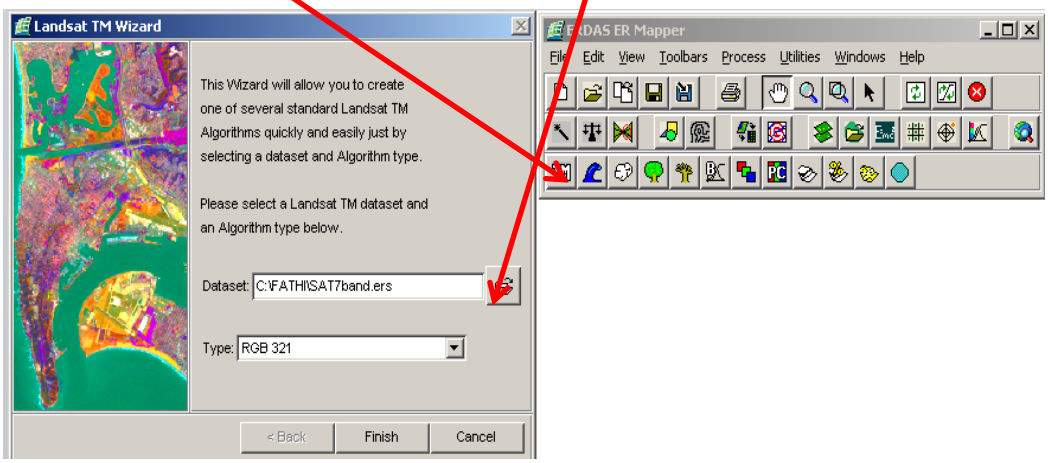

and note the appropriate RGB display.

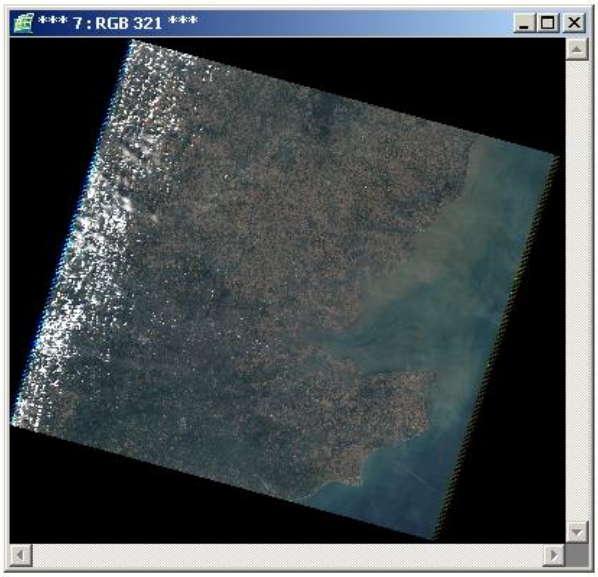

The data set is now ready for more sophisticated analysis (such as an unsupervised classification……)

Appendix 3: Showing how to produce a scene of an appropriate size for work.

1. Display the whole scene, using Open, selecting an appropriate file and clicking 'OK':

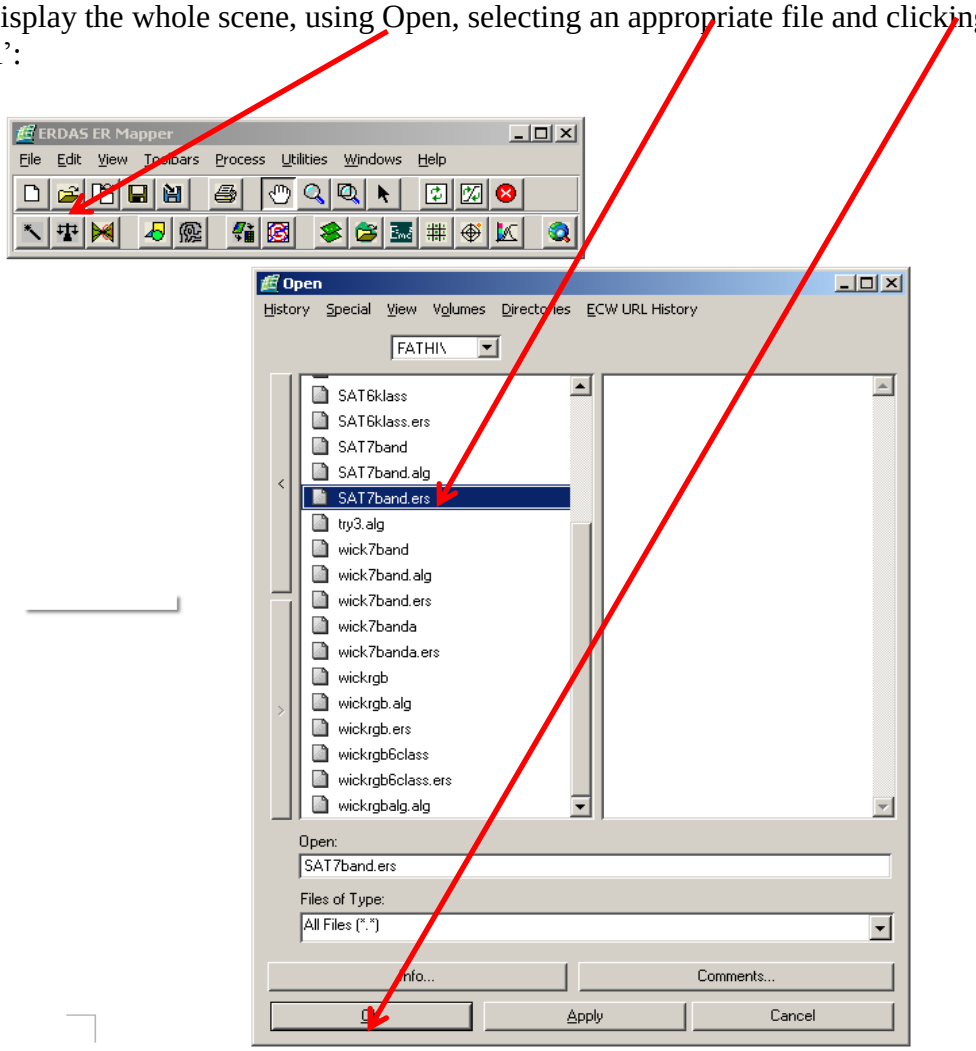

2. To select a subset of the image, select Utilities/File maintenance/Datasets/Save a subset of image

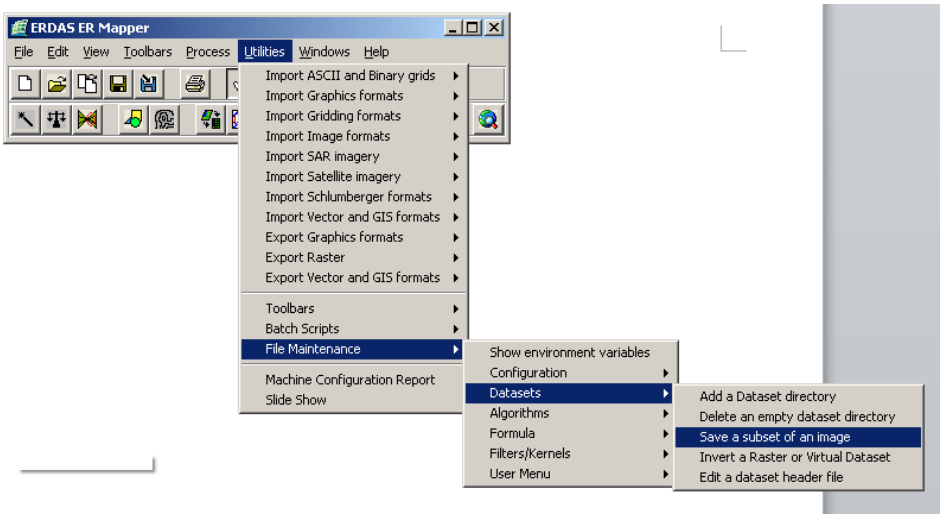

Selecting an appropriate WINDOW from the subset, to save as a separate working scene:

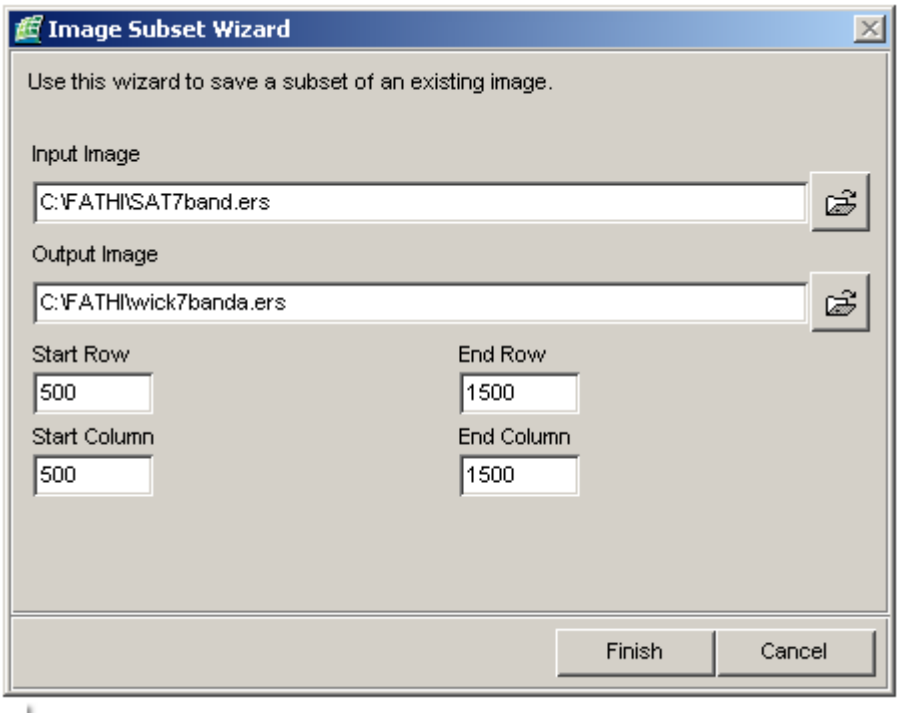

(note: to do this you will have to have discovered the appropriate rows and columns you require to bound your study area. PAINT is a useful tool for this!).

3. To display your new area, again use ‘Open’, but select your new data set.

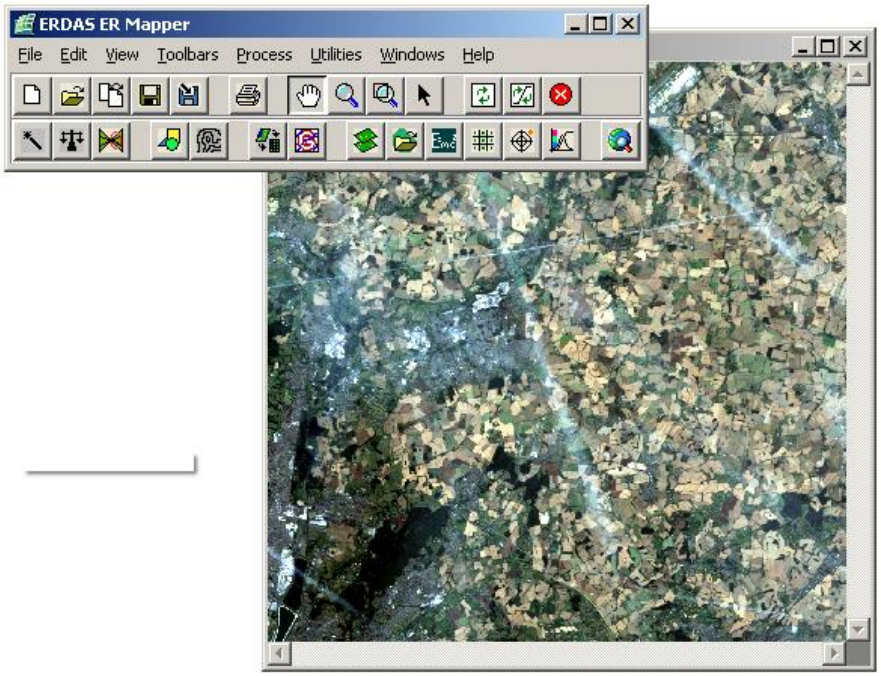

Appendix 4a: Plant taxa recorded from 40 quadrats in Wicken Fen with common names, density and frequency.

Family	Species Name	Common Name	Density (m^{-2})	Frequency %
Asteraceae	*Bellis perennis* L.	Daisy	1	2.5
Asteraceae	*Cirsium arvense* (L.) Scop	Creeping Thistle	1.025	12.5
Asteraceae	*Cirsium palustre* (L.) Scop	Marsh Thistle	0.2	7.5
Asteraceae	*Cirsium vulgare* (Savi) Ten.	Spear Thistle	0.175	2.5
Asteraceae	*Centaurea nigra* L.	Common Knapweed	0.55	2.5
Apiaceae	*Angelica sylvestris L.*	Wild Angelica	0.15	2.5
Apiaceae	*Berula erecta* (Huds.) Coville	Lesser Water-parsnip	0.625	2.5
Apiaceae	*Hydrocotyle vulgaris* L.	Marsh Pennywort	5	5
Alismataceae	*Alisma plantago-aquatica* L.	Water-plantain	0.025	2.5
Ranunculaceae	*Ranunculus flammula* L	Lesser Spearwort	0.025	2.5
Betulaceae	*Betula pendula* Roth	Silver Birch	0.275	5
Brassicaceae	*Cardamine hirsute* L.	Hairy Bittercress	0.2	2.5
Boraginaeae	*Myosotis scorpioides* L.	Water Forget-me-not	0.1	5
Boraginaeae	*Symphytum officinale* L.	Common Comfrey	1.55	12.5
Convolvulaceae	*Calystegia sepium* (L.) R. Br.	Hedge Bindweed	4.55	25
Cyperacaea	*Carex acutiformis* Ehrh.	Lesser Pond-sedge	3.75	7.5
Cyperacaea	*Carex distans* L.	Brown Sedge	0.5	2.5
Cyperacaea	*Carex flacca* Schreb.	Glaucous Sedge	5.125	15
Cyperacaea	*Carex otrubae* Podp.	False Fox-sedge	0.025	2.5
Cyperacaea	*Carex panicea* L.	Carnation Sedge	2.05	7.5
Cyperacaea	*Carex riparia* Curtis	Greater Pond-sedge	0.5	2.5
Cyperacaea	*Cladium mariscus* (L.) Pohl	Great Fen-sedge	8.125	12.5
Cyperacaea	*Eleocharis uniglumis* (Link) Schult.	Slender Spike-rush	8.75	10
Crassulaceae	*Crassula helmsii* (Kirk) Cockayne	Australian swamp stonecrop	0.1	2.5
Caryophyllaceae	*Lychnis flos-cuculi* L.	Ragged-Robin	0.125	2.5
Caryophyllaceae	*Stellaria alsine* Grimm	Bog starwort	0.425	2.5

Appendix 4a

Family	Species Name	Common Name	Density (m^{-2})	Frequency %
Dryopteridaceae	*Athyrium filix-femina* (L.) Roth	Lady Fern	2.525	5
Euphorbiaceae	*Mercurialis perennis* L.	Dog's mercury	0.1	2.5
Salicaceae	*Salix repens* L.	Creeping Willow	0.025	2.5
Fabaceae	*Lathyrus pratensis* L.	Meadow Vetchling	0.05	2.5
Iridaceae	*Iris pseudacorus* L.	Yellow Flag	1.925	17.5
Juncaceae	*Juncus bufonius* L.	Toad Rush	1.275	5
Juncaceae	*Juncus effusus* L.	Soft-rush	4.65	7.5
Juncaceae	*Juncus inflexus* L.	Hard Rush	10	17.5
Lamiaceae	*Ajuga reptans* L.	Bugle	0.1	2.5
Lamiaceae	*Glechoma hederacea* L	Ground-ivy	1.5	10
Lamiaceae	*Lycopus europaeus* L.	Gypsywort	0.25	2.5
Lamiaceae	*Mentha aquatica* L.	Water Mint	4.775	27.5
Lemnaceae	*Lemna minor* L.	Common Duckweed	65	10
Lemnaceae	*Lemna trisulca* L.	Ivy-leaved Duckweed	0.125	2.5
Onagraceae	*Chamerion augustifolium* (L.) Holub	Rosebay Willowherb	0.15	2.5
Onagraceae	*Epilobium hirsutum* L.	Great Willowherb	3.075	10
Poaceae	*Trifolium repens* L	White Clover	0.125	2.5
Poaceae	*Agrostis stolonifera* L.	Creeping Bent	16.85	30
Poaceae	*Alopecurus geniculatus* L.	Marsh Foxtail	5	5
Poaceae	*Anthoxanthum odoratum* L.	Sweet Vernal-grass	0.5	2.5
Poaceae	*Arrhenatherum elatius* (L.) P. Beauv. Ex J. Presl & C. Presl	False Oat-grass	0.15	2.5
Poaceae	*Dactylis glomerata* L.	Cock's-foot	0.3	5
Poaceae	*Festuca pratensis* Huds.	Meadow Fescue	0.5	2.5
Poaceae	*Festuca rubra* L.	Red Fescue	15.5	22.5
Poaceae	*Helictotrichon pubescens* (Huds.) Pilg.	Downy Oat-grass	4.025	7.5
Poaceae	*Holcus lanatus* L.	Yorkshire-fog	2.625	7.5
Poaceae	*Lolium perenne* L.	Perennial Rye-grass	0.15	2.5

Appendix 4a

Family	Species Name	Common Name	Density (m^{-2})	Frequency %
Poaceae	*Molinia caerulea* (L.) Moench	Purple Moor-grass	0.925	7.5
Poaceae	*Phalaris arundinacea* L.	Reed Canary-grass	4.8	15
Poaceae	*Phragmites australis* (Cav.) Trin. Ex Steud.	Common Reed	21.9	72.5
Poaceae	*Poa palustris* L.	Fowl bluegrass	3.775	10
Poaceae	*Poa pratensis* L.	Smooth Meadow-grass	6.925	12.5
Poaceae	*Poa trivialis* L.	Rough Meadow-grass	6.3	15
Plantaginaceae	*Callitriche platycarpa* Kuetz.	Various-leaved Water-starwort	0.25	2.5
Primulaceae	*Lysimachia vulgaris* L.	Yellow Loosestrife	2.42	22.5
Polygonaceae	*Rumex acetosa* L.	Common Sorrel	0.05	2.5
Polygonaceae	*Rumex hydrolapathum* Huds.	Water Dock	0.075	2.5
Polygonaceae	*Rumex obtusifolius* L.	Broad-leaved Dock	0.125	2.5
Rosaceae	*Crataegus monogyna* Jacq.	Hawthorn	0.025	2.5
Rosaceae	*Rubus fruticosus* L.	Bramble	1.175	7.5
Rosaceae	*Filipendula ulmaria* (L.) Maxim.	Meadowsweet	1.3	10
Rosaceae	*Potentilla erecta* (L.) Raeusch.	Tormentil	0.075	2.5
Ranunculacaea	*Ranunculus lingua* L.	Greater Spearwort	0.125	2.5
Ranunculacaea	*Ranunculus trichophyllus* Chaix	Thread-leaved Water-crowfoot	2.85	12.5
Ranunculacaea	*Thalictrum flavum* L.	Common Meadow-rue	0.65	5
Ranunculacaea	*Caltha palustris* L.	Marsh-marigold	0.25	2.5
Resedaceae	*Reseda lutea* L.	Wild Mignonette	0.975	10
Rubiaceae	*Galium aparine* L	Cleavers	5.25	7.5
Rubiaceae	*Galium palustre* L.	Common Marsh-bedstraw	7.875	37.5
Salicaceae	*Salix caprea* L.	Goat Willow	2.1	12.5
Salicaceae	*Salix pentandra* L.	Bay Willow	0.25	2.5
Salicaceae	*Salix purpurea* L.	Purple Willow	0.225	2.5
Sparganiaceae	*Sparganium erectum* L.	Branched Bur-reed	0.15	5
Solanaceae	*Solanum dulcamara* L.	Bittersweet	0.175	2.5
Typhaceae	*Typha latifolia* L.	Greater Reedmace	1.475	5
Urticaeae	*Urtica dioica* L.	Common Nettle	1.8	17.5

Appendix 4b: Field data collected from 40 quadrats at Wicken Fen during June 2010. (T = Line transect; Q = Quadrat).

Species	Abb.	T1Q1	T1Q2	T1Q3	T1Q4	T1Q5	T1Q6	T1Q7	T1Q8
Angelica sylvestris	Ansy	0	0	0	0	0	0	0	0
Agrostis stolonifera	Agst	0	20	0	0	0	0	0	0
Ajuga reptans	Ajre	0	4	0	0	0	0	0	0
Alisma plantago-aquatica	Alpa	0	0	0	0	0	0	0	0
Alopecurus geniculatus	Alge	0	0	0	0	0	0	0	0
Anthoxanthum odoratum	Anod	0	0	0	0	0	0	0	0
Arrhenatherum elatius	Arel	0	0	0	0	0	0	0	0
Athyrium filix-femina	Atff	0	31	0	0	0	0	0	0
Ranunculus flammula	Rafl	0	0	0	0	0	0	0	0
Bellis perennis	Blpe	0	0	0	0	0	0	0	0
Berula erecta	Beer	0	0	0	0	0	0	0	0
Betula pendula	Btpe	0	0	0	0	0	0	0	0
Callitriche platycarpa	Clpl	0	0	0	0	0	0	0	0
Caltha palustris	Capa	0	0	0	0	0	0	0	0
Calystegia sepium	Clse	9	0	0	48	0	0	0	0
Cardamine hirsuta	Cahi	0	0	0	0	0	0	0	0
Carex acutiformis	Cxac	0	0	0	0	60	0	0	50
Carex distans	Cxdi	0	0	0	0	0	0	0	0
Carex flacca	Cxfl	0	0	0	0	0	0	0	0
Carex otrubae	Cxot	0	0	0	0	0	0	0	0
Carex panicea	Cxpa	0	0	60	16	0	0	0	0
Carex riparia	Cari	0	0	0	0	0	0	0	0
Centaurea nigra	Cnni	0	0	0	22	0	0	0	0
Chamerion augustifolium	Chau	0	0	0	0	0	0	0	0
Cirsium arvense	Ciar	0	0	0	0	0	0	0	0
Cirsium palustre	Cipa	0	0	0	0	0	0	0	0
Cirsium vulgare	Civu	0	0	0	0	0	0	0	0
Cladium mariscus	Clma	0	0	0	0	0	0	0	20
Crassula helmsii	Crhe	0	0	0	0	0	0	0	0
Crataegus monogyna	Crmo	0	0	0	0	0	0	0	0
Dactylis glomerata	Dcgl	0	0	0	0	0	0	0	0
Eleocharis uniglumis	Elun	0	0	0	0	0	0	0	0
Epilobium hirsutum	Ephi	0	0	0	0	0	0	0	0
Festuca pratensis	Fepr	0	0	0	0	0	0	0	0
Festuca rubra	Feru	0	0	0	0	0	0	0	0
Filipendula ulmaria	Fiul	0	0	0	0	0	0	23	0
Galium aparine	Gaap	0	0	0	0	0	0	0	0
Galium palustre	Gapa	0	11	14	23	1	10	15	0
Glechoma hederacea	Glhe	0	0	0	0	0	0	0	0
Helictotrichon pubescens	Hepu	0	0	0	0	0	0	0	0
Holcus lanatus	Hola	0	0	0	0	0	0	0	0

Appendix 4b

Species	Abb.	T1Q1	T1Q2	T1Q3	T1Q4	T1Q5	T1Q6	T1Q7	T1Q8
Hydrocotyle vulgaris	Hyvu	0	0	100	100	0	0	0	0
Iris pseudacorus	Irps	0	0	0	0	0	6	0	0
Juncus bufonius	Jubu	0	0	0	0	0	0	0	0
Juncus effusus	Juef	0	0	0	0	0	0	0	0
Juncus inflexus	Juin	100	0	100	100	0	0	0	0
Lathyrus pratensis	Lapr	0	0	0	0	0	0	0	0
Lemna minor	Lemi	0	0	0	0	0	0	1	0
Lemna trisulca	Letr	0	0	0	0	0	0	0	0
Lolium perenne	Lope	0	0	0	0	0	0	0	0
Lychnis flos-cuculi	Lyfc	0	0	0	0	0	0	0	0
Lycopus europaeus	Lyeu	0	0	0	0	0	0	0	0
Lysimachia vulgaris	Lyvu	17	0	2	0	0	14	0	0
Mentha aquatica	Meaq	0	0	22	14	0	12	0	0
Molinia caerulea	Moca	0	0	0	0	0	0	0	0
Myosotis scorpioides	Mssc	0	0	0	0	0	0	0	0
Trifolium repens	Trre	0	0	0	0	0	0	0	0
Phalaris arundinacea	Phar	0	0	0	20	10	0	0	0
Phragmites australis	Phau	17	15	24	0	100	35	3	21
Poa pratensis	Papr	0	8	0	0	0	0	50	0
Poa trivialis	Patr	0	0	0	0	0	0	0	0
Potentilla erecta	Pter	0	0	0	0	0	0	0	0
Ranunculus lingua	Rali	0	0	0	0	0	0	0	0
Ranunculus trichophyllus	Ratr	0	0	0	0	0	4	0	0
Reseda lutea	Relu	0	0	0	0	0	0	0	0
Rubus fruticosus	Rufr	0	0	0	0	0	0	0	16
Rumex acetosa	Ruac	0	0	0	0	0	0	0	0
Rumex hydrolapathum	Ruhy	0	3	0	0	0	0	0	0
Rumex obtusifolius	Ruob	0	0	0	0	0	0	0	0
Salix caprea	Saca	0	0	0	0	0	0	0	0
Salix pentandra	Sape	0	0	0	0	0	0	0	0
Salix purpurea	Sapu	0	0	0	0	0	0	0	0
Solanum dulcamara	Sodu	0	0	0	0	0	0	0	0
Sparganium erectum	Sper	0	0	0	0	0	0	0	0
Stellaria media	Stme	0	0	0	0	0	0	0	0
Symphytum officinale	Syof	11	0	0	0	0	0	0	0
Thalictrum flavum	Thfl	0	0	4	22	0	0	0	0
Typha latifolia	Tyla	0	0	0	0	0	0	0	0
Urtica dioica	Urdi	0	0	0	0	0	0	0	0
Salix repens	Sare	0	0	0	0	0	0	0	0

Appendix 4b

Species	Abb.	T1Q9	T1Q10	T2Q1	T2Q2	T2Q3	T2Q4	T2Q5	T2Q6
Angelica sylvestris	Ansy	6	0	0	0	0	0	0	0
Agrostis stolonifera	Agst	0	0	0	0	0	24	0	0
Ajuga reptans	Ajre	0	0	0	0	0	0	0	0
Alisma plantago-aquatica	Alpa	0	0	0	0	0	0	0	0
Alopecurus geniculatus	Alge	0	0	0	0	0	0	0	100
Anthoxanthum odoratum	Anod	0	0	0	0	0	0	0	0
Arrhenatherum elatius	Arel	0	0	0	0	0	0	0	0
Athyrium filix-femina	Atff	0	0	0	0	0	0	0	0
Ranunculus flammula	Rafl	0	0	0	0	0	0	0	0
Bellis perennis	Blpe	0	0	0	0	0	40	0	0
Berula erecta	Beer	0	0	0	0	0	0	0	0
Betula pendula	Btpe	0	0	0	0	0	0	0	0
Callitriche platycarpa	Clpl	0	0	0	0	0	0	10	0
Caltha palustris	Capa	0	0	0	0	0	0	10	0
Calystegia sepium	Clse	0	0	0	0	0	0	0	12
Cardamine hirsuta	Cahi	0	8	0	0	0	0	0	0
Carex acutiformis	Cxac	40	0	0	0	0	0	0	0
Carex distans	Cxdi	0	0	20	0	0	0	0	0
Carex flacca	Cxfl	0	0	30	0	0	25	0	0
Carex otrubae	Cxot	0	0	0	0	0	0	0	0
Carex panicea	Cxpa	0	0	0	6	0	0	0	0
Carex riparia	Cari	0	0	0	0	0	0	0	20
Centaurea nigra	Cnni	0	0	0	0	0	0	0	0
Chamerion augustifolium	Chau	0	0	0	0	0	0	0	0
Cirsium arvense	Ciar	0	0	0	0	0	0	0	0
Cirsium palustre	Cipa	5	1	2	0	0	0	0	0
Cirsium vulgare	Civu	0	0	0	0	0	0	0	0
Cladium mariscus	Clma	0	0	0	100	0	0	0	0
Crassula helmsii	Crhe	0	0	0	0	0	0	0	0
Crataegus monogyna	Crmo	0	1	0	0	0	0	0	0
Dactylis glomerata	Dcgl	0	0	0	0	0	0	0	0
Eleocharis uniglumis	Elun	0	0	0	0	0	0	0	0
Epilobium hirsutum	Ephi	0	15	0	0	6	0	0	0
Festuca pratensis	Fepr	0	0	0	0	0	0	0	0
Festuca rubra	Feru	0	0	0	0	0	0	0	0
Filipendula ulmaria	Fiul	0	3	0	0	0	0	0	0
Galium aparine	Gaap	0	0	10	0	0	0	0	0
Galium palustre	Gapa	20	0	0	0	0	0	50	40
Glechoma hederacea	Glhe	0	4	0	0	0	0	0	0
Helictotrichon pubescens	Hepu	0	0	100	55	0	0	0	0
Holcus lanatus	Hola	0	0	0	0	0	0	0	0

Appendix 4b

Species	Abb.	T1Q9	T1Q10	T2Q1	T2Q2	T2Q3	T2Q4	T2Q5	T2Q6
Hydrocotyle vulgaris	Hyvu	0	0	0	0	0	0	0	0
Iris pseudacorus	Irps	5	0	0	0	0	35	1	0
Juncus bufonius	Jubu	0	0	0	0	0	0	0	1
Juncus effusus	Juef	0	0	0	0	0	0	0	0
Juncus inflexus	Juin	0	0	0	15	15	40	0	0
Lathyrus pratensis	Lapr	0	2	0	0	0	0	0	0
Lemna minor	Lemi	0	0	0	0	0	0	0	0
Lemna trisulca	Letr	0	0	0	0	0	0	0	0
Lolium perenne	Lope	0	0	0	0	0	0	0	0
Lychnis flos-cuculi	Lyfc	0	0	0	0	0	0	0	0
Lycopus europaeus	Lyeu	0	0	0	0	0	0	0	0
Lysimachia vulgaris	Lyvu	12	0	10	25	0	0	0	8
Mentha aquatica	Meaq	0	0	0	0	5	26	0	0
Molinia caerulea	Moca	0	0	0	0	25	0	0	2
Myosotis scorpioides	Mssc	0	0	0	0	0	0	0	0
Trifolium repens	Trre	0	0	0	0	0	0	0	0
Phalaris arundinacea	Phar	0	0	0	0	0	0	0	0
Phragmites australis	Phau	12	0	0	7	18	0	27	0
Poa pratensis	Papr	100	89	0	0	0	0	0	0
Poa trivialis	Patr	0	0	0	0	0	0	0	0
Potentilla erecta	Pter	0	0	0	3	0	0	0	0
Ranunculus lingua	Rali	0	0	0	0	0	0	0	0
Ranunculus trichophyllus	Ratr	0	0	0	0	0	0	0	1
Reseda lutea	Relu	0	0	0	0	0	0	0	0
Rubus fruticosus	Rufr	0	0	0	0	0	0	0	0
Rumex acetosa	Ruac	0	0	0	0	0	0	0	0
Rumex hydrolapathum	Ruhy	0	0	0	0	0	0	0	0
Rumex obtusifolius	Ruob	0	0	5	0	0	0	0	0
Salix caprea	Saca	0	0	0	50	3	0	0	0
Salix pentandra	Sape	0	0	0	0	0	0	0	0
Salix purpurea	Sapu	0	0	0	0	0	0	0	0
Solanum dulcamara	Sodu	0	0	0	0	0	0	0	0
Sparganium erectum	Sper	0	0	0	0	0	0	0	0
Stellaria media	Stme	0	0	0	0	0	0	0	0
Symphytum officinale	Syof	0	0	0	0	8	0	0	0
Thalictrum flavum	Thfl	0	0	0	0	0	0	0	0
Typha latifolia	Tyla	0	0	0	0	0	0	0	9
Urtica dioica	Urdi	12	0	0	0	0	0	0	0
Salix repens	Sare	0	0	0	0	0	0	0	0

Appendix 4b

Species	Abb.	T2Q7	T2Q8	T3Q1	T3Q2	T3Q3	T3Q4	T3Q5	T3Q6
Angelica sylvestris	Ansy	0	0	0	0	0	0	0	0
Agrostis stolonifera	Agst	100	0	0	0	0	15	0	5
Ajuga reptans	Ajre	0	0	0	0	0	0	0	0
Alisma plantago-aquatica	Alpa	0	0	0	0	0	0	0	0
Alopecurus geniculatus	Alge	0	0	0	100	0	0	0	0
Anthoxanthum odoratum	Anod	0	0	0	0	0	0	0	0
Arrhenatherum elatius	Arel	0	0	0	0	0	0	0	0
Athyrium filix-femina	Atff	0	0	0	0	0	0	0	0
Ranunculus flammula	Rafl	0	0	0	0	0	0	0	0
Bellis perennis	Blpe	0	0	0	0	0	0	0	0
Berula erecta	Beer	0	0	0	0	0	0	0	0
Betula pendula	Btpe	10	1	0	0	0	0	0	0
Callitriche platycarpa	Clpl	0	0	0	0	0	0	0	0
Caltha palustris	Capa	0	0	0	0	0	0	0	0
Calystegia sepium	Clse	0	3	0	0	0	0	0	10
Cardamine hirsuta	Cahi	0	0	0	0	0	0	0	0
Carex acutiformis	Cxac	0	0	0	0	0	0	0	0
Carex distans	Cxdi	0	0	0	0	0	0	0	0
Carex flacca	Cxfl	0	0	0	0	0	0	100	0
Carex otrubae	Cxot	0	0	0	0	0	0	0	0
Carex panicea	Cxpa	0	0	0	0	0	0	0	0
Carex riparia	Cari	0	0	0	0	0	0	0	0
Centaurea nigra	Cnni	0	0	0	0	0	0	0	0
Chamerion augustifolium	Chau	6	0	0	0	0	0	0	0
Cirsium arvense	Ciar	0	0	5	0	0	0	0	15
Cirsium palustre	Cipa	0	0	0	0	0	0	0	0
Cirsium vulgare	Civu	0	0	0	0	0	0	0	0
Cladium mariscus	Clma	0	0	0	0	0	0	0	0
Crassula helmsii	Crhe	0	0	0	0	0	0	0	0
Crataegus monogyna	Crmo	0	0	0	0	0	0	0	0
Dactylis glomerata	Dcgl	0	0	0	0	0	0	0	0
Eleocharis uniglumis	Elun	0	0	0	0	0	0	0	0
Epilobium hirsutum	Ephi	0	2	0	0	0	0	0	0
Festuca pratensis	Fepr	0	0	0	0	0	0	0	0
Festuca rubra	Feru	10	10	0	3	0	10	100	0
Filipendula ulmaria	Fiul	0	0	0	0	0	0	0	0
Galium aparine	Gaap	0	0	0	0	0	0	0	100
Galium palustre	Gapa	0	0	0	0	0	0	0	0
Glechoma hederacea	Glhe	0	0	0	0	0	0	20	0
Helictotrichon pubescens	Hepu	0	0	0	0	0	0	0	0
Holcus lanatus	Hola	0	0	0	0	0	0	0	0

Appendix 4b

Species	Abb.	T2Q7	T2Q8	T3Q1	T3Q2	T3Q3	T3Q4	T3Q5	T3Q6
Hydrocotyle vulgaris	Hyvu	0	0	0	0	0	0	0	0
Iris pseudacorus	Irps	12	0	0	0	0	0	10	0
Juncus bufonius	Jubu	0	0	0	0	0	0	0	0
Juncus effusus	Juef	0	0	0	0	0	0	0	0
Juncus inflexus	Juin	0	0	0	0	0	0	0	0
Lathyrus pratensis	Lapr	0	0	0	0	0	0	0	0
Lemna minor	Lemi	0	0	0	0	0	0	0	0
Lemna trisulca	Letr	0	0	0	0	0	0	0	0
Lolium perenne	Lope	0	0	0	0	0	0	0	0
Lychnis flos-cuculi	Lyfc	0	0	0	0	0	0	0	0
Lycopus europaeus	Lyeu	0	0	0	0	0	0	0	0
Lysimachia vulgaris	Lyvu	0	1	0	4	0	0	0	0
Mentha aquatica	Meaq	20	0	0	0	0	0	0	0
Molinia caerulea	Moca	0	0	0	0	0	0	0	0
Myosotis scorpioides	Mssc	0	0	0	0	0	0	0	0
Trifolium repens	Trre	0	0	0	0	5	0	0	0
Phalaris arundinacea	Phar	0	0	0	0	0	0	50	0
Phragmites australis	Phau	0	15	7	1	100	20	10	25
Poa pratensis	Papr	0	0	0	0	0	0	0	30
Poa trivialis	Patr	0	100	100	0	0	0	0	0
Potentilla erecta	Pter	0	0	0	0	0	0	0	0
Ranunculus lingua	Rali	0	0	0	0	0	0	0	0
Ranunculus trichophyllus	Ratr	0	0	0	0	0	0	0	0
Reseda lutea	Relu	0	0	0	0	20	6	3	10
Rubus fruticosus	Rufr	0	0	17	0	0	0	0	0
Rumex acetosa	Ruac	0	0	0	0	0	0	0	0
Rumex hydrolapathum	Ruhy	0	0	0	0	0	0	0	0
Rumex obtusifolius	Ruob	0	0	0	0	0	0	0	0
Salix caprea	Saca	12	0	13	0	0	0	0	0
Salix pentandra	Sape	0	0	0	0	0	0	0	0
Salix purpurea	Sapu	0	0	9	0	0	0	0	0
Solanum dulcamara	Sodu	0	0	0	0	0	0	0	0
Sparganium erectum	Sper	0	0	0	0	5	0	0	0
Stellaria media	Stme	0	0	0	0	0	17	0	0
Stellaria palustris	Stpa	0	0	0	0	0	0	0	0
Symphytum officinale	Syof	0	7	18	0	0	0	0	0
Thalictrum flavum	Thfl	0	0	0	0	0	0	0	0
Typha latifolia	Tyla	0	0	0	0	0	0	0	0
Urtica dioica	Urdi	0	0	0	0	10	6	0	0
Salix repens	Sare	0	0	0	0	0	1	0	0

Appendix 4b

Species	Abb.	T3Q7	T4Q1	T4Q2	T4Q3	T5Q1	T5Q2	T5Q3	T5Q4
Angelica sylvestris	Ansy	0	0	0	0	0	0	0	0
Agrostis stolonifera	Agst	100	0	0	0	100	100	100	10
Ajuga reptans	Ajre	0	0	0	0	0	0	0	0
Alisma plantago-aquatica	Alpa	0	0	0	0	0	0	0	0
Alopecurus geniculatus	Alge	0	0	0	0	0	0	0	0
Anthoxanthum odoratum	Anod	0	0	0	0	0	0	0	0
Arrhenatherum elatius	Arel	0	0	0	0	0	0	0	0
Athyrium filix-femina	Atff	0	0	0	0	0	0	0	0
Ranunculus flammula	Rafl	0	0	0	0	0	0	0	0
Bellis perennis	Blpe	0	0	0	0	0	0	0	0
Berula erecta	Beer	0	0	0	0	0	0	0	0
Betula pendula	Btpe	0	0	0	0	0	0	0	0
Callitriche platycarpa	Clpl	0	0	0	0	0	0	0	0
Caltha palustris	Capa	0	0	0	0	0	0	0	0
Calystegia sepium	Clse	0	1	7	70	0	0	0	0
Cardamine hirsuta	Cahi	0	0	0	0	0	0	0	0
Carex acutiformis	Cxac	0	0	0	0	0	0	0	0
Carex distans	Cxdi	0	0	0	0	0	0	0	0
Carex flacca	Cxfl	0	0	0	0	0	0	0	0
Carex otrubae	Cxot	0	0	0	0	0	0	1	0
Carex panicea	Cxpa	0	0	0	0	0	0	0	0
Carex riparia	Cari	0	0	0	0	0	0	0	0
Centaurea nigra	Cnni	0	0	0	0	0	0	0	0
Chamerion augustifolium	Chau	0	0	0	0	0	0	0	0
Cirsium arvense	Ciar	0	0	0	0	2	0	14	0
Cirsium palustre	Cipa	0	0	0	0	0	0	0	0
Cirsium vulgare	Civu	0	0	0	0	0	0	0	0
Cladium mariscus	Clma	0	100	5	100	0	0	0	0
Crassula helmsii	Crhe	0	0	0	0	0	0	0	4
Crataegus monogyna	Crmo	0	0	0	0	0	0	0	0
Dactylis glomerata	Dcgl	0	0	0	0	2	0	0	0
Eleocharis uniglumis	Elun	0	0	0	0	0	100	0	100
Epilobium hirsutum	Ephi	0	0	0	0	0	0	0	0
Festuca pratensis	Fepr	0	0	0	0	0	0	0	0
Festuca rubra	Feru	25	0	0	0	90	0	30	0
Filipendula ulmaria	Fiul	0	0	0	6	0	0	0	0
Galium aparine	Gaap	0	0	0	0	0	0	0	0
Galium palustre	Gapa	6	0	0	5	0	0	0	0
Glechoma hederacea	Glhe	0	0	0	0	0	0	0	0
Helictotrichon pubescens	Hepu	0	0	0	0	0	0	0	0
Holcus lanatus	Hola	0	0	0	0	50	0	40	0

Appendix 4b

Species	Abb.	T3Q7	T4Q1	T4Q2	T4Q3	T5Q1	T5Q2	T5Q3	T5Q4
Hydrocotyle vulgaris	Hyvu	0	0	0	0	0	0	0	0
Iris pseudacorus	Irps	0	0	0	0	0	0	0	0
Juncus bufonius	Jubu	0	0	0	0	0	0	0	0
Juncus effusus	Juef	0	0	0	43	100	0	43	0
Juncus inflexus	Juin	0	0	0	0	0	0	0	0
Lathyrus pratensis	Lapr	0	0	0	0	0	0	0	0
Lemna minor	Lemi	0	0	0	0	0	0	0	10
Lemna trisulca	Letr	0	0	0	0	0	0	0	0
Lolium perenne	Lope	0	0	0	0	0	0	0	0
Lychnis flos-cuculi	Lyfc	0	0	0	0	0	0	0	0
Lycopus europaeus	Lyeu	0	0	0	0	0	10	0	0
Lysimachia vulgaris	Lyvu	0	0	0	0	0	0	0	0
Mentha aquatica	Meaq	0	0	0	0	0	17	0	12
Mercurialis perennis	Mrpe	0	0	0	0	0	0	0	0
Molinia caerulea	Moca	0	0	0	0	0	0	0	0
Myosotis scorpioides	Mssc	0	0	0	0	0	0	0	1
Trifolium repens	Trre	0	0	0	0	0	0	0	0
Phalaris arundinacea	Phar	0	0	0	0	0	0	0	2
Phragmites australis	Phau	10	10	40	4	0	0	0	0
Poa pratensis	Papr	0	0	0	0	0	0	0	0
Poa trivialis	Patr	0	40	1	0	0	0	0	0
Potentilla erecta	Pter	0	0	0	0	0	0	0	0
Ranunculus lingua	Rali	0	0	0	0	0	0	0	0
Ranunculus trichophyllus	Ratr	0	0	0	0	0	0	0	7
Reseda lutea	Relu	0	0	0	0	0	0	0	0
Rubus fruticosus	Rufr	0	0	0	14	0	0	0	0
Rumex acetosa	Ruac	0	0	0	0	0	2	0	0
Rumex hydrolapathum	Ruhy	0	0	0	0	0	0	0	0
Rumex obtusifolius	Ruob	0	0	0	0	0	0	0	0
Salix caprea	Saca	0	6	0	0	0	0	0	0
Salix pentandra	Sape	0	0	0	0	0	0	0	0
Salix purpurea	Sapu	0	0	0	0	0	0	0	0
Solanum dulcamara	Sodu	0	0	0	0	0	0	0	0
Sparganium erectum	Sper	0	0	2	0	0	0	0	0
Stellaria media	Stme	0	0	0	0	0	0	0	0
Symphytum officinale	Syof	0	0	0	0	0	0	0	0
Thalictrum flavum	Thfl	0	0	0	0	0	0	0	0
Typha latifolia	Tyla	0	0	0	0	0	0	0	0
Urtica dioica	Urdi	0	0	19	7	0	0	0	0
Salix repens	Sare	0	0	0	0	0	0	0	0

Appendix 4b

Species	Abb.	T5Q5	T5Q6	T5Q7	T6Q1	T6Q2	T6Q3	T6Q4	T6Q5
Angelica sylvestris	Ansy	0	0	0	0	0	0	0	0
Agrostis stolonifera	Agst	0	0	10	0	0	0	90	0
Ajuga reptans	Ajre	0	0	0	0	0	0	0	0
Alisma plantago-aquatica	Alpa	0	0	1	0	0	0	0	0
Alopecurus geniculatus	Alge	0	0	0	0	0	0	0	0
Anthoxanthum odoratum	Anod	0	0	0	0	0	0	20	0
Arrhenatherum elatius	Arel	6	0	0	0	0	0	0	0
Athyrium filix-femina	Atff	0	0	0	0	0	70	0	0
Ranunculus flammula	Rafl	0	0	1	0	0	0	0	0
Bellis perennis	Blpe	0	0	0	0	0	0	0	0
Berula erecta	Beer	0	25	0	0	0	0	0	0
Betula pendula	Btpe	0	0	0	0	0	0	0	0
Callitriche platycarpa	Clpl	0	0	0	0	0	0	0	0
Caltha palustris	Capa	0	0	0	0	0	0	0	0
Calystegia sepium	Clse	0	0	0	7	0	0	15	0
Cardamine hirsuta	Cahi	0	0	0	0	0	0	0	0
Carex acutiformis	Cxac	0	0	0	0	0	0	0	0
Carex distans	Cxdi	0	0	0	0	0	0	0	0
Carex flacca	Cxfl	0	0	0	22	0	16	12	0
Carex otrubae	Cxot	0	0	0	0	0	0	0	0
Carex panicea	Cxpa	0	0	0	0	0	0	0	0
Carex riparia	Cari	0	0	0	0	0	0	0	0
Centaurea nigra	Cnni	0	0	0	0	0	0	0	0
Chamerion augustifolium	Chau	0	0	0	0	0	0	0	0
Cirsium arvense	Ciar	5	0	0	0	0	0	0	0
Cirsium palustre	Cipa	0	0	0	0	0	0	0	0
Cirsium vulgare	Civu	0	0	0	0	0	0	7	0
Cladium mariscus	Clma	0	0	0	0	0	0	0	0
Crassula helmsii	Crhe	0	0	0	0	0	0	0	0
Crataegus monogyna	Crmo	0	0	0	0	0	0	0	0
Dactylis glomerata	Dcgl	0	0	0	0	10	0	0	0
Eleocharis uniglumis	Elun	0	50	100	0	0	0	0	0
Epilobium hirsutum	Ephi	100	0	0	0	0	0	0	0
Festuca pratensis	Fepr	0	0	0	0	0	0	20	0
Festuca rubra	Feru	0	0	0	0	0	25	0	96
Filipendula ulmaria	Fiul	0	0	0	0	0	0	20	0
Galium aparine	Gaap	100	0	0	0	0	0	0	0
Galium palustre	Gapa	0	100	5	0	10	5	0	0
Glechoma hederacea	Glhe	0	0	0	1	0	0	0	35
Helictotrichon pubescens	Hepu	0	0	0	0	0	0	6	0
Holcus lanatus	Hola	0	0	0	0	0	0	15	0

Appendix 4b

Species	Abb.	T5Q5	T5Q6	T5Q7	T6Q1	T6Q2	T6Q3	T6Q4	T6Q5
Hydrocotyle vulgaris	Hyvu	0	0	0	0	0	0	0	0
Iris pseudacorus	Irps	0	0	0	0	0	0	8	0
Juncus bufonius	Jubu	0	0	0	0	0	0	50	0
Juncus effusus	Juef	0	0	0	0	0	0	0	0
Juncus inflexus	Juin	0	0	0	0	0	0	30	0
Lathyrus pratensis	Lapr	0	0	0	0	0	0	0	0
Lemna minor	Lemi	0	10	5	0	0	0	0	0
Lemna trisulca	Letr	0	0	5	0	0	0	0	0
Lolium perenne	Lope	6	0	0	0	0	0	0	0
Lychnis flos-cuculi	Lyfc	0	0	0	0	0	0	5	0
Lycopus europaeus	Lyeu	0	0	0	0	0	0	0	0
Lysimachia vulgaris	Lyvu	0	0	0	0	0	0	0	0
Mentha aquatica	Meaq	0	25	33	0	5	0	0	0
Molinia caerulea	Moca	0	0	0	10	0	0	0	0
Myosotis scorpioides	Mssc	0	0	3	0	0	0	0	0
Trifolium repens	Trre	0	0	0	0	0	0	0	0
Phalaris arundinacea	Phar	0	0	0	10	100	0	0	0
Phragmites australis	Phau	14	25	1	100	100	100	15	0
Poa pratensis	Papr	0	0	0	0	0	0	0	0
Poa trivialis	Patr	3	0	0	10	0	0	0	0
Potentilla erecta	Pter	0	0	0	0	0	0	0	0
Ranunculus lingua	Rali	0	0	0	0	5	0	0	0
Ranunculus trichophyllus	Ratr	0	0	2	0	100	0	0	0
Reseda lutea	Relu	0	0	0	0	0	0	0	0
Rubus fruticosus	Rufr	0	0	0	0	0	0	0	0
Rumex acetosa	Ruac	0	0	0	0	0	0	0	0
Rumex hydrolapathum	Ruhy	0	0	0	0	0	0	0	0
Rumex obtusifolius	Ruob	0	0	0	0	0	0	0	0
Salix caprea	Saca	0	0	0	0	0	0	0	0
Salix pentandra	Sape	0	0	0	10	0	0	0	0
Salix purpurea	Sapu	0	0	0	0	0	0	0	0
Solanum dulcamara	Sodu	0	6	0	0	0	0	0	0
Sparganium erectum	Sper	0	0	0	0	0	0	0	0
Stellaria media	Stme	0	0	0	0	0	0	0	0
Symphytum officinale	Syof	0	0	0	0	0	18	0	0
Thalictrum flavum	Thfl	0	0	0	0	0	0	0	0
Typha latifolia	Tyla	0	50	0	0	0	0	0	0
Urtica dioica	Urdi	0	0	0	0	0	10	0	8
Salix repens	Sare	0	0	0	0	0	0	0	0

Appendix 4c: Environmental variables recorded from sample quadrats in June 2010 at Wicken Fen. (T = Line transect; Q = Quadrat).

Line transect & Quadrat number	Soil pH	Soil conductivity (µS/cm)	Water conductivity (µS/cm)	% Shade	Water depth (m)	Vegetation layer (m)			
						Herb	Tall herb	Shrub	Tree
T1Q1	7.42	700	859	none	none	0.28	0.71	absent	absent
T1Q2	6.76	491	none	44	none	0.29	1.22	3.67	absent
T1Q3	7.11	580	none	none	0.01	0.23	0.94	absent	absent
T1Q4	6.97	576	none	none	0.01	0.61	1.11	absent	absent
T1Q5	7.31	779	none	none	none	0.83	2.11	absent	absent
T1Q6	6.95	700	876	none	0.15	0.68	1.34	absent	absent
T1Q7	6.85	460	none	93	none	0.25	0.81	5.5	absent
T1Q8	7.22	704	none	86	none	0.25	2.02	2.97	16
T1Q9	5.6	690	none	78	none	0.32	1.8	4.73	absent
T1Q10	6.59	520	none	74	none	0.07	0.93	absent	11
T2Q1	7.8	318	none	none	none	0.11	0.49	absent	absent
T2Q2	7.89	232	none	none	none	0.69	1.26	1.31	absent
T2Q3	7.8	252	none	none	none	0.33	1.21	absent	absent
T2Q4	7.35	629	none	none	none	0.19	0.51	absent	absent
T2Q5	6.91	542	718	none	0.1	0.18	1.04	absent	absent
T2Q6	7.8	245	758	none	0.16	0.47	1.79	absent	absent
T2Q7	7.34	595	none	none	none	0.4	1.06	3.33	absent
T2Q8	7.2	618	none	none	none	0.57	1.22	3	absent
T3Q1	7.49	622	none	none	none	0.11	1.1	1.9	absent
T3Q2	7.6	670	none	95	none	0.14	0.71	4	12
T3Q3	7.44	571	none	95	none	0.76	1.36	5.33	absent
T3Q4	7.42	765	none	99.4	none	0.23	0.69	absent	16
T3Q5	7.7	758	none	98	none	0.25	.95	absent	20
T3Q6	7.79	600	none	none	none	0.33	1.02	absent	absent
T3Q7	7.72	570	none	97	none	0.34	0.87	absent	7.3

Appendix 4c

Line transect & Quadrat number	Soil pH	Soil conductivity (µS/cm)	Water conductivity (µS/cm)	% Shade	Water depth (m)	Vegetation layer (m)			
						Herb	Tall herb	Shrub	Tree
T4Q1	6.86	512	none	none	none	0.7	2.14	2.5	absent
T4Q2	7.36	537	none	98	none	0.86	1.75	absent	5
T4Q3	7.74	569	none	90	none	0.48	1.71	absent	8
T5Q1	7.77	635	none	none	none	0.36	0.6	absent	absent
T5Q2	7.59	785	none	none	none	0.15	absent	absent	absent
T5Q3	7.55	658	none	none	none	0.35	0.81	absent	absent
T5Q4	7.47	908	875	none	0.42	0.29	absent	absent	absent
T5Q5	7.72	631	none	93	none	0.67	1.35	6	absent
T5Q6	6.8	841	629	none	0.09	0.49	1.89	absent	absent
T5Q7	6.9	758	758	none	0.13	0.44	absent	absent	absent
T6Q1	7.66	806	none	93	none	0.47	1.24	absent	10
T6Q2	6.72	2610	2820	none	0.1	0.56	1.98	absent	8
T6Q3	7.52	550	none	97	none	0.49	1.56	6	absent
T6Q4	7.36	686	none	none	none	0.26	1.15	absent	absent
T6Q5	7.6	925	none	99	none	0.2	absent	absent	9

Appendix 5: TWINSPAN Analysis depicting final Table from 40 quadrats in Wicken Fen.

Plant species in first column), entries in the table are the pseudospecies levels not quantitative values, the right and bottom sides define the dendrogram of the classification of species and samples, respectively.

```
                 1 22341231 1112 3 2211  3 3333 11322232
                7091380143912386568785634760245274925910

 63 Papr       555-----5----------------------3--------  0000
 26 Cipa       -13----2-----------------------------------  000100
  1 Aepo       --3------------------------------------  000101
 16 Cahi       -3-------------------------------------  000101
 30 Crmo       -1-------------------------------------  000101
 32 Defl       ----555--------------------------------  000101
 40 Glhe       -2--5-5----------1---------------------  000101
 48 Lapr       -2-------------------------------------  000101
 59 Oxac       ---3-----------------------------------  000101
 77 Sodu       ---3---------------2------------------  00011
 83 Urdi       --44-43------------43--------------3----  00011
 34 Ephi       -4-------5---32-------------------------  001000
  7 Arel       ---------3-----------------------------  001001
 18 Cxdi       -------5-------------------------------  001001
 38 Gaap       -------455-----------------------------  001001
 51 Lope       ---------3-----------------------------  001001
 72 Ruob       -------3-------------------------------  001001
 13 Clpl       ---------------------4-----------------  001010
 14 Capa       ---------------------4-----------------  001010
 22 Cxve       ----------------------5----------------  001010
 28 Clma       ------------5--5--535------------------  001010
 57 Moca       -------------5---4----2----------------  001010
 62 Papa       --------------55-4-1-------------------  001010
 64 Patr       ---------25----------------------------  001010
 65 Pter       ------------2---------------------------  001010
 69 Rufr       ----------4-------4-4------------------  001010
 74 Sape       ----------------4---------------------  001010
 75 Sapu       ----------3-----------------------------  001010
 17 Cxac       --5-------------5-5--------------------  001011
 80 Syof       -----4----44-33------------------------  001011
 15 Clse       --------4--3--21-3-35-4-5---------4-----  0011
 41 Hepu       -------5----5----------------------3-----  0011
 54 Lyvu       --4----4---45-1-------32--4-------------  0011
 73 Saca       ----------4-52-3----------------4-------  0011
 19 Cxfl       ----54-5---------5---------------54-----  010
 37 Fiul       52------------------3-------------5-----  010
 68 Relu       ---52---4----------------------------3----  010
  5 Alge       ----------------------5----------------5  011
 25 Ciar       --------433--------------------------24-  011
 61 Phau       2-4545--54343444555525-5-55--514--454--1  011
  8 Atff       -----5-------------------------5--------  100
 39 Gapa       4-5--3----------1---3554544--534----3---  100
 60 Phar       ----5-----------44------55--2-----------  100
 47 Juin       -----------544---------55--------55-----  101
 82 Tyla       ----------------------3------5----------  101
 44 Irps       --3-4----------------1----3-----453-----  1100
 45 Jubu       ----------------------1-----------5-----  1100
 21 Cxpa       ------------3----------54---------------  110100
  3 Ajre       -------------------------------2--------  110101
  4 Alpa       --------------------------------1--------  110101
  6 Anod       -----------------------------------5-----  110101
  9 Bara       --------------------------------1--------  110101
 10 Blpe       -----------------------------------5------  110101
 11 Beer       -------------------------------5---------  110101
 12 Btpe       --------------1-----------------4-------  110101
```

Appendix 5

```
23 Cnni       ----------------------5---------------  110101
24 Chau       -------------------------------3-------  110101
27 Civu       ---------------------------------3-----  110101
29 Craq       ---------------------------2-----------  110101
33 Elun       ---------------------------5555---------  110101
35 Fepr       ---------------------------------5-----  110101
43 Hyvu       ----------------------55----------------  110101
49 Lemi       1---------------------------443---------  110101
50 Letr       -------------------------------3---------  110101
52 Lyfc       ---------------------------------3-----  110101
53 Lyeu       ----------------------------4------------  110101
55 Meaq       -------------3---------54344455-55------  110101
58 Mssc       ----------------------------1-2---------  110101
66 Rali       -------------------------3--------------  110101
67 Ratr       ----------------------1--52-3-2---------  110101
70 Ruac       ----------------------------2------------  110101
71 Ruhy       -------------------------------2--------  110101
76 Sper       ----------------------------3----------  110101
79 Stpa       ---------------------------------5-----  110101
81 Thfl       ----------------------25----------------  110101
 2 Agst       --------3------------------54-455554555-  11011
31 Dcgl       -------------------------4-----------2--  11011
42 Hola       ---------------------------------4--55-  11100
20 Cxot       ---------------------------------------1-  111010
56 Mrpe       ---------------------------------------2  111010
78 Stal       ---------------------------------4----  111010
84 Vamy       -------------------------------1----  111010
36 Feru       --------------4-----------------4--45552  111011
46 Juef       --------------------5----------------55-  1111

              00000000000000000000000111111111111111111
              00000001111111111111111100000000000011111
              00111110001111111111111100000000001100001
                01111   00000000000110001111111
                        00000011111     0000001
                        01111100111     000001
```

Appendix 6: TWINSPAN groups in Wicken Fen with Ellenberg's indicator values for light -L; Moisture- F; and Reaction (soil pH or water pH) – R. (source: Hill et al., 1999).

Group	Species	Abb.	L	F	R
1	*Aegopodium podagraria* L.	Aepo	6	5	6
	Cardamine hirsute L.	Cahi	8	5	6
	Carex acutiformis Ehrh.	Cxac	7	8	7
	Carex flacca Schreb.	Cxfl	6	5	6
	Cirsium palustre (L.) Scop	Cipa	7	8	5
	Crataegus monogyna Jacq.	Crmo	7	5	7
	Deschampsia flexuosa (L.) Trin	Defl	6	5	2
	Epilobium hirsutum L.	Ephi	7	8	7
	Filipendula ulmaria (L.) Maxim.	Fiul	7	8	6
	Galium aparine L.	Gaap	7	9	7
	Glechoma hederacea L	Glhe	6	6	7
	Iris pseudacorus L.	Irps	7	9	6
	Lathyrus pratensis L.	Lapr	7	6	6
	Lemna minor L.	Lemi	7	11	7
	Lysimachia vulgaris L	Lyvu	7	9	7
	Oxalis acetosella L.	Oxac	4	6	4
	Phragmites australis (Cav.) Trin. Ex Steud.	Phau	7	5	7
	Poa pratensis L.	Popr	7	10	6
	Reseda lutea L.	Rebu	7	4	7
	Solanum dulcamara L.	Sodu	7	8	7
	Symphytum officinale L.	Syof	7	7	7
	Urtica dioica L.	Urdi	6	6	7
2	*Agrostis stolonifera* L.	Agst	7	6	7
	Alopecurus geniculatus L.	Alge	8	7	6
	Arrhenatherum elatius (L.) P. Beauv. Ex J. Presl & C. Presl	Arel	7	5	7
	Betula pendula Roth	Bepe	7	5	4
	Callitriche platycarpa Kuetz.	Capl	6	11	7
	Calystegia sepium (L.) R. Br.	Case	7	8	7
	Carex acutiformis Ehrh.	Caac	7	8	7
	Carex distans L.	Cadi	8	6	7
	Carex flacca Schreb.	Cafl	7	5	6
	Carex panicea L.	Capa	8	8	4
	Carex vesicaria L.	Cave	8	10	5
	Cirsium arvense (L.) Scop	Ciar	8	6	7
	Cirsium palustre (L.) Scop	Cipa	7	8	5
	Cladium mariscus (L.) Pohl	Clma	8	9	8
	Epilobium hirsutum L.	Ephi	7	8	7
	Festuca rubra L	Feru	8	5	6
	Filipendula ulmaria (L.) Maxim.	Fiul	7	8	6
	Galium aparine L.	Gaap	6	6	7

Appendix 6:

Group	Species	Abb.	L	F	R
2	*Galium palustre* L.	Gapa	7	9	5
	Glechoma hederacea L	Glhe	6	6	7
	Helictotrichon pubescens (Huds.) Pilg.	Hepu	7	4	7
	Iris pseudacorus L.	Irps	7	9	6
	Juncus bufonius L.	Jubu	7	7	6
	Juncus effusus L.	Juef	7	7	4
	Juncus inflexus L.	Juin	7	7	7
	Lolium perenne L.	Lope	8	5	6
	Lycopus europaeus L.	Lyeu	7	8	7
	Mentha aquatica L.	Meaq	7	8	7
	Molinia caerulea (L.) Moench	Moca	7	8	3
	Phalaris arundinacea L.	Phar	7	8	7
	Phragmites australis (Cav.) Trin. Ex Steud	Phau	7	10	7
	Poa palustris L.	Popa	7	9	7
	Poa pratensis L.	papr	7	5	6
	Poa trivialis L.	potr	7	6	6
	Potentilla erecta (L.) Raeusch.	poer	7	7	3
	Ranunculus trichophyllus Chaix	Ratr	7	12	6
	Reseda lutea L.	Relu	7	4	7
	Rubus fruticosus L.	Rufr	6	6	6
	Rumex obtusifolius L.	Ruob	7	5	7
	Salix caprea L.	Saca	7	7	7
	Salix pentandra L.	Sapu	7	8	6
	Salix purpurea L.	Sopu	8	9	7
	Solanum dulcamara L.	Sodu	7	8	7
	Symphytum officinale L	Syof	7	7	7
	Typha latifolia L.	Tyla	8	10	7
	Urtica dioica L.	Urdi	6	6	7
3	*Agrostis stolonifera* L.	Agst	7	6	7
	Ajuga reptans L.	Ajre	5	7	5
	Alisma plantago-aquatica L.	Alpl	7	10	7
	Anthoxanthum odoratum L.	Anod	7	6	4
	Athyrium filix-femina (L.) Roth	Atfi	5	7	5
	Baldellia ranunculoides (L.) Parl.	Bara	8	10	6
	Berula erecta (Huds.) Coville	Beer	7	10	7
	Bellis perennis L.	Bepe	8	5	6
	Calystegia sepium (L.) R. Br.	Case	7	8	7
	Carex flacca Schreb.	Cafl	7	5	6
	Carex panicea L.	Capa	8	8	4
	Cirsium vulgare (Savi) Ten.	Civu	7	5	6
	Dactylis glomerata L.	Dagl	7	5	7
	Eleocharis uniglumis (Link) Schult.	Elun	8	9	7

Appendix 6:

Group	Species Name	Abb.	L	F	R
3	*Festuca pratensis* Huds.	Fepr	7	6	6
	Filipendula ulmaria (L.) Maxim.	Fiul	7	8	6
	Galium palustre L.	Gapa	7	9	5
	Helictotrichon pubescens (Huds.) Pilg.	Hepu	7	4	7
	Holcus lanatus L.	Hola	7	6	6
	Hydrocotyle vulgaris L.	Hyvu	8	8	6
	Iris pseudacorus L.	Irps	7	9	6
	Juncus bufonius L.	Jubu	7	7	6
	Juncus inflexus L.	Juin	7	7	7
	Lemna minor L.	Lemi	7	11	7
	Lemna trisulca L.	Letr	7	12	7
	Lychnis flos-cuculi L.	Lyfl	7	9	6
	Lycopus europaeus L.	Lyeu	7	8	7
	Mentha aquatica L.	Meaq	7	8	7
	Myosotis scorpioides L	Mysc	7	9	6
	Phalaris arundinacea L.	Phar	7	8	7
	Phragmites australis (Cav.) Trin. Ex Steud.	Phau	7	10	7
	Poa pratensis L.	Popr	7	9	6
	Ranunculus lingua L.	Rali	7	10	6
	Ranunculus trichophyllus Chaix	Ratr	7	12	6
	Rumex acetosa L.	Ruac	7	5	5
	Rumex hydrolapathum Huds.	Ruhy	7	10	7
	Sparganium erectum L.	Sper	7	10	7
	Stellaria palustris Retz.	Stpa	7	8	6
	Thalictrum flavum L.	Thfl	7	8	7
	Typha latifolia L.	Tyla	8	10	7
4	*Agrostis stolonifera* L.	Agat	7	6	7
	Alopecurus geniculatus L	Alge	8	7	6
	Carex otrubae Podp.	Caot	6	8	7
	Cirsium arvense (L.) Scop	Ciar	8	6	7
	Dactylis glomerata L.	Dagl	7	5	7
	Festuca rubra L	Feru	8	5	6
	Galium palustre L.	Gapa	7	9	5
	Holcus lanatus L.	Hola	7	6	6
	Juncus effusus L.	Juef	7	7	4
	Mercurialis perennis L	Mepe	3	6	7
	Phragmites australis (Cav.) Trin. Ex Steud	Phau	7	10	7
	Reseda lutea L.	Relu	7	4	7
	Stellaria alsine Grimm	Stal	7	8	5
	Urtica dioica L.	Urdi	6	6	7
	Vaccinium myrtillus L.	Vamy	6	6	2

Appendix 7a: Plant taxa recorded from 48 quadrats in July 2011 at Caerlaverock Reserve with common names, density and frequency.

Family	Species Name	Common Name	Density (m^{-2})	Frequency %
Asteraceae	*Senecio jacobeae* L.	Common Ragwort	1.25	6.25
Asteraceae	*Cirsium arvense* (L.) Scop.	Creeping Thistle	2.81	8.33
Asteraceae	*Aster tripolium* L.	Sea Aster	1.17	6.25
Asteraceae	*Bellis perennis* L.	Daisy	1.52	12.5
Asteraceae	*Leontodon autumnalis* L.	Autumn Hawkbit	1.54	10.42
Asteraceae	*Tripleurospermum maritimum* (L.) W.D.J.Koch	Sea Mayweed	0.42	2.08
Apiacaea	*Oenanthe lachenallii* C.Gmelin.	Parsley Water-dropwort	0.38	8.33
Araliaceae	*Hedera helix* L.	Common Ivy	0.27	6.25
Apiaceae	*Heracleum sphondylium* L.	Hogweed	0.04	2.08
Brassicaceae	*Cardamine pratense* L.	Cuckooflower	0.04	2.08
Brassicaceae	*Capsella bursa-pastoris* (L.) Medik.	shepherds-purse	0.02	2.08
Brassicaceae	*Cochlearia officinalis* L.	Common Scurvygrass	0.13	2.08
Brassicaceae	*Cochlearia anglica* L.	English Scurvygrass	0.02	2.08
Boraginaceae	*Symphytum tuberosum* L.	Tuberous Comfrey	0.15	2.08
Caryophyllaceae	*Stellaria nemorum* L.	Wood Stitchwort	0.33	4.17
Caryophyllaceae	*Stellaria holostea* L.	Greater Stitchwort	0.79	8.33
Caryophyllaceae	*Silene dioica* (L.) Clairv.	Red Campion	0.06	2.08
Chenopodiaceae	*Atriplex hastata* L.	Hastate orach	0.75	8.33
Chenopodiaceae	*Salicornia europaea* L.	Common Glasswort	0.31	6.25
Cyperaceae	*Carex flacca* Schreb.	Glaucous Sedge	2.6	6.25
Cyperaceae	*Carex distans* L.	Distant Sedge	0.67	8.33
Cyperaceae	*Scirpus maritimus* L.	Sea Clubrush	1.52	4.17
Cyperaceae	*Carex nigra* (L.) Reichard.	Common Sedge	1.98	6.25
Cyperaceae	*Eleocharis uniglumis* (Link) Schult	Slender Spike-rush	1.7	4.17
Cyperaceae	*Carex disticha* Huds.	Brown Sedge	0.21	2.08
Dryopteridaceae	*Dryopteris filix-mas* (L.) Schott	Male-fern	0.17	6.25
Equisetaceae	*Equisetum arvense* L.	Field Horsetail	0.15	4.17

Appendix 7a

Family	Species Name	Common Name	Density (m^{-2})	Frequency %
Fabaceae	*Lathyrus pratensis* L.	Meadow Vetchling	1.2	8.3
Fabaceae	*Lotus corniculatus* L.	Common Bird's-foot-trefoil	2.37	12.5
Fabaceae	*Trifolium repens* L.	White Clover	11.27	31.25
Fabaceae	*Ulex europaeus* L.	Gorse	4.23	14.58
Geraniaceae	*Geranium robertianum* L.	Herb-Robert	0.3	2.08
Juncaceae	*Juncus gerardii* Loisel.	Saltmarsh Rush	15.19	22.92
Juncaceae	*Juncus bufonius* L.	Toad Rush	0.42	2.08
Juncaceae	*Juncus effusus* L.	Soft-rush	9.02	14.58
Juncaceae	*Juncus inflexus* L.	Hard Rush	3.63	10.42
Juncaginaceae	*Triglochin maritima* L.	Sea Arrowgrass	4.63	22.92
Onagraceae	*Epilobium angustifolium* L.	Alpine Willowherb	0.08	2.08
Plantoginaceae	*Plantago maritima* L.	Sea Plantain	2.02	8.33
Plumbaginaceae	*Armeria maritima* (Mill.) Willd.	Thrift	7.42	18.75
Polygonaceae	*Rumex acetosa* L.	Common Sorrel	0.19	2.08
Polygonaceae	*Polygonum persicaria* L.	Spotted ladysthumb , redshank	0.17	2.08
Poaceae	*Elymus pycnanthus* (Godr.) Barkworth	Sea Couch	3.33	4.17
Poaceae	*Holcus mollis* L.	Creeping Soft-grass	0.38	4.17
Poaceae	*Agrostis capillaris* L.	Common Bent	5.94	12.5
Poaceae	*Glyceria declinata* Breb.	Small Sweet-grass	1.02	4.17
Poaceae	*Elymus repens* (L.) Gould.	Common Couch	0.542	6.25
Poaceae	*Cynosurus cristatus* L.	Crested Dog's-tail	1.23	4.17
Poaceae	*Dactylis glomerata L.*	Cock's-foot	3.13	8.33
Poaceae	*Lolium perenne* L.	Perennial Rye-grass	6.65	14.58
Poaceae	*Anthoxanthum odoratum L.*	Sweet Vernal-grass	0.25	4.17
Poaceae	*Puccinellia maritima* (Hudson) Parl.	Common Saltmarsh-grass	12.31	16.67
Poaceae	*Phleum pratense* L.	Timothy	0.63	2.08

Appendix 7a

Family	Species Name	Common Name	Density (m^{-2})	Frequency %
Poaceae	*Agrostis stolonifera* L.	Creeping Bent	7.17	20.83
Poaceae	*Poa trivialis L.*	Rough Meadow-grass	4.125	10.42
Poa ceae	*Poa annua* L.	Annual Meadow-grass	0.1	2.08
Poaceae	*Holcus lanatus* L.	Yorkshire-fog	8.85	22.92
Poaceae	*Festuca rubra* L.	Red Fescue	27.77	39.58
Poaceae	*Alopecurus geniculatus* L.	Marsh Foxtail	0.17	2.08
Poaceae	*Spartina maritima* (Curtis) Fernald.	Small Cord-grass	2.08	2.08
Poaceae	*Poa subcaerulea* Smith.	Spreading Meadow-grass	2.21	8.33
Poaceae	*Festuca arundinacea* Schreb.	Tall Fescue	4.27	6.25
Primulaceae	*Glaux maritima* L.	Sea-milkwort	4.75	18.75
Ranunculaceae	*Ranunculus baudotii* Godr.	Brackish Water-crowfoot	0.35	2.08
Ranunculaceae	*Ranunculus acris* L	Meadow Buttercup	1.56	10.42
Ranunculaceae	*Ranunculus repens L.*	Creeping Buttercup	4.58	18.75
Rosaceae	*Potentilla anserina* L.	Silverweed	3.13	20.83
Rosaceae	*Rubus fruticosus* L.	Bramble	0.1	2.08
Rubiaceae	*Galium aparine L.*	Cleavers	0.92	12.5
Rubiaceae	*Galium palustre* L.	Common Marsh-bedstraw	0.31	2.08
Urticaceae	*Urtica dioica L.*	Common Nettle	4.33	18.75

Appendix 7b: Field data collected from 48 quadrats at Caerlaverock Reserve during July 2011. (T = Line transect; Q = Quadrat)

Species	Abb.	T1Q1	T1Q2	T1Q3	T1Q4	T1Q5	T1Q6	T1Q7	T1Q8
Agrostis capillaris	agr cap	0	0	40	0	0	0	0	0
Agrostis stolonifera	agr sto	0	100	0	0	0	0	100	0
Alopecurus geniculatus	alo gen	0	8	0	0	0	0	0	0
Anthoxanthum odoratum	ant odo	0	0	0	0	0	0	0	0
Armeria maritima	arm mar	0	0	0	0	0	0	5	2
Aster tripolium	ast tri	0	0	0	0	0	0	0	0
Atriplex hastata	atr has	0	0	0	0	0	0	0	0
Bellis perennis	bel per	0	0	0	0	10	20	0	0
Capsella bursa-pastoris	cap bur	0	0	0	0	0	0	0	0
Cardamine pratense	car pra	0	0	0	0	0	0	0	0
Carex distans	car dist	0	0	4	0	0	0	0	0
Carex disticha	car dis	0	10	0	0	0	0	0	0
Carex flacca	car flac	0	0	45	0	5	0	0	0
Carex nigra	car nig	0	0	0	33	0	0	0	0
Cirsium arvense	cir arv	44	0	0	0	0	55	0	0
Cochlearia anglica	coc ang	0	0	0	0	0	0	0	0
Cochlearia officinalis	coc off	0	0	0	0	0	0	0	0
Cynosurus cristatus	cyn cri	0	0	0	30	29	0	0	0
Dactylis glomerata	dac glo	0	0	0	0	0	0	0	0
Dryopteris filix-mas	dry fil	0	0	0	0	0	0	0	0
Eleocharis uniglumis	ele uni	0	0	0	0	0	0	0	0
Elymus pycnanthus	ely pyc	0	0	0	0	0	0	0	0
Elymus repens	ely rep	6	0	0	0	0	0	0	0
Epilobium angustifolium	epi ang	0	0	0	0	0	0	0	0
Equisetum arvense	equ arv	0	0	0	0	0	0	0	0
Festuca arundinacea	fes aru	0	0	0	50	0	100	0	0
Festuca rubra	fes rub	0	17	100	0	10	0	0	100
Galium aparine	gal apa	0	0	0	0	0	0	0	0
Galium palustre	gal pal	0	0	0	0	0	0	0	0
Geranium robertianum	ger rob	0	0	0	0	0	0	0	0
Glaux maritima	gla mar	0	12	19	0	0	0	19	0
Gyceria declinata	gyc dec	0	0	0	0	0	0	0	0
Hedera helix	hed hel	0	0	0	0	0	0	0	0
Heracleum sphondylium	her sph	0	0	0	0	0	0	0	0
Holcus lanatus	hol lan	0	0	0	25	5	0	0	0
Holcus mollis	hol mol	0	0	0	0	0	0	0	0
Juncus gerardi	jun ger	0	0	50	0	0	0	100	0
Juncus bufonius	jun buf	0	0	0	0	0	0	0	0
Juncus effusus	jun eff	0	0	0	0	0	0	0	0
Juncus inflexus	jun inf	0	0	0	0	0	0	0	0

Appendix 7b

Species	Abb.	T1Q1	T1Q2	T1Q3	T1Q4	T1Q5	T1Q6	T1Q7	T1Q8
Lathyrus pratensis	lat pra	0	0	0	0	0	20	0	0
Leontodon autumnalis	leo aut	0	0	0	0	0	0	0	0
Lolium perenne	lol per	0	0	0	0	0	0	0	0
Lotus corniculatus	lot cor	0	0	0	0	0	0	0	0
Oenanthe lachenallii	oen lac	0	0	0	5	0	0	0	0
Phleum pratense	phl pra	0	0	0	0	0	0	0	0
Plantago maritima	pla mar	0	0	0	0	0	0	31	0
Poa annua	poa ann	0	0	0	0	0	0	0	0
Poa subcaerulea	poa sub	0	0	0	0	0	0	0	0
Poa trivialis	poa tri	50	0	0	0	0	0	0	0
Polygonum persicaria	pol per	0	0	0	0	0	0	0	0
Potentilla anserina	pot ans	0	0	0	0	6	0	0	0
Puccinellia maritima	puc mar	0	0	0	0	0	0	0	0
Ranunculus acris	ran acr	0	0	0	0	10	0	0	0
Ranunculus baudotii	ran bau	0	17	0	0	0	0	0	0
Ranunculus repens	ran rep	50	0	0	0	0	0	0	0
Rubus fruticosus	rub fru	0	0	0	0	0	0	0	0
Rumex acetosa	rum ace	0	0	0	0	0	0	0	0
Salicornia europaeus	sal eur	0	0	0	0	0	0	0	0
Scirpus maritimus	sci mar	0	0	0	0	0	0	0	0
Senecio jacobea	sen jac	5	0	0	0	0	0	0	0
Silene dioica	sil dio	0	0	0	0	0	0	0	0
Spartina maritima	spa mar	0	0	0	0	0	0	0	0
Stellaria holostea	ste hol	0	0	0	0	0	0	0	0
Stellaria nemorum	ste nem	15	0	0	0	0	0	0	0
Symphytum tuberosum	sym tub	0	0	0	0	0	0	0	0
Trifolium repens	tri rep	0	13	34	35	40	0	0	0
Triglochin maritima	tri mar	0	16	4	0	0	0	11	80
Tripleurospermum maritimum	tri mar	0	0	0	0	0	0	0	0
Ulex europaeus	ule eur	71	0	0	0	0	0	0	0
Urtica dioica	urt dio	28	0	0	0	0	0	0	0

Appendix 7b

Species	Abb.	T2Q1	T2Q2	T2Q3	T2Q4	T2Q5	T3Q1	T3Q2	T3Q3
Agrostis capillaris	agr cap	0	50	25	50	20	0	0	0
Agrostis stolonifera	agr sto	0	0	0	0	0	0	0	0
Alopecurus geniculatus	alo gen	0	0	0	0	0	0	0	0
Anthoxanthum odoratum	ant odo	0	0	0	0	0	0	2	0
Armeria maritima	arm mar	0	0	0	0	0	0	0	0
Aster tripolium	ast tri	0	0	0	0	0	0	0	0
Atriplex hastata	atr has	7	0	0	0	0	0	0	0
Bellis perennis	bel per	0	0	0	0	0	0	24	12
Capsella bursa-pastoris	cap bur	0	0	0	0	0	0	0	0
Cardamine pratense	car pra	0	0	2	0	0	0	0	0
Carex distans	car dist	0	0	0	0	0	0	0	0
Carex disticha	car dis	0	0	0	0	0	0	0	0
Carex flacca	car flac	0	0	0	0	0	0	0	0
Carex nigra	car nig	0	2	0	0	0	0	0	0
Cirsium arvense	cir arv	0	0	15	0	0	0	0	0
Cochlearia anglica	coc ang	0	0	0	0	0	0	0	0
Cochlearia officinalis	coc off	0	0	0	0	0	0	0	0
Cynosurus cristatus	cyn cri	0	0	0	0	0	0	0	0
Dactylis glomerata	dac glo	0	0	0	0	0	40	1	0
Dryopteris filix-mas	dry fil	0	0	0	0	0	0	0	0
Eleocharis uniglumis	ele uni	0	0	0	30	0	0	0	0
Elymus pycnanthus	ely pyc	0	0	0	0	0	0	0	0
Elymus repens	ely rep	0	0	0	0	0	0	0	0
Epilobium angustifolium	epi ang	0	0	4	0	0	0	0	0
Equisetum arvense	equ arv	0	0	6	0	0	0	0	0
Festuca arundinacea	fes aru	55	0	0	0	0	0	0	0
Festuca rubra	fes rub	0	100	0	0	0	0	0	0
Galium aparine	gal apa	0	0	0	0	0	10	0	0
Galium palustre	gal pal	0	0	0	15	0	0	0	0
Geranium robertianum	ger rob	0	0	0	0	0	0	0	0
Glaux maritima	gla mar	19	0	0	0	0	0	0	0
Gyceria declinata	gyc dec	0	0	0	9	0	0	0	0
Hedera helix	hed hel	0	0	0	0	0	0	0	0
Heracleum sphondylium	her sph	0	0	0	0	0	0	0	0
Holcus lanatus	hol lan	0	0	0	0	12	0	3	100
Holcus mollis	hol mol	0	0	0	0	0	0	0	0
Juncus gerardi	jun ger	93	30	0	0	0	0	0	0
Juncus bufonius	jun buf	0	0	20	0	0	0	0	0
Juncus effusus	jun eff	0	0	100	100	0	0	0	0
Juncus inflexus	jun inf	0	0	0	10	0	0	0	0
Lathyrus pratensis	lat pra	0	0	0	0	0	0	0	0

Appendix 7b

Species	Abb.	T2Q1	T2Q2	T2Q3	T2Q4	T2Q5	T3Q1	T3Q2	T3Q3
Leontodon autumnalis	leo aut	0	8	0	0	0	0	0	0
Lolium perenne	lol per	0	0	0	0	0	0	100	16
Lotus corniculatus	lot cor	0	0	0	0	17	0	0	0
Oenanthe lachenallii	oen lac	0	0	0	0	0	0	0	0
Phleum pratense	phl pra	0	0	0	0	0	0	0	0
Plantago maritima	pla mar	0	0	0	0	0	0	0	0
Poa annua	poa ann	0	0	0	0	0	0	0	0
Poa subcaerulea	poa sub	0	0	0	0	0	0	0	0
Poa trivialis	poa tri	0	0	0	0	30	0	0	0
Polygonum persicaria	pol per	0	0	8	0	0	0	0	0
Potentilla anserina	pot ans	0	0	0	10	3	0	0	0
Puccinellia maritima	puc mar	0	0	0	0	0	0	0	0
Ranunculus acris	ran acr	0	0	0	0	20	0	21	0
Ranunculus baudotii	ran bau	0	0	0	0	0	0	0	0
Ranunculus repens	ran rep	0	0	16	0	0	15	0	8
Rubus fruticosus	rub fru	0	0	5	0	0	0	0	0
Rumex acetosa	rum ace	0	0	0	0	0	0	0	0
Salicornia europaeus	sal eur	0	0	0	0	0	0	0	0
Scirpus maritimus	sci mar	25	0	0	0	0	0	0	0
Senecio jacobea	sen jac	0	0	0	0	0	0	4	51
Silene dioica	sil dio	0	0	0	0	0	0	0	0
Spartina maritima	spa mar	0	0	0	0	0	0	0	0
Stellaria holostea	ste hol	0	0	0	0	2	0	0	0
Stellaria nemorum	ste nem	0	0	0	0	0	0	0	0
Symphytum tuberosum	sym tub	0	0	0	7	0	0	0	0
Trifolium repens	tri rep	0	100	0	0	0	0	2	0
Triglochin maritima	tri mar	0	25	0	0	0	0	0	0
Tripleurospermum maritimum	tri mar	0	0	0	0	0	0	0	0
Ulex europaeus	ule eur	0	0	26	13	51	0	0	0
Urtica dioica	urt dio	0	0	44	0	3	54	0	0

Appendix 7b

Species	Abb.	T3Q4	T3Q5	T3Q6	T3Q7	T4Q1	T4Q2	T4Q3	T4Q4
Agrostis capillaris	agr cap	0	0	0	0	100	0	0	0
Agrostis stolonifera	agr sto	0	0	20	0	0	12	0	10
Alopecurus geniculatus	alo gen	0	0	0	0	0	0	0	0
Anthoxanthum odoratum	ant odo	0	0	0	0	0	0	0	0
Armeria maritima	arm mar	0	0	0	0	0	0	0	0
Aster tripolium	ast tri	0	0	0	0	0	0	0	0
Atriplex hastata	atr has	0	0	0	0	0	0	0	0
Bellis perennis	bel per	0	0	0	0	0	0	3	0
Capsella bursa-pastoris	cap bur	0	0	0	0	0	0	0	1
Cardamine pratense	car pra	0	0	0	0	0	0	0	0
Carex distans	car dist	0	0	0	0	0	0	0	0
Carex disticha	car dis	0	0	0	0	0	0	0	0
Carex flacca	car flac	0	0	0	0	0	0	0	0
Carex nigra	car nig	0	0	0	0	0	0	0	0
Cirsium arvense	cir arv	0	0	0	0	0	0	0	0
Cochlearia anglica	coc ang	0	0	0	0	0	0	0	0
Cochlearia officinalis	coc off	0	0	0	0	0	0	0	0
Cynosurus cristatus	cyn cri	0	0	0	0	0	0	0	0
Dactylis glomerata	dac glo	0	9	0	0	0	0	0	0
Dryopteris filix-mas	dry fil	0	0	0	0	0	0	0	0
Eleocharis uniglumis	ele uni	0	0	0	0	0	0	0	0
Elymus pycnanthus	ely pyc	0	0	0	0	0	0	0	0
Elymus repens	ely rep	0	0	0	0	0	0	0	10
Epilobium angustifolium	epi ang	0	0	0	0	0	0	0	0
Equisetum arvense	equ arv	0	0	0	0	0	0	0	0
Festuca arundinacea	fes aru	0	0	0	0	0	0	0	0
Festuca rubra	fes rub	0	0	100	55	0	54	0	0
Galium aparine	gal apa	0	0	0	0	0	0	0	0
Galium palustre	gal pal	0	0	0	0	0	0	0	0
Geranium robertianum	ger rob	0	0	0	0	0	0	0	0
Glaux maritima	gla mar	0	0	18	0	0	0	0	0
Gyceria declinata	gyc dec	0	0	0	0	0	40	0	0
Hedera helix	hed hel	0	0	0	0	0	0	0	0
Heracleum sphondylium	her sph	0	0	0	0	0	0	0	0
Holcus lanatus	hol lan	35	5	0	0	90	0	0	0
Holcus mollis	hol mol	0	0	0	0	0	0	0	0
Juncus gerardi	jun ger	0	0	100	0	0	10	0	0
Juncus bufonius	jun buf	0	0	0	0	0	0	0	0
Juncus effusus	jun eff	100	70	0	0	10	0	0	0
Juncus inflexus	jun inf	20	0	0	0	40	0	0	0
Lathyrus pratensis	lat pra	8	0	0	0	0	0	0	0

Appendix 7b

Species	Abb.	T3Q4	T3Q5	T3Q6	T3Q7	T4Q1	T4Q2	T4Q3	T4Q4
Leontodon autumnalis	leo aut	0	0	0	0	0	0	0	0
Lolium perenne	lol per	40	0	0	0	0	0	50	100
Lotus corniculatus	lot cor	38	0	0	0	10	0	0	0
Oenanthe lachenallii	oen lac	0	0	0	0	0	0	0	0
Phleum pratense	phl pra	0	0	0	0	0	0	0	30
Plantago maritima	pla mar	0	0	20	0	0	0	0	0
Poa annua	poa ann	0	0	0	0	0	0	0	5
Poa subcaerulea	poa sub	0	0	0	0	0	0	0	0
Poa trivialis	poa tri	0	0	5	0	0	0	0	0
Polygonum persicaria	pol per	0	0	0	0	0	0	0	0
Potentilla anserina	pot ans	0	0	0	0	8	38	0	0
Puccinellia maritima	puc mar	0	0	20	60	0	0	0	0
Ranunculus acris	ran acr	0	0	0	0	0	0	0	0
Ranunculus baudotii	ran bau	0	0	0	0	0	0	0	0
Ranunculus repens	ran rep	3	3	0	0	0	0	100	0
Rubus fruticosus	rub fru	0	0	0	0	0	0	0	0
Rumex acetosa	rum ace	0	9	0	0	0	0	0	0
Salicornia europaeus	sal eur	0	0	0	0	0	0	0	0
Scirpus maritimus	sci mar	0	0	0	0	0	48	0	0
Senecio jacobea	sen jac	0	0	0	0	0	0	0	0
Silene dioica	sil dio	0	0	0	0	0	0	0	0
Spartina maritima	spa mar	0	0	0	0	0	0	0	0
Stellaria holostea	ste hol	0	0	0	0	0	0	0	1
Stellaria nemorum	ste nem	0	1	0	0	0	0	0	0
Symphytum tuberosum	sym tub	0	0	0	0	0	0	0	0
Trifolium repens	tri rep	0	0	30	0	0	0	100	29
Triglochin maritima	tri mar	0	0	10	0	0	0	0	0
Tripleurospermum maritimum	tri mar	0	0	0	0	0	0	0	20
Ulex europaeus	ule eur	0	21	0	0	0	0	0	0
Urtica dioica	urt dio	0	0	0	0	0	0	0	0

Appendix 7b

Species	Abb.	T5Q1	T5Q2	T5Q3	T5Q4	T5Q5	T5Q6	T5Q7	T5Q8
Agrostis capillaris	agr cap	0	0	0	0	0	0	0	0
Agrostis stolonifera	agr sto	0	0	0	0	5	0	20	27
Alopecurus geniculatus	alo gen	0	0	0	0	0	0	0	0
Anthoxanthum odoratum	ant odo	0	0	0	0	0	0	0	0
Armeria maritima	arm mar	0	33	1	100	0	0	0	0
Aster tripolium	ast tri	0	9	43	0	0	0	0	0
Atriplex hastata	atr has	0	0	0	0	9	8	0	0
Bellis perennis	bel per	0	0	0	0	0	0	0	0
Capsella bursa-pastoris	cap bur	0	0	0	0	0	0	0	0
Cardamine pratense	car pra	0	0	0	0	0	0	0	0
Carex distans	car dist	0	0	0	0	0	0	0	0
Carex disticha	car dis	0	0	0	0	0	0	0	0
Carex flacca	car flac	0	0	0	0	0	0	75	0
Carex nigra	car nig	0	0	0	0	0	0	0	0
Cirsium arvense	cir arv	0	0	0	0	0	0	0	0
Cochlearia anglica	coc ang	0	0	0	0	0	0	0	0
Cochlearia officinalis	coc off	0	0	6	0	0	0	0	0
Cynosurus cristatus	cyn cri	0	0	0	0	0	0	0	0
Dactylis glomerata	dac glo	0	0	0	0	0	0	0	0
Dryopteris filix-mas	dry fil	0	0	0	0	0	0	0	0
Eleocharis uniglumis	ele uni	0	0	0	0	0	0	0	50
Elymus pycnanthus	ely pyc	0	0	0	0	0	0	0	0
Elymus repens	ely rep	0	0	0	0	0	0	0	0
Epilobium angustifolium	epi ang	0	0	0	0	0	0	0	0
Equisetum arvense	equ arv	0	0	0	0	0	0	0	0
Festuca arundinacea	fes aru	0	0	0	0	0	0	0	0
Festuca rubra	fes rub	0	0	0	100	50	45	100	48
Galium aparine	gal apa	0	0	0	0	0	0	0	0
Galium palustre	gal pal	0	0	0	0	0	0	0	0
Geranium robertianum	ger rob	0	0	0	0	0	0	0	0
Glaux maritima	gla mar	0	0	0	100	0	0	0	1
Gyceria declinata	gyc dec	0	0	0	0	0	0	0	0
Hedera helix	hed hel	0	0	0	0	0	0	0	0
Heracleum sphondylium	her sph	0	0	0	0	0	0	0	0
Holcus lanatus	hol lan	0	0	0	0	0	0	0	0
Holcus mollis	hol mol	0	0	0	0	0	0	0	0
Juncus gerardi	jun ger	0	0	0	0	100	0	100	21
Juncus bufonius	jun buf	0	0	0	0	0	0	0	0
Juncus effusus	jun eff	0	0	0	0	0	0	0	0
Juncus inflexus	jun inf	0	0	0	0	0	0	0	0

Appendix 7b

Species	Abb.	T5Q1	T5Q2	T5Q3	T5Q4	T5Q5	T5Q6	T5Q7	T5Q8
Lathyrus pratensis	lat pra	0	0	0	0	0	0	0	0
Leontodon autumnalis	leo aut	0	0	0	0	4	0	2	0
Lolium perenne	lol per	0	0	0	0	0	0	0	0
Lotus corniculatus	lot cor	0	0	0	0	0	10	0	0
Oenanthe lachenallii	oen lac	0	0	0	0	0	0	2	0
Phleum pratense	phl pra	0	0	0	0	0	0	0	0
Plantago maritima	pla mar	0	25	0	0	0	0	0	0
Poa annua	poa ann	0	0	0	0	0	0	0	0
Poa subcaerulea	poa sub	0	0	0	0	0	0	0	0
Poa trivialis	poa tri	0	0	0	0	0	0	0	0
Polygonum persicaria	pol per	0	0	0	0	0	0	0	0
Potentilla anserina	pot ans	0	0	0	0	0	0	55	4
Puccinellia maritima	puc mar	57	100	100	0	0	0	0	0
Ranunculus acris	ran acr	0	0	0	0	0	0	0	0
Ranunculus baudotii	ran bau	0	0	0	0	0	0	0	0
Ranunculus repens	ran rep	0	0	0	0	0	0	0	0
Rubus fruticosus	rub fru	0	0	0	0	0	0	0	0
Rumex acetosa	rum ace	0	0	0	0	0	0	0	0
Salicornia europaeus	sal eur	3	0	4	0	0	0	0	0
Scirpus maritimus	sci mar	0	0	0	0	0	0	0	0
Senecio jacobea	sen jac	0	0	0	0	0	0	0	0
Silene dioica	sil dio	0	0	0	0	0	0	0	0
Spartina maritima	spa mar	0	0	0	0	0	100	0	0
Stellaria holostea	ste hol	0	0	0	0	0	0	0	0
Stellaria nemorum	ste nem	0	0	0	0	0	0	0	0
Symphytum tuberosum	sym tub	0	0	0	0	0	0	0	0
Trifolium repens	tri rep	0	0	0	0	3	0	6	10
Triglochin maritima	tri mar	0	0	0	37	10	0	4	0
Tripleurospermum maritimum	tri mar	0	0	0	0	0	0	0	0
Ulex europaeus	ule eur	0	0	0	0	0	0	0	0
Urtica dioica	urt dio	0	0	0	0	0	0	0	0

Appendix 7b

Species	Abb.	T5Q9	T6Q1	T6Q2	T6Q3	T6Q4	T6Q5	T6Q6	T6Q7
Agrostis capillaris	agr cap	0	0	0	0	0	0	0	0
Agrostis stolonifera	agr sto	0	0	0	0	0	0	0	0
Alopecurus geniculatus	alo gen	0	0	0	0	0	0	0	0
Anthoxanthum odoratum	ant odo	0	0	0	0	0	0	0	0
Armeria maritima	arm mar	2	0	23	90	100	0	0	0
Aster tripolium	ast tri	0	0	0	4	0	0	0	0
Atriplex hastata	atr has	0	0	0	0	0	0	12	0
Bellis perennis	bel per	0	0	0	0	0	0	0	0
Capsella bursa-pastoris	cap bur	0	0	0	0	0	0	0	0
Cardamine pratense	car pra	0	0	0	0	0	0	0	0
Carex distans	car dist	0	0	0	0	0	8	10	0
Carex disticha	car dis	0	0	0	0	0	0	0	0
Carex flacca	car flac	0	0	0	0	0	0	0	0
Carex nigra	car nig	0	0	0	0	0	0	0	0
Cirsium arvense	cir arv	0	0	0	0	0	0	0	0
Cochlearia anglica	coc ang	0	0	0	0	0	1	0	0
Cochlearia officinalis	coc off	0	0	0	0	0	0	0	0
Cynosurus cristatus	cyn cri	0	0	0	0	0	0	0	0
Dactylis glomerata	dac glo	100	0	0	0	0	0	0	0
Dryopteris filix-mas	dry fil	0	0	0	0	0	0	0	0
Eleocharis uniglumis	ele uni	0	0	0	0	0	0	0	0
Elymus pycnanthus	ely pyc	0	0	0	0	0	0	0	100
Elymus repens	ely rep	10	0	0	0	0	0	0	0
Epilobium angustifolium	epi ang	0	0	0	0	0	0	0	0
Equisetum arvense	equ arv	0	0	0	0	0	0	0	0
Festuca arundinacea	fes aru	0	0	0	0	0	0	0	0
Festuca rubra	fes rub	0	0	14	0	100	40	100	100
Galium aparine	gal apa	0	0	0	0	0	0	0	0
Galium palustre	gal pal	0	0	0	0	0	0	0	0
Geranium robertianum	ger rob	0	0	0	0	0	0	0	0
Glaux maritima	gla mar	0	0	0	27	13	0	0	0
Gyceria declinata	gyc dec	0	0	0	0	0	0	0	0
Hedera helix	hed hel	0	0	0	0	0	0	0	0
Heracleum sphondylium	her sph	0	0	0	0	0	0	0	0
Holcus lanatus	hol lan	20	0	0	0	0	0	0	0
Holcus mollis	hol mol	0	0	0	0	0	0	0	0
Juncus gerardi	jun ger	0	0	0	0	0	100	0	0
Juncus bufonius	jun buf	0	0	0	0	0	0	0	0
Juncus effusus	jun eff	8	0	0	0	0	0	0	0
Juncus inflexus	jun inf	0	0	0	0	0	0	0	0

Appendix 7b

Species	Abb.	T5Q9	T6Q1	T6Q2	T6Q3	T6Q4	T6Q5	T6Q6	T6Q7
Lathyrus pratensis	lat pra	0	0	0	0	0	0	0	0
Leontodon autumnalis	leo aut	5	0	0	0	0	0	0	0
Lolium perenne	lol per	10	0	0	0	0	0	0	0
Lotus corniculatus	lot cor	0	0	0	0	0	0	27	0
Oenanthe lachenallii	oen lac	0	0	0	0	0	0	0	6
Phleum pratense	phl pra	0	0	0	0	0	0	0	0
Plantago maritima	pla mar	0	0	21	0	0	0	0	0
Poa annua	poa ann	0	0	0	0	0	0	0	0
Poa subcaerulea	poa sub	0	0	0	0	50	0	10	0
Poa trivialis	poa tri	0	0	0	0	0	0	0	0
Polygonum persicaria	pol per	0	0	0	0	0	0	0	0
Potentilla anserina	pot ans	4	0	0	0	0	0	0	12
Puccinellia maritima	puc mar	0	54	100	100	0	0	0	0
Ranunculus acris	ran acr	0	0	0	0	0	0	0	0
Ranunculus baudotii	ran bau	0	0	0	0	0	0	0	0
Ranunculus repens	ran rep	0	0	0	0	0	0	0	0
Rubus fruticosus	rub fru	0	0	0	0	0	0	0	0
Rumex acetosa	rum ace	0	0	0	0	0	0	0	0
Salicornia europaeus	sal eur	0	8	0	0	0	0	0	0
Scirpus maritimus	sci mar	0	0	0	0	0	0	0	0
Senecio jacobea	sen jac	0	0	0	0	0	0	0	0
Silene dioica	sil dio	0	0	0	0	0	0	0	0
Spartina maritima	spa mar	0	0	0	0	0	0	0	0
Stellaria holostea	ste hol	0	0	0	0	0	0	0	0
Stellaria nemorum	ste nem	0	0	0	0	0	0	0	0
Symphytum tuberosum	sym tub	0	0	0	0	0	0	0	0
Trifolium repens	tri rep	9	0	0	0	100	0	0	0
Triglochin maritima	tri mar	0	0	0	0	15	10	0	0
Tripleurospermum maritimum	tri mar	0	0	0	0	0	0	0	0
Ulex europaeus	ule eur	13	0	0	0	0	0	0	0
Urtica dioica	urt dio	0	0	0	0	0	0	0	0

Appendix 7b

Species	Abb.	T6Q8	T6Q9	T6Q10	T7Q1	T7Q2	T7Q3	T7Q4	T7Q5
Agrostis capillaris	agr cap	0	0	0	0	0	0	0	0
Agrostis stolonifera	agr sto	10	0	40	0	0	0	0	0
Alopecurus geniculatus	alo gen	0	0	0	0	0	0	0	0
Anthoxanthum odoratum	ant odo	0	10	0	0	0	0	0	0
Armeria maritima	arm mar	0	0	0	0	0	0	0	0
Aster tripolium	ast tri	0	0	0	0	0	0	0	0
Atriplex hastata	atr has	0	0	0	0	0	0	0	0
Bellis perennis	bel per	0	0	0	0	0	0	0	4
Capsella bursa-pastoris	cap bur	0	0	0	0	0	0	0	0
Cardamine pratense	car pra	0	0	0	0	0	0	0	0
Carex distans	car dist	10	0	0	0	0	0	0	0
Carex disticha	car dis	0	0	0	0	0	0	0	0
Carex flacca	car flac	0	0	0	0	0	0	0	0
Carex nigra	car nig	60	0	0	0	0	0	0	0
Cirsium arvense	cir arv	0	0	21	0	0	0	0	0
Cochlearia anglica	coc ang	0	0	0	0	0	0	0	0
Cochlearia officinalis	coc off	0	0	0	0	0	0	0	0
Cynosurus cristatus	cyn cri	0	0	0	0	0	0	0	0
Dactylis glomerata	dac glo	0	0	0	0	0	0	0	0
Dryopteris filix-mas	dry fil	0	0	0	0	0	3	4	1
Eleocharis uniglumis	ele uni	0	0	0	0	0	0	0	0
Elymus pycnanthus	ely pyc	0	0	0	0	0	60	0	0
Elymus repens	ely rep	0	0	0	0	0	0	0	0
Epilobium angustifolium	epi ang	0	0	0	0	0	0	0	0
Equisetum arvense	equ arv	0	0	0	1	0	0	0	0
Festuca arundinacea	fes aru	0	0	0	0	0	0	0	0
Festuca rubra	fes rub	100	0	0	0	0	0	0	0
Galium aparine	gal apa	0	0	3	4	15	5	7	0
Galium palustre	gal pal	0	0	0	0	0	0	0	0
Geranium robertianum	ger rob	0	0	0	0	0	0	0	14
Glaux maritima	gla mar	0	0	0	0	0	0	0	0
Gyceria declinata	gyc dec	0	0	0	0	0	0	0	0
Hedera helix	hed hel	0	0	0	0	0	2	4	7
Heracleum sphondylium	her sph	0	0	0	0	0	0	2	0
Holcus lanatus	hol lan	0	100	30	0	0	0	0	0
Holcus mollis	hol mol	0	0	0	10	8	0	0	0
Juncus gerardi	jun ger	25	0	0	0	0	0	0	0
Juncus bufonius	jun buf	0	0	0	0	0	0	0	0
Juncus effusus	jun eff	0	0	45	0	0	0	0	0
Juncus inflexus	jun inf	0	100	4	0	0	0	0	0

Appendix 7b

Species	Abb.	T6Q8	T6Q9	T6Q10	T7Q1	T7Q2	T7Q3	T7Q4	T7Q5
Lathyrus pratensis	lat pra	0	30	0	0	0	0	0	0
Leontodon autumnalis	leo aut	55	0	0	0	0	0	0	0
Lolium perenne	lol per	0	0	3	0	0	0	0	0
Lotus corniculatus	lot cor	0	12	0	0	0	0	0	0
Oenanthe lachenallii	oen lac	5	0	0	0	0	0	0	0
Phleum pratense	phl pra	0	0	0	0	0	0	0	0
Plantago maritima	pla mar	0	0	0	0	0	0	0	0
Poa annua	poa ann	0	0	0	0	0	0	0	0
Poa subcaerulea	poa sub	16	0	0	0	0	0	30	0
Poa trivialis	poa tri	0	0	0	60	53	0	0	0
Polygonum persicaria	pol per	0	0	0	0	0	0	0	0
Potentilla anserina	pot ans	10	0	0	0	0	0	0	0
Puccinellia maritima	puc mar	0	0	0	0	0	0	0	0
Ranunculus acris	ran acr	0	0	0	0	17	0	0	7
Ranunculus baudotii	ran bau	0	0	0	0	0	0	0	0
Ranunculus repens	ran rep	0	20	5	0	0	0	0	0
Rubus fruticosus	rub fru	0	0	0	0	0	0	0	0
Rumex acetosa	rum ace	0	0	0	0	0	0	0	0
Salicornia europaeus	sal eur	0	0	0	0	0	0	0	0
Scirpus maritimus	sci mar	0	0	0	0	0	0	0	0
Senecio jacobea	sen jac	0	0	0	0	0	0	0	0
Silene dioica	sil dio	0	0	0	0	0	0	0	3
Spartina maritima	spa mar	0	0	0	0	0	0	0	0
Stellaria holostea	ste hol	0	15	20	0	0	0	0	0
Stellaria nemorum	ste nem	0	0	0	0	0	0	0	0
Symphytum tuberosum	sym tub	0	0	0	0	0	0	0	0
Trifolium repens	tri rep	30	0	0	0	0	0	0	0
Triglochin maritima	tri mar	0	0	0	0	0	0	0	0
Tripleurospermum maritimum	tri mar	0	0	0	0	0	0	0	0
Ulex europaeus	ule eur	0	0	8	0	0	0	0	0
Urtica dioica	urt dio	0	0	0	10	8	13	43	5

Appendix 7c: Environmental variables recorded from sample quadrats in Caerlaverock.

Line transect & Quadrat number	Soil pH	Conductivity soil (μS/cm)	% Shade	Water depth (m)	Vegetation layer (m)			
					Herb	Tall herb	Shrub	Tree
T1Q1	5.4	127	none	none	0.077	0.873	0.883	none
T1Q2	7.39	2704	none	none	0.62	none	none	none
T1Q3	6.41	863	none	none	0.223	none	none	none
T1Q4	7.77	435	none	none	0.16	none	none	none
T1Q5	5.37	247	none	none	0.21	none	none	none
T1Q6	6.78	282	none	none	none	0.93	none	none
T1Q7	7.13	1550	none	none	0.31	none	none	none
T1Q8	7.19	3310	none	none	0.13	none	none	none
T2Q1	7.3	4230	none	0.17	0.5	none	none	none
T2Q2	7.00	4160	none	none	0.09	none	none	none
T2Q3	6.02	675	56.29	none	0.08	0.75	1.02	none
T2Q4	6.06	3432	50	none	0.21	1.02	none	none
T2Q5	6.39	1716	46.60	none	0.04	0.23	0.68	none
T3Q1	6.09	435	17.86	none	0.4	0.68	none	none
T3Q2	6.2	130	none	none	0.04	none	none	none
T3Q3	6.2	117	none	none	0.12	0.49	none	none
T3Q4	5.51	93	none	none	0.04	0.45	none	none
T3Q5	5.76	344	40.91	none	0.13	0.68	0.53	none
T3Q6	7.69	551	none	none	0.15	none	none	none
T3Q7	7.92	263	none	none	0.06	none	none	none
T4Q1	5.48	173	none	none	0.53	none	none	none
T4Q2	7.2	1140	none	0.29	0.22	none	none	none
T4Q3	5.45	96	none	none	0.06	none	none	none
T4Q4	6.17	118	none	none	0.17	none	none	none

Appendix 7c

Line transect & Quadrat number	Soil pH	Conductivity soil (µS/cm)	% Shade	Water depth (m)	Vegetation layer (m)			
					Herb	Tall herb	Shrub	Tree
T5Q1	6.97	12950	none	none	0.02	none	none	none
T5Q2	7.33	4650	none	none	0.12	none	none	none
T5Q3	7.21	5570	none	none	0.02	none	none	none
T5Q4	6.8	118	none	none	0.13	none	none	none
T5Q5	7.51	2433	none	0.12	none	0.42	none	none
T5Q6	7.45	1483	none	none	0.17	0.6	none	none
T5Q7	6.08	1037	none	none	0.13	none	none	none
T5Q8	6.22	1078	none	0.08	0.12	none	none	none
T5Q9	5.33	139	10.6	none	0.15	none	0.58	none
T6Q1	7.1	8520	none	none	0.05	none	none	none
T6Q2	6.98	4580	none	0.05	0.12	none	none	none
T6Q3	7.15	4330	none	none	0.08	none	none	none
T6Q4	7.37	2033	none	none	0.16	none	none	none
T6Q5	6.94	2460	none	none	0.21	none	none	none
T6Q6	7.24	1421	none	none	none	0.42	none	none
T6Q7	7.07	732	none	none	none	0.55	none	none
T6Q8	7.15	1393	none	none	0.14	none	none	none
T6Q9	5.53	651	none	none	none	0.47	none	none
T6Q10	6.4	190	28.32	none	0.07	0.67	0.77	none
T7Q1	5.65	113	29.88	none	0.16	0.65	none	5
T7Q2	6.37	165	19.70	none	0.26	1.4	none	7
T7Q3	6.5	112	5.88	none	0.19	1.18	none	4
T7Q4	6.05	222	17.04	none	0.16	1.1	none	4
T7Q5	5.57	242	7.6	none	none	0.92	none	8

Appendix 8: TWINSPAN Analysis depicting final Table from 48 quadrats in Caerlaverock Reserve

Plant species in first column), entries in the table are the pseudospecies levels not quantitative values, the right and bottom sides define the dendrogram of the classification of species and samples, respectively.

```
                TTTTTTTTTTTTTTTTTTTTTTTTTTTTTTTTTTTTTTTTTTTTTTTTTTTTTTTTT
                77737712223534663441113564566112555661133256655 6
                QQQQQQQQQQQQQQQQQQQQQQQQQQQQQQQQQQQQQQQQQQQQQQQQQQQQQQQQQ
                51213413545941913344562662778382458452767122313 1
                ..............0..............................
                ..............................................
                ..............................................
                ..............................................



                444144 111131244122   1332344  122333  12 233223
                84546711328371236344565092101380892782790965657 4

 22 fest  aru  ------------------5-5------------------5------  0000
 27 ranu  acr  3-4-----5----------4-5-----------------------  000100
  8 sene  jac  ------3---------5-----2-----------------------  000101
 23 cyno  cri  ------------------55--------------------------  000101
 29 bell  per  2---------------42--455---------------------- -  000101
 30 lath  pra  -------------5------4-------------------------  000101
 31 lath  pal  ------------3--------4-------------------------  000101
 53 loli  per  -----------45--2455---5-----------------------  000101
 57 phle  pra  ------------------5--------------------------  000101
 58 trip  mar  ------------------5--------------------------  000101
 59 caps  bur  -----------------1---------------------------  000101
 60 poa  annu  -----------------3---------------------------  000101
  2 cirs  arv  ------54-------5-----5-------------------------  000110
  4 elym  rep  ------3----4------4---------------------------  000110
 24 holc  lan  --------4-3555555--53-2-----------------------  000110
 41 junc  eff  -------5-55354-5-----------------------------  000110
 44 gali  pal  ---------4-----------------------------------  000110
 46 junc  inf  ---------4--5552-----------------------------  000110
 47 symp  tub  ---------3-----------------------------------  000110
 50 stel  hol  --------2-----45--1---------------------------  000110
 54 anth  odo  --------------4-------2-----------------------  000110
 55 rume  ace  ----------3-----------------------------------  000110
  1 ulex  eur  ------555454---3-------------------------------  000111
  6 ranu  rep  ---4--54--2-2-5335-----------------------------  000111
  7 stel  nem  ------4---1-------------------------------------  000111
 37 junc  buf  -------5-------------------------------------  000111
 38 card  pra  -------2-------------------------------------  000111
 39 equi  arv  -1-----3-------------------------------------  000111
 40 rubu  fru  -------3-------------------------------------  000111
 42 poly  per  -------3-------------------------------------  000111
 43 epil  ang  -------2-------------------------------------  000111
 49 lotu  sub  --------4-------------------------------------  000111
 51 dact  glo  ---5------35----------1-----------------------  000111
 17 agro  cap  -------555---5---------------5-5--------------  001
 21 lotu  cor  ------------544--------45----------------------  001
 45 eleo  uni  ---------5-----------------------5-------------  001
  5 poa  triv  -55---5-5-------------------------------3-------  0100
  3 urti  dio  343545552---------------------------------------  01010
 52 gali  apa  -24433---------2-------------------------------  010110
 68 holc  mol  -43-------------------------------------------  010110
 69 dryo  fil  1---22----------------------------------------  010111
```

Appendix 8

```
70 hede  hel  3---22-----------------------------------------  010111
71 hera  sph  -----2-----------------------------------------  010111
72 gera  rob  4-----------------------------------------------  010111
73 sile  dio  2-----------------------------------------------  010111
67 elym  pyc  ----5----------------------5-------------------  011
16 trif  rep  -----------3-----5555-2---3-55-5-245-4-5--------  100
25 care  nig  --------------------5--------5--2---------------  100
28 pote  ans  --------24-2-3------3----5544-----2-------------  100
48 gyce  dec  ---------3---------------5----------------------  100
20 care  fla  --------------------3-----5--5------------------  101
26 oena  lac  --------------------3------233------------------  101
10 agro  sto  ---------------5--4------45-4----35--555--------  1100
36 leon  aut  -----------3--------------2-5--3-2--------------  1100
65 poa  subc  -----5------------------4---4------5------------  1100
18 care  din  ------------------------4---42------3-----------  110100
35 atri  has  ------------------------34--------3-------3------  110100
64 spar  mar  ------------------------5------------------------  110100
11 fest  rub  --------------------4--555555555555554-55--4----  110101
19 junc  ger  -------------------------45-55-5-55-5-55-5------  110101
34 scir  mar  -------------------------5---------------5------  110101
 9 ranu  bau  ------------------------------------4----------  110110
12 trig  mar  -------------------------2--25554-44444--------  110110
13 alop  gen  ------------------------------------3----------  110110
14 care  dis  ------------------------------------4----------  110110
66 coch  ang  -----------------------------------1-----------  110110
15 glau  mar  ----------------------------4--5-14-444-4--5---  110111
32 plan  mar  ---------------------------------------55--55----  1110
33 arme  mar  -----------2------------------2-5--5--3---555-1-  1110
56 pucc  mar  ---------------------------------------55-555555  1111
61 sali  eur  ------------------------------------------------223  1111
62 aste  tri  ---------------------------------------3-2-5-  1111
63 coch  off  ------------------------------------------------3-  1111

              00000000000000000000001111111111111111111111111
              00000011111111111111111000000000000000000000111111
              01111100000000001111111001111111111111111111000111
               0011100011111110001111  00001111111111111
                       0001111            0000000000001
                                          000000001111
```

Appendix 9: TWINSPAN groups in Caerlaverock Reseve with Ellenberg's indicator values for light --L; Moisture -- F; and Salt – S, (Source: Hill et al., 1999).

Group	Species	Abbreviation name	L	F	S
1	*Bellis perennis* L.	bell pere	8	5	0
	Dactylis glomerata L.	dact glom	7	5	0
	Dryopteris filix-mas (L.) Schott	dryo fili	5	6	0
	Elymus pycnanthus (Godr.) Barkworth	elym pycn			
	Equisetum arvense L.	equi arve	7	6	0
	Galium aparine L.	gali apar	6	6	0
	Hedera helix L.	hede heli	4	5	0
	Heracleum sphondylium L.	hera spho	7	5	0
	Holcus mollis L.	holc moll	6	6	0
	Poa subcaerulea Smith.	poa subc	7	5	0
	Poa trivialis L.	poa triv	7	6	0
	Ranunculus acris L	ranu acri	7	6	0
	Ranunculus repens L.	ranu repe	6	7	0
	Geranium robertianum L	gera robe	5	6	0
	Silene dioica (L.) Clairv.	sile dioi	5	6	0
	Urtica dioica L.	urti dioi	6	6	0
2	*Agrostis capillaris* L.	agro capi	6	5	0
	Armeria maritima (Mill.) Willd.	arme mari	8	7	3
	Cardamine pratense L.	card prat	7	8	0
	Eleocharis uniglumis (Link) Schult.	eleo unig	8	9	3
	Epilobium angustifolium L.	epil angu	6	5	0
	Equisetum arvense L.	equi arve	7	6	0
	Galium aparine L.	gali apar	6	6	0
	Galium palustre L.	gali palu	7	9	0
	Gyceria declinata Breb.	gyce decl	7	8	0
	Juncus bufonius L.	junc bufo	7	7	1
	Juncus effusus L.	junc effu	7	7	0
	Juncus inflexus L.	junc infl	7	7	1
	Leontodon autumnalis L.	leon autu	8	6	1
	Lotus corniculatus L.	lotu corn	7	4	1
	Lotus subbiflorus Lag.	lotu subb	7	5	0
	Polygonum persicaria L.	poly peri	7	8	0
	Rubus fruticosus L.	rubu frut	6	6	0
	Rumex acetosa L.	rume acet	7	5	0
	Stellaria nemorum L.	stel nemo	4	6	0
	Symphytum tuberosum L.	symp tube	6	6	0
	Ulex europaeus L.	ulex euro	7	5	0
	Urtica dioica L.	urti dioi	6	6	0

Appendix 9:

Group	Species	Abbreviation name	L	F	S
3	*Agrostis stolonifera* L.	agro stol	7	6	1
	Anthoxanthum odoratum L.	anth odor	7	6	0
	Bellis perennis L.	bell pere	8	5	0
	Capsella bursa-pastoris (L.) Medik.	caps bura	7	5	0
	Carex flacca Schreb.	care flacc	7	5	0
	Carex nigra (L.) Reichard.	care nigr	7	8	0
	Cirsium arvense (L.) Scop.	cirs arve	8	6	0
	Cynosurus cristatus L.	cyno cris	7	5	0
	Dactylis glomerata L.	dact glom	7	5	0
	Elymus repens (L.) Gould.	elym repe	7	5	2
	Festuca arundinacea Schreb.	fest arun	8	6	1
	Festuca rubra L.	fest rubr	8	5	2
	Holcus lanatus L.	holc lana	7	6	0
	Lathyrus palustris L.	lath palu	7	9	0
	Lathyrus pratensis L.	lath prat	7	6	0
	Lolium perenne L.	loli pere	8	5	0
	Oenanthe lachenallii C.Gmelin.	oena lach	8	8	3
	Phleum pretense L.	phle prat	8	5	0
	Poa annua L.	poa annu	7	5	1
	Potentilla anserina L.	pote anse	8	7	2
	Ranunculus acris L	ranu acri	7	6	0
	Ranunculus repens L.	ranu repe	6	7	0
	Senecio jacobeae L.	sene jaco	7	4	0
	Stellaria holostea L.	stel holo	5	5	0
	Trifolium repens L.	trif repe	7	5	0
4	*Agrostis capillaris* L.	agro capi	6	5	0
	Agrostis stolonifera L.	agro stol	7	6	1
	Alopecurus geniculatus L.	alop geni	8	7	1
	Armeria maritima (Mill.) Willd.	arme mari	8	7	3
	Atriplex hastata L.	atri hast	8	7	2
	Carex distans L.	care distn	8	6	3
	Carex disticha Huds.	care dist	7	8	0
	Carex flacca Schreb.	care flacc	7	5	0
	Carex nigra (L.) Reichard.	care nigr	7	8	0
	Cochlearia anglica L.	coch angl	8	8	6
	Eleocharis uniglumis (Link) Schult.	eleo unig	8	9	3
	Elymus pycnanthus (Godr.) Barkworth	elym pycn			
	Festuca rubra L.	fest rubr	8	5	2
	Glaux maritima L.	glau mari	8	7	4
	Gyceria declinata Breb.	gyce decl	7	8	0
	Juncus gerardi Loisel.	junc gera	8	7	3

Appendix 9:

Group	Species	Abbreviation name	L	F	S
4	*Leontodon autumnalis* L.	leon autu	8	6	1
	Lotus corniculatus L.	lotu corn	7	4	1
	Oenanthe lachenallii C.Gmelin.	oena lach	8	8	3
	Plantago maritima L.	plan mari	8	7	3
	Poa subcaerulea Smith.	poa subc	7	5	0
	Poa trivialis L.	poa triv	7	6	0
	Potentilla anserina L.	pote anse	8	7	2
	Puccinellia maritima (Hudson) Parl.	pucc mari	9	8	5
	Ranunculus baudotii Godr.	ranu baud	7	11	4
	Scirpus maritimus L.	scir mari	8	10	4
	Spartina maritima (Curtis) Fernald.	spar mari	9	9	6
	Trifolium repens L.	trif repe	7	5	0
	Tripleurospermum maritimum (L.) W.D.J.Koch	trip mari	8	5	1
5	*Armeria maritima* (Mill.) Willd.	arme mari	8	7	3
	Aster tripolium L.	aste trip	9	8	5
	Cochlearia officinalis L.	coch offi	8	6	3
	Festuca rubra L.	fest rubr	8	5	2
	Glaux maritima L.	glau mari	8	7	4
	Plantago maritima L.	plan mari	8	7	3
	Puccinellia maritima (Hudson) Parl.	pucc mari	9	8	5
	Salicornia europaea L.	sali euro	9	8	9

Appendix 10: Shows results from digitized polygons A, B and C of Figure 3-5 five times and Figure 3-8 four times.

Wicken Fen 1984

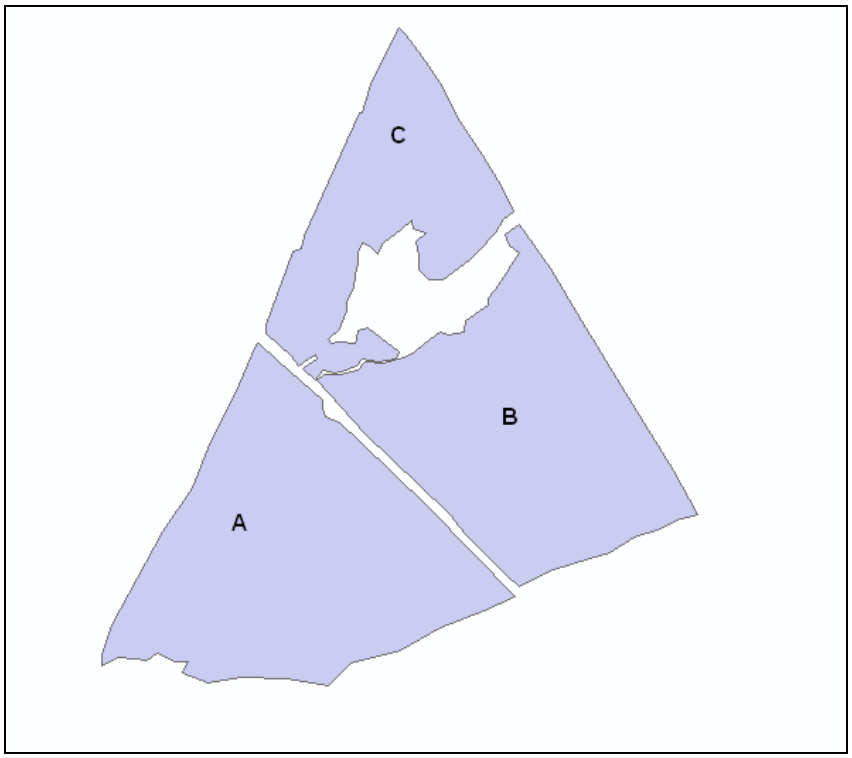

A digitizing No.	Area of polygon **A** (m^2)	Area of polygon **B** (m^2)	Area of polygon **C** (m^2)	Total area of three polygons m^2
1	10045	85744	50992	146784
2	10102	90106	48046	148254
3	10169	91007	47902	149078
4	10294	86789	52178	149261
5	10104	90849	46796	147752

Appendix 10

Wicken Fen 2009

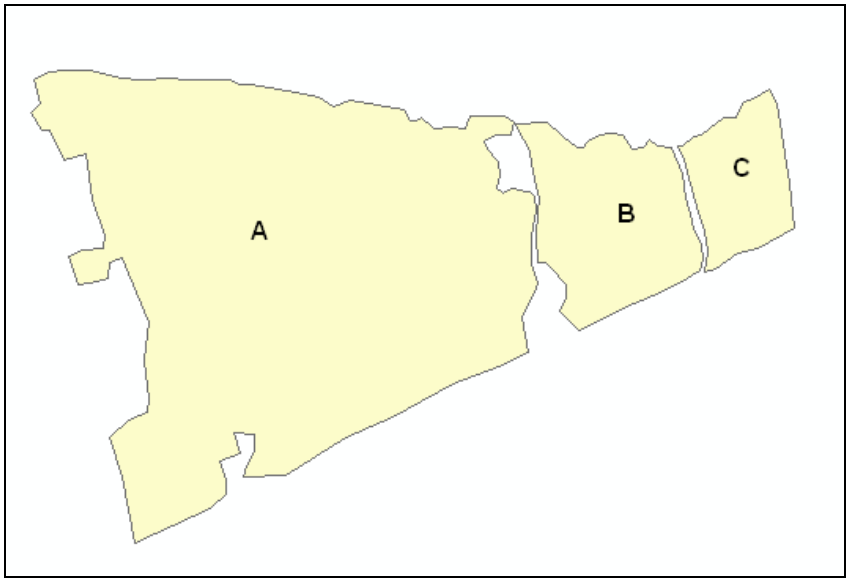

A digitizing No.	Area of polygon **A** (m^2)	Area of polygon **B** (m^2)	Area of polygon **C** (m^2)	Total area of three polygons m^2
1	85055	14465	7693	107213
2	85195	14446	7572	107213
3	85194	14598	7636	107428
4	85068	14473	7547	107088